Czech University of Life Sciences Prague

Faculty of Forestry and Wood Sciences

The use of remote sensing imagery for the estimation of tree health characteristics related to bark beetle attack

Ph.D., Dissertation thesis (Diss T)

Author: Ing. Aleksei Trubin

Field of study: Applied geoinformatics and remote sensing in forestry

Supervisor: doc. Ing. Peter Surový, Ph.D.

Consultant: Ing. Rastislav Jakuš, PhD.

Place & Year : Prague, 2024

CZECH UNIVERSITY OF LIFE SCIENCES PRAGUE

Faculty of Forestry and Wood Sciences

Ph.D. THESIS ASSIGNMENT

Ing. Aleksei Trubin

Applied geoinformatics and remote sensing in forestry

Thesis title

The use of remote sensing imagery for the estimation of tree health characteristics related to bark beetle attack

---

Objectives of thesis

Objectives of the dissertation thesis:
1) Development and validation of remote sensing methods for early detection and health assessment of Norway spruce.
2) Spectral analysis and characterization of Norway spruce during different phases of bark beetle infestation.
3) Evaluation of the synergistic use of satellite remote sensing data and auxiliary data for bark beetle infestation assessment

Methodology

The methodology of this thesis is based on the utilization of advanced remote sensing (RS) technologies and the integration of meteorological data to study the susceptibility and response of Norway spruce to bark beetle infestations.

The causes of bark beetle damage depend on many factors but one of the main hypotheses is that acute or chronic drought stress predisposes the tree to bark beetle attack. With the use of modern equipment, such as multispectral sensors and satellite imagery, it becomes possible to make more and more precise detection of specific trees potentially predisposed to bark beetle attack at the initial stages, as well as to provide data for further modelling of the process. Many studies (A. Lausch, R. Näsi, R. Jakuš) confirm the effectiveness of using various sensors and vehicles to acquire RS data for identifying potentially predisposed trees to bark beetle attack.

Experimental plots will be used for the assessment of spectral signatures of spruce exposed to acute and chronic stress. The obtained signatures will be used for assessment of predisposition to attack in bark beetle outbreak areas.

To deepen our understanding of the broader environmental context, this study integrates a range of meteorological data, including temperature, precipitation, wind speed and duration of solar radiation. These climate variables are crucial for developing predictive models of tree mortality and understanding its geographical variations.

By using RS data, ground truth data and meteorological variables, the research aims to uncover patterns, detect susceptibility and establish models that can predict mortality more accurately.

The proposed extent of the thesis

70 – 80stran

Keywords

Ips typographus, Picea abies, Bark beetle outbreaks, Drought, spectral vegetation indices

Recommended information sources

ABDOLLAHNEJAD, Azadeh; SUROVÝ, Peter; ČESKO. MINISTERSTVO ŽIVOTNÍHO PROSTŘEDÍ. *Detection and modeling of forest attributes in forest with defferent density using remote sensing and auxiliary data : doctoral dissertation.* Dissertation thesis. Praha: 2018.

Abdullah, H., Skidmore, A.K., Darvishzadeh, R., Heurich, M., 2019. Sentinel-2 accurately maps green-attack stage of European spruce bark beetle (Ips typographus , L.) compared with Landsat-8. Remote Sens Ecol Conserv 5, 87–106. https://doi.org/10.1002/rse2.93

Hansen, M.C., Potapov, P.V., Moore, R., Hancher, M., Turubanova, S.A., Tyukavina, A., Thau, D., Stehman, S.V., Goetz, S.J., Loveland, T.R., Kommareddy, A., Egorov, A., Chini, L., Justice, C.O., Townshend, J.R.G., 2013. High-Resolution Global Maps of 21st-Century Forest Cover Change. Science 342, 850–853. https://doi.org/10.1126/science.1244693

Hlásny, T., Krokene, P., Liebhold, A., Montagné-Huck, C., Müller, J., Qin, H., Raffa, K., Schelhaas, M.-J., Seidl, R., Svoboda, M., Viiri, H., European Forest Institute, 2019. Living with bark beetles: impacts, outlook and management options (From Science to Policy), From Science to Policy. European Forest Institute. https://doi.org/10.36333/fs08

Mezei, P., Jakuš, R., Pennerstorfer, J., Havašová, M., Škvarenina, J., Ferenčík, J., Slivinský, J., Bičárová, S., Bilčík, D., Blaženec, M., Netherer, S., 2017. Storms, temperature maxima and the Eurasian spruce bark beetle Ips typographus—An infernal trio in Norway spruce forests of the Central European High Tatra Mountains. Agricultural and Forest Meteorology 242, 85–95. https://doi.org/10.1016/j.agrformet.2017.04.004

Netherer, S., Matthews, B., Katzensteiner, K., Blackwell, E., Henschke, P., Hietz, P., Pennerstorfer, J., Rosner, S., Kikuta, S., Schume, H., Schopf, A., 2015. Do water-limiting conditions predispose Norway spruce to bark beetle attack? New Phytologist 205, 1128–1141. https://doi.org/10.1111/nph.13166

PANAGIOTIDIS, Dimitrios; SUROVÝ, Peter; ČESKO. MINISTERSTVO ŽIVOTNÍHO PROSTŘEDÍ. *Assessment of forest parameters usinf modern remote sensing approaches : doctoral dissertation.* Dissertation thesis. Praha: 2017.

Seidel, H., Schunk, C., Matiu, M., and Menzel, A. (2016). Diverging drought resistance of scots pine provenances revealed by infrared thermography. Front. Plant Sci. 7:1247. doi: 10.3389/fpls.2016.01247

SUROVÝ, Peter; KUŽELKA, Karel; ČESKO. MINISTERSTVO ŽIVOTNÍHO PROSTŘEDÍ. *Aplikace dálkového průzkumu Země v lesnictví.* Praha: Česká zemědělská univerzita, 2019. ISBN 978-80-213-3008-5.

Wermelinger, B., 2004. Ecology and management of the spruce bark beetle Ips typographus—a review of recent research. Forest Ecology and Management 202, 67–82. https://doi.org/10.1016/j.foreco.2004.07.018

Expected date
2023/24 WS – FFWS – State Doctoral Examinations

The Dissertation Thesis Supervisor
doc. Ing. Peter Surový, PhD.

Supervising department
Department of Forest Management and Remote Sensing

Advisor of thesis
Ing. Rastislav Jakuš, PhD.

Electronic approval: 22. 1. 2024
doc. Ing. Peter Surový, PhD.
Head of department

Electronic approval: 22. 1. 2024
prof. RNDr. Tomáš Hlásny, PhD.
Chairperson of Field of Study Board

Electronic approval: 23. 1. 2024
prof. Ing. Róbert Marušák, PhD.
Dean

Prague on 23. 01. 2024

Annotation

This thesis examines the impact of climate-induced drought stress and bark beetle infestations on European spruce forests, particularly the Eurasian spruce bark beetle (*Ips typographus* L.) attacks on Norway and Siberian spruce. Utilizing satellite remote sensing, ground truth, and meteorological data, the study explores tree health assessment during various bark beetle infestation phases.

Four scientific publications form the core of this thesis. Two studies (Trubin et al., 2023; 2024) apply PlanetScope multispectral imagery and ground truth data to identify forest spectral characteristics before and during early bark beetle attacks. Key findings highlight the effectiveness of specific spectral vegetation indices (Enhanced Vegetation Index (EVI) and Visible Atmospherically Resistant Index (VARI)) in early detection of beetle-related tree decline, offering a novel approach to forest health monitoring.

The other two studies (Trubin et al., 2022 and Pirtskhalava-Karpova et al., 2024) focus on modeling tree mortality using meteorological variables. These studies identify key climatic factors influencing annual tree loss in forests with different spruce species. Results enhance predictive models for bark beetle outbreaks and highlight climatic patterns predictive of potential infestations.

Overall, this thesis contributes significantly to forest management and conservation strategies. By integrating satellite imagery with terrestrial and climatic data, it provides a comprehensive framework for early detection and continuous monitoring of bark beetle infestations. This proactive methodology aids in identifying vulnerable and affected areas, enabling timely and targeted interventions to reduce damage. Moreover, the developed mortality models using climatic variables empower forest managers to better anticipate and prepare for potential outbreaks, optimizing resource management and response tactics.

Keywords: *Ips typographus*, *Picea abies*, bark beetle outbreaks, drought, spectral vegetation indices.

Declaration

I declare that I have independently written the dissertation on the topic "The use of remote sensing imagery for the estimation of tree health characteristics related to bark beetle attack", with the use of literature and based on consultations and supervisor's recommendations. I agree to publishing of the dissertation according to Act no. 111/1998 Coll., on schools, as amended, regardless of the outcome of its defense.

Prague, 2024   Ing. Aleksei Trubin

Acknowledgements

I'd like to thank Rastislav Jakuš and Peter Surový for their guidance and support during my time at the Czech University of Life Sciences. Their practical advice and constructive feedback were invaluable. Their expertise was a constant source of inspiration, and I am grateful for the insights they brought to my research.

I would also like to acknowledge the central project, EXTEMIT-K, for providing the framework and resources necessary for my research. I am also thankful to IGA and NAZVA for contributing additional depth to my work.

A big thanks goes to Miroslav Blaženec and the Institute of Forest Ecology for the internship opportunity. The experience contributed significantly to my skillset and understanding of the subject matter.

My office mates deserve mention for making the daily grind more bearable. Your company, support, and the occasional brainstorming sessions were greatly appreciated. Lastly, my family has been my constant support system. Their encouragement has been crucial in helping me stay focused and motivated. Thank you for standing by me through the ups and downs.

In closing, I want to express my gratitude to all who have contributed in one way or another to this academic endeavor. Your support has been essential, and I am truly thankful.

Table of Contents

List of figures

List of table

List of original publications

I. **Trubin, A.**, Kozhoridze, G., Zabihi, K., Modlinger, R., Singh, V. V., Surový, P., and Jakuš, R. (2023). Detection of susceptible Norway spruce to bark beetle attack using PlanetScope multispectral imagery. *Front. For. Glob. Change* 6, 1130721. doi: 10.3389/ffgc.2023.1130721.

II. **Trubin, A.**, Kozhoridze, G., Zabihi, K., Modlinger, R., Singh, V. V., Surový, P., and Jakuš, R. Detection of Green Attack and Bark Beetle Susceptibility in Norway Spruce Trees using PlanetScope Multispectral Imagery. Manuscript.

III. **Trubin, A.**, Mezei, P., Zabihi, K., Surový, P., and Jakuš, R. (2022). Northernmost European spruce bark beetle *Ips typographus* outbreak: Modelling tree mortality using remote sensing and climate data. Forest Ecology and Management 505, 119829. doi: 10.1016/j.foreco.2021.119829.

IV. Pirtskhalava-Karpova, N., **Trubin, A.**, Karpov A., and Jakuš, R. (2024). Drought initialised bark beetle outbreak in Central Europe: meteorological factors and infestation dynamic. Forest Ecology and Management 554, 121666. https://doi.org/10.1016/j.foreco.2023.121666

1. Introduction and literary analysis

Eurasian spruce bark beetle (*Ips typographus* L.) is one of Eurasia's most economically significant forest pests (Wermelinger, 2004), that leads to significant loss of coniferous forests within the whole Palearctic region (Christiansen and Bakke, 1988) and severe damage to coniferous forests in the Northern Hemisphere (Raffa et al., 2015). Despite their vital function in conifer-dominated forest ecosystems in the Northern Hemisphere's regeneration and succession (Bače et al., 2015; Winter et al., 2015; Zeppenfeld et al., 2015), bark beetle outbreaks in recent years have significantly exceeded their earlier recorded frequencies and effects (Winter et al., 2015). Considering the growing threat from the Eurasian spruce bark beetle, especially in conditions of climate change, it is crucial to explore triggers that global forests face, especially severe environmental stresses.

In European spruce forests, the primary abiotic elements impacting their health are typically identified as drought and wind (Kärvemo et al., 2014; Komonen et al., 2011; Marini et al., 2017). These factors are anticipated to escalate due to climate change (Haarsma et al., 2013; Seidl et al., 2017; Jactel et al., 2019).

1.1 Main drivers of the bark beetle outbreaks

Traditionally, storms have been the primary cause of spruce bark beetle infestations in Europe, but in recent times, there has been a notable rise in outbreaks induced by drought conditions (Kärvemo et al., 2023, Hlásny et al., 2021a, Hlásny et al., 2021b).

1.1.1 Wind

In recent decades, European coniferous forests, particularly Norway spruce forests, have witnessed a surge in windthrow disturbances, intensifying in both regularity and impact (Nilsson et al., 2004; Seidl et al., 2011). This phenomenon, coupled with the activities of the Eurasian spruce bark beetle (*Ips typographus* L.), constitutes a dual threat to these ecosystems. Upon the proliferation of windthrown spruces, bark beetle populations burgeon, as these trees become primary hosts, facilitating beetles' reproduction and, subsequently, attacks on healthier trees, which typically unfold one to three years post-windthrow (Marini et al., 2013; Økland and Berryman, 2004; Wermelinger, 2004; Sauvard, 2004). This ecological chain reaction not

only threatens protected areas, especially those adhering to a non-intervention management approach near managed forests (Havašová et al., 2017), but also becomes distinctly challenging during outbreaks when beetles overcome even robust trees' defences (Lindman et al., 2023). While storms, the initial catalysts, usually affect confined geographical spaces (Seidl et al., 2016; Hlásny et al., 2021b; Wermelinger and Jakoby, 2022), subsequent bark beetle infestations and their severity have been notably correlated with factors such as wind-felled spruces, host-tree volumes and age, neighboring infestations, and conditions related to aridity and temperature (Kärvemo et al., 2014a; Pasztor et al., 2014; Kärvemo et al., 2016; Brůna et al., 2013; Stadelmann et al., 2014; Netherer and Nopp-Mayr, 2005; Sproull et al., 2017; Blomqvist et al., 2018; Mezei et al., 2017; Kärvemo et al., 2023).

1.1.2 Drought

Globally, forests are increasingly susceptible to dieback due to physiological stress caused by heat and drought (McDowell et al., 2008), which is often linked to the accelerated growth of forest insect pests (Allen et al., 2010; DeRose et al., 2013; Kolb et al., 2016; White, 2015).

Research indicates that wind and drought are the two key non-biological factors affecting the health of spruce forests in Europe (Komonen et al., 2011; Kärvemo et al., 2014; Marini et al., 2017). Nonetheless, the specific physiological mechanisms that determine conifer survival and death under drought conditions remain largely unknown (McDowell et al., 2008). While conifers exhibit varying degrees of drought tolerance, extended periods of water scarcity can greatly increase their vulnerability to bark beetle attacks (Krokene, 2015). Environmental elements believed to accelerate bark beetle outbreaks include more frequent droughts and rising temperatures, which directly influence insect population dynamics as well as the growth and resistance of host plants (Jactel et al., 2012; Weed et al., 2013; Bentz and Jönsson, 2015; Meddens et al., 2015; Raffa et al., 2015). For instance, extended droughts coupled with high temperatures can reduce tree hydration, rendering them more prone to *Ips typographus* L. attacks (Wermelinger, 2004; Netherer et al., 2015). It is observed that plant defense chemicals may increase during moderate droughts but decrease during prolonged, severe droughts (Gely et al., 2020). Müller et al. (2022) identified that a heightened likelihood of bark beetle infestations is linked to factors such as high average canopy height, high spruce volume, reduced soil moisture, proximity to recent clear-cut areas and earlier beetle outbreaks.

1.2 Remote sensing of bark beetle attack stages
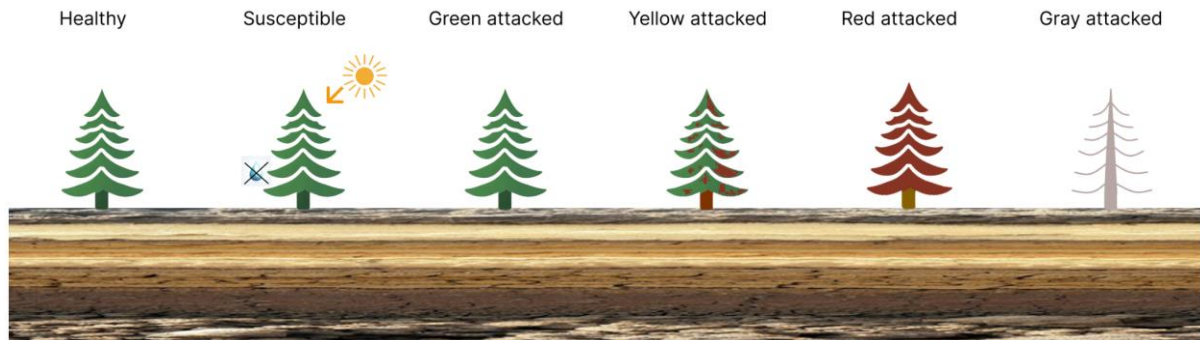
Figure 1- Stages of the development of bark beetle attack

Lots of studies show the great results of using RS imagery to detect the Yellow and Red attack stages in different locations and landscapes (Wulder et al., 2006; Zabihi et al., 2021; Marvasti-Zadeh et al., 2023). The promising results of these studies led researchers to investigate the possibilities of detecting the latest stage of infestation, and even before it.

In terms of the phases of bark beetle attack, the current research focused on the mortality phase to have a complete understanding of the entire bark beetle outbreak cycle and the early phase (green attack), to understand forest characteristics before the attack (having signs of stress) and in the first days and weeks of the attack to be able to detect traceable signs using remote sensing data (Figure 1).

The latest review on the early detection of *Ips typographus* was performed by Zabihi et al., 2021 and Marvasti-Zadeh et al., 2023.

Georgiev et al., 2023 indicated the efficiency of using free Sentinel-2 satellite imagery for the early detection of *Ips typographus* infestations in Norway spruce forests in their study near Smolyan (Bulgaria) around windbreak and windfalls in mountain areas. By analyzing the Normalized Difference Vegetation Index (NDVI), the research demonstrated that significant deviations in NDVI values from 2018 (the year of severe windthrow) to 2020 provided evidence of pest attacks before observable symptoms. The study's findings underscore the potential of NDVI data to facilitate the early identification of bark beetle infestations, thereby enabling more effective forest management and mitigation strategies.

Advanced approaches to using Machine Learning and Deep Learning in the detection of bark beetle infestation with remote sensing data are quite advanced, allowing it to cover large landscapes (Zhang et al., 2022). However, the performance of current ML methods for

early detection is limited, often achieving less than 80% accuracy. This performance is influenced by several factors including the type of imagery sensors, resolutions, acquisition dates, and the features and algorithms used. Deep learning networks and the random forest algorithm have shown promise, particularly for detecting subtle changes in the visible, thermal, and short-wave infrared spectral regions (Marvasti-Zadeh et al., 2023).

1.3 Aims of this thesis

This thesis integrates three primary study areas related to the susceptibility, green attack, and mortality phases of Norway spruce (*Picea abies* (L.) Karst) trees in response to bark beetle infestations. It offers an in-depth analysis of these phases and their spectral characteristics, guided by the following hypotheses.

Susceptibility Phase: The first study aimed to identify the potential for detecting trees susceptible to beetle attacks early in the growing season. By leveraging spectral bands and/or spectral vegetation indices (SVIs) derived from individual wavelengths, the goal was to establish the significant differences between healthy trees and those predisposed to attacks, developing a robust methodology using remotely sensed and ground-truth data to track the health status of Norway spruce on a temporal scale, specifically before and during infestation episodes.

Green Attack Phase: The second study took a closer look at the spectral properties of forests under green attack, assuming they are significantly different due to the differing levels of damage caused by bark beetles. Assuming that the spectral signatures of affected trees would have unique features indicative of the ongoing physiological changes, this research aimed to identify these meaningful differences among the forest classes. The spectral properties of healthy forests were used as a reference point, giving insights into the undisturbed state of these stands.

Mortality Phase: The third and fourth research was aimed primarily at identifying the most effective models using meteorological variables, such as temperature, precipitation, and previous-year damage, that accurately represent annual tree-cover loss. The objective was to investigate how these selected variables might influence annual fluctuations in tree loss, as per the simplest and most explanatory model. An additional aim was to investigate whether the variables linked to tree mortality vary according to geographical location, specifically comparing the northernmost limits of spruce occurrence to lower latitudes. This was achieved by integrating variables related to solar radiation into the analysis. The main goal of this study

was to refine our understanding of tree cover loss, particularly in the context of beetle-induced tree mortality, by leveraging robust predictive models grounded in meteorological data.

2. Summary of work methodology

2.1 Study area and sites

2.1.1 The School Forest Enterprise

The School Forest Enterprise (ŠLP) is situated in the vicinity of Kostelec nad Černými Lesy, roughly 50 kilometers southeast of Prague in the Czech Republic. This area, managed by the Czech University of Life Sciences Prague (CZU), encompasses a forested region of about 5,700 hectares. These forests are situated at the juncture of the Central Bohemia Uplands and the Polabí lowlands, part of the Česká křídová tabule geomorphological area, with elevations ranging from 300 to 527 meters. The region is classified within the temperate zone, experiencing mild winters. Historical climatic data indicates average annual temperatures fluctuating between 7.0 and 7.5 °C, with annual rainfall averaging around 650 mm. The vegetation period typically spans from 150 to 160 days annually. The forest composition is diverse: conifers, primarily Norway spruce (*Picea abies*), which accounts for nearly half of this category, dominate 70% of the forest cover. Scots pine (*Pinus sylvestris*) and other coniferous species also contribute significantly to this percentage. The remaining 30% comprises broadleaved species, predominantly European beech (*Fagus sylvatica*) and oak species (*genus Quercus*), alongside other varieties. The area's forest health has been increasingly challenged by recurring drought conditions in recent years. Notably, the severe drought of 2018 led to a significant bark beetle infestation, primarily caused by *I. typographus*, with localized occurrences of *I. duplicatus*, *I. amitinus*, and *Pityogenes chalcographus*. In response, forest management practices have been geared towards sanitary logging, focusing on the fast identification and removal of affected trees to mitigate further damage.
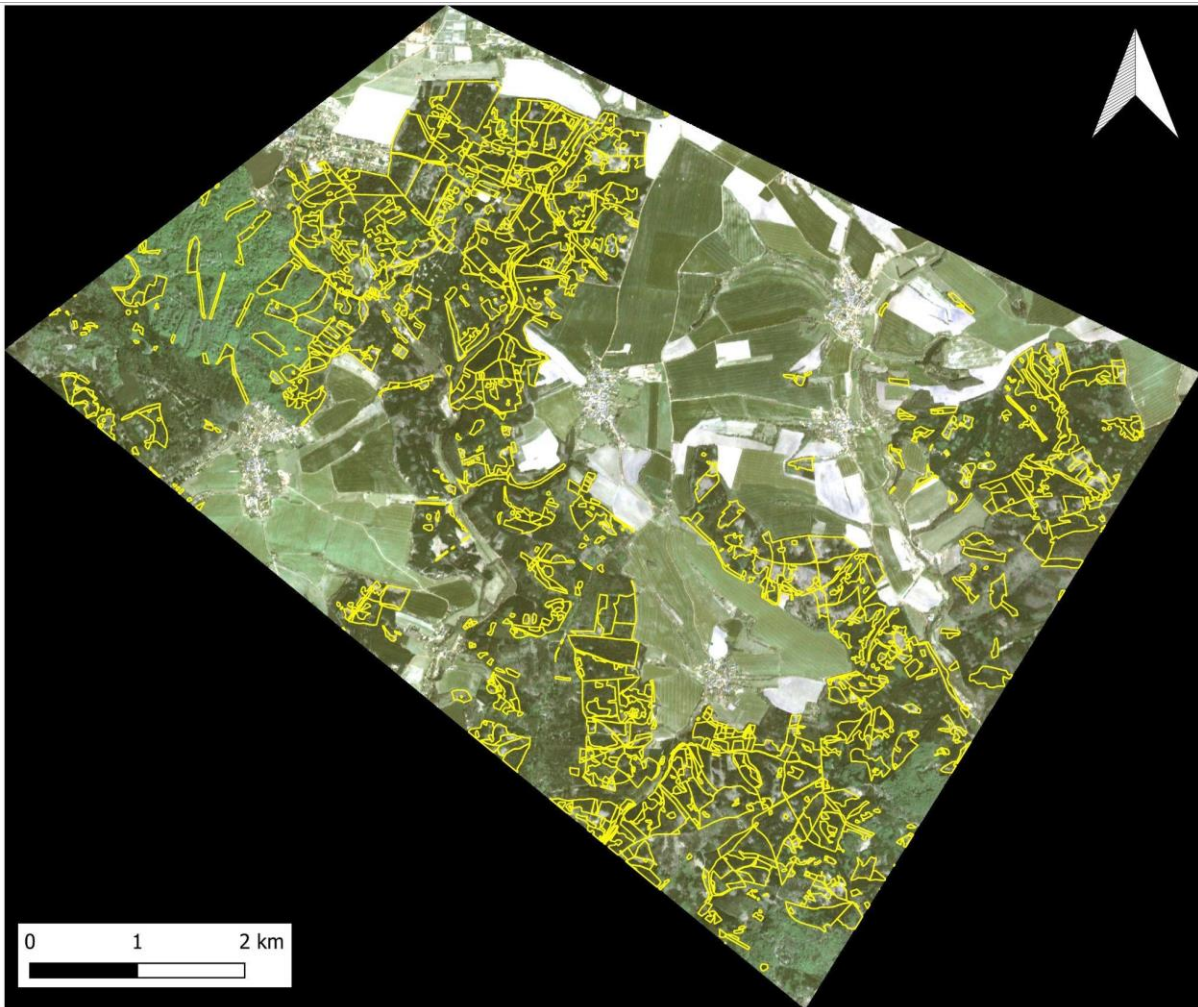
Figure 2 - Overlay of Forest Management Plan of The School Forest Enterprise on Planet Imagery dated April 23, 2022, cropped to the Area of Interest (AOI).

2.1.2 Dvinsko-Pinegskiy reserve

The Dvinsko-Pinegskiy reserve in Arkhangelsk region, Russia is a state-protected area between 62°30′ and 64°00′ N and 42°00′ W to 46°00′ E, untouched by significant human activities. Encompassing 300,420 hectares, the study area is predominantly forested (over 90%), with Siberian spruce being the dominant species.

In 2020, as compensation for 150 hectares of illegally felled forest in the Dvinsko-Pinezhsky nature reserve, a logging company took under voluntary protection an area of taiga of 1,834 hectares, which was not included in the original configuration.
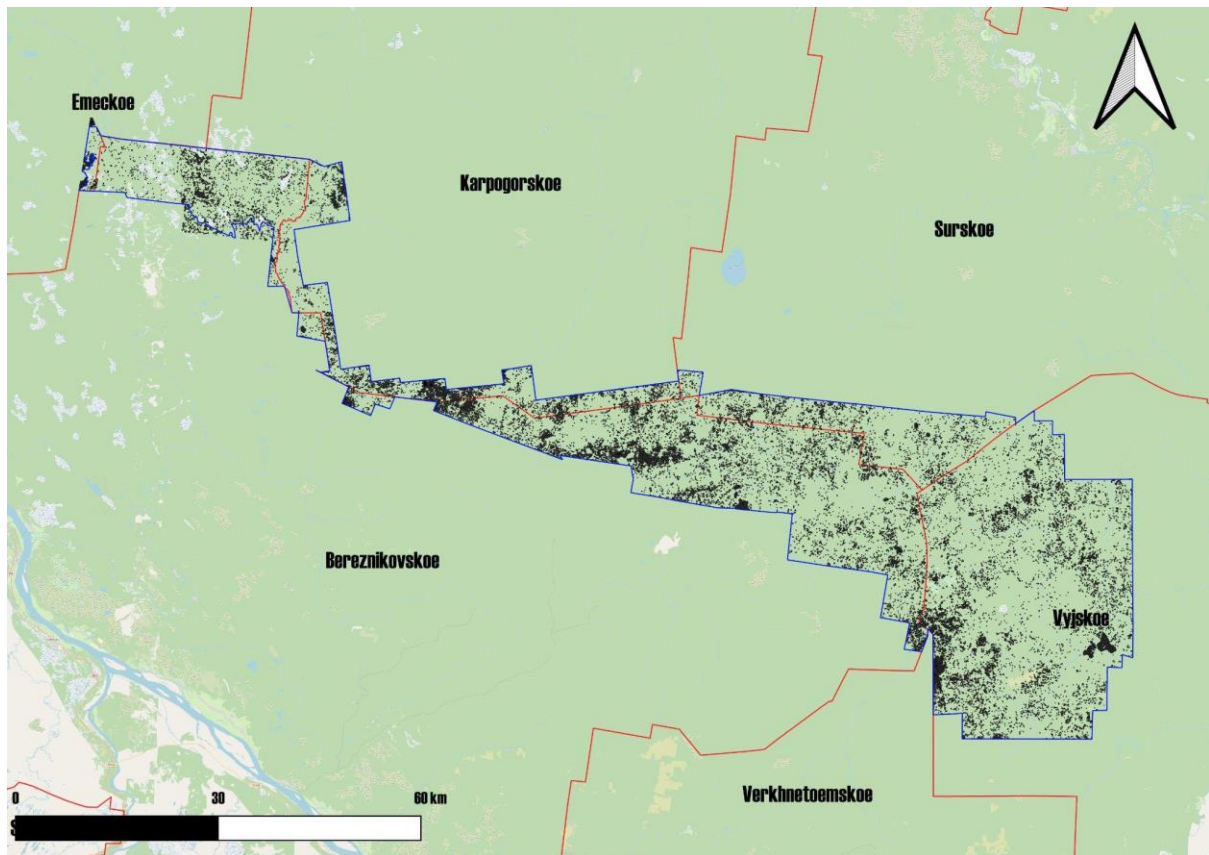
Figure 3 - Dvinsko-Pinezhsky natural reserve with Global Forest Watch 2004-2014 dataset with forestry borders.

The spruce stands, originating from past wildfires, naturally decay when reaching 180-200 years of age, contributing to forest regeneration. The forest landscape is impacted by localized spruce death, infrequent disturbances, windthrows, insect outbreaks, and fires, with droughts often exacerbating these events. The Eurasian spruce bark beetle infestation that started in 1999 is linked to severe drought conditions in 1997 and heavy snowfall damage in 2001-2002 (Trubin et al., 2022).

2.2 Remote sensing data acquisition and processing

The selection of remote sensing data sources is predicated on their unique strengths in monitoring and analyzing the health of trees affected by bark beetle infestation. In this context, PlanetScope data have been selected, leveraging the participation in Planet's Education and Research (E&R) Program, which provides specialized access to these high-quality satellite data for academic purposes. This access is particularly beneficial given PlanetScope's exceptional temporal resolution, offering frequent updates that surpass the capabilities of alternatives like

Sentinel 2. This high-frequency data acquisition is critical in capturing dynamic changes in forest health, a task that would be prohibitively expensive and labor-intensive using UAVs, especially considering the spatial extent of the study area.

Global Forest Watch (GFW), leveraging processed Landsat data, provides a comprehensive view of forest loss. This platform offers a distinct advantage over developing custom solutions for forest loss detection, such as training, validation and applying complex machine learning and AI models, which can be time-consuming and resource-intensive on large areas. GFW's data significantly streamline the process, offering accurate and readily available information on forest changes, essential for quantifying the impact of bark beetle attacks.

These data sources, with their respective strengths, not only enhance the efficiency of data acquisition but also ensure the reliability and accuracy of the analyses conducted in this study. In subsequent research endeavors beyond this thesis, the integration of diverse data sources will be explored to enhance the specificity and accuracy of monitoring bark beetle impacts on forest health.

2.2.1 Global Forest Watch

Global Forest Watch (GFW) is an online platform that provides data and tools for monitoring forests worldwide. Launched by the World Resources Institute along with over 40 partners, GFW harnesses the power of satellite technology, open data, and crowdsourcing to deliver near-real-time information about the state of forests. This initiative aims to increase transparency and facilitate better management of forest landscapes by enabling policymakers, researchers, and the general public to access detailed information about forest cover changes. The GFW's data, which includes metrics like gross forest cover loss, is crucial for understanding and analyzing global deforestation patterns and trends. This data is particularly valuable for environmental research, as it offers precise and consistent measurements of forest change over time, captured through advanced analysis of Landsat satellite imagery. Such comprehensive and accessible data are important for the development of sustainable forest management strategies and conservation efforts in different geographical regions.

The gross forest cover loss (lossyear) layers (Marini et al., 2013) were used from 2001 to 2014 derived from Global Forest Watch data (ver. 1.2, Hansen et al., 2013), based on time-series analysis of Landsat imagery, to create annual maps from 2001 to 2019 at 30 by 30 meters

spatial resolution. These raster images were derived from the original $10 \times 10°$ granules and then were vectorized using the Polygonize plugin (GDAL 3.1.4), cut by the polygon of the reserve's boundaries in the QGIS environment (ver. 3.16).

2.2.2 PlanetScope

PlanetScope imagery are high-resolution multispectral satellite images captured by the Dove satellite constellation, operated by Planet Labs. The numerous small satellites that make up this constellation, known as the "Doves", combine to cover the Earth's surface comprehensively and frequently. The primary benefit of PlanetScope imagery is its high temporal resolution, allowing the ability to monitor changes on the Earth's surface nearly on a daily basis. Applications requiring regular and up-to-date observations, including disaster response, agricultural management, and environmental monitoring, would especially benefit from this capability. With a spatial resolution of three meters, the imagery obtained by the Dove satellites, especially the Dove Classic (PS2) sensor utilized in this study, offers comprehensive visual information. In addition, the Dove satellites capture data in a number of spectral bands, including Red, Green, and Blue (RGB) and Near Infrared (NIR), which offers insightful information on a range of environmental topics.

Cloud-free PlanetScope imagery (instrument–Dove Classic (PS2)) in the GeoTIFF format with surface reflectance data type (harmonized to Sentinel-2 for consistent radiometry) were used from April 2 to 5 September 2020 (22 imageries).

The individual four bands and the SVIs were used to differentiate three defined classes. These three classes were non-attacked trees during our year of study, assumed and considered as the "Healthy" class; trees were attacked in the later stages of the growing season, assumed and considered as the "Susceptible" class; trees that were previously classified as "Susceptible", but had since reached the date of bark beetle green attack and, consequently, are designated as the "Green-attack" class in Paper 2. For Paper 1, only the first two classes were selected.
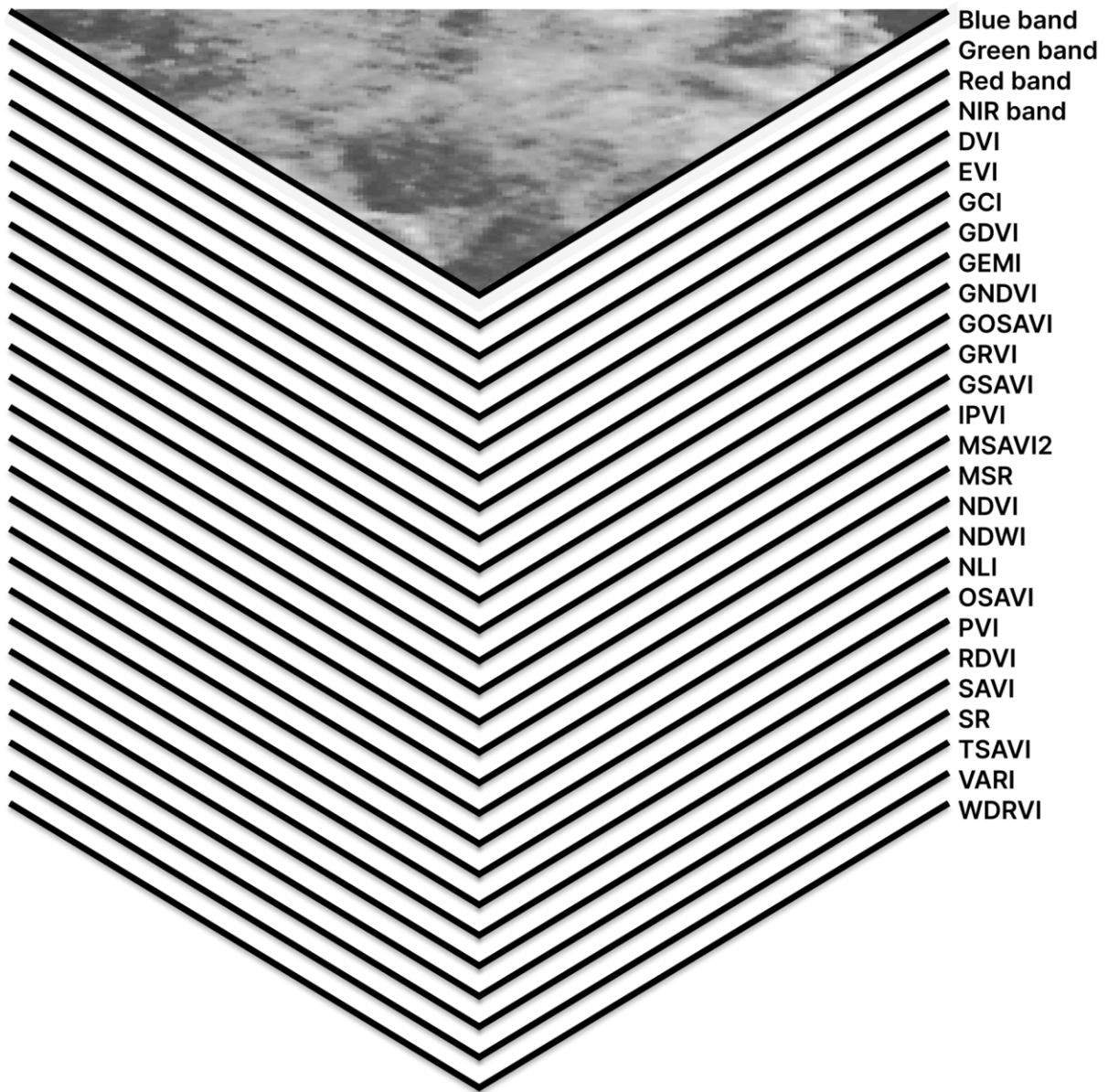
Figure 4 Stacked multiband data cube containing individual bands and SVI

For each acquisition in the time series, 23 SVIs were calculated using the Raster Calculator plugin in QGIS version 3.16.16 (QGIS Development Team, 2009). All individual bands and SVIs were merged into a single GeoTIFF file to make a cube image of 27 bands, for further statistical analysis (Figure 4).

2.3 GIS and ground truth data collection and validation

2.3.1 Cross-platform ArcGIS application

The coordinates of the areas of evidence of bark beetle in The School Forest Enterprise (ŠLP) in Kostelec nad Cernými lesy were recorded by employers of the company and CZU FLD and EXTEMIT-K project using cross-platform ArcGIS application. A cross-platform ArcGIS application is a set of compatible tools and applications within the ArcGIS system, intended to perform a variety of GIS tasks on various devices. Esri's ArcGIS is a versatile mapping and spatial analysis platform which is used in resource management, urban planning, and environmental research, among other fields of study. The ArcGIS platform makes it possible for data to be seamlessly integrated and synchronized across various hardware and software environments via a cross-platform architecture. Since it enables users to perform more in-depth analysis and visualization on desktop computers, as well as to record and access data on-the-go via smartphones and tablets, this versatility is especially important for field data collection and subsequent analysis.

The aim of the application was to have the ability to record, store, analyse and visualize data on different platforms. ArcGIS Collector was used for smartphones (both iOS and Android-based) to record points with coordinates of the hotspot and ArcGIS Online portal and ArcMap 10.8 desktop application were used for storing, analysis, visualising and report creation.
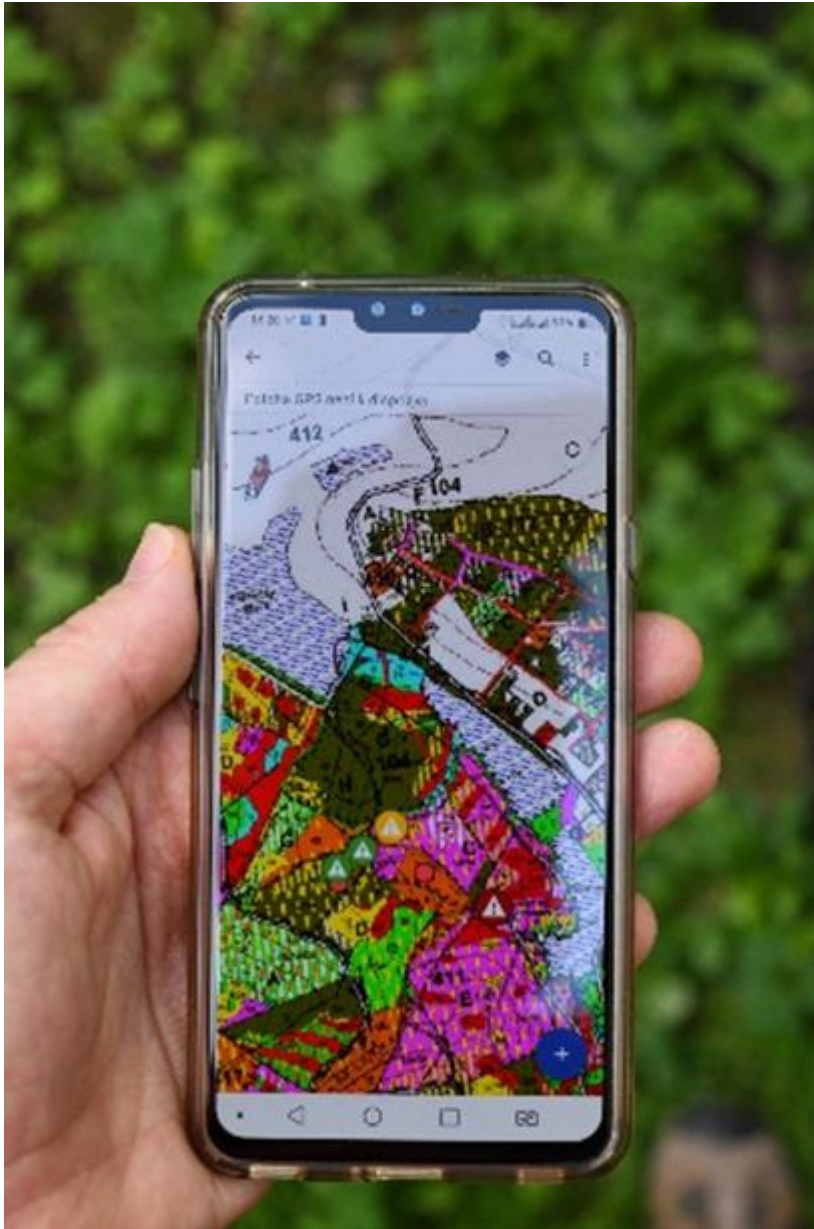
` Figure 5 - Mobile application (Photo by Roman Modlinger)
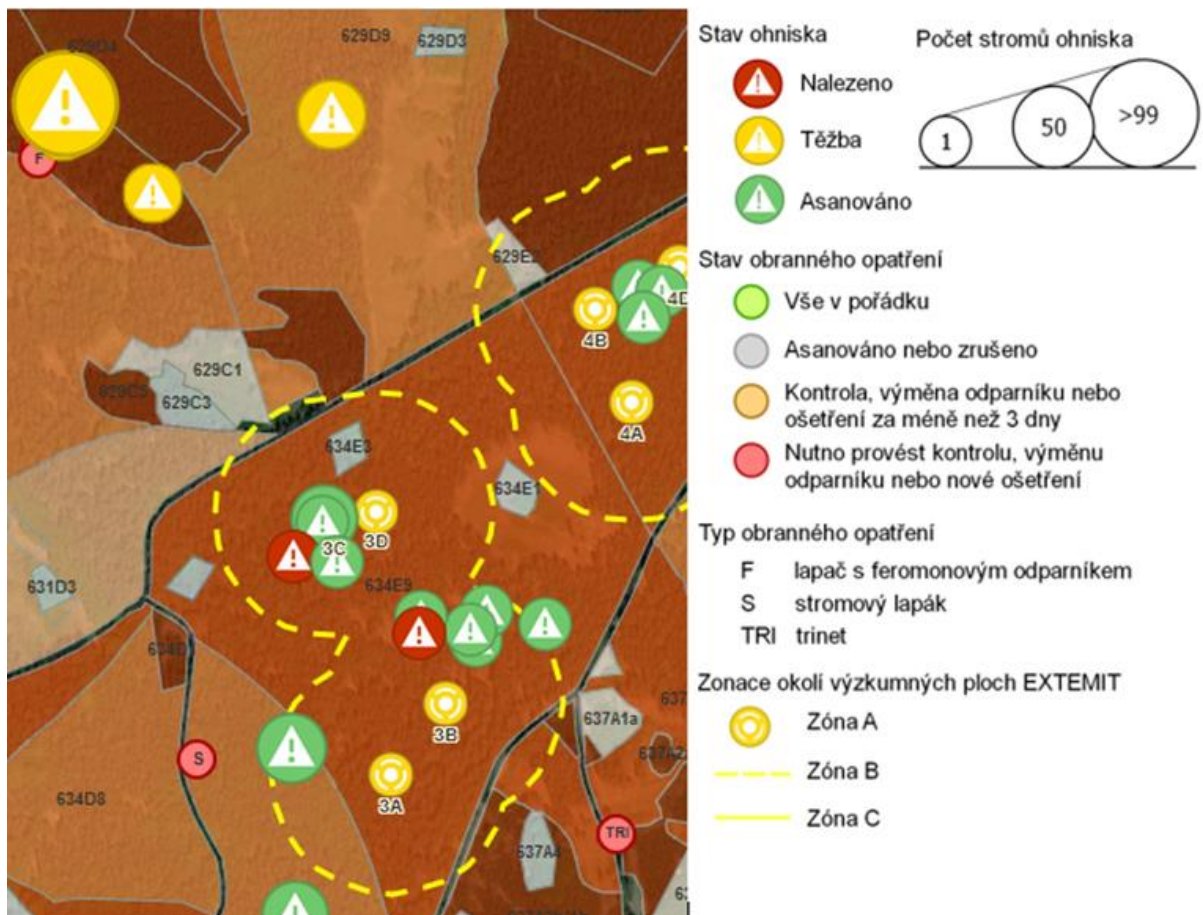
Figure 6 Desktop application
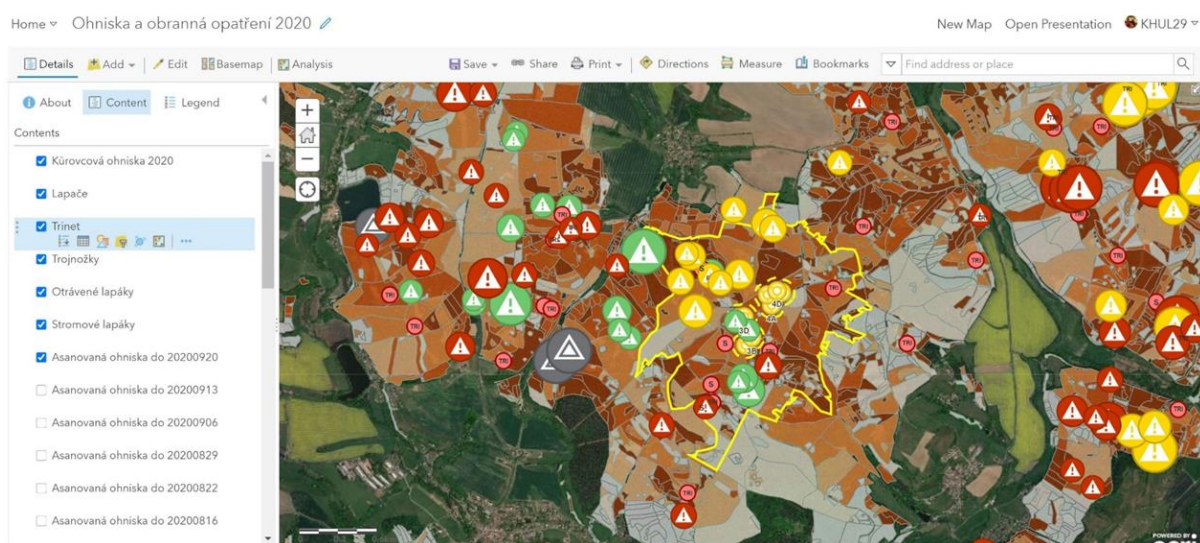
Figure 7 Overview of desktop application and layer description

Table 1 - Attributes of layers, used in the application for collecting information about hotspots

Attribute #	Attribute name	Description	Type and Options
1	Date of collection	Filled by forest managers and other users of Collector for ArcGIS.	
2	Number of attacked trees on the date of first collection	Filled by forest managers and other users of Collector for ArcGIS.	
3	Development stage of bark beetles	Filled by forest managers and other users of Collector for ArcGIS. There is a list of available choices (domains).	Entry holes, Eggs, 1st instar larvae, 2nd instar larvae, 3rd instar larvae, pupae, yellow beetle, brown beetle, emerging holes, dry dead tree
4	Hot spot state	Filled by forest managers and other users of Collector for ArcGIS. There is a list of available choices (domains).	
5	Date, Number of attacked trees, Maximum developed stage of bark beetles at the first and next inspections	Filled by forest managers and other users of Collector for ArcGIS.	
6	Type of bark beetle	Filled by forest managers and other users of Collector for ArcGIS. Users are using the list of choices, which are Yes/No.	Eurasian spruce bark beetle (*Ips typographus*), Six-toothed spruce bark beetle (pityogenes chalcographus), Double-spined bark beetle (*Iplicatups dus*), Small spruce bark beetle (*Polygraphus*

			poligraphus)
7	JPRL	Forest stand code. Filled by GIS administrator.	
8	Estimated volume	Cubic meters of affected trees at the time of collection.	
9	Forest management area (numeric code)	Filled manually by GIS administrator	

Date of collection (implied as date of attack), Number of attacked trees on the date of first collection, Development stage of bark beetles, Hot spot state, Date, Number of attacked trees, Maximum developed stage of bark beetles at the first and next inspections, Type of bark beetle, JPRL, Estimated volume and Forest management area (numeric code) in the day of inspection were recorded using the ArcGIS Collector app.

Foresters conducted weekly surveys in their assigned regions to identify initial bark beetle infestations. Simultaneously, EXTEMIT-K project researchers collected similar data around six experimental plots. They employed visual inspections and sniffer dogs to spot early-stage infested trees within a 500-meter radius of these plots (Vošvrdová et al., 2023; Trubin et al., 2023). Each experimental plot was divided into four subplots, which include 8–10 neighbour trees (Özçelik et al., 2022; Stříbrská et al., 2022).

2.4 Meteorological variables

In the Dvinsko-Pinegskiy reserve study area, the meteorological variables were crucial for understanding the impact of climate on bark beetle epidemics and tree mortality from 2001 to 2014. The dataset included monthly temperature, precipitation, and duration of solar radiation, obtained from the Sura meteorological station, and calculated indices - JJA (June, July, and August average air temperature), DJF (December, January, and February average air temperature), annual variables and the Selyaninov hydrothermal coefficient, calculated to assess moisture during the growing season.

The ŠLP study, focusing on a bark beetle outbreak in Central Europe, also heavily relied on meteorological variables to understand annual tree cover loss and bark beetle damage from 2012 to 2022. Conducted near Kostelec nad Černými Lesy in the Czech Republic, the study

used data from the nearest weather station (Ondřejov). The meteorological variables analyzed included the same variables as in the Dvinsko-Pinegskiy study, excluding the Selyaninov hydrothermal coefficient and adding April to September wind speed

2.5 Statistical analysis

2.5.1 Difference between two and three classes

For each distinct class, mean values of individual spectral bands and Spectral Vegetation Indices (SVI), compiled in the multilayer spectral data cube, were utilized to identify significant differences between classes. The suitability of parametric statistical methods was verified using the Shapiro-Wilk and Levene tests. Shapiro-Wilk test checks for normal distribution, while Levene's test assesses the equality of variances across groups. To identify statistically significant differences in spectral values (individual bands and SVIs) for each image capture date, Welch's t-test and Linear Discriminant Analysis (LDA) with leave-one-out cross-validation accuracy (LOOCV) were applied for two categories ("Healthy" and "Susceptible"). Welch's t-test is used when data have unequal variances and sample sizes, and LDA is a method for finding the linear combination of features that best separates two or more classes of objects. LOOCV is a method of cross-validation for model assessment. In the case of three categories ("Healthy", "Susceptible", and "Green-attack"), a One-Way Analysis of Variance (ANOVA) with Three Factors was conducted. This was followed by the Games-Howell test for datasets meeting the Levene test's assumptions, and Tukey's Honestly Significant Difference test (Tukey's HSD) for those that did not. ANOVA is used to compare mean values between three or more groups. Games-Howell and Tukey's HSD are post-hoc tests for multiple comparisons. For datasets not conforming to these assumptions, the nonparametric Kruskal-Wallis H Test (also known as "one-way ANOVA on ranks") with Three Independent Groups, and subsequently Dunn's post hoc tests, were used.

The extraction of mean values from data cube bands was carried out using QGIS, the OTB package, and the ZonalStatistics plugin. All statistical analyses were performed in Python, employing the SciPy library (ver. 1.7.1), scikit-learn (ver. 1.1.2), the statsmodels package (ver. 0.13.5), and scikit-posthocs (ver. 0.7.0).

2.5.2 Modelling tree mortality using remote sensing and climate data

Prior to analysis, the data was inspected for outliers and collinearity. Data exploration involved plotting the response variable against each covariate to examine their interrelationships. Based on this exploration, the correlation between tree mortality and explanatory variables was investigated using linear regression in Article 3, as well as Generalised Additive Models (GAMs) and Ridge regression in Article 4. Linear regression is employed to examine the association between a dependent variable and one or multiple independent variables. GAMs are a flexible approach to modelling complex data, and Ridge regression is a technique used to analyze multiple regression data that suffer from multicollinearity.

A selection of a priori models was predefined for analysis to determine which model best describes tree infestation by *I. typographus* in Article 3, and the initiation and spread of spots, as well as tree infestation in Article 4. These models were developed using known variables relevant to the dynamics of bark beetle populations, primarily climatic factors.

For linear regression and GAMs, the Information-Theoretic (I-T) method was employed to evaluate competing models. Models were ranked by the Akaike Information Criterion (AIC) for small sample datasets, with the delta AIC (ΔAIC) indicating the AIC difference between a model and the top-performing model in the candidate set; the model was chosen based on the lowest ΔAIC. AIC serves as an indicator of the relative quality of a statistical model in relation to a specific data set. Models within the ΔAIC of less than 2 were considered comparable to the best, while those within the ΔAIC range of 2–7 were also plausible. Akaike weights were computed to rank candidate models in terms of parsimony, reflecting the likelihood of each model being the most suitable given the data and set of candidates (Burnham et al., 2011).

For ridge regression, an error-based assessment method was utilized for model comparison. Models were evaluated using the Root Mean Square Error (RMSE) criterion, with the most accurate model identified by the smallest RMSE. RMSE measures the average magnitude of the error. The alpha parameter, acting as a regularization term, penalizes large coefficients in the model, thus reducing overfitting risks. A higher alpha value increases regularization strength, favoring simplicity, while a lower value allows more flexibility but may capture noise.

In Article 4, Annual bark beetle spot initiation (ha), spread (ha), and Annual tree loss change (the natural logarithm of the ratio between tree mortality in a given year and the previous year) were used as response variables; in Article 3, only Annual tree loss change.

To address the issue of high correlations among variables, we implemented a criterion where variables were selected based on a correlation coefficient threshold of 0.7. The relationship between yearly fluctuations in tree cover loss and its previous years' changes was examined by computing the autocorrelation function (ACF). Additionally, the cross-correlation functions (CCFs) were employed to analyze the relationship between the predictor time series and the variables identified in the most effective model.

In the context of Article 3, all computational and statistical analyses were performed using R (Version 3.6.1) within RStudio (Version 1.3.1093, R Development Core Team 2018). Conversely, for Article 4, the analyses were carried out in VSCode 1.73.1 using the Jupyter Notebook and Python (Version 3.11.1). The Python environment included various libraries such as pandas (Version 1.5.0), Matplotlib (Version 3.6.0), statsmodels (Version 0.15.0), pygam (Version 0.5.5), and scikit-learn (Version 1.3.0).

3. Results

The PhD dissertation thesis consists of three first-author articles (one as a manuscript) and one second-author article. The first part of the results focuses on the detection of susceptible Norway spruce trees to *I. typographus* attack (section 3.1.1). The second part demonstrates spectral differences of Norway spruce forests before and during green attack in comparison with healthy forests (section 3.1.2). The third part (section 3.2.1) examines a study that models annual changes in tree cover loss (mortality) using climate variables in the northernmost mass Eurasian spruce bark beetle outbreak. The fourth part (section 3.2.2) describes the results of modelling the bark beetle-driven spot initialisation, spot spreading and annual tree loss change using meteorological variables in central Europe.

Article I (Trubin et al., 2023) shows that using PlanetScope satellite imagery and field data, spectral vegetation indices (SVIs), specifically the Enhanced Vegetation Index (EVI) and Visible Atmospherically Resistant Index (VARI), can successfully distinguish healthy trees from those susceptible to infestations early in the growing season in central Europe's Norway spruce-dominated forests. This article responds to Objectives 1, 2 and partly 3.

Article II (Trubin et al., 2024) expands on the approach outlined in Article I, applying PlanetScope satellite imagery and field data to not only distinguish healthy Norway spruce trees from those susceptible to infestations in central Europe but also to identify trees under green attack. The study utilized the Enhanced Vegetation Index (EVI) and Visible Atmospherically Resistant Index (VARI) to differentiate these three classes, employing a variety of statistical methods to increase the accuracy and robustness of the classification process. This article responds to Objectives 1, 2 and partly 3.

Article III (Trubin et al., 2022) reports that Siberian spruce forests in the Arkhangelsk region, Russia, have experienced unprecedented tree cover loss over the past two decades due to the Eurasian spruce bark beetle, marking the first recorded outbreak of this kind at higher latitudes. Utilizing remote sensing and climate data, we modelled annual tree-loss changes over a 14-year period, pinpointing a combination of average annual temperature and precipitation, temperature and precipitation in June, as key factors driving these changes. This article responds to Objective 3.

Article IV (Pirtskhalava-Karpova et al., 2024) expands on the approach outlined in Article III for the different study area (The School Forest Enterprise, Kostelec nad Černými Lesy, the Czech Republic), with new statistical approaches (GAM and ridge regression), periods division (initialization, spread and annual total tree cover loss change) and adding new

variable - wind speed. Applying the same GFW tree cover loss dataset and meteorological data, we found that spot initialization was strongly related to April's solar radiation from the previous year; spot spreading - with the current year's average air temperature and annual tree loss with solar radiation in June and September (and the previous year's average precipitation, using ridge regression). This article responds to Objective 3.

3.1 Assessment of the predisposition of trees to bark beetle

3.1.1 Detection of susceptible Norway spruce to bark beetle attack using PlanetScope multispectral imagery

Published as:

Trubin Aleksei, Kozhoridze Giorgi, Zabihi Khodabakhsh, Modlinger Roman, Singh Vivek Vikram, Surový Peter, Jakuš Rastislav (2023). Detection of susceptible Norway spruce to bark beetle attack using PlanetScope multispectral imagery. Front. For. Glob. Change 6, 1130721. doi: 10.3389/ffgc.2023.1130721.

Authors' contributions

AT, GK, KZ, VVS, PS, and RJ contributed to the conception and design of the study. AT organized the database. AT and GK performed the statistical analysis. AT and RJ wrote the first draft of the manuscript. AT, GK, KZ, RM, VVS, and RJ wrote sections of the manuscript. All authors contributed to the manuscript revision, read, and approved the submitted version.

Extended summary

Introduction

Global forests, particularly coniferous ones, are becoming increasingly vulnerable to dieback due to physiological stress caused by heat, drought, and increased pest growth, with the European spruce bark beetle (*I. typographus*) being a key economic pest in Eurasia. The bark beetle's life cycle, its impact on trees, and how it can lead to infestations are affected by environmental factors, tree age, and density. Recent outbreaks have been significant, driven by climate change, leading to increased tree mortality, particularly in spruce forests. Gathering precise, up-to-date spatial information on infestations can help create effective plans for removal and sanitation, though this remains challenging due to limited access in large areas. Remote sensing (RS) data, using active and passive sensors, has proven to be an effective method for tracking vegetation stress and infestations. The use of PlanetScope satellite imagery has allowed for better tracking of small changes in land cover within broad areas. Individual bandwidths and Spectral Vegetation Indices (SVIs) can be used to detect changes in needle pigments, chlorophyll content, and water content due to bark beetle attacks. This study seeks to investigate if trees susceptible to beetle attacks can be detected before or early in the growing season and to develop a methodology for using remotely sensed and ground-truth data to characterize the health status of Norway spruce before and during infestations.

Materials and methods

The research was conducted in forests southeast of Prague, Czech Republic, managed by the Czech University of Life Sciences (CULS). The forests, located in a temperate climate zone, experienced a bark beetle outbreak in 2018 due to severe drought. The vegetation mainly consists of spruce, pine, beech, and oak. We utilized 22 cloud-free PlanetScope (instrument Dove Classic (PS2)) images from April to September 2020 for our study. Each image consisted of Red, Green, Blue (RGB), and Near Infrared (NIR) bands. Using QGIS software, we calculated 23 Spectral Vegetation Indices (SVIs) for each image. These were used to distinguish between non-attacked ("Healthy") and those that were attacked in the later stages of the growing season ("Susceptible") trees. The positions of attacked trees were recorded using the ArcGIS Collector application on smartphones, along with the date of the attack, the bark beetle species involved, and the number of trees attacked each day. For the "Susceptible" class, we excluded samples showing signs of later logging, which led to a reduction in sample size

and the exclusion of the last five dates of imagery from the time-series datasets. Statistical analyses involved the use of Welch's t-test to identify if there were significant differences in the means of spectral reflectance between the "Healthy" and "Susceptible" classes. Linear Discriminant Analysis (LDA) was employed to evaluate the separability of the individual bands and SVIs for differentiating the two classes.

Results

The study revealed two peak periods of bark beetle swarming and infestations during the growing season: mid-June and mid-July to early August. Susceptible trees had a higher mean value for individual bands than healthy trees, especially during the first half of the growing season. However, the top-ranked Spectral Vegetation Indices (SVIs), EVI and VARI, showed the opposite trend, with healthy trees generally having higher values. Individual bands demonstrated significant differences between healthy and susceptible trees, particularly between days 93 to 114. However, these bands could not sufficiently distinguish between the healthy and susceptible classes, as classification accuracy from the Linear Discriminant Analysis (LDA) did not meet the 70% threshold. SVIs showed significant differences between the two classes, especially from days 93 to 129. However, only EVI and VARI displayed significant differences at other dates during the first half of the growing season. Accuracy from the LDA test only passed or almost reached the 70% threshold for VARI and EVI, respectively, at days 93 to 114. The study determined that the most effective SVIs for differentiating between the classes were EVI on days 114 and 183, and VARI on days 93, 100, 108, 114, and 183.

Discussion

The study found that all four PlanetScope wavebands (Red, Green, Blue, and NIR) have the potential to detect trees susceptible to bark beetle attacks, with the NIR being the most reliable spectral reflectance for susceptible trees during the first half of a growing season. Among spectral vegetation indices, EVI and VARI were most effective in detecting susceptible trees, with EVI showing potential as a key index for predicting bark beetle attacks and managing forest pests. Seasonal SVI patterns revealed an increase until late July without significant declines, and the mean EVI values for predisposed trees were significantly lower than those for non-attacked trees. The study, however, had limitations such as the spectral resolution, limited by the choice of sensor with 4 bands due to the period of observation in 2020. Future research should consider data sets with additional bands such as SWIR to track early stressed trees more effectively, potentially using products from third-generation

PlanetScope sensors, available from mid-March 2020, or other satellites like Sentinel-2. Additional coefficients not connected with band values could be integrated into vegetation indices to improve performance if accurate ground truth data are collected. The infestation causes weren't determined, and the process by which drought conditions cause bark beetle-induced Norway spruce mortality remains to be fully understood. Despite these limitations, the findings of EVI and VARI as significant spectral vegetation indices offer insights into detecting water-stressed trees, thus facilitating changes in the physiological and biochemical processes in trees. Further research is recommended to enhance these methods.

Conclusions

Amidst a warming climate, the increased severity of droughts and associated bark beetle outbreaks necessitates proactive forest management and policy measures, including continuous monitoring of forest health and timely sanitation procedures. Utilizing vegetation indices like EVI and VARI can help detect water-stressed trees susceptible to attacks early in the growing season, thus allowing a proactive response. The ability to discern different phases of attack—from initial attacks on stressed trees to the spreading of infestations to neighbouring trees—has been noted. The complexity of these patterns can influence the ability to detect susceptible trees using a single Spectral Vegetation Index (SVI). Hence, an integrated approach using multiple SVIs sensitive to both healthy and susceptible trees and different attack phases is recommended. Furthermore, establishing thresholds for these indices can aid in creating classified maps, serving as practical tools for predicting vulnerable trees and potential infestation hotspots. Future research should explore additional bands from new generations of PlanetScope satellites and formulate new SVIs for better detection of water-stressed trees. A spectral difference based on SVI could be used to preemptively identify stress and predisposition to bark beetle infestations.

Detection of susceptible Norway spruce to bark beetle attack using PlanetScope multispectral imagery

Aleksei Trubin[1]*, Giorgi Kozhoridze[1], Khodabakhsh Zabihi[1], Roman Modlinger[1], Vivek Vikram Singh[1], Peter Surový[1] and Rastislav Jakuš[1,2]

[1]Faculty of Forestry and Wood Sciences, Czech University of Life Sciences Prague, Prague, Czechia, [2]Institute of Forest Ecology, Slovak Academy of Sciences, Zvolen, Slovakia

Climate change-related acute or long-term drought stress can weaken forest ecosystems and result in widespread bark beetle infestations. Eurasian spruce bark beetle (*Ips typographus* L.) infestations have been occurring in Norway spruce [*Picea abies* (L.) Karst.]-dominated forests in central Europe including the Czechia. These infestations appear regularly, especially in homogeneous spruce stands, and the impact varies with the climate-induced water stress conditions. The removal of infected trees before the beetles leave the bark is an important step in forest pest management. Early identification of susceptible trees to infestations is also very important but quite challenging since stressed tree-tops show no sign of discolouration in the visible spectrum. We investigated if individual spectral bandwidths or developed spectral vegetation indices (SVIs), can be used to differentiate non-attacked trees, assumed to be healthy, from trees susceptible to attacks in the later stages of a growing season. And, how the temporal-scale patterns of individual bands and developed SVIs of susceptible trees to attacks, driven by changes in spectral characteristics of trees, behave differently than those patterns observed for healthy trees. The multispectral imagery from the PlanetScope satellite coupled with field data were used to statistically test the competency of the individual band and/or developed SVIs to differentiate two designated classes of healthy and susceptible trees. We found significant differences between SVIs of the susceptible and healthy spruce forests using the Enhanced Vegetation Index (EVI) and Visible Atmospherically Resistant Index (VARI). The accuracy for both indices ranged from 0.7 to 0.78; the highest among all examined indices. The results indicated that the spectral differences between the healthy and susceptible trees were present at the beginning of the growing season before the attacks. The existing spectral differences, likely caused by water-stress stimuli such as droughts, may be a key to detecting forests susceptible to early infestations. Our introduced methodology can also be applied in future research, using new generations of the PlanetScope imagery, to assess forests susceptibility to bark beetle infestations early in the growing season.

KEYWORDS

Picea abies, Ips typographus, spectral vegetation indices, bark beetle infestations, Enhanced Vegetation Index, Visible Atmospherically Resistant Index

38

1. Introduction

Forests worldwide are becoming increasingly more sensitive to dieback due to physiological stress driven by heat and drought (McDowell et al., 2008), which is frequently coupled with increased growth of forest insect pests (Allen et al., 2010; DeRose et al., 2013). Several studies found two most significant abiotic factors, wind and drought, have been impacting the health of spruce forests in Europe, (e.g., Komonen et al., 2011; Kärvemo et al., 2014; Marini et al., 2017). However, the physiological processes underlying conifer survival and mortality under drought conditions are yet to be fully understood (McDowell et al., 2008). Conifers have a wide range of drought tolerance; however, prolonged water deficit frequency in trees may significantly increase their susceptibility to bark beetle infestation (Krokene, 2015). Critical environmental factors thought to expedite bark beetle outbreaks are the combination of more frequent droughts and warmer temperatures, directly impacting insect population dynamics and host plant development and resistance (Jactel et al., 2012; Weed et al., 2013; Bentz and Jönsson, 2015; Meddens et al., 2015; Raffa et al., 2015). For example, prolonged dry periods accompanied by high temperatures might decrease tree water supplies and make them more vulnerable to *Ips typographus* L. attacks (Wermelinger, 2004; Netherer et al., 2015). Plant defense chemicals may rise during periods of moderate drought whereas these chemicals may decrease during prolonged severe drought (Gely et al., 2020).

One of Eurasia's most economically significant forest pests (Wermelinger, 2004) is the European spruce bark beetle (*I. typographus*), which is severely damaging coniferous forests in the Palearctic region (Christiansen and Bakke, 1988).

For most bark beetle species, the females deposit their eggs inside the bark and intracortical layer of trees, consisting of phloem and cambium zone tissues, where larvae develop (Keeling, 2016). The first generation of bark beetle exits the bark when the accumulated thermal sum on average passes a threshold for several weeks (Öhrn et al., 2014), highly variable on regional- and continental-scales, starting from the early growing season (May to October; Zabihi et al., 2021b).

Factors such as tree aging and density, and drought effects were found to be important in weakening trees' resistance to bark beetle attacks (Christiansen and Bakke, 1988; Raffa, 1988; Fettig et al., 2007; Bentz et al., 2010). The tree- and stand-level factors such as tree vigor and size and stand density are critical in the endemic level of infestation at which infestation occurs locally (Raffa and Berryman, 1983; Simard et al., 2012). However, landscape-level factors facilitate the transition of infestation from a local eruption toward regional outbreaks (Wallin and Raffa, 2004; Raffa et al., 2008; Simard et al., 2012). Some of the influential landscape-level variables on beetle outbreaks were found to be favorable climatic conditions, adjacency to the incipient populations, surface terrain, an abundance of mature host trees, and former disturbances, such as fire and outbreaks (Aukema et al., 2006). The spread of outbreaks was also found to be autocorrelated within the spatial- and temporal-scales despite the host tree vigor (Aukema et al., 2006, 2008; Simard et al., 2012).

Recent bark beetle outbreaks in spruce-dominated forests have significantly outperformed previously known frequencies and consequences, despite their crucial role in forest regeneration and succession (Bače et al., 2015; Zeppenfeld et al., 2015; Zabihi et al., 2021a). The number of *I. typographus* generations per year may increase due to climate change (i.e., increased temperature) which could also drive further outbreaks than previously documented (Hlásny et al., 2011; Marini et al., 2013). For example, at least two generations and sister broods were found to occur in central European forests due to favorable summer temperatures (Netherer et al., 2019). The most devastating *I. typographus* outbreak in Central Europe to date was found to be in the Czechia from 2014 to 2015, which was initialized and led mainly by climatic factors (Hlásny et al., 2021). Due to the shift of climatic conditions in Europe, with more extreme weather anomalies, such as severe droughts, storms, floods (Lindner et al., 2010), and intense heat, mortality for most tree species in forests, including spruce, is expected to rise (Hlásny et al., 2022).

Precise up-to-date spatial information on the presence and dynamics of infestations is essential to make an efficient plan for the removal and sanitation of infested trees, aiming to keep the remaining forest intact. Gathering such data in large areas with limited access is still challenging (Stereńczak et al., 2019). The spatio-temporal dynamics of the bark beetle population have been investigated in Europe, (e.g., Kärvemo et al., 2014; Havašová et al., 2017; Mezei et al., 2017), and in North America, (e.g., Meddens and Hicke, 2014; Senf et al., 2015). However, the success in detecting and mapping tree mortality related to bark beetle infestations highly depends on the forest composition and structure (Koontz et al., 2021). For example, the detection and monitoring of infested forest stands composed only of coniferous host species are rather straightforward. In such stands or forests, newly infested trees appear mostly in large and easily definable groups as bark beetles continue to attack mostly nearby infested trees (Lausch et al., 2011). One of the most effective ways to track vegetation stress is using remote sensing (RS) data (Lawley et al., 2016). Multispectral aerial and satellite imagery has been successfully used for mapping insect outbreaks and other forest disturbances (Väisänen and Heliövaara, 1994; White et al., 2007; Long and Lawrence, 2016). To characterize tree health status, the integrated approach of using RS data from different sources, such as imagery acquired by active (e.g., synthetic aperture radar; SAR) and passive sensors (e.g., multi- and hyper-spectral imagery) could be applied (Niemann et al., 2015). For example, Ortiz et al. (2013), Abdullah et al. (2019a), and Ali et al. (2021) used satellite imagery, and Ortiz et al. (2013) used X-band SAR, to detect early infestations.

The availability of RS data at various spectral, temporal, and spatial resolutions plays an important role in detecting forest infestation phenomena (Zabihi et al., 2021b). For example, coarse-resolution Landsat imagery (Meddens et al., 2013), medium-resolution SPOT-5 and Sentinel-2 imagery (Abdullah et al., 2019a), and fine-resolution aerial photography (Minařík and Langhammer, 2016; Brovkina et al., 2018; Klouček et al., 2019; Abdollahnejad and Panagiotidis, 2020) have been used to map infested trees. PlanetScope imagery with a spatial resolution of 3.7 meters (Planet Labs, Inc, 2022), allows better tracking of small changes in the land cover within a relatively broad area. The daily image acquisition of the PlanetScope (at the nadir) allows prompt monitoring of forests susceptible to beetle attacks. All these specifications of the PlanetScope help to avoid or minimize labor-intensive visual surveys and/or costly UAVs- or aircrafts-use to detect susceptible- or already attacked trees. The PlanetScope satellite

39

FIGURE 1
The study area, located in The School Forest Enterprise in Kostelec nad Černými lesy, in the Czechia. The forest management layer, cropped by the border of the study area, is marked in purple on the RGB true-color composite of planet imagery (9 April 2020).
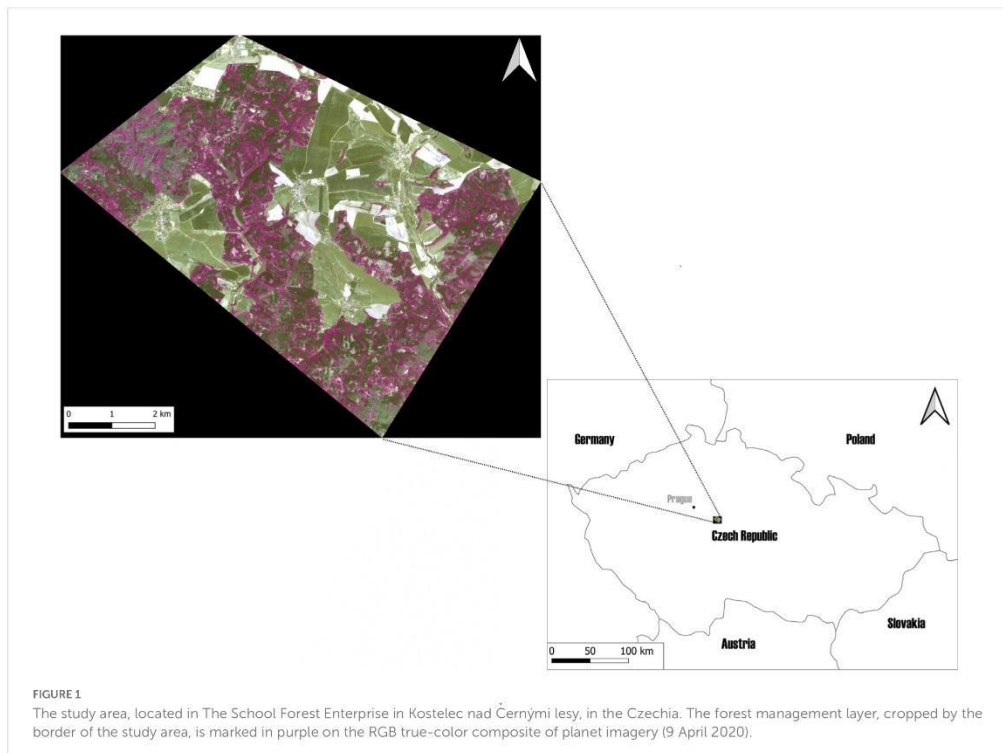
initially launched in 2014, and its second generation that we used, known as Dove-R or PS2.SD, provides imagery at four spectral bands, including Blue, Green, Red, and near-infrared (NIR) wavelengths (Planet Labs, Inc, 2022).

Most individual bandwidths [e.g., visible, red-edge, NIR, and shortwave-infrared (SWIR)] and several SVIs that were developed, were found to be useful for detecting changes in needle pigments, including chlorophyll content, degree of greenness, and water content due to bark beetle attacks (Zabihi et al., 2021b). In general, beetle-induced water-stressed trees reflect a higher amount of visible light than healthy trees (Ortiz et al., 2013). The severe stress in infested trees causes chlorophyll loss that consequently reduces the absorption rate of visible light by photosynthetically active pigments (Blackburn, 1998, 2006; Carter and Knapp, 2001; Mullen, 2016; Mullen et al., 2018). Similarly, water-stressed trees reflect more red-edge light than healthy trees due to a decrease in chlorophyll *a* contents (Ortiz et al., 2013), and changes in the structure of spongy mesophyll (Mullen et al., 2018). The changes in the structure of spongy mesophyll, so-called foliage desiccation, also reduce the absorption rate of NIR wavelengths in water-stressed infested trees (Ortiz et al., 2013; Mullen et al., 2018), and a similar pattern was observed for SWIR wavelengths (Immitzer et al., 2016).

Some of the top-ranked indices used to represent changes in needle pigments and greenness were found to be Red-Edge NDVI (RENDVI or NDVI705; Ortiz et al., 2013), and Normalized

Difference Red-Edge (NDRE 2 and 3; Abdullah et al., 2019a,b). Disease-Water Stress Index (DWSI), Normalized Difference Water Index (NDWI), Leaf Water Content Index (LWCI), Ratio Drought Index (RDI), and Moisture Stress Index (MSI) were found to be top-ranked indices, used in former research (Abdullah et al., 2019a,b; Yang, 2019) to detect changes in leaf water contents due to bark beetle attacks (Zabihi et al., 2021b). A normalized distance red and shortwave infrared (NDRS; Huo et al., 2021), developed based on red and SWIR wavelengths, was found to be a useful index to estimate forest susceptibility to bark beetle attacks in April, or to detect infested trees during the attacks from May to October. However, changes in forest parameters affect the reflectance of longer wavelengths such as SWIR, greater than shorter wavelengths such as visible lights in healthy coniferous forests (Rautiainen et al., 2018). Those forest parameters include forest structure, needle age and intracellular structure of air-to-cell wall interfaces, moisture content of forest floors, and tree physiological changes over the growing seasons (Rautiainen et al., 2018; Zabihi et al., 2021b). Thus, SWIR-dependent indices may propagate uncertainty to some extent in the model developments and validations (Zabihi et al., 2021b). In a recent review by Zabihi et al. (2021b), using visible bands such as RGB and red-edge (a bandwidth close to NIR) were recommended to develop SVIs in order to map the early stage of bark beetle infestations. We based our study on the assumption that some trees may be more susceptible to *I. typographus* attacks, than others, in uninfested

40

TABLE 1 Day number in 2020 with the associated dates of planet images used; imagery after July 14 were removed at the later stage of analyses because of having clearcuts due to bark beetle attacks.

#	Day number in 2020	Date
1	93	2 April 2020
2	100	9 April, 2020
3	108	17 April 2020
4	114	23 April 2020
5	129	8 May 2020
6	139	18 May 2020
7	153	1 June 2020
8	180	28 June 2020
9	183	1 July 2020
10	194	12 July 2020
11	196	14 July 2020
12	204	22 July 2020
13	214	1 August 2020
14	218	5 August 2020
15	226	13 August 2020
16	229	16 August 2020
17	246	2 September 2020
18	249	5 September 2020
19	257	13 September 2020
20	259	15 September 2020
21	266	22 September 2020

forests. And, those trees can be detected/predicted using SVIs derived from high spatial and multispectral resolution imagery acquired by PlanetScope satellite. We also assumed non-attacked trees, within the vicinity of attacked trees, as healthy trees over a growing season.

We proposed to investigate if trees susceptible to beetle attacks can be detected before or early in the growing season. If so, what spectral bands and/or SVIs, developed using individual wavelengths, could be used to indicate significant differences between healthy trees and those susceptible to attacks. We eventually aim to develop a methodology for using remotely-sensed and ground-truth data to characterize the health status of Norway spruce on a temporal scale before and during the course of infestations.

2. Materials and methods

2.1. Study area

The study was conducted in forests, approximately 50 km southeast of Prague (Czechia or the Czech Republic) (Figure 1), owned and managed by the Czech University of Life Sciences (CULS). The CULS forests cover a total area of ∼ 5,700 ha, lie in the temperate climate zone. The mean annual temperature and sum of precipitation ranged 7–7.5°C and 600–650 mm, respectively,

with a vegetation period lasts 150–160 days (Tolasz et al., 2007). In recent years, periodic droughts negatively affected the vitality of forests (Remeš, 2017). The forest stands consist of 70% conifers, mainly spruce (50%) followed by pine (16%), and the rest for other species. In terms of broadleaved trees (the remaining 30% cover), beech covers the most, 14%, followed by oak at 10%, and the rest for other species. If the area was not managed by the CULS, beech and oak may have been dominated, followed by pine and spruce trees, similar to nearby unmanaged forest composition. The CULS forests are managed using a clearcutting silvicultural system in a combination with the shelterwood system (Remeš, 2017). Due to the extreme drought in 2018, the whole area was affected by the bark beetle outbreak, mainly by *I. typographus*; however, other species such as *I. duplicatus, I. amitinus,* and *Pityogenes chalcographus* may have been infesting some local spots (Hlásny et al., 2021). The forest management strategy has been recently focusing on sanitary logging to promptly remove infested trees, as soon as observed.

2.2. Satellite data acquisition and processing

We used 22 PlanetScope imagery [instrument–Dove Classic (PS2)] from April 2 to 5 September 2020 (Table 1). Only cloud-free images were used for further analysis; the image acquired on Day 145 was excluded due to having cloud cover. All imageries were downloaded in the GeoTIFF format and surface reflectance data type (harmonized to Sentinel-2 for consistent radiometry) was selected as the initial product option. Every image had four bands including Red, Green, Blue (RGB), and Near Infrared (NIR) with a spatial resolution of 3 m.

For each acquisition in the time series (Table 1), we calculated 23 SVIs (Table 2) using the Raster Calculator plugin in QGIS version 3.16.16 (QGIS Development Team, 2009).

The individual four bands and the SVIs computed from Table 2 were used to differentiate two defined classes. These two classes were non-attacked trees during our year of study, assumed and considered as the "Healthy" class, and trees were attacked in the later stages of the growing season, assumed and considered as the "Susceptible" class.

All individual bands and SVIs (Table 2) developed using individual bands, were merged into a single GeoTIFF file to make a cube image of 27-bands, for further statistical analysis.

2.3. GIS data collection and validation

The spatial position (X- and Y-coordinates) of attacked trees, named as susceptible trees, were recorded by foresters and researchers using the ArcGIS Collector application developed and installed on smartphones. The date of the attack, the name of the bark beetle species, and the number of attacked trees per day were also recorded using the ArcGIS Collector app. Foresters have been detecting early infestations on a weekly basis in their designated areas. Researchers from the EXTEMIT-K project were also recording the same datasets around six experimental plots designed and established by the EXTEMIT-K project. Researchers

41

TABLE 2 Spectral vegetation indices (SVIs), their acronyms, equations, and publishers, used to detect trees susceptible to bark beetle attack.

Spectral vegetation index	Acronym	Equation	References
Difference Vegetation Index	DVI	$NIR - R$	Tucker, 1979
Enhanced Vegetation Index	EVI	$2.5 * \frac{(NIR - R)}{(NIR + 6 * R - 7.5 * B + 1)}$	Huete et al., 2002
Green Chlorophyll Index	GCI	$\left(\frac{NIR}{G}\right) - 1$	Gitelson et al., 2003
Green Difference Vegetation Index	GDVI	$NIR - G$	Sripada, 2005
Global Environmental Monitoring Index	GEMI	$eta * (1 - 0.25 * eta) - \frac{R - 0.125}{1 - R}$ $eta = \frac{2(NIR^2 - R^2) + 1.5 * NIR + 0.5 * R}{NIR + R + 0.5}$	Pinty and Verstraete, 1992
Green Normalized Difference Vegetation Index	GNDVI	$\frac{NIR - G}{NIR + G}$	Gitelson et al., 1996
Green Optimized Soil Adjusted Vegetation Index	GOSAVI	$\frac{NIR - G}{NIR + G + 0.16}$	Sripada, 2005
Green Ratio Vegetation Index	GRVI	$\frac{NIR}{G}$	Sripada et al., 2006
Green Soil Adjusted Vegetation Index	GSAVI	$1.5 * \frac{(NIR - G)}{(NIR + G + 0.5)}$	Sripada, 2005
Infrared Percentage Vegetation Index	IPVI	$\frac{NIR}{NIR + R}$	Crippen, 1990
Modified Soil Adjusted Vegetation Index	MSAVI2	$\frac{2 * NIR + 1 - \sqrt{(2 * NIR + 1)^2 - 8(NIR - R)}}{2}$	Qi et al., 1994
Modified Simple Ratio	MSR	$\frac{\left(\frac{NIR}{R}\right) - 1}{\left(\sqrt{\frac{NIR}{R}}\right) + 1}$	Chen, 1996
Normalized Difference Vegetation Index	NDVI	$\frac{NIR - R}{NIR + R}$	Rouse et al., 1973
Normalized Difference Water Index	NDWI	$\frac{G - NIR}{G + NIR}$	Gao, 1995
Non-Linear Index	NLI	$\frac{NIR^2 - R}{NIR^2 + R}$	Goel and Qin, 1994
Optimized Soil Adjusted Vegetation Index	OSAVI	$\frac{NIR - R}{NIR + R + 0.16}$	Rondeaux et al., 1996
Perpendicular Vegetation Index	PVI	$\frac{NIR - a*R - b}{\sqrt{(1 + a^2)}}$ a—slope of the soil line, b—gradient of the soil line	Richardson and Wiegand, 1977
Renormalized Difference Vegetation Index	RDVI	$\frac{NIR - R}{\sqrt{NIR + R}}$	Roujean and Breon, 1995
Soil Adjusted Vegetation Index	SAVI	$\frac{1.5*(NIR - R)}{(NIR + R + 0.5)}$	Huete, 1988
Simple Ratio	SR	$\frac{NIR}{R}$	Birth and McVey, 1968
Transformed Soil Adjusted Vegetation Index	TSAVI	$\frac{(s * (NIR - s * R - a))}{(a * NIR + R - a * s + X * (1 + s^2))}$ s—a slope of the soil line, a— the soil line intercept, X - the adjustment factor that is set to minimize soil noise.	Baret and Guyot, 1991
Visible Atmospherically Resistant Index	VARI	$\frac{G - R}{G + R - B}$	Gitelson et al., 2002
Wide Dynamic Range Vegetation Index	WDRVI	$\frac{(a * NIR - R)}{(a * NIR + R)}$ a - the weighting coefficient	Gitelson, 2004

TABLE 3 List of sampling (training) and ancillary data used, with their types, stage and method of collection, application or software used to drive data from, required for further steps in the statistical analyses and classifications.

Data	Type	Stage of collection	Collection method	Application/ software used	Additional data used	Data derived from	Number of plots	Final purposes
Infested trees	Vector and categorical	Mid-growing season and later on	Field survey/ sampling	ArcGIS collector app	UAV imagery, used as base imagery in collector app	Creating polygons of susceptible class	61	Training data for the "Susceptible" class
Non-attacked trees	Vector and categorical	N/A	Random sampling points	QGIS	PlanetScope Imagery	Creating polygons of Healthy class	61	Training data for the "Healthy" class
Forest management units	Vector and categorical	N/A	Provided by the Forestry Department	QGIS	N/A	Average area, age, and percent category of Norway Spruce	2,541	Area for the "Healthy" class, with similar characteristics found for the "Susceptible" class

used both visual observations and detection by a sniffer dog to detect early-attacked trees within the 500-m zone around the experimental plots (Vošvrdová et al., 2023).

The EXTEMIT-K project was proposed to conduct research experiments aiming to provide potential science-based approaches to deal with current and future challenges of protecting forest ecosystems in the Czechia. The bark beetle infestations and drought effects on spruce trees and beetle activities were found to be the core challenges, and have been investigated by the research team.

FIGURE 2
Sample size scatterplot of the time-series dataset of the "Susceptible" class. Five images with a sample size of 2, records after day no. 196 corresponding to July 14, were excluded from the analyses (highlighted in the rectangle).

FIGURE 3
The frequency of bark beetle infestations observed throughout the 2020 growing season (May to October).
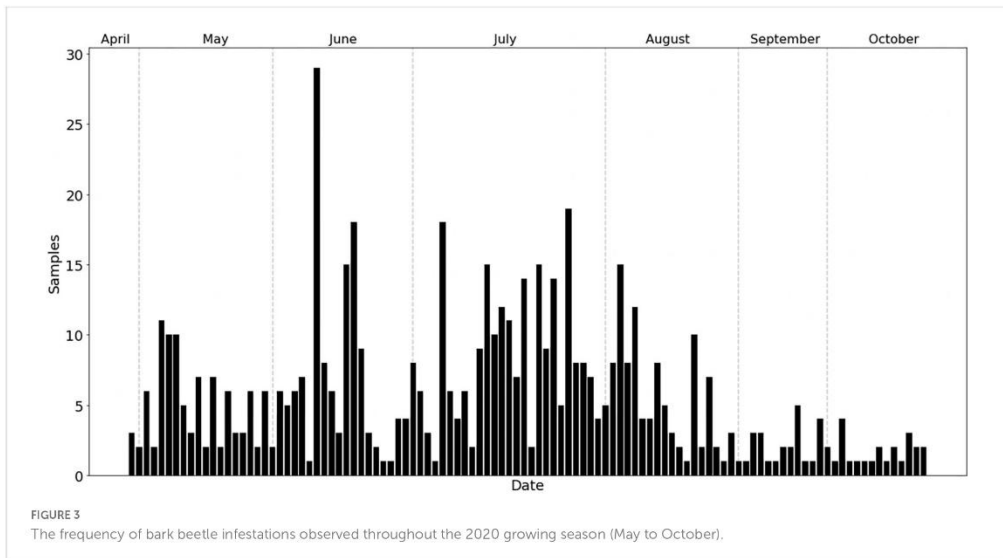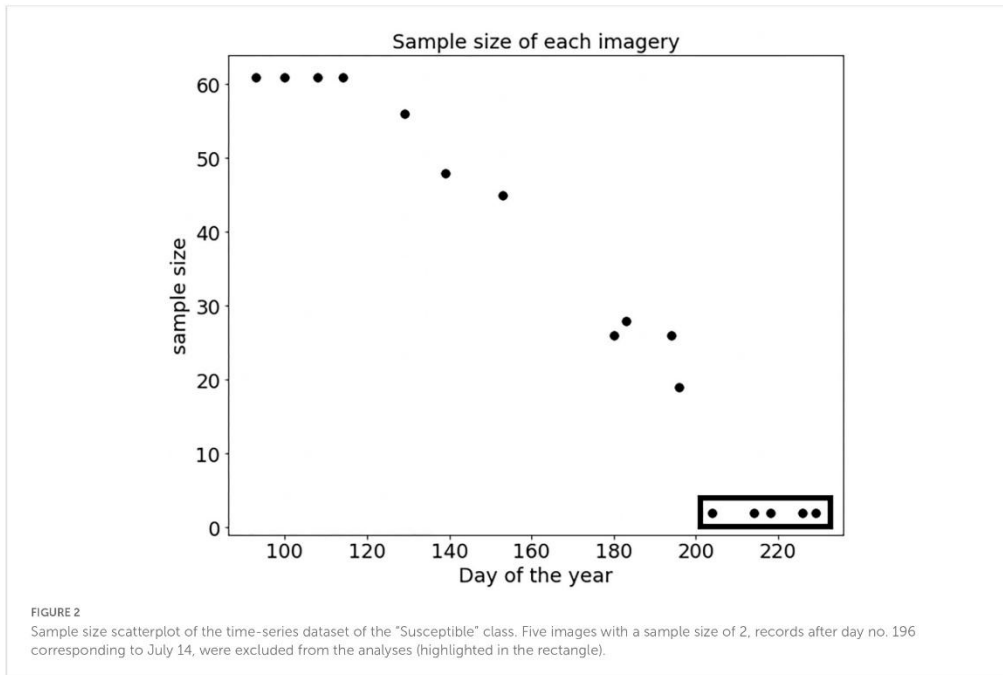
Every experimental plot consisted of four subplots, with 8–10 neighbor trees selected within (Özçelik et al., 2022; Stříbrská et al., 2022). All the field survey data were stored and visualized in the Online Web version of ArcGIS. This allowed us to export field survey data for further analyses in QGIS at the end of the season.

The spatial positions of total sample points of 61 areas with attacked trees, at the later stages of the growing season, were used to create polygons/boundaries of these trees, which were assumed as susceptible to attacks before and during the first half of the growing season.

FIGURE 4
Behavior of the single bands (mean and standard error) before and during the first half of the growing season for healthy trees and trees predicted to be attacked by bark beetles. Solid vertical lines on the trend lines represent the standard error of the mean and dashed vertical lines represent the monthly division.
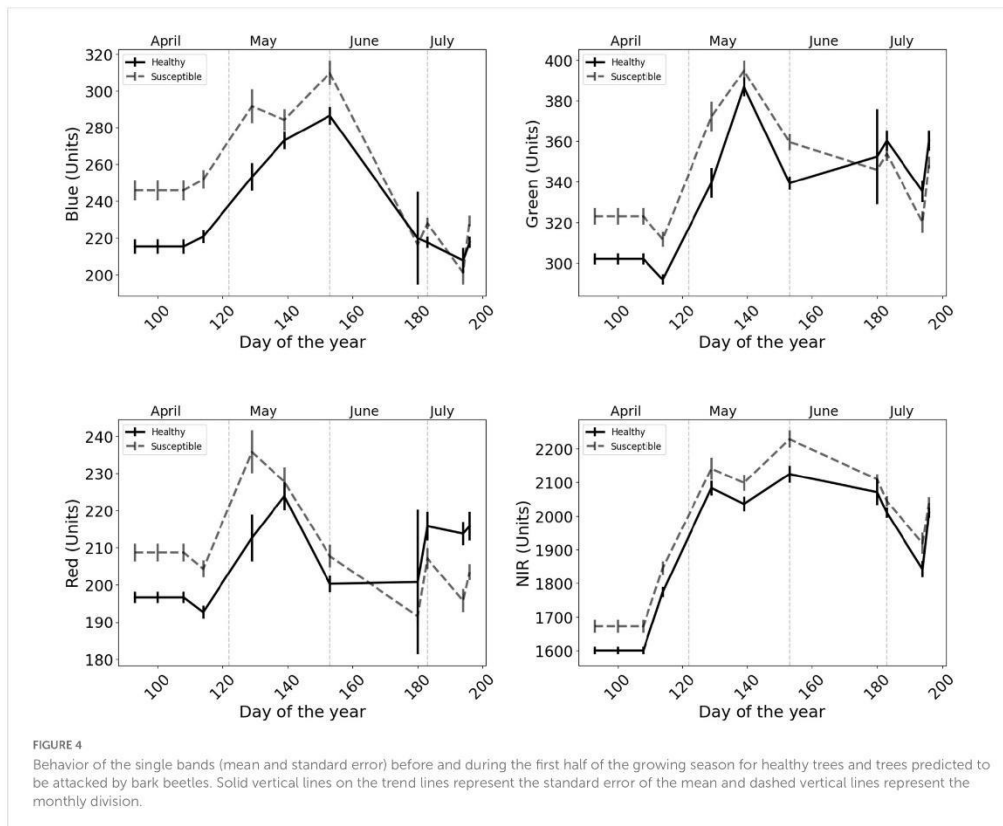
On the last PlanetScope imagery in the dataset (September 22), the K-means clustering algorithm was performed to detect unbiased, square-like (pixelated) borders of 61 objects, based on the clear-cut year in 2020 detection cluster (which has different spectral features, comparing to forest stand) and points locations of areas with attacked trees using the open-source Orfeo ToolBox (OTB) package (version 7.2.0; Grizonnet et al., 2017). Sizes and shapes of the 61 areas, identified as clear-cuts on the last imagery in the dataset were used for further analysis on the other imageries. We overlaid each PlanetScope image with very high spatial resolutions (20-cm) UAV orthophotos to ensure the accurate spatial positioning of target objects. The vectorization of 61 boundaries was visually validated to avoid any error in tree positions, collected by the ArcGIS collector app, in addition to potential misclassified areas among trees such as bare soil, using the Poligonize (GDAL) plugin.

We generated a random sampling for the class "Healthy" with similar characteristics found for the class "Susceptible" (Table 3). For example, similarity in the age ranges, percentage of Norway spruce (based on forest management data), sample size, and average area (Table 3). Sixty-one circle-shaped samples with an area of 0.165 ha each in forest management units at the age ranging from 78 to 130 years were randomly selected within the forest management units with 80–100% Norway spruce cover. Based on forest inventory data, spruce cover in the forest management units is more than 80%, therefore we assume that the sample polygons and related spectral signal represent spruce stands.

2.4. Data cleaning

The sample size of the "Healthy" class (61 trees) was the same for every image, with no need for any data cleaning. For the "Susceptible" class, we initially removed samples with traces of later on logging found on any date of imagery, and thus, we only kept those samples not reaching the start date of the green-attack phase during our temporal-scale analyses. The criteria of having a balanced sample size between two classes of "Healthy" and "Susceptible" trees caused us to exclude the last five dates of imagery from the time-series datasets (all imagery after July 14; Figure 2). However, we kept imagery from days no. 180 to 196, to complete our proposed temporal-scale analyses, even though the sample size for the "Susceptible" class decreased more than twice that of the earlier dates. The data cleaning and plotting were performed in

44
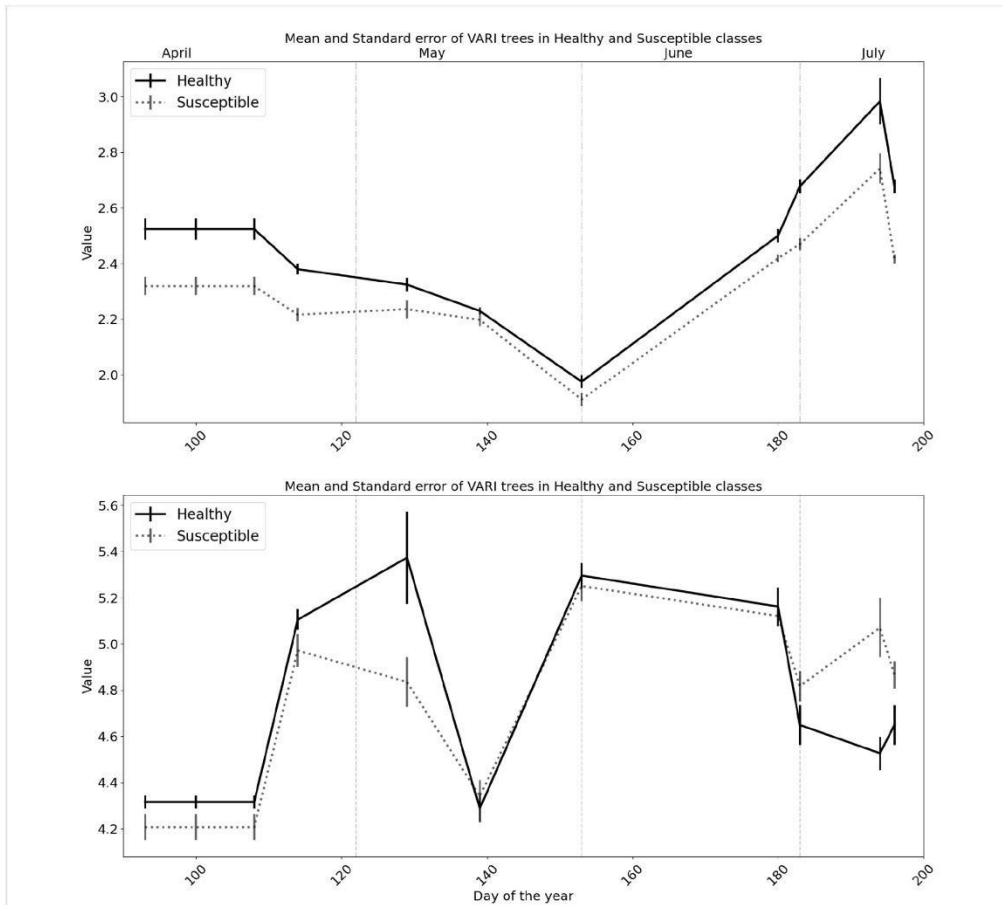
FIGURE 5
The behavior of the spectral vegetation indices of the Enhanced Vegetation Index (EVI) and Visible Atmospherically Resistant Index (VARI) before and during the first half of the growing season for healthy trees, and trees predicted to be attacked by bark beetles. Solid vertical lines on the trend lines represent the standard error of the mean and dashed vertical lines represent the monthly division.

FIGURE 6
Welch's *t*-test *p*-values between two classes of healthy and susceptible trees to attacks, on different days before and during the first half of the growing season, using individual bands.

45

FIGURE 7
The overall classification accuracy (CA), using leave-one-out cross-validation on the LDA test for individual bands, to differentiate two classes of healthy and susceptible trees to attacks, on different days before and during the first half of the growing season.
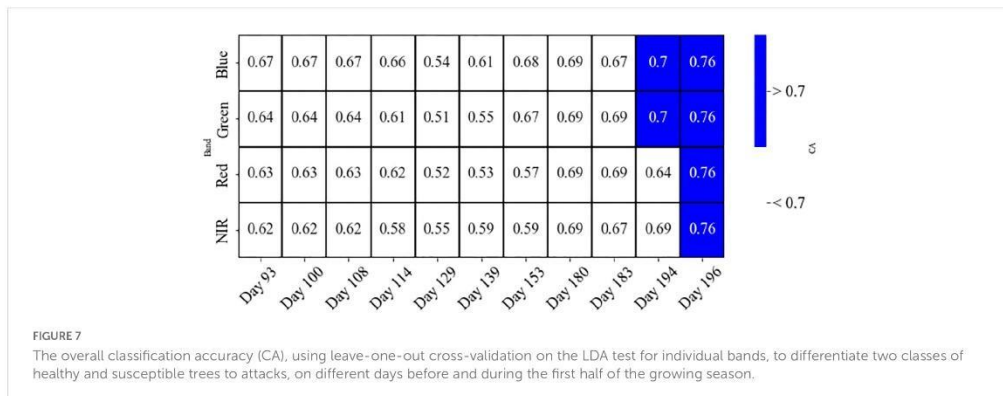
VSCode 1.73.1 in Jupiter Notebook using, Python programming language (ver. 3.8.5; Van Rossum and Drake, 2010), and pandas 1.5.0 and Matplotlib 3.6.0, respectively.

2.5. Statistical analyses

We extracted the mean value for 4 bands of spectral reflectance and the proposed 23 SVIs (Table 2) for every polygon of the "Healthy" and "Susceptible" class, using the Zonal Statistics-plugin from the OTB package in QGIS.

The Welch's t-test was used to determine if the means of spectral reflectance of individual bands and developed SVIs for the "Healthy" and "Susceptible" classes were statistically different for each date of imagery, using the SciPy library (ver. 1.7.1; Virtanen et al., 2020).

Linear discriminant analysis (LDA) was used to evaluate the separability of individual bands and/or SVIs to differentiate two classes, using the scikit-learn library (ver. 1.1.2; Pedregosa et al., 2011). The LDA is a supervised classification that uses a linear classifiers algorithm based on the distribution of features (Hastie et al., 2009).

The LDA maximizes the distance among classes and minimizes the variance within classes, and was performed on every band of the 27-bands-cube imagery. The leave-one-out cross-validation accuracy (LOOCV) was performed to examine the overall classification accuracy (CA) of the performed LDA on either individual bands or SVIs of two designated classes.

3. Results

Based on the frequency plot of daily attacks, using the datasets from the ArcGIS Collector app., the emergence and initial attacks of bark beetles on trees were found to be from April 27 to 4 May 2020 (Figure 3). There seemed to be two peaks of beetle swarming and infestations during the growing seasons; the first peak occurred around mid-June and the second peak seemed to be around mid-July to early-August (Figure 3).

The class of trees susceptible to attacks generally revealed a higher mean value, for individual bands, than the class of healthy trees, before and during the first half of the growing season (early April to late July; Figure 4 and Supplementary Table 1).

For the top-ranked SVIs, EVI and VARI, the observed patterns between the two classes were opposite to that observed in individual bands; the "Healthy" class generally revealed higher values than the "Susceptible" class (Figure 5 and Supplementary Table 1).

The differentiation between the mean value for the polygons of the two classes followed a more steady pattern for the EVI, similar to the NIR, whereas the values sometimes overlapped for the VARI, mostly after May 18 (Figure 5 and Supplementary Table 1).

3.1. Individual bands

Individual bands showed statistically significant differences between the two classes of healthy and susceptible trees, mostly for Days 93 to 114 ($p < 0.05$ for the Welch's t-test; Figure 6).

Results for the linear discriminant analysis, LDA, showed high accuracy for individual bands on only days 194 and 196 (CA 64–76%; Figure 7). However, we may not be able to validate these results as the sample size of the susceptible class for these days dropped more than twice that for earlier dates. Therefore, "Healthy" and "Susceptible" classes may not be sufficiently distinguished using only individual bands (Figure 7) as the CA values from the LDA test did not reach the 70% threshold for any bands.

3.2. Spectral vegetation indices (SVIs)

Spectral vegetation indices, such as DVI, EVI, MSAVI, NDVI, PVI, SAVI, TSAVI, VARI, and WDRVI, showed statistically significant differences between two classes of healthy and susceptible trees, mostly for Days 93 to 129, at a different rate of type I error for the Welch's t-test (Figure 8). However, the EVI and VARI were the only two indices showed significant differences between classes at other dates during the first half of the growing season (Figure 8).

Results for the linear discriminant analysis, LDA, were showing high accuracy for the most of SVIs on days 194 and 196 (CA

46

	Day 93	Day 100	Day 108	Day 114	Day 129	Day 139	Day 153	Day 180	Day 183	Day 194	Day 196
DVI	0.009	0.009	0.009	0.015	0.376	0.087	0.016	0.146	0.123	0.096	0.232
EVI	0	0	0	0	0.04	0.255	0.089	0.012	0	0.048	0
GCI	0.088	0.088	0.088	0.117	0.022	0.595	0.637	0.707	0.207	0.016	0.131
GDVI	0.018	0.018	0.018	0.031	0.506	0.099	0.024	0.138	0.141	0.094	0.246
GEMI	0.021	0.021	0.021	0.051	0.41	0.107	0.074	0.324	0.417	0.106	0.625
GNDVI	0.084	0.084	0.084	0.094	0.018	0.694	0.537	0.768	0.139	0.035	0.082
GOSAVI	0.084	0.084	0.084	0.094	0.018	0.694	0.537	0.768	0.139	0.035	0.082
GRVI	0.088	0.088	0.088	0.117	0.022	0.595	0.637	0.707	0.207	0.016	0.131
GSAVI	0.084	0.084	0.084	0.094	0.018	0.694	0.538	0.767	0.139	0.035	0.082
IPVI	0.246	0.246	0.246	0.173	0.035	0.689	0.621	0.667	0.054	0.007	0.023
MSAVI	0.001	0.001	0.001	0.001	0.006	0.717	0.443	0.817	0.255	0.259	0.207
MSR	0.3	0.3	0.3	0.238	0.039	0.623	0.566	0.813	0.088	0.003	0.042
NDVI	0.001	0.001	0.001	0	0.006	0.726	0.465	0.535	0.257	0.238	0.21
NDWI	0.084	0.084	0.084	0.094	0.018	0.694	0.537	0.768	0.139	0.035	0.082
NLI	0.806	0.806	0.806	0.859	0.177	0.353	0.106	0.214	0.04	0.052	0.039
OSAVI	0.247	0.247	0.247	0.173	0.035	0.689	0.621	0.667	0.054	0.007	0.023
PVI	0.007	0.007	0.007	0.013	0.245	0.087	0.018	0.321	0.25	0.151	0.445
RDVI	0.064	0.064	0.064	0.079	0.936	0.126	0.031	0.064	0.066	0.05	0.11
SAVI	0.001	0.001	0.001	0	0.006	0.726	0.465	0.535	0.258	0.237	0.21
SR	0.328	0.328	0.328	0.277	0.053	0.597	0.545	0.645	0.108	0.003	0.054
TSAVI	0	0	0	0	0.007	0.738	0.488	0.379	0.261	0.219	0.213
VARI	0	0	0	0	0.034	0.307	0.508	0.002	0	0.402	0
WDRVI	0.001	0.001	0.001	0.003	0.088	0.07	0.015	0.646	0.224	0.154	0.396

Legend:
- p > 0.05
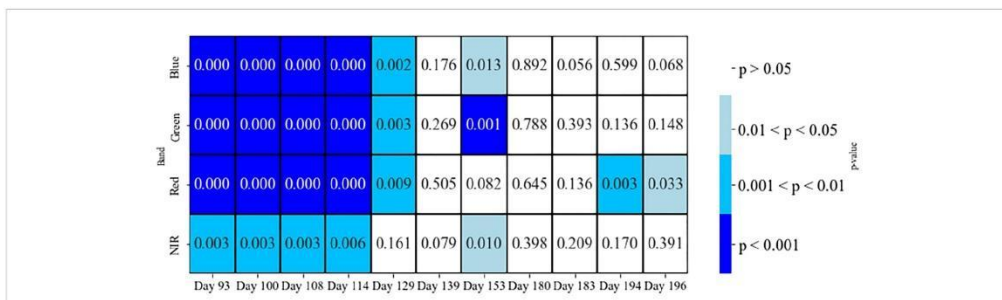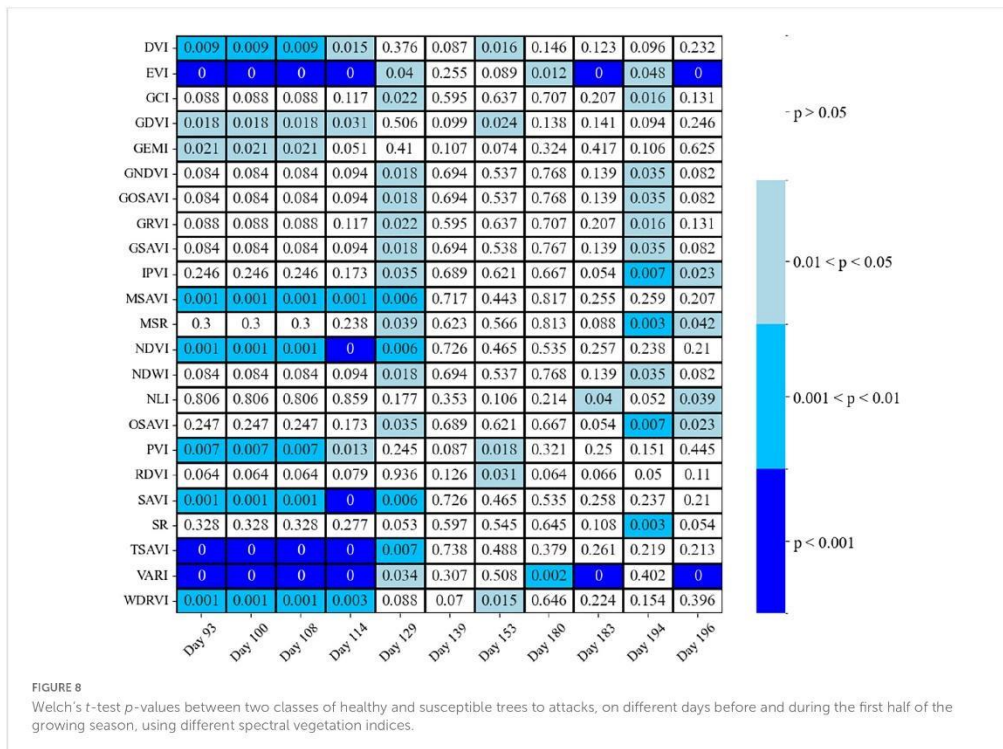- 0.01 < p < 0.05
- 0.001 < p < 0.01
- p < 0.001

FIGURE 8
Welch's t-test p-values between two classes of healthy and susceptible trees to attacks, on different days before and during the first half of the growing season, using different spectral vegetation indices.

68–83%; **Figure 9**). However, we may not be able to validate these results as the sample size of the susceptible class for these days decreased more than twice that for earlier dates, similar to individual bands. Beyond these dates, the accuracy of the LDA test passed or almost reached the 70% threshold only for the VARI and EVI, respectively, at days 93 to 114 (**Figure 9**).

3.2.1. Evaluations of SVIs using combined Welch's t-test and LDA

The two classes were found to be differentiated at most using two SVIs based on combined evaluations of using Welch's t-test and LDA; the EVI on Days 114 and 183, and the VARI on Days 93, 100, 108, 114, and 183 resulted in the LDA accuracy greater than 0.7 and p-value for the Weltch's t-test less than 0.05 (**Figures 8, 9**).

4. Discussion

4.1. Wavelengths and spectral vegetation indices suitable for prediction of bark beetle attack

Our results show that all four wavebands of PlantScope, including Red, Green, Blue, and NIR, have the potential to detect susceptible trees and thus predict the occurrences of bark beetle

attacks (Welch's t-test; **Figure 6**). Nevertheless, the CA for none of them passed the defined 70% threshold. Considering the overall temporal patterns from early April to late July, the differentiation between the two classes of healthy and susceptible trees followed a more steady pattern for NIR than other visible bands (**Figure 4**). This may indicate that the NIR could be a more reliable spectral reflectance than other visible lights to detect susceptible trees, before and during the first half of a growing season (**Figure 4**).

Among all spectral vegetation indices we investigated, EVI and VARI were found to be the best indices to detect trees susceptible to attacks (**Figures 8, 9**; the lowest Welch's t-test p-value and the highest CA), similar to Huo et al. (2021). The VARI Index on Day 183 was significantly different between healthy and susceptible trees (significant Welch's t-test and LDA with the CA higher than 70%) so the values for the susceptible trees were much higher than the healthy/control trees. However, the EVI shows the best performance during the entire season. In contrast to the VARI, susceptible trees were always showing lower values for the EVI than healthy trees. The observed patterns may indicate that the EVI could be the best index for the prediction of bark beetle attack occurrences within a forest, which could also be used for general applications in forest pest management to detect water-stressed trees. For example, Kim (2013) found EVI sensitive to drought and rising temperatures in the ecosystems of northern Arizona, USA. In addition, Scots pine (*Pinus sylvestris L.*), a sensitive species to drought effects (Seidel et al., 2016), showed early signs of vitality

Index	Day 93	Day 100	Day 108	Day 114	Day 129	Day 139	Day 153	Day 180	Day 183	Day 194	Day 196
DVI	0.61	0.61	0.61	0.56	0.52	0.58	0.58	0.69	0.67	0.7	0.75
EVI	0.67	0.67	0.67	0.74	0.54	0.58	0.57	0.69	0.79	0.7	0.8
GCI	0.55	0.55	0.55	0.52	0.55	0.54	0.57	0.69	0.67	0.77	0.76
GDVI	0.61	0.61	0.61	0.55	0.47	0.57	0.58	0.68	0.67	0.71	0.75
GEMI	0.61	0.61	0.61	0.53	0.5	0.58	0.55	0.69	0.67	0.71	0.76
GNDVI	0.57	0.57	0.57	0.56	0.53	0.56	0.57	0.69	0.69	0.75	0.76
GOSAVI	0.57	0.57	0.57	0.56	0.53	0.56	0.57	0.69	0.69	0.75	0.76
GRVI	0.55	0.55	0.55	0.52	0.55	0.54	0.57	0.69	0.67	0.77	0.76
GSAVI	0.57	0.57	0.57	0.56	0.53	0.56	0.57	0.69	0.69	0.75	0.76
IPVI	0.53	0.53	0.53	0.52	0.54	0.56	0.57	0.69	0.69	0.71	0.76
MSAVI	0.66	0.66	0.66	0.67	0.48	0.55	0.56	0.69	0.69	0.7	0.76
MSR	0.55	0.55	0.55	0.53	0.53	0.55	0.56	0.69	0.67	0.75	0.76
NDVI	0.66	0.66	0.66	0.66	0.48	0.55	0.57	0.69	0.69	0.7	0.76
NDWI	0.57	0.57	0.57	0.56	0.53	0.56	0.57	0.69	0.69	0.75	0.76
NLI	0.31	0.31	0.31	0	0.48	0.51	0.53	0.7	0.66	0.71	0.76
OSAVI	0.53	0.53	0.53	0.52	0.54	0.56	0.57	0.69	0.69	0.71	0.76
PVI	0.61	0.61	0.61	0.56	0.56	0.59	0.57	0.69	0.67	0.69	0.76
RDVI	0.55	0.55	0.55	0.53	0.51	0.56	0.57	0.67	0.64	0.7	0.75
SAVI	0.66	0.66	0.66	0.66	0.48	0.55	0.57	0.69	0.69	0.7	0.76
SR	0.54	0.54	0.54	0.53	0.49	0.54	0.56	0.69	0.67	0.74	0.76
TSAVI	0.66	0.66	0.66	0.66	0.48	0.55	0.57	0.69	0.69	0.7	0.76
VARI	0.7	0.7	0.7	0.74	0.56	0.59	0.6	0.69	0.78	0.72	0.83
WDRVI	0.62	0.62	0.62	0.58	0.56	0.59	0.57	0.69	0.67	0.69	0.75

Legend: > 0.7 / < 0.7 (CA)

FIGURE 9
The overall classification accuracy (CA), using leave-one-out cross-validation on the LDA test for SVIs, to differentiate two classes of healthy and susceptible trees to attacks, on different days before and during the first half of the growing season.

decline in Italy, which may be remotely detected using the EVI (Vacchiano et al., 2012).

4.2. Seasonal changes of spectral characteristics of susceptible trees to attacks

The overall patterns of the SVIs behavior before and during the first half of the growing season were found to be increasing, without any significant declines from early April to mid-season. However, the patterns slowed down by late July and early August. Most of the SVIs, even the most significant (for both classes), had declines as well.

Generally, the value of SVIs has been showing a seasonal trend (Karkauskaite et al., 2017; Yang et al., 2017). We found all the mean values of EVI of the predisposed trees were significantly

lower than for non-attacked trees (Figure 5), and thus, suggesting the EVI as a potential spectral vegetation index to predict bark beetle-infestation occurrences.

4.3. Limitations of the study

The spectral resolution of the available remote sensing products that we used was limited by the choice of the sensor with 4 bands due to the year of our observation, a period in 2020. For future research, it is preferable to use datasets with SWIR band in addition to NIR, visible, and red-edge spectral reflectances due to their effectiveness in tracking early stressed trees, though with different levels of detection uncertainty (Zabihi et al., 2021b). This could be achieved with the PlanetScope products of the 3rd generation sensors, known as SuperDove or PSB.SDafter, available from mid-March 2020. The 3rd generation sensors acquire imagery at eight bands, including Coastal Blue, Green I, Yellow, and Red Edge plus

the four bands we have already used (Planet Labs, Inc, 2022). The specified 8-bands allow computing more spectral vegetation indices than we were able to. In addition to the PlanetScope imagery, there are other satellites, e.g., Sentinel-2, which acquires imagery in the SWIR band even though its spatial resolution is coarser than the PlanetScope. Given this very important advantage, we recommend comparing products, e.g., SVIs, developed on imagery acquired from Sentinel-2 and the 3rd generation of PlanetScope, for future research investigations. Vegetation indices such as PVI, TSAVI and WDRVI have additional coefficients, which are not connected with band values. Those coefficients, such as slope, gradient, and intercept of the soil line and others, were set as recommended (default) values due to limitations in GIS data collection campaigns. More precise ground truth data with these additional parameter records could improve index performances.

Ground truth data with the locations of all bark beetle infestations were identified by foresters and researchers on a weekly frequency. Nevertheless, the cause of the infestation has not been determined. Each bark beetle infestation area potentially could be triggered by the internal and/or neighboring tree(s), attacked but not harvested in 2019.

The mechanism of bark beetle-induced Norway spruce mortality under drought conditions, such as changes in the physiological and biochemical processes of trees susceptible to attacks, is yet to be fully understood (Netherer et al., 2021). However, our findings of two spectral vegetation indices, EVI and VARI, may offer key indices to detect trees that are under water-stressed conditions, causing changes in the physiological and biochemical processes in trees. For example, Wei et al. (2023) found a positive correlation between spatial and temporal variations of tree-ring width (TRW) and the Enhanced Vegetation Index (EVI). The relationship between the TRW and EVI became stronger in more arid regions where trees were under more drought and subsequent water-stress conditions (Wei et al., 2023).

5. Conclusion

In the warming climate, drought and drought-induced bark beetle outbreaks may become more severe. Therefore, forest managers and policymakers need to provide monitoring of forest health status on a continuous, e.g., bidaily to weekly basis with subsequent sanitation measures, which otherwise may result in further bark beetle infestations with its ongoing rapid developments (Zabihi et al., 2021b). Our study was conducted to examine and thus offer the best indices, EVI and possibly VARI, to detect trees susceptible to attacks, likely due to water-stress conditions, before and/or during the first half of the growing season. Thus, a proactive management strategy can be practiced at this stage to better suppress or control the infestations.

We may still be able to distinguish the phase of attack from the spot initialization, at which very few trees are attacked, toward spot spreading, when the attacked area includes several adjacent trees (Colombari et al., 2013). In the phase of spot initialization, bark beetles attack stressed trees, while in the phase of spot spreading, the infestation spreads to neighbor trees regardless of their resistance to attack, considered as spatial and temporal autocorrelation of attacks (Aukema et al., 2006, 2008; Jakuš et al.,

2011; Simard et al., 2012). These spatial and temporal patterns of attack likely result in different spectral signatures observed during different phases of attacks in addition to different spectral signatures observed from non-attacked trees but highly susceptible. This complexity may impact the level of uncertainty in detecting susceptible trees, using a single SVI, during the period of beetle flight activities at which different phases of attacks may co-occur. Therefore, we recommend using an integrated approach of employing several SVIs, e.g., sensitive to healthy vs. susceptible trees, and different phases of attacks, simultaneously.

We finally recommend defining thresholds for these two vegetation indices, EVI and VARI, to provide a classified map for practical applications in forestry. The classified map would be used as a spatial tool to predict trees vulnerable to attacks and thus, to highlight hotspots regions with a high probability of infestation occurrences. Our proposed methodology offers an approach for future research to replicate using additional bands coming from new generations of PlantScope satellites. Further investigations of formulating and developing new SVIs, more sensitive to water-stressed- and thus susceptible-trees to attacks, are also recommended to improve the mapping accuracy.

The spectral difference based on SVI could be used to detect stress before attacks using the methods proposed in the present paper. Also, the new broadband SVI formula should be researched for more precise identification of predisposition to the bark beetle infestations.

Data availability statement

The raw data supporting the conclusions of this article will be made available by the authors, without undue reservation.

Author contributions

AT, GK, KZ, VVS, PS, and RJ contributed to the conception and design of the study. AT organized the database. AT and GK performed the statistical analysis. AT and RJ wrote the first draft of the manuscript. AT, GK, KZ, RM, VVS, and RJ wrote sections of the manuscript. All authors contributed to the manuscript revision, read, and approved the submitted version.

Funding

49

Conflict of interest

The authors declare that the research was conducted in the absence of any commercial or financial relationships that could be construed as a potential conflict of interest.

Publisher's note

All claims expressed in this article are solely those of the authors and do not necessarily represent those of their affiliated organizations, or those of the publisher, the editors and the reviewers. Any product that may be evaluated in this article, or claim that may be made by its manufacturer, is not guaranteed or endorsed by the publisher.

Supplementary material

The Supplementary Material for this article can be found online at: https://www.frontiersin.org/articles/10.3389/ffgc.2023.1130721/full#supplementary-material

References

Abdollahnejad, A., and Panagiotidis, D. (2020). Tree species classification and health status assessment for a mixed broadleaf-conifer forest with UAS multispectral imaging. *Remote Sens.* 12:3722. doi: 10.3390/rs12223722

Abdullah, H., Skidmore, A. K., Darvishzadeh, R., and Heurich, M. (2019a). Sentinel-2 accurately maps green-attack stage of European spruce bark beetle (*Ips typographus.* L.) compared with Landsat-8. *Remote Sens. Ecol. Conserv.* 5, 87–106. doi: 10.1002/rse2.93

Abdullah, H., Skidmore, A. K., Darvishzadeh, R., and Heurich, M. (2019b). Timing of red-edge and shortwave infrared reflectance critical for early stress detection induced by bark beetle (*Ips typographus*, L.) attack. *Int. J. Appl. Earth Observ. Geoinform.* 82, 101900. doi: 10.1016/j.jag.2019.101900

Ali, A. M., Abdullah, H., Darvishzadeh, R., Skidmore, A. K., Heurich, M., Roeoesli, C., et al., (2021). Canopy chlorophyll content retrieved from time series remote sensing data as a proxy for detecting bark beetle infestation. *Remote Sens. Appl. Soc. Envi.* 22:100524.

Allen, C. D., Macalady, A. K., Chenchouni, H., Bachelet, D., McDowell, N., Vennetier, M., et al., (2010). A global overview of drought and heat-induced tree mortality reveals emerging climate change risks for forests. *For. Ecol. Manag.* 259, 660–684. doi: 10.1016/j.foreco.2009.09.001

Aukema, B. H., Carroll, A. L., Zheng, Y., Zhu, J., Raffa, K. F., Moore, R. D., et al., (2008). Movement of outbreak populations of mountain pine beetle: Influences of spatiotemporal patterns and climate. *Ecography* 31, 348–358.

Aukema, B. H., Carroll, A. L., Zhu, J., Raffa, K. F., Sickley, T., and Taylor, S. W. (2006). Landscape level analysis of mountain pine beetle in British Columbia, Canada: Spatiotemporal development and spatial synchrony within the present out-break. *Ecography* 29, 427–441.

Bače, R., Svoboda, M., Janda, P., Morrissey, R. C., Wild, J., Clear, J. L., et al., (2015). Legacy of pre-disturbance spatial pattern determines early structural diversity following severe disturbance in montane spruce forests. *PLoS One* 10:e0139214. doi: 10.1371/journal.pone.0139214

Baret, F., and Guyot, G. (1991). Potentials and limits of vegetation indices for LAI and APAR assessment. *Remote Sens. Environ.* 35, 161–173.

Bentz, B. J., and Jönsson, A. M. (2015). "Modeling bark beetle responses to climate change," in *Bark beetles*, eds F. E. Vega and R. W. Hofstetter (London: Elsevier), 533–553. doi: 10.1016/B978-0-12-417156-5.00013-7

Bentz, B. J., Régnière, J., Fettig, C. J., Hansen, E. M., Hayes, J. L., Hicke, J. A., et al., (2010). Climate change and bark beetles of the western United States and Canada: Direct and indirect effects. *BioScience* 60, 602–613.

Birth, G., and McVey, G. (1968). Measuring the color of growing turf with a reflectance spectrophotometer. *Agron. J.* 60, 640–643.

Blackburn, G. A. (1998). Spectral indices for estimating photosynthetic pigment concentrations: A test using senescent tree leaves. *Int. J. Remote Sens.* 19, 657–675. doi: 10.1080/014311698215919

Blackburn, G. A. (2006). Hyperspectral remote sensing of plant pigments. *J. Exp. Bot.* 58, 855–867. doi: 10.1093/jxb/erl123

Brovkina, O., Cienciala, E., Surový, P., and Janata, P. (2018). Unmanned aerial vehicles (UAV) for assessment of qualitative classification of Norway spruce in temperate forest stands. *Geospatial Inform. Sci.* 21, 12–20. doi: 10.1080/10095020.2017.1416994

Carter, G. A., and Knapp, A. K. (2001). Leaf optical properties in higher plants: Linking spectral characteristics to stress and chlorophyll concentration. *Am. J. Bot.* 88, 677–684. doi: 10.2307/2657068

Chen, J. (1996). Evaluation of vegetation indices and modified simple ratio for boreal applications. *Can. J. Remote Sens.* 22, 229–242.

Christiansen, E., and Bakke, A. (1988). "The spruce bark beetle of Eurasia," in *Dynamics of forest insect populations*, ed. A. A. Berryman (Boston, MA: Springer US), 479–503. doi: 10.1007/978-1-4899-0789-9_23

Colombari, F., Schroeder, M. L., Battisti, A., and Faccoli, M. (2013). Spatio-temporal dynamics of an Ips acuminatus outbreak and implications for management. *Agric. For. Entomol.* 15, 34–42. doi: 10.1111/j.1461-9563.2012.00589.x

Crippen, R. (1990). Calculating the vegetation index faster. *Remote Sens. Environ.* 34, 71–73.

DeRose, R. J., Bentz, B. J., Long, J. N., and Shaw, J. D. (2013). Effect of increasing temperatures on the distribution of spruce beetle in *Engelmann spruce* forests of the Interior West USA. *For. Ecol. Manag.* 308, 198–206. doi: 10.1016/j.foreco.2013.07.061

Fettig, C. J., Klepzig, K. D., Billings, R. F., Munson, A. S., Nebeker, T. E., Negrón, J. F., et al., (2007). The effectiveness of vegetation management practices for prevention and control of bark beetle infestations in coniferous forests of the western and southern United States. *For. Ecol. Manag.* 238, 24–53.

Gao, B.-C. (1995). "Normalized difference water index for remote sensing of vegetation liquid water from space," in *Proceedings of the SPIE*, eds M. R. Descour, J. M. Mooney, D. L. Perry, and L. R. Illing (Orlando, FL), 225. doi: 10.1117/12.210877

Gely, C., Laurance, S. G. W., and Stork, N. E. (2020). How do herbivorous insects respond to drought stress in trees? *Biol. Rev.* 95, 434–448. doi: 10.1111/brv.12571

Gitelson, A. A. (2004). Wide dynamic range vegetation index for remote quantification of biophysical characteristics of vegetation. *J. Plant Physiol.* 161, 165–173. doi: 10.1078/0176-1617-01176

Gitelson, A. A., Kaufman, Y. J., and Merzlyak, M. N. (1996). Use of a green channel in remote sensing of global vegetation from EOS-MODIS. *Remote Sens. Environ.* 58, 289–298. doi: 10.1016/S0034-4257(96)00072-7

Gitelson, A., Gritz, Y., and Merzlyak, M. (2003). Relationships between leaf chlorophyll content and spectral reflectance and algorithms for non-destructive chlorophyll assessment in higher plant leaves. *J. Plant Physiol.* 160, 271–282. doi: 10.1078/0176-1617-00887

Gitelson, A., Stärk, R. F., Grits, U., Rundquist, D. C., Kaufman, Y. J., and Derry, D. (2002). Vegetation and soil lines in visible spectral space: A concept and technique for remote estimation of vegetation fraction. *Int. J. Remote Sens.* 23, 2537–2562.

Goel, N., and Qin, W. (1994). Influences of canopy architecture on relationships between various vegetation indices and LAI and Fpar: A computer simulation. *Remote Sens. Rev.* 10, 309–347.

Grizonnet, M., Michel, J., Poughon, V., Inglada, J., Savinaud, M., and Cresson, R. (2017). Orfeo ToolBox: Open source processing of remote sensing images. *Open Geospatial Data Softw. Stand.* 2:15. doi: 10.1186/s40965-017-0031-6

Hastie, T., Tibshirani, R., and Friedman, J. H. (2009). *The elements of statistical learning: Data mining, inference, and prediction*, 2nd Edn. New York, NY: Springer.

Havašová, M., Ferenčík, J., and Jakuš, R. (2017). Interactions between windthrow, bark beetles and forest management in the TATRA national parks. *For. Ecol. Manag.* 391, 349–361. doi: 10.1016/j.foreco.2017.01.009

Hlásny, T., Barka, I., Merganičová, K., Koístek, Š, Modlinger, R., Turčáni, M., et al., (2022). A new framework for prognosing forest resources under intensified disturbance impacts: Case of the Czech Republic. *For. Ecol. Manag.* 523:120483. doi: 10.1016/j.foreco.2022.120483

Hlásny, T., Zajíčková, L., Turčáni, M., Holuša, J., and Sitková, Z. (2011). Geographical variability of spruce bark beetle development under climate change in the Czech Republic. *J. For. Sci.* 57, 242–249. doi: 10.17221/104/2010-JFS

Hlásny, T., Zimová, S., Merganičová, K., Štěpánek, P., Modlinger, R., and Turčáni, M. (2021). Devastating outbreak of bark beetles in the Czech Republic: Drivers,

50

impacts, and management implications. *For. Ecol. Manag.* 490:119075. doi: 10.1016/j.foreco.2021.119075

Huete, A. (1988). A soil-adjusted vegetation index (SAVI). *Remote Sens. Environ.* 25, 295–309.

Huete, A., Didan, K., Miura, T., Rodriguez, E. P., Gao, X., and Ferreira, L. G. (2002). Overview of the radiometric and biophysical performance of the MODIS vegetation indices. *Remote Sens. Environ.* 83, 195–213.

Huo, L., Persson, H. J., and Lindberg, E. (2021). Early detection of forest stress from European spruce bark beetle attack, and a new vegetation index: Normalized distance red & SWIR (NDRS). *Remote Sens. Environ.* 255:112240. doi: 10.1016/j.rse.2020.112240

Immitzer, M., Vuolo, F., and Atzberger, C. (2016). First experience with Sentinel-2 data for crop and tree species classifications in central Europe. *Remote Sens.* 8:166. doi: 10.3390/rs8030166

Jactel, H., Petit, J., Desprez-Loustau, M.-L., Delzon, S., Piou, D., Battisti, A., et al., (2012). Drought effects on damage by forest insects and pathogens: A meta-analysis. *Glob. Change Biol.* 18, 267–276. doi: 10.1111/j.1365-2486.2011.02512.x

Jakuš, R., Zajíčkova, L., Cudlín, P., Blaženec, M., Turčani, M., Ježík, M., et al., (2011). Landscape-scale *Ips typographus* attack dynamics: From monitoring plots to GIS-based disturbance models. *iForest* 4, 256–261. doi: 10.3832/ifor0589-004

Karkauskaite, P., Tagesson, T., and Fensholt, R. (2017). Evaluation of the plant phenology index (PPI), NDVI and EVI for start-of-season trend analysis of the Northern Hemisphere boreal zone. *Remote Sens.* 9:485. doi: 10.3390/rs9050485

Kärvemo, S., Van Boeckel, T. P., Gilbert, M., Grégoire, J.-C., and Schroeder, M. (2014). Large-scale risk mapping of an eruptive bark beetle – Importance of forest susceptibility and beetle pressure. *For. Ecol. Manag.* 318, 158–166. doi: 10.1016/j.foreco.2014.01.025

Keeling, C. I. (2016). "Bark beetle research in the postgenomic Era," in *Advances in Insect physiology*, Vol. 50, eds T. Claus and G. J. Blomquist (Cambridge, MA: Academic Press), 265–293.

Kim, Y. (2013). Drought and elevation effects on MODIS vegetation indices in northern Arizona ecosystems. *Int. J. Remote Sens.* 34, 4889–4899. doi: 10.1080/2150704X.2013.781700

Klouček, T., Komárek, J., Surový, P., Hrach, K., Janata, P., and Vašíček, B. (2019). The use of UAV mounted sensors for precise detection of bark beetle infestation. *Remote Sens.* 11:1561. doi: 10.3390/rs11131561

Komonen, A., Schroeder, L. M., and Weslien, J. (2011). *Ips typographus* population development after a severe storm in a nature reserve in southern Sweden: *Ips typographus* after storm disturbance. *J. Appl. Entomol.* 135, 132–141. doi: 10.1111/j.1439-0418.2010.01520.x

Koontz, M. J., Latimer, A. M., Mortenson, L. A., Fettig, C. J., and North, M. P. (2021). Cross-scale interaction of host tree size and climatic water deficit governs bark beetle-induced tree mortality. *Nat. Commun.* 12:129. doi: 10.1038/s41467-020-20455-y

Krokene, P. (2015). "Conifer defense and resistance to bark beetles," in *Bark beetles*, eds F. E. Vega and R. W. Hofstetter (Amsterdam: Elsevier), 177–207. doi: 10.1016/B978-0-12-417156-5.00005-8

Lausch, A., Fahse, L., and Heurich, M. (2011). Factors affecting the spatio-temporal dispersion of *Ips typographus* (L.) in Bavarian Forest National Park: A long-term quantitative landscape-level analysis. *For. Ecol. Manag.* 261, 233–245. doi: 10.1016/j.foreco.2010.10.012

Lawley, V., Lewis, M., Clarke, K., and Ostendorf, B. (2016). Site-based and remote sensing methods for monitoring indicators of vegetation condition: An Australian review. *Ecol. Indic.* 60, 1273–1283. doi: 10.1016/j.ecolind.2015.03.021

Lindner, M., Maroschek, M., Netherer, S., Kremer, A., Barbati, A., Garcia-Gonzalo, J., et al., (2010). Climate change impacts, adaptive capacity, and vulnerability of European forest ecosystems. *For. Ecol. Manag.* 259, 698–709. doi: 10.1016/j.foreco.2009.09.023

Long, J. A., and Lawrence, R. L. (2016). Mapping percent tree mortality due to mountain pine beetle damage. *For. Sci.* 62, 392–402. doi: 10.5849/forsci.15-046

Marini, L., Lindelöw, Å., Jönsson, A. M., Wulff, S., and Schroeder, L. M. (2013). Population dynamics of the spruce bark beetle: A long-term study. *Oikos* 122, 1768–1776. doi: 10.1111/j.1600-0706.2013.00431.x

Marini, L., Økland, B., Jönsson, A. M., Bentz, B., Carroll, A., Forster, B., et al., (2017). Climate drivers of bark beetle outbreak dynamics in Norway spruce forests. *Ecography* 40, 1426–1435. doi: 10.1111/ecog.02769

McDowell, N., Pockman, W. T., Allen, C. D., Breshears, D. D., Cobb, N., Kolb, T., et al., (2008). Mechanisms of plant survival and mortality during drought: Why do some plants survive while others succumb to drought? *New Phytol.* 178, 719–739. doi: 10.1111/j.1469-8137.2008.02436.x

Meddens, A. J. H., and Hicke, J. A. (2014). Spatial and temporal patterns of Landsat-based detection of tree mortality caused by a mountain pine beetle outbreak in Colorado USA. *For. Ecol. Manag.* 322, 78–88. doi: 10.1016/j.foreco.2014.02.037

Meddens, A. J. H., Hicke, J. A., Macalady, A. K., Buotte, P. C., Cowles, T. R., and Allen, C. D. (2015). Patterns and causes of observed piñon pine mortality in the southwestern United States. *New Phytol.* 206, 91–97. doi: 10.1111/nph.13193

Meddens, A. J. H., Hicke, J. A., Vierling, L. A., and Hudak, A. T. (2013). Evaluating methods to detect bark beetle-caused tree mortality using single-date and multi-date Landsat imagery. *Remote Sens. Environ.* 132, 49–58. doi: 10.1016/j.rse.2013.01.002

Mezei, P., Jakuš, R., Pennerstorfer, J., Havašová, M., Škvarenina, J., Ferenčík, J., et al., (2017). Storms, temperature maxima and the *Eurasian spruce* bark beetle *Ips typographus*—An infernal trio in Norway spruce forests of the Central European High Tatra Mountains. *Agric. For. Meteorol.* 242, 85–95. doi: 10.1016/j.agrformet.2017.04.004

Minařík, R., and Langhammer, J. (2016). Use of a multispectral uav photogrammetry for detection and tracking of forest disturbance dynamics. *Int. Arch. Photogramm. Remote Sens. Spatial Inf. Sci.* XLI-B 8, 711–718. doi: 10.5194/isprsarchives-XLI-B8-711-2016

Mullen, K. E. (2016). *Early detection of mountain pine beetle damage in ponderosa pine forests of the black hills using hyperspectral and worldview-2 data. Master's thesis.* Mankato, MN: Minnesota State University.

Mullen, K., Yuan, F., and Mitchell, M. (2018). The mountain pine beetle epidemic in the black hills, South Dakota: The consequences of long term fire policy, climate change and the use of remote sensing to enhance mitigation. *JGG* 10:69. doi: 10.5539/jgg.v10n1p69

Netherer, S., Kandasamy, D., Jirosová, A., Blanka, K., Schebeck, M., and Schlyter, F. (2021). Interactions among Norway spruce, the bark beetle *Ips typographus* and its fungal symbionts in times of drought. *J. Pest Sci.* 94, 591–614. doi: 10.1007/s10340-021-01341-y

Netherer, S., Matthews, B., Katzensteiner, K., Blackwell, E., Henschke, P., Hietz, P., et al., (2015). Do water-limiting conditions predispose Norway spruce to bark beetle attack? *New Phytol.* 205, 1128–1141. doi: 10.1111/nph.13166

Netherer, S., Panassiti, B., Pennerstorfer, J., and Matthews, B. (2019). Acute drought is an important driver of bark beetle infestation in Austrian Norway spruce stands. *Front. For. Glob. Change* 2:39. doi: 10.3389/ffgc.2019.00039

Niemann, K. O., Quinn, G., Stephen, R., Visintini, F., and Parton, D. (2015). Hyperspectral remote sensing of mountain pine beetle with an emphasis on previsual assessment. *Can. J. Remote Sens.* 41, 191–202. doi: 10.1080/07038992.2015.1065707

Öhrn, P., Langstrom, B., LindelÖw, A., and Bjrklund, N. (2014). Seasonal flight patterns of *Ips typographus* in southern Sweden and thermal sums required for emergence. *Agric. For. Entomol.* 16, 1–23.

Ortiz, S., Breidenbach, J., and Kändler, G. (2013). Early detection of bark beetle green attack using terraSAR-X and rapideye data. *Remote Sens.* 5, 1912–1931. doi: 10.3390/rs5041912

Özçelik, M. S., Tomášková, I., Surový, P., and Modlinger, R. (2022). Effect of forest edge cutting on transpiration rate in *Picea abies* (L.) H. *Karst. For.* 13:1238. doi: 10.3390/f13081238

Pedregosa, F., Varoquaux, G., Gramfort, A., Michel, V., Thirion, B., Grisel, O., et al., (2011). Scikit-learn: Machine learning in python. *J. Mach. Learn. Res.* 12, 2825–2830.

Pinty, B., and Verstraete, M. (1992). GEMI: A non-linear index to monitor global vegetation from satellites. *Vegetation* 101, 15–20.

Planet Labs, Inc (2022). *Planet planet imagery product specifications.* San Francisco, CA: Planet Labs, Inc.

QGIS Development Team (2009). *QGIS geographic information system. Open source geospatial foundation.* Pittsburgh, PA: Q Development Team.

Qi, J., Chehbouni, A., Huete, A., Kerr, Y., and Sorooshian, S. (1994). A modified soil adjusted vegetation index. *Remote Sens. Environ.* 48, 119–126.

Raffa, K. F. (1988). "The mountain pine beetle in western North America," in *Dynamics of forest insect populations: Patterns, causes, and implications*, ed. A. A. Berryman (New York, NY: Plenum), 556–576.

Raffa, K. F., and Berryman, A. A. (1983). The role of host plant resistance in the colonization behavior and ecology of bark beetles (Coleoptera: Scolytidae). *Ecol. Monogr.* 53, 27–49.

Raffa, K. F., Aukema, B. H., Bentz, B. J., Carroll, A. L., Hicke, J. A., Turner, M. G., et al., (2008). Crossscale drivers of natural disturbances prone to anthropogenic amplification: The dynamics of bark beetle eruptions. *Bioscience* 58, 501–517.

Raffa, K. F., Grégoire, J.-C., and Staffan Lindgren, B. (2015). "Natural history and ecology of bark beetles," in *Bark beetles*, eds F. E. Vega and R. W. Hofstetter (San Diego, CA: Elsevier), 1–40. doi: 10.1016/B978-0-12-417156-5.00001-0

Rautiainen, M., Lukeš, P., Homolová, L., Hovi, A., Pisek, J., and Mõttus, M. (2018). Spectral properties of coniferous forests: A review of in situ and laboratory measurements. *Remote Sens.* 10:207. doi: 10.3390/rs10020207

Remeš, J. (2017). "The university forest enterprise in Kostelec nad Černými Lesy – a basis for practical education and research at the Faculty of forestry and wood sciences in Prague," in *Proceedings of the Forests for university education: Examples and experiences – SILVA network conference, Faculty of forestry and wood sciences, Czech university of live sciences, Prague, Jun 26th – 28th, 2017, Technische Universität Dresden*

51

and Sächsische Landesbibliotek, Dresden, eds P. Schmidt, S. Lewark, J. Remeš, and N. Weber (Prague), 17–22.

Richardson, A. J., and Wiegand, C. L. (1977). Distinguishing vegetation from soil background information. *Photogram. Eng. Remote Sens.* 43, 1541–1552.

Rondeaux, G., Steven, M., and Baret, F. (1996). Optimization of soil-adjusted vegetation indices. *Remote Sens. Environ.* 55, 95–107.

Roujean, J., and Breon, F. (1995). Estimating PAR absorbed by vegetation from bidirectional reflectance measurements. *Remote Sens. Environ.* 51, 375–384.

Rouse, J., Haas, R., Schell, J., and Deering, D. (1973). "Monitoring vegetation systems in the great plains with ERTS," in *Proceedings of the 3rd ERTS Symposium, NASA*, (Washington, DC), 309–317.

Seidel, H., Schunk, C., Matiu, M., and Menzel, A. (2016). Diverging drought resistance of scots pine provenances revealed by infrared thermography. *Front. Plant Sci.* 7:1247. doi: 10.3389/fpls.2016.01247

Senf, C., Pflugmacher, D., Wulder, M. A., and Hostert, P. (2015). Characterizing spectral–temporal patterns of defoliator and bark beetle disturbances using Landsat time series. *Remote Sens. Environ.* 170, 166–177. doi: 10.1016/j.rse.2015.09.019

Simard, M., Powell, E. N., Raffa, K. F., and Turner, M. G. (2012). What explains landscape patterns of bark beetle outbreaks in Greater Yellowstone? *Glob. Ecol. Biogeogr.* 21, 556–567.

Sripada, R. (2005). *Determining in-season nitrogen requirements for corn using aerial color-infrared photography*. Ph.D. dissertation. Raleigh, NC: North Carolina State University.

Sripada, R., Heiniger, R. W., White, J. G., and Meijer, A. D. (2006). Aerial color infrared photography for determining early in-season nitrogen requirements in corn. *Agron.* J. 98, 968–977.

Stereńczak, K., Mielcarek, M., Modzelewska, A., Kraszewski, B., Fassnacht, F. E., and Hilszczański, J. (2019). Intra-annual *Ips typographus* outbreak monitoring using a multi-temporal GIS analysis based on hyperspectral and ALS data in the Białowieża Forests. *For. Ecol. Manag.* 442, 105–116. doi: 10.1016/j.foreco.2019.03.064

Stříbrská, B., Hradecký, J., Čepl, J., Tomášková, I., Jakuš, R., Modlinger, R., et al., (2022). Forest margins provide favourable microclimatic niches to swarming bark beetles, but Norway spruce trees were not attacked by *Ips typographus* shortly after edge creation in a field experiment. *Remote Sens. Environ.* 506:119950. doi: 10.1016/j.foreco.2021.119950

Tolasz, R., Míková, T., Valeriánová, A., and Voženílek, V. (eds) (2007). *Climate atlas of Czechia*, 1st Edn. Prague: Olomouc: Czech Hydrometeorological Institute, Palackého University, 255.

Tucker, C. (1979). Red and photographic infrared linear combinations for monitoring vegetation. *Remote Sens. Environ.* 8, 127–150.

Vacchiano, G., Garbarino, M., Borgogno Mondino, E., and Motta, R. (2012). Evidences of drought stress as a predisposing factor to Scots pine decline in Valle d'Aosta (Italy). *Eur. J. For. Res.* 131, 989–1000. doi: 10.1007/s10342-011-0570-9

Väisänen, R., and Heliövaara, K. (1994). Assessment of insect occurrence in boreal forests based on satellite imagery and field measurements. *Acta For. Fenn.* 243:7505. doi: 10.14214/aff.7505

Van Rossum, G., and Drake, F. L. (2010). *The Python language reference. Release 3.0.1 [Repr.]*. Hampton, NH: Python Software Foundation.

Virtanen, P., Gommers, R., Oliphant, T. E., Haberland, M., Reddy, T., Cournapeau, D., et al., (2020). SciPy 1.0: Fundamental algorithms for scientific computing in Python. *Nat. Methods* 17, 261–272. doi: 10.1038/s41592-019-0686-2

Vošvrdová, N., Johansson, A., Turčáni, M., Jakuš, R., Tyšer, D., Schlyter, F., et al., (2023). Dogs trained to recognise a bark beetle pheromone locate recently attacked spruces better than human experts. *For. Ecol. Manag.* 528:120626. doi: 10.1016/j.foreco.2022.120626

Wallin, K. F., and Raffa, K. (2004). Feedback between individual host selection behavior and population dynamics in an eruptive herbivore. *Ecol. Monogr.* 74, 101–116.

Weed, A. S., Ayres, M. P., and Hicke, J. A. (2013). Consequences of climate change for biotic disturbances in North American forests. *Ecol. Monogr.* 83, 441–470. doi: 10.1890/13-0160.1

Wei, M., Jiao, L., Zhang, P., Wu, X., Xue, R., and Du, D. (2023). Spatio-temporal diversity in the link between tree radial growth and remote sensing vegetation index of qinghai spruce on the northeastern margin of the tibetan plateau. *Forests* 14:260. doi: 10.3390/f14020260

Wermelinger, B. (2004). Ecology and management of the spruce bark beetle *Ips typographus*—a review of recent research. *For. Ecol. Manag.* 202, 67–82. doi: 10.1016/j.foreco.2004.07.018

White, J. C., Coops, N. C., Hilker, T., Wulder, M. A., and Carroll, A. L. (2007). Detecting mountain pine beetle red attack damage with EO-1 Hyperion moisture indices. *Int. J. Remote Sens.* 28, 2111–2121. doi: 10.1080/01431160600944028

Yang, H., Yang, X., Zhang, Y., Heskel, M. A., Lu, X., Munger, J. W., et al., (2017). Chlorophyll fluorescence tracks seasonal variations of photosynthesis from leaf to canopy in a temperate forest. *Glob. Change Biol.* 23, 2874–2886. doi: 10.1111/gcb.13590

Yang, S. (2019). *Detecting bark beetle damage with Sentinel-2 multi-temporal data in Sweden. Master's thesis*. Lund: Lund University.

Zabihi, K., Surovy, P., Trubin, A., Singh, V. V., and Jakuš, R. (2021b). A review of major factors influencing the accuracy of mapping green-attack stage of bark beetle infestations using satellite imagery: Prospects to avoid data redundancy. *Remote Sens. Appl.* 24:100638. doi: 10.1016/j.rsase.2021.100638

Zabihi, K., Huettmann, F., and Young, B. (2021a). Predicting multi-species bark beetle (Coleoptera: Curculionidae: Scolytinae) occurrence in Alaska: First use of open access big data mining and open source GIS to provide robust inference and a role model for progress in forest conservation. *Biodiv. Inf.* 16, 1–19. doi: 10.17161/bi.v16i1.14758

Zeppenfeld, T., Svoboda, M., DeRose, R. J., Heurich, M., Müller, J., Čížková, P., et al., (2015). Response of mountain *Picea abies* forests to stand-replacing bark beetle outbreaks: Neighbourhood effects lead to self-replacement. *J. Appl. Ecol.* 52, 1402–1411. doi: 10.1111/1365-2664.12504

52

3.1.2 Detection of Green Attack and Bark Beetle Susceptibility in Norway Spruce Trees using PlanetScope Multispectral Imagery

Published as:

Trubin Aleksei, Kozhoridze Giorgi, Zabihi Khodabakhsh, Modlinger Roman, Singh Vivek Vikram, Surový Peter, Jakuš Rastislav. Detection of Green Attack and Bark Beetle Susceptibility in Norway Spruce Trees using PlanetScope Multispectral Imagery.

Authors' contributions

AT, GK, KZ, VVS, PS, and RJ contributed to the conception and design of the study. AT organized the database. AT and GK performed the statistical analysis. AT and RJ wrote the first draft of the manuscript. AT, GK, KZ, RM, VVS, and RJ wrote sections of the manuscript. All authors contributed to the manuscript revision, read, and approved the submitted version.

Extended summary

Introduction

Recent studies have highlighted the escalating vulnerability of global coniferous forests to the Eurasian spruce bark beetle (*I. typographus*), a significant economic pest in Eurasia. These forests are increasingly susceptible to dieback due to physiological stress from factors like heat, drought, and pest spreading. Environmental factors, tree aging, and density significantly influence the life cycle of bark beetles, their impact on trees, and the resultant infestations. Notably, climate change has driven substantial outbreaks, leading to heightened mortality rates in spruce forests. The task of accurately mapping these hotspots is critical to developing effective removal and sanitation strategies but is often challenged by the vastness and inaccessibility of the affected areas. In this context, remote sensing (RS) data has emerged as a valuable tool for monitoring vegetation stress and pest infestations. Specifically, the use of PlanetScope satellite imagery has enhanced the ability to detect subtle changes in land cover over extensive areas. This study focuses on the application of individual bands and Spectral Vegetation Indices (SVIs) to identify alterations in spectral signatures in trees attacked by bark beetles. The main objective is to determine whether trees at risk of beetle attack can be identified before or at the beginning of the growing season. In addition, this study aims to develop a methodology that combines remote sensing data with ground-based observations to assess the health status of Norway spruce before and during bark beetle infestation.

Materials and methods

This research was conducted in a 5,700-hectare forest near Prague, Czech Republic, primarily composed of conifers, among which spruce is the most common. The area, managed by the Czech University of Life Sciences Prague, has experienced recent droughts, exacerbating bark beetle infestations, particularly by *I. typographus*. The study utilized cloud-free PlanetScope satellite imagery captured between April and September 2020. These images, with RGB and NIR bands, were processed to compute 23 Spectral Vegetation Indices (SVIs) for each image. The study identified three tree classes: Healthy (unattacked trees), Susceptible (trees attacked later in the season but before green-attack phase), and Green-attack (trees that had reached the green-attack phase). GIS data on attacked trees were collected weekly using the ArcGIS Collector app, and 61 locations were identified for the study. The data was validated and cleaned, with adjustments made for logged trees and changes in attack stages.

Statistical analysis of spectral reflectance and SVIs was conducted using Python, including ANOVA and Kruskal-Wallis tests with relevant post-hoc tests to assess differences among the three classes.

Results

In this study, 122 forest polygons, split evenly between 61 "Healthy" and 61 attacked samples (further classified as "Susceptible" or "Green-attack"), were analyzed. Each polygon averaged 0.165 hectares, with the total area for attacked and healthy samples being approximately 10.089 ha and 10.065 ha respectively. Statistical analysis of individual bands across 72 datasets revealed non-normal distribution in 32 datasets. Additionally, 11 of the 24 datasets in individual bands showed unequal variances. Regarding the Spectral Vegetation Indices (SVIs), out of 414 datasets, 188 did not follow a normal distribution, broken down as 105 in "Healthy," 22 in "Susceptible," and 61 in "Green-attack." In SVIs, 33/138 datasets showed unequal variances. Significant differences were identified between at least two classes using individual bands, particularly noted in the Green band on Days 153 and 183, and the Red band on Day 194. In the case of Spectral Vegetation Indices (SVIs), out of the 23 Vegetation Indices (VIs) studied, 17 showed significant differences between at least two classes. Particularly, marked differences were observed between two pairs of classes for the Enhanced Vegetation Index (EVI) and Visible Atmospherically Resistant Index (VARI) on Day 196, as well as for the Infrared Percentage Vegetation Index (IPVI), Modified Soil-Adjusted Vegetation Index (MSR), Optimized Soil-Adjusted Vegetation Index (OSAVI), and Simple Ratio (SR) on Day 194.

Discussion

This study reveals that while PlanetScope's four wavebands and several vegetation indices are capable of detecting trees vulnerable to bark beetle infestation and green-attack phases, no single waveband or vegetation index could consistently distinguish between healthy, susceptible, and green-attacked trees. Key wavebands showed potential in identifying Norway spruce trees at risk of infestation and during green-attack phases, particularly on specific days within the vegetation season. The Green waveband was most effective in differentiating between healthy and green-attacked trees in May and July. The Red waveband was also effective, particularly towards the study's end, correlating with a decrease in chlorophyll content leading to higher reflectance. The NIR waveband was less significant for spectral

separability. Spectral vegetation indices provided significant results mainly in the study's latter half. The Enhanced Vegetation Index (EVI) and Visible Atmospherically Resistant Index (VARI) emerged as the most promising indices for detecting susceptible and green-attacked trees. These indices, particularly EVI, consistently distinguished between healthy and susceptible trees throughout the season. The study also noted that different sets of Spectral Vegetation Indices might be needed for different halves of the growing season. Moreover, individual wavebands like Blue, Green, and Red could be prioritized for differentiating the three classes of trees across the season. Additionally, the study observed seasonal spectral separations between susceptible and green-attacked areas starting from July, supporting the theory that abiotic stress and initial bark beetle infestation affect trees' spectral signatures similarly. The study faced limitations due to the spectral resolution of the sensor and the challenge of determining the exact cause of infestations. Advancing to an individual tree level could enhance detection accuracy but requires additional data collection and preprocessing. In terms of management implications, large-scale bark beetle outbreaks are expected in the future, and satellite data with high-frequency scanning, such as PlanetScope products, could be crucial for early detection. Combining this with field surveys and phenology models can help determine optimal times for airborne sensing. The study suggests that drone imagery may offer better spatial resolution for early attack detection, but the challenge lies in covering extensive outbreak areas and ensuring early tree removal to prevent further spread.

Conclusions

This study highlights the effectiveness of PlanetScope imagery and spectral analysis in distinguishing healthy, susceptible, and green-attacked trees, with the Green and Red wavebands proving particularly useful. Additionally, EVI and VARI indices emerged as significant in detecting trees prone to bark beetle infestation. These findings enhance understanding of bark beetle infestation dynamics and tree predisposition, suggesting the need for further research and the potential of integrated high-resolution satellite systems for early detection.

1   **Detection of Green Attack and Bark Beetle Susceptibility in Norway Spruce**

2   **Trees using PlanetScope Multispectral Imagery**

3

4   Aleksei Trubin[1,*], Giorgi Kozhoridze[1,2], Khodabakhsh Zabihi[1], Roman Modlinger[3],

5   Vivek Vikram Singh[1], Peter Surový[1] and Rastislav Jakuš[1,4]

6

7   [1]Faculty of Forestry and Wood Sciences, Czech University of Life Sciences in Prague,

8   16500 Kamýcká 129, Suchdol, Prague 6, Czech Republic

9   [2] Faculty of Environmental Sciences, Czech University of Life Sciences in Prague,

10   16500 Kamýcká 129, Suchdol, Prague 6, Czech Republic

11   [3] Forest Risk Research Centre, Czech University of Life Sciences in Prague, 16500

12   Kamýcká 129, Suchdol, Prague 6, Czech Republic

13   [4] Institute of Forest Ecology, Slovak Academy of Sciences, Štúrova 2, 960 53 Zvolen,

14   Slovakia

15   *Correspondence: Aleksei Trubin trubin@fld.czu.cz*

16

17   Abstract

18

19   The detection of susceptible and attacked trees is a key factor in the

20   management of bark beetle infestations. Early detection remains a challenge because

21   there are no visible changes in the canopy during the early stages, making it difficult to

22   detect outbreaks in a timely manner. The green-attack phase, which occurs without

23   discernible needle discoloration, further complicates early detection. While studies

24   have examined spectral characteristics during green-attack, few have focused on pre-

25   infestation spectral responses alongside accurate field identification of attack timing.

26   Our paper investigates the spectral differences among three classes of forest areas:

27   healthy, susceptible to bark beetle attacks, and green-attacked trees. The study aims to

28   differentiate these classes using individual wavebands or spectral vegetation indices

29   (SVIs). The research is based on the assumption that the spectral characteristics of

30   these forests vary significantly due to differing levels of damage caused by the bark

31   beetle. The study utilises satellite data acquired from 16 PlanetScope images, that were

32   captured between 2 April and 5 September 2020. Various SVIs and four individual

33   bands are used to differentiate the three tree classes. The spatial position of attacked

34   trees is recorded using GIS data collection, and data cleaning is performed. Statistical

35   analyses are conducted to assess the separability among the tree classes. The findings

36   indicate that the Green and Red wavebands show promise in distinguishing between

37   healthy, susceptible, and green-attacked trees. The study also reveals spectral

38   differences between healthy and susceptible trees before bark beetle attacks,

39   suggesting the presence of abiotic stress and initial infestation processes. Multiple

40   wavebands and spectral indices are found to be important for accurate detection. The

41   EVI and VARI indices demonstrate potential in detecting susceptible trees and their

42   predisposition to infestation.

43

44   **Keywords:** *Picea abies, Ips typographus*, spectral vegetation indices, bark

45   beetle infestations, green attack, Enhanced Vegetation Index, Visible Atmospherically

46   Resistant Index

47

48   **1 INTRODUCTION**

49

50   Among several bark beetle species, the outbreaks of *Ips typographus* (L.) have

51   been severely damaging the central European forests, especially in the Czech

52   Republic, during the 2018-2019 period, and they are thought to be associated with

53   drought (Hlásny et al., 2021). The population growth of forest insects, including the

54   bark beetles, and the consequent infestations, have been exacerbated by water-stress

55   conditions in trees, due to heat and drought effects (McDowell et al., 2008; Allen et

56   al., 2010; Trubin et al., 2022). Further, wind and drought effects have been

57   deteriorating spruce forest health in Europe (Komonen et al., 2011; Kärvemo et al.,

58   2014; Marini et al., 2017). Although conifers have a high tolerance capacity for

59   drought effects, a long-term high frequency of droughts can surpass the limits of their

60   tolerance and thus make conifers, e.g., Norway spruce (*Picea abies* (L.) Karst),

61   susceptible to bark beetle infestations (Krokene, 2015). For example, trees were found

62   to be more vulnerable to *I. typographus* attacks after long-term dry periods

63   accompanied by high-temperature regimes (Wermelinger, 2004; Netherer et al., 2015)

64   due to a significant decrease in their defence chemicals (Gely et al., 2020). The high-

65   temperature regimes not only deteriorate tree defence capability, but also they may

66   influence the breeding behaviour of bark beetles, which would increase the number of

67   their yearly generations (Netherer et al., 2019).

68   Remotely sensed imagery and the associated techniques, with which to process

69   the data, offer a tool to monitor infestations over continuous spatial and temporal

70　scales (Fernandez-Carrillo et al., 2020; Zabihi et al., 2021, Trubin et al., 2023). The

71　spatio-temporal patterns of bark beetle infestations and population dynamics have been

72　investigated in different parts of the world. For example, there are studies by Kärvemo

73　et al., 2014, Havašová et al., 2017, Mezei et al., 2017, Abdullah et al., 2019a, Abdullah

74　et al., 2019b, Abdollahnejad, and Panagiotidis, 2020 in Europe, and Meddens and

75　Hicke, 2014, Senf et al., 2015, and Mullen et al., 2018 in North America. Among

76　several sources of available remotely sensed imagery, multispectral aerial and satellite

77　imagery have been promising resources, with which to map forest disturbances, such

78　as insect outbreaks (Väisänen and Heliövaara, 1994; White et al., 2007; Long and

79　Lawrence, 2016). As bark beetle attacks are spatially and temporally autocorrelated

80　(Aukema et al., 2006; Aukema et al., 2008; Simard et al., 2011), the availability of

81　remote sensing data with diverse spectral, spatial, and temporal resolutions enables

82　mapping the infestation dynamics/patterns (Zabihi et al., 2021; Marvasti-Zadeh et al.,

83　2023). For example, Meddens et al. (2013) and Abdullah et al. (2019a) used coarse-

84　resolution Landsat imagery and medium-resolution SPOT-5 & Sentinel-2 imagery to

85　map early infestations, respectively. In addition, fine-resolution aerial photography has

86　been used to detect infested trees (e.g., Minařík and Langhammer, 2016; Brovkina et

87　al., 2018; Klouček et al., 2019; Abdollahnejad and Panagiotidis, 2020; Bárta et al.,

88　2022).

89　　　　Detecting susceptible trees and infested trees is crucial for practical bark beetle

90　control. However, early detection is challenging due to the lack of visible changes in

91　tree crowns during the initial stages. The absence of colouration alterations hampers

92　identifying attacks (Niemann and Visintini, 2005; Zabihi et al., 2021). The green-

93 attack stage, without needle discolouration, occurs initially when beetles colonise host

94 trees (Niemann and Visintini, 2005; Zabihi et al., 2021). The challenge of early

95 detection arises from the intricate integration of multiple factors, including the

96 dynamic interplay of bark beetle life cycles, site-specific conditions, and tree vitality,

97 alongside the concurrent temporal evolution of weather elements, such as temperature

98 and precipitation within the local ecosystem (Wulder et al., 2009; Bárta et al., 2022).

99 Locating and removing infested trees before new beetle generations emerge is

100 critical to suppress the spread of an attack (Zabihi et al., 2021). Determining whether

101 remote sensing can detect green-attacks is a crucial research question, that seeks to

102 enhance forest monitoring and early warning techniques (Huo et al., 2023).

103 Studies on European spruce bark beetles have consistently reported low

104 accuracy in identifying 'green-attacks' (Abdullah et al., 2019; Huo et al., 2021;

105 Dalponte et al., 2023). These 'green-attacks' exhibit variations in timing among

106 individual trees, and are influenced by the initial attack timing and the climate zone

107 (Huo et al., 2021). While several studies have investigated the spectral characteristics

108 during 'green-attacks', only a few studies have focused on the pre-infestation spectral

109 responses, combined with precise field identification of the time of bark beetle attack

110 (Huo et al., 2021, 2023; Trubin et al., 2023). Huo et al. (2021) conducted a study

111 which examined the differences in spectral signals between healthy trees and trees

112 attacked by spruce bark beetles. Their findings revealed that these signal differences

113 were present before the attacks, and did not show significant changes during the early-

114 stage infestation. However, these differences became more pronounced during the late-

115 stage infestation in autumn. It is important to emphasise that spectral differences

116   between healthy and stressed trees exist, even before the attacks occur (Huo et al.,

117   2021; Trubin et al., 2023). Therefore, it is incorrect to solely attribute these differences

118   as a response to infestation. In that, simply demonstrating spectral differences between

119   healthy and attacked samples is insufficient evidence for effectively detecting 'green-

120   attacks'.

121   The existence of spectral differences prior to attacks suggests a relationship

122   between these differences, the weakness and stress of trees, and the susceptibility of

123   trees to infestation by bark beetles. The significance of this hypothesis is underscored

124   by the preference of bark beetles for weaker trees, with lower defence mechanisms, as

125   the first target for attack (Wermelinger, 2004; Korolyova et al., 2022). After the

126   successful colonisation of the first target trees, the remaining beetles attack

127   neighbouring trees independently from their vitality. Furthermore, topographic-related

128   data, such as potential solar radiation, have proven valuable in bark beetle attack

129   prediction models, significantly enhancing their predictive capability (Ďuračiová et al.,

130   2020). Considering these factors, in conjunction with spectral analysis, can further

131   improve the accuracy of detecting bark beetle infestations.

132   According to Bárta et al. (2022), with the use of aerial hyperspectral imagery, it

133   is possible to distinguish between healthy and bark beetle-attacked trees within 23

134   days after infestation. Huo et al. (2023) performed an experiment with an artificial *I.*

135   *typographus* attack on trees, with no significant spectral differences before

136   infestations. They used commercial pheromones to induce attack, and they did not see

137   any indication that infested trees can be detected sufficiently enough during the first 5

138   weeks of infestation.

139   Recent works have been focusing on SVIs to detect trees that are susceptible to

140   bark beetle attacks, which enables resource managers and policy-makers to establish

141   proactive forest pest management. For example, Huo et al. (2021) developed a

142   normalized distance red and shortwave infrared (NDRS) index using Red and Short-

143   wave infrared (SWIR) wavebands. The NDRS index was found to be a promising

144   index with which to estimate forest susceptibility to bark beetle infestations in April,

145   or to detect infested trees during the growing season from May to October (Huo et al.,

146   2021). In addition, Trubin et al. (2023) found significant differences between

147   susceptible and healthy trees using the Enhanced Vegetation Index (EVI) and the

148   Visible Atmospherically Resistant Index (VARI) on a temporal scale from April to

149   mid-growing season. Trubin et al. (2023) used visible light wavebands from the 2nd

150   generation of PlanetScope satellite (Planet Labs, Inc., San Francisco, CA) to

151   differentiate healthy trees and trees that are susceptible to bark beetle attacks.

152   Although numerous studies have been using satellite imagery, such as Landsat,

153   SPOT-5, and Sentinel-2 to map bark beetle infestations, limited studies have been

154   using PlanetScope imagery to map the green-attack stage of infestations. As an

155   advantage, PlanetScope acquires imagery at high spatial resolution (3.7 m) at a short

156   temporal scale on a daily basis. The second generation of PlanetScope, named Dove-R

157   or PS2.SD, which we used in the present study, provides imagery at four spectral

158   wavebands, including Blue, Green, Red, and near-infrared (NIR). Recently, Dalponte

159   et al. (2023) successfully used the second generation of PlanetScope imagery in a

160   spectral separability study of healthy, green-attack, and red-attack stages.

161   Most individual wavebands, such as visible, Red-edge, NIR, and Shortwave-

162   infrared (SWIR), and SVIs, that have been developed from these bands have, to date,

163   been successful in detecting beetle-induced changes in needle pigments, such as

164   chlorophyll contents, greenness, and water contents (Zabihi et al., 2021). For example,

165   the loss of chlorophyll contents in highly water-stressed trees reduces the absorption of

166   visible lights, e.g., Blue, Green, and Red, by photosynthetically active pigments in

167   infested trees (Blackburn, 1998, 2007; Carter and Knapp, 2001; Mullen, 2016; Mullen

168   et al., 2018). Similarly, the loss of chlorophyll α contents in beetle-induced water-

169   stressed trees causes more reflection in red-edge light than in healthy trees (Ortiz et al.,

170   2013). The severe water stress conditions cause foliage desiccation due to changes in

171   the structure of spongy mesophyll and, thus, reduce the absorption of red-edge and

172   NIR wavebands (Oritz et al., 2013; Mullen et al., 2018). Similarly, SWIR wavebands

173   have been reflected more in water-stressed trees than in healthy trees (Immitzer et al.,

174   2016).

175   Among several investigated SVIs to detect changes in needle pigments and

176   greenness, Red-Edge NDVI (Ortiz et al., 2013) and Normalized Difference Red-Edge

177   (NDRE 2 and 3; Abdullah et al., 2019a; Abdullah et al., 2019b) were found to be

178   promising indices. The top-ranked indices for detecting beetle-induced water-stressed

179   needles were found to be the Disease-Water Stress Index (DWSI), the Normalized

180   Difference Water Index (NDWI), the Leaf Water Content Index (LWCI), and the Ratio

181   Drought Index (RDI; Abdullah et al., 2019a; Abdullah et al., 2019b).

182   The use of visible lights and Red-edge (a bandwidth close to NIR) to develop

183   SVIs was recommended, in order to minimise the mapping uncertainty of the green-

184   attack stage of bark beetle infestations (Zabihi et al., 2021).

185   Based on patterns of differences in spectral characteristics in predisposed and

186   bark beetle attacked trees described by Huo et al. (2021, 2023) and Trubin et al.

187   (2022), we investigated the spectral differences among three distinct classes of forest

188   areas in relation to *I. typographus* attacks during the growing season. The first class

189   included forest areas that were attacked during the growing season and were assumed

190   to be susceptible to *I. typographus* attacks. Within this class, when the green-attack

191   stage of bark beetle infestations occurred for different areas at different times of the

192   growing season, these trees were excluded from the class that was susceptible to *I.*

193   *typographus* attacks and was assumed to be the class of green-attacked trees (Figure

194   3). The third class was areas that were not attacked during the year of observations

195   and, thus, were assumed to be healthy. We aim to differentiate among these classes,

196   using either individual wavebands or SVIs, that have been developed from individual

197   wavebands.

198   Firstly, we assumed that the spectral characteristics of these forests would vary

199   significantly, due to the differing levels of damage caused by the bark beetle.

200   Additionally, we presumed that the spectral signatures of trees under a green-attack

201   would exhibit unique features, reflecting the ongoing physiological changes within the

202   affected vegetation. Finally, we expected that the spectral properties of healthy forests

203   would serve as a baseline for comparison, providing valuable insights into the normal

204   state of unaffected stands. These assumptions guided our research and helped us

205 uncover meaningful distinctions among the forest classes, thus contributing to a deeper

206 understanding of the impacts of *I. typographus* on forest ecosystems. The present

207 paper is a continuation of previous work that is focused on tree predisposition to bark

208 beetle attacks (Trubin et al., 2023). In contrast to Dalponte et al. 2023, we were

209 focused also on predisposition to bark beetle attack. We were also not able to analyse

210 later stages of attack due to sanitary felling.

211   We have used PlanetScope multispectral data. In the study period, it was the

212 only satellite service providing data every day in reasonable resolution enabling the

213 identification of bark beetle-caused tree mortality on a relatively small scale.

214

215

216 **2 MATERIALS AND METHODS**

217   2.1 Study area

218   The study was conducted in forests that are located about 50 km southeast of

219 Prague (in Czechia or the Czech Republic) (Figures 1 and 2), and owned and managed

220 by the Czech University of Life Sciences Prague (CULS; CZU is the Czech acronym).

221
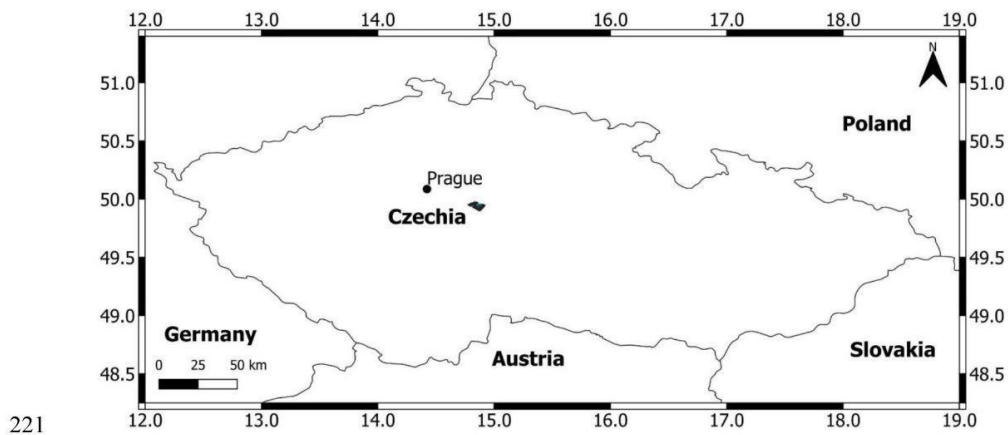
222   **FIGURE 1** | The study area location in the CULS forests, to the southeast of
223   Prague.

224   Spanning an area of approximately 5,700 hectares, the CULS forests are located
225   in a temperate climatic region. Historically, the mean annual temperature of this area
226   has been in the range of 7 to 7.5 °C, and the annual sum of precipitation has been
227   measured in the range of 600 to 650 mm (Tolasz et al., 2007). In recent times, the
228   region has been experiencing recurrent droughts, which have adversely impacted
229   forest health (Remeš, 2017). The majority of the tree species in the forests are conifers,
230   constituting about 70% of the total vegetation. Spruce is the predominant species
231   among conifers, making up 50%, while pines account for 16%, with other species
232   comprising the remainder. Broadleaved trees make up the remaining 30% of the
233   woodland, with beech being the most common at 14%, followed by oak which
234   constitutes around 10%, and other species making up the rest. In 2018, the forests
235   experienced a severe drought, which led to a significant bark beetle outbreak. *I.*
236   *typographus* was the primary species behind the infestation, but there were also

237   indications of localised infestations by other species, including *Ips duplicatus*

238   (Sahlberg), *Ips amitinus* (Eichhoff), and *Pityogenes chalcographus* (L.) (Hlásny et al.,

239   2021). Recent forest management efforts have been oriented towards sanitary logging,

240   in order to expedite the removal of trees that have been affected by these infestations,

241   as they are identified (Trubin et al., 2023; Pirtskhalava-Karpova et al., 2024).
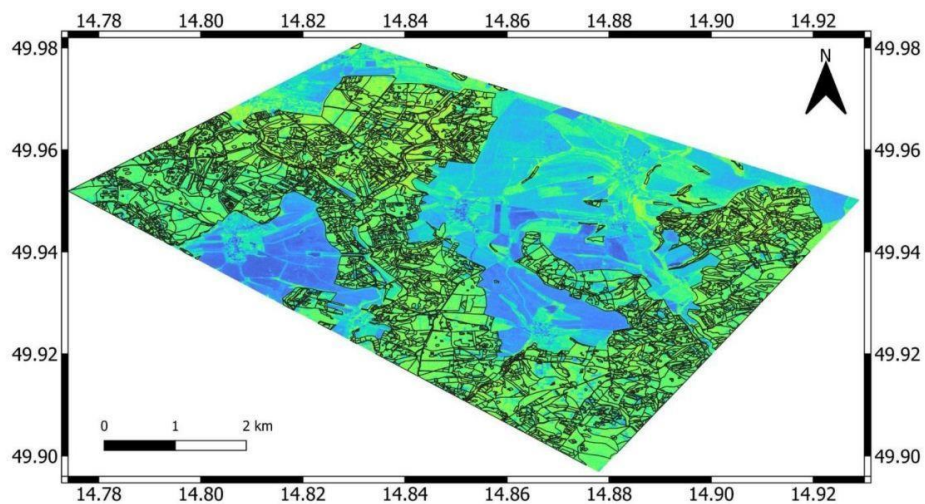
242

243   **FIGURE 2** | The School Forest Enterprise in Kostelec nad Černými lesy (town

244   in the Czech Republic), with forest management layer, clipped by the border of the

245   study area on the EVI vegetation index of Planet Imagery (14 July 2020).

246

247   2.2 Satellite data acquisition and processing

248   For satellite data acquisition and processing, GIS data collection and validation,

249   and data cleaning, we have used the methodology described by Trubin et al. (2023).

250   For our analysis, we used 16 PlanetScope images that were captured between 2 April

251 and 5 September 2020. Only cloud-free images were selected for further processing.

252 All images were downloaded in the GeoTIFF format, and surface reflectance data type

253 was selected. Every image had four bands, including Red, Green, Blue (RGB), and

254 Near Infrared (NIR), with a spatial resolution of 3 m. We computed 23 Spectral

255 Vegetation Indices for each image in the time series.

256 To differentiate between three classes of trees, we utilised the individual bands

257 and the SVIs (Table 1; formulas are provided in Supplementary Materials).

258 **TABLE 1** Spectral Vegetation Indices, their acronyms and publishers, used in the study. The

259 selection of SVI was aimed to capture a wide range of vegetative health indicators but limited with

260 number of available bands.

Spectral Vegetation Index	Acronym	Reference
Difference Vegetation Index	DVI	Tucker, 1979
Enhanced Vegetation Index	EVI	Huete et al., 2002
Green Chlorophyll Index	GCI	Gitelson et al., 2003
Green Difference Vegetation Index	GDVI	Sripada et al., 2005
Global Environmental Monitoring Index	GEMI	Pinty and Verstraete, 1992
Green Normalized Difference Vegetation Index	GNDVI	Gitelson et al., 1996
Green Optimized Soil Adjusted Vegetation Index	GOSAVI	Sripada et al., 2005
Green Ratio Vegetation Index	GRVI	Sripada et al., 2006
Green Soil Adjusted Vegetation Index	GSAVI	Sripada et al., 2005
Infrared Percentage Vegetation Index	IPVI	Crippen, 1990
Modified Soil Adjusted Vegetation Index	MSAVI2	Qi et al., 1994
Modified Simple Ratio	MSR	Chen, 1996
Normalized Difference Vegetation Index	NDVI	Rouse et al., 1974

Normalized Difference Water Index	NDWI	Gao, 1995
Non-Linear Index	NLI	Goel and Qin, 1994
Optimized Soil Adjusted Vegetation Index	OSAVI	Rondeaux et al., 1996
Perpendicular Vegetation Index	PVI	Richardson and Wiegard, 1977
Renormalized Difference Vegetation Index	RDVI	Roujean and Breon, 1995
Soil Adjusted Vegetation Index	SAVI	Huete, 1988
Simple Ratio	SR	Birth and McVey, 1968
Transformed Soil Adjusted Vegetation Index	TSAVI	Baret and Guyot, 1991
Visible Atmospherically Resistant Index	VARI	Gitelson et al., 2002
Wide Dynamic Range Vegetation Index	WDRVI	Gitelson et al., 1996
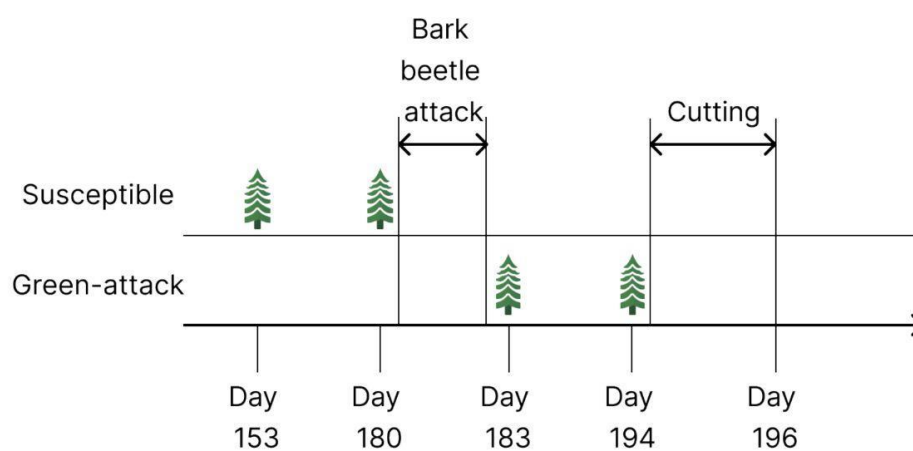
261
262   FIGURE 3 - Progression of sample class status from "Susceptible" to "Green-

263   attack" and subsequent removal.

264   The first class consisted of trees that did not exhibit any signs of attack during

265   our study year and are, therefore, labelled as the "Healthy" class. The second class is

266   comprised of trees that were attacked later in the growing season, but before the green-

267   attack phase, and they are referred to as the "Susceptible" class. The third class

268   consists of trees that were previously classified as "Susceptible", but had since reached

269   the date of bark beetle green-attack and, consequently, are designated as the "Green-

270   attack" class.

271   2.3 GIS data collection and validation

272   Foresters and researchers from the EXTEMIT-K project (partly with the help of

273   a detection dog (i.e., sniffer dog), Vošvrdová et al., 2023) logged the spatial

274   coordinates (X and Y) of trees under attack, as well as the date of the attack, the

275   species of the bark beetle, and the number of trees attacked, using the ArcGIS

276   Collector smartphone app on a weekly basis in their designated areas.

277   For this study, the spatial coordinates of a total of 61 locations, that were

278   attacked in the growing season, were used to construct polygons of these forest areas.

279   To ensure accuracy, the vectorised boundaries of the trees were visually validated to

280   avoid any spatial error. We also created a random sample of the "Healthy" class, with

281   similar attributes found for attacked areas (Table 2). Sixty-one (61) circular polygons,

282   each encompassing an area of 0.165 hectares, were randomly chosen within forest

283   management units, aged between 78 to 130 years, and having 80-100% Norway spruce

284   coverage (Trubin et al., 2023).

285

286   TABLE 2 Summary of GIS dataset used including sampling (training) datasets

287   collected in the field and from satellite imagery, and ancillary datasets of forest

288   management units. The type of datasets, e.g., vector vs. raster, and categorical vs.

289   binary, and the stage of collection during the growing season and later on, the

290   collection method, and the application or software used to extract data from them are

291   provided.

Data	Type	Stage of collection	Collection method	Application/ software used	Additional data used	Data derived from	Number of plots	Final purposes
Infested trees	Vector and categorical	Mid-growing season and later on	Field survey/sampling	ArcGIS Collector app	UAV imagery, used as base imagery in app and the date of the attack	Creating polygons of "Susceptible" and "Green attack" classes based on the date of the attack	61	Data for the "Susceptible" and "Green attack" class
Non-attacked trees	Vector and categorical	N/A	Random sampling points	QGIS	PlanetScope Imagery	Creating polygons of Healthy	61	Training data for the "Healthy" class

						class		
Forest management units	Vector and categorical	N/A	Provided by the Forestry Department	QGIS	N/A	Average area, age, and percent category of Norway Spruce	2541	Area for the "Healthy" class, with similar characteristics found for the "Susceptible" and "Green-attack" class

292

293   2.4 Data cleaning

294   The sample size of the "Healthy" class remained constant at 61 trees across all

295 images, requiring no data cleaning. However, for the "Susceptible" and "Green-attack"

296 classes, we removed samples that exhibited evidence of logging during any of the

297 imaging dates. We also excluded samples from the "Susceptible" class that had not

298 reached the green-attack phase, by the time of our temporal-scale analyses, and

299 transferred them to the "Green-attack" class once they had reached that phase. In order

300 to maintain a balanced sample size across all classes, we decided to exclude the first

301 and last five dates of imagery from our time-series datasets, specifically, all imagery

302 captured before 18 May and after 14 July (as shown in Figure 4).

Sample size of each imagery

303
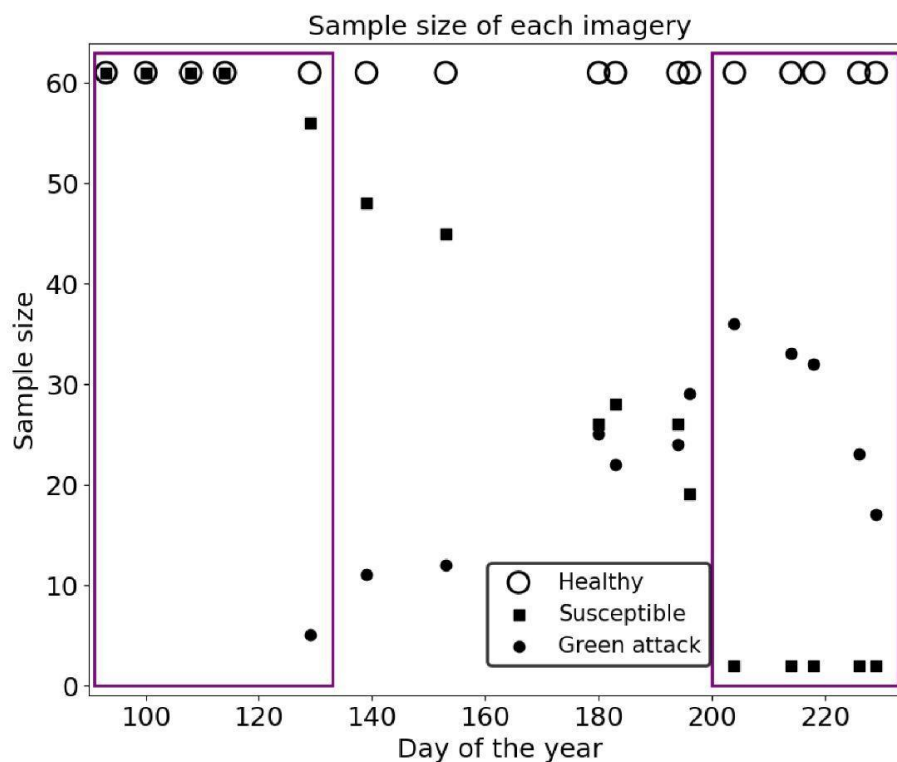
FIGURE 4 | Sample size scatterplot of the time-series dataset of the "Healthy", "Susceptible",
and "Green attack" classes. Five images with a sample size of 2 (records after Day no. 196,
corresponding to 14 July), and five images with a missing or low sample size of 5 (records before Day
no. 139, corresponding to 18 May) were excluded from the analyses (highlighted in the rectangle).

2.5 Statistics

The mean value of bands of spectral reflectance and SVIs for each polygon of
the "Healthy", "Susceptible", and "Green-attack" classes were extracted using the

313　ZonalStatistics-plugin from the OTB package in QGIS (Open Source Geographic

314　Information System).

315　　　　Assumptions for the use of parametric statistics were tested (Shapiro-Wilk test

316　and Levene test; Underwood, 2001). For the data that complied with the assumptions,

317　a One-Way Analysis of Variance (ANOVA) with Three Factors was performed,

318　followed by the Games-Howell test for the data that complied with the assumptions of

319　the Levene test, and Tukey's honestly significant difference test (Tukey's HSD) for

320　the data that did not comply. For the data that did not comply with the assumptions,

321　the nonparametric Kruskal-Wallis H Test (also termed as "one-way ANOVA on

322　ranks") with Three Independent Groups, and then Dunn's post hoc tests, were used

323　(Figure 5).
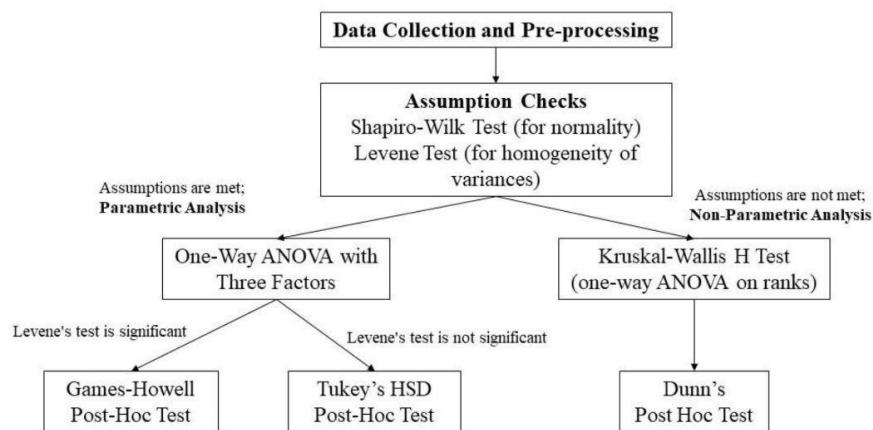
324

325　Figure 5 Description of statistics

326　　　　All statistical calculations were done in Python programming language, using

327　the SciPy library (ver. 1.7.1; Virtanen et al., 2020), statsmodels package (ver. 0.13.5;

328　Seabold and Perktold, 2010), scikit-posthocs (ver. 0.7.0; Terpilovskii, 2019).

329

330   **3 RESULTS**

331   We analysed a total of 122 polygons, comprising 61 "Healthy" class and 61

332   attacked samples, which were further categorised into either "Susceptible" or "Green-

333   attack" classes, based on the date of imagery and attack. The average area covered by

334   the forest polygons in each sample was 0.165 hectares (ha), for both the "Healthy"

335   class and attacked categories. Cumulatively, the total area spanned by the 61 attacked

336   polygons was 10.089 ha, while the "Healthy" polygons covered an area of 10.065 ha.

337   Focusing on individual bands, it was observed that out of the 72 datasets, 32 did

338   not conform to a normal distribution. When broken down by class, the "Susceptible"

339   class had 8 out of 24 datasets that were not normally distributed, the "Green attack"

340   class had 10 out of 24, and the "Healthy" class had 14 out of 24.

341   In addition, 11 of the 24 datasets in individual bands exhibited unequal

342   variances. Notably, all individual bands displayed unequal variances on Day 139.

343   Furthermore, all datasets, with the exception of the data on Day 180 in the Red band,

344   exhibited unequal variances.

345   Regarding the Spectral vegetation indices, of the 414 datasets, 188 did not

346   follow a normal distribution. Within the classes, the "Healthy" class had 105 datasets

347   that were not normally distributed, the "Susceptible" class had 22, and the "Green-

348   attack" class had 61.

349   Finally, in the SVIs, 33 out of the 138 datasets analysed showed unequal

350   variances.

351

352   3.1 Individual bands

353   One pair of classes were found to be significantly different using all individual

354 bands, based on combined evaluations of using One-Way ANOVA with Three Factors

355 or Kruskal-Wallis H Test with Three Independent Groups, and Tukey's honestly

356 significant difference test (Tukey's HSD), or Games-Howell, or Dunn's post hoc tests.

357 However, two pairs of classes were found to be significantly different, using the Green

358 band on Days 153 and 183, and the Red band on Day 194 (Table 3 and Table 4).

359   For all single bands, we found significant differences, at least between the two

360 classes (Table 3). The significant differences between the two couples of classes were

361 found for the Green band on Day 153 and 183 and the Red band on Day 194 (Table 4,

362 Figure 6).

363   TABLE 3 Test results for One-Way ANOVA with Three Factors or Kruskal-Wallis H Test

364 with Three Independent Groups: P-values for each day, using individual bands. In the table, *

365 represents $p < 0.05$, ** represents $p < 0.01$, and *** represents $p < 0.001$.

366

| Band	Day 139	Day 153	Day 180	Day 183	Day 194	Day 196
Blue	0.237	0.053	0.979	0.002**	0.696	0.004**
Green	0.336	0.001***	0.977	0.022*	0.24	0.033*
Red	0.263	0.068	0.928	0.109	0.002**	0.139
NIR	0.279	0.044*	0.742	0.454	0.312	0.533

367

368   **TABLE 4** | The results for Tukey's honestly significant difference test (Tukey's HSD),

369 Games-Howell and Dunn's post hoc tests between two classes after significant One-Way ANOVA

370 with Three Factors, or Kruskal-Wallis H Test with Three Independent Groups: P-values for each day,

371 using individual bands. In the table, * represents $p < 0.05$, ** represents $p < 0.01$, and *** represents p

372 < 0.001.

Band	Day	Healthy versus Susceptible	Healthy versus Green attack	Susceptible versus Green attack
Blue	183	0.15	0.0021**	0.28
Blue	196	0.17	0.0043**	0.66
Green	153	0.0023**	0.016*	0.8
Green	183	1	0.038*	0.035*
Red	194	0.01*	0.81	0.0023**
NIR	153	0.034*	0.67	0.76

373

374

375
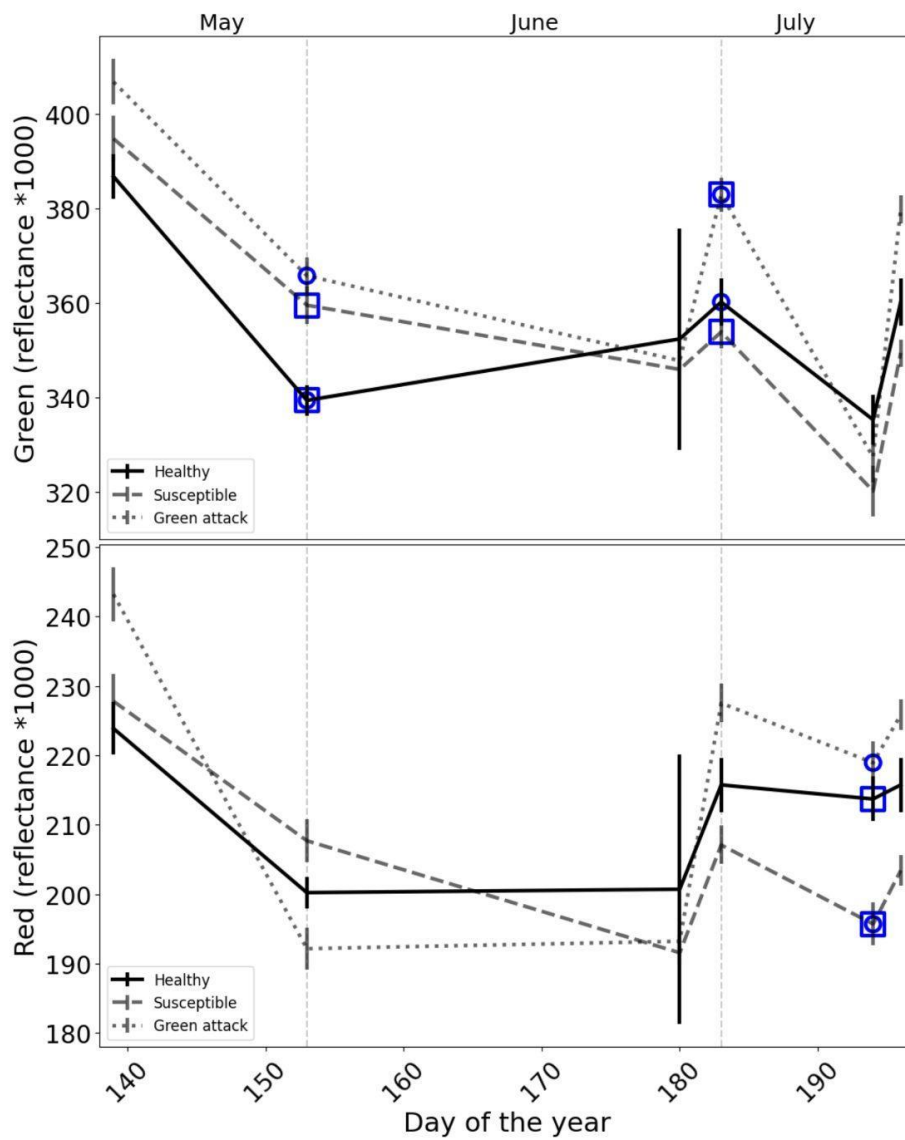
FIGURE 6 | Green and Red bands graph with mean and standard error, that had significant differences between two couples of classes. Each shape of blue figures (circles and rectangles) identifies a pair of classes where significant differences were met.

379

380   3.2 Spectral Vegetation Indices

381   One pair of classes was found to be significantly different at most of the SVIs,

382   based on combined evaluations of using One-Way ANOVA with Three Factors, or

383   Kruskal-Wallis H Test with Three Independent Groups and Tukey's honestly

384   significant difference test (Tukey's HSD), or Games-Howell, or Dunn's post hoc tests.

385   However, the two pairs of classes were found to be differentiated, at most, using two

386   SVIs; the EVI and VARI on Day 196 resulted in the p-value of post hoc test being less

387   than 0.001 or between 0.01 and 0.01, and the p-value for One-Way ANOVA with

388   Three Factors or Kruskal-Wallis H Test with Three Independent Groups being less

389   than 0.001 (Table 5 and Table 6).

390   For SVI 17 of 23 VI, we found significant differences, at least between the two

391   classes (Table 5). The significant differences between the two couples of classes were

392   found for EVI and VARI on Day 196 and IPVI, MSR, OSAVI, and SR on Day 194

393   (Table 6, Figure 7).

394

395   TABLE 5 - Test results for One-Way ANOVA with Three Factors or Kruskal-Wallis H Test

396   with Three Independent Groups: P-values for each day, using different spectral vegetation indices. In

397   the table, * represents $p < 0.05$, ** represents $p < 0.01$, and *** represents $p < 0.001$.

Index	Day 139	Day 153	Day 180	Day 183	Day 194	Day 196
DVI	0.25	0.059	0.39	0.26	0.16	0.44
EVI	0.48	0.23	0.019*	9.10E-05***	0.038*	1.20E-05***

|						
GCI	0.45	0.16	0.92	0.027*	0.014*	0.063
GDVI	0.27	0.088	0.37	0.22	0.17	0.46
GEMI	0.28	0.19	0.66	0.51	0.2	0.87
GNDVI	0.34	0.1	0.97	0.015*	0.037*	0.038*
GOSAVI	0.34	0.1	0.97	0.015*	0.037*	0.038*
GRVI	0.45	0.16	0.92	0.027*	0.014*	0.063
GSAVI	0.34	0.1	0.97	0.015*	0.037*	0.038*
IPVI	0.27	0.18	0.95	0.033*	0.0021**	0.05*
MSAVI	0.41	0.31	0.8	0.0069**	0.43	0.028*
MSR	0.4	0.15	0.95	0.053	0.00072***	0.078
NDVI	0.45	0.3	0.6	0.0073**	0.39	0.029*
NDWI	0.34	0.1	0.97	0.015*	0.037*	0.038*
NLI	0.17	0.11	0.6	0.04*	0.033*	0.091
OSAVI	0.27	0.18	0.95	0.033*	0.0021**	0.05*
PVI	0.28	0.067	0.67	0.49	0.28	0.64
RDVI	0.21	0.083	0.23	0.11	0.064	0.24
SAVI	0.45	0.3	0.6	0.0073**	0.39	0.029*
SR	0.45	0.15	0.91	0.065	0.00051***	0.095
TSAVI	0.48	0.31	0.48	0.0078**	0.36	0.03*
VARI	0.49	0.22	0.01**	1.30E-05***	0.47	1.10E-06***
WDRVI	0.23	0.054	0.89	0.46	0.29	0.61

398

399   **TABLE 6** The results for Tukey's honestly significant difference test (Tukey's HSD), Games-

400   Howell and Dunn's post hoc tests between two classes after significant One-Way ANOVA with Three

401   Factors or Kruskal-Wallis H Test with Three Independent Groups: P-values for each day, using

402 different spectral vegetation indices. In the table, * represents p < 0.05, ** represents p < 0.01, and ***

403 represents p < 0.001.

Index	Day	Healthy versus Susceptible	Healthy versus Green attack	Susceptible versus Green attack
EVI	180	0.16	0.025**	0.77
	183	0.0001***	0.2	0.097
	194	0.12	0.38	0.012*
	196	0.001**	0.27	0.0025**
GNDVI	183	0.37	0.089	0.011*
	196	0.19	0.27	0.016*
MSAVI	183	0.49	0.0048*	0.14
	196	0.44	0.023*	0.61
NDVI	183	0.5	0.0051**	0.15
	196	0.44	0.024*	0.61
NDWI	183	0.37	0.089	0.011*
	196	0.19	0.27	0.016*
SAVI	183	0.5	0.0051**	0.15
	196	0.44	0.024*	0.61
TSAVI	183	0.5	0.0054**	0.15
	196	0.45	0.025*	0.62
VARI	180	0.0055**	0.092	0.9
	183	0***	0.054	0.15
	196	0***	0.06	0.0056**
GCI	183	0.49	0.11	0.021*
	194	0.041*	0.69	0.35
GOSAVI	183	0.37	0.089	0.011*

	196	0.19	0.27	0.016*
GRVI	183	0.49	0.11	0.021*
	194	0.041*	0.69	0.35
GSAVI	183	0.37	0.089	0.011*
	196	0.19	0.27	0.016*
IPVI	183	0.2	0.33	0.026*
	194	0.006**	0.71	0.004**
	196	0.059	0.57	0.017*
MSR	194	0.0017**	0.82	0.0023**
NLI	183	0.14	0.53	0.038*
	194	0.067	0.77	0.042*
OSAVI	183	0.2	0.33	0.026*
	194	0.006**	0.71	0.004**
	196	0.059	0.57	0.017*
SR	194	0.0011**	0.86	0.002**

404
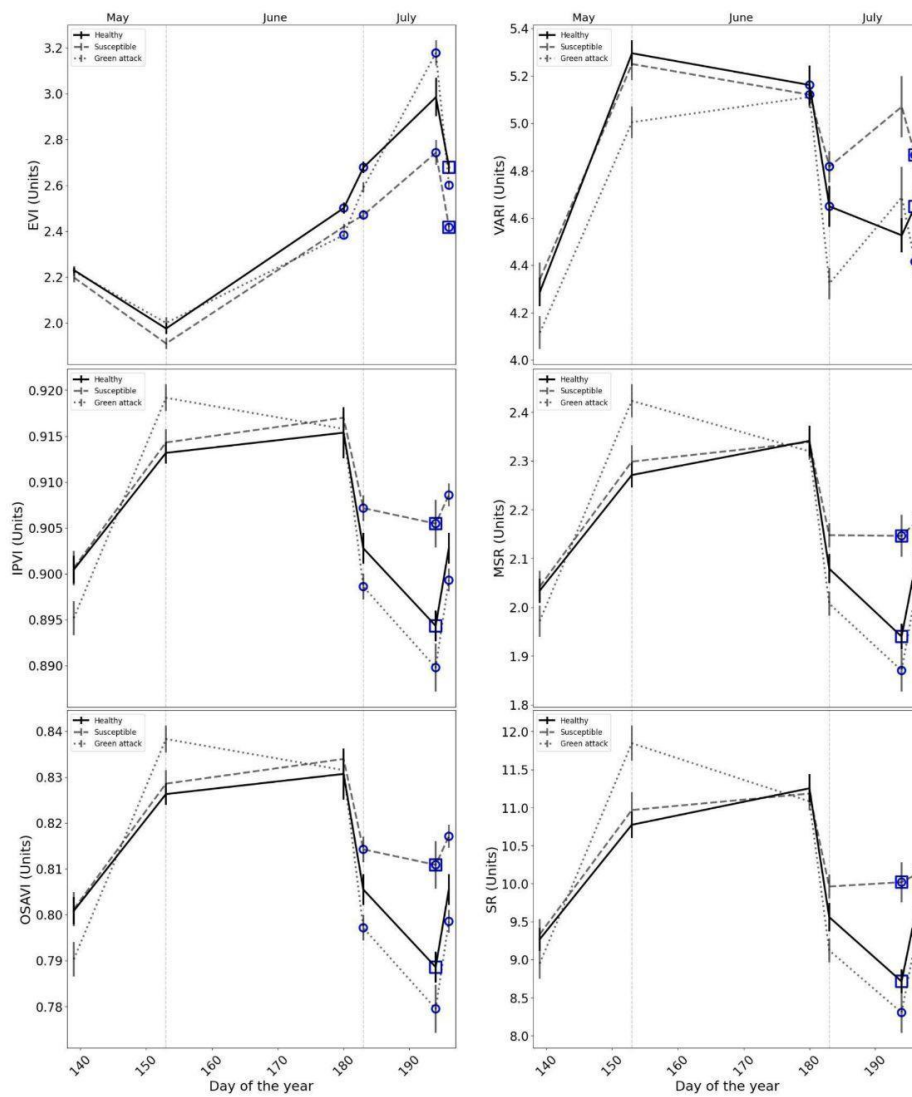
FIGURE 7 | EVI, VARI, IPVI, MSR, OSAVI, and SR vegetation indices graph with mean and
standard error that had significant differences between one or two couples of classes. Each shape of
blue figures (circles and rectangles) identifies a pair of classes where significant differences were met.

408

409   **4. DISCUSSION**

410   Our results show that all four wavebands of PlanetScope and several vegetation

411   indices allow to detect trees that are susceptible to bark beetle infestation and green-

412   attack phases. However, the studied wavebands and spectral vegetation indices had

413   relatively high variability and seasonal dynamics (Figures 6 and 7). We have not found

414   a single waveband or vegetation index that would be able to distinguish between

415   healthy, susceptible, and green-attacked trees, even on a single date, with statistically

416   significant results.

417

418   4.1 Wavebands with potential for the detection of Norway spruce trees

419   susceptible to bark beetle infestation and green-attack.

420   All four wavebands allow to detect trees that are susceptible to bark beetle

421   infestation and green-attack phases (Table 3, Table 4, Figure 6) on specific days (Blue

422   – days 183 and 196; Green – days 153 and 183; Red – day 194, NIR – day 153) during

423   vegetation season. However, the Red and especially Green wavebands have shown the

424   best results. Green waveband has shown the best results in distinguishing between

425   healthy and green-attacked trees in May and July (Figure 6). In May, there were

426   statistically significant differences between healthy and jointly susceptible and green-

427   attacked trees. However, in July, there was the strongest difference between green-

428   attacked and susceptible trees. In the case of days with statistically significant results,

429   Green waveband was consistent in distinguishing between healthy and green-attacked

430   trees, and green-attacked trees had higher reflectance than healthy trees. The results

431   that are connected with the green reflectance performance in the second half of the

432   season are in agreement with the findings of Huo et al. (2023).

433   Red waveband was able to distinguish between healthy and green-attacked trees

434   at the end of the study period. This finding is in agreement with the results of Huo et

435   al. (2021), Bárta et al. (2022), and Dalponte et al. (2023). The decrease in chlorophyll

436   content leads to a reduction in spectral absorption in the visible region, resulting in

437   higher reflectance, particularly in the Red band (Carter and Knapp, 2001).

438   The NIR waveband was the least important for spectral separability. It is also in

439   agreement with the works of Huo et al. (2021), Bárta et al. (2022), and Dalponte et al.

440   (2023).

441

442   4.2 Spectral vegetation indices that are suitable for the detection of Norway

443   spruce trees, which are susceptible to bark beetle infestation and green-attack phases

444   Spectral vegetation indices show statistically significant results only in the

445   second half of the study period (Table 5, Table 6, Figure 7). Similar to the results of a

446   single-result-set analysis, this finding is in agreement with the results of Dalponte et al.

447   (2023). Only GNDVI and NDVI were used in our study, and in the study by Dalponte

448   et al. (2023), with similar performances in both studies. However, both indexes did not

449   achieve the best results in our study. Among all spectral vegetation indices we

450   investigated, EVI and VARI were found to be the indices with the best potential to,

451   simultaneously, detect trees that are susceptible to bark beetle infestation and green-

452   attack phases (Table 6; the lowest p-value), similar to the works of Huo et al. (2021)

453   and Trubin et al. (2023). The VARI Index on Day 196 was significantly different

454   between healthy trees, and trees that are susceptible to bark beetle infestation, and

455   green-attack (significant post hoc test for two pairs); hence, the values for the

456   susceptible trees were much higher than for the healthy/control trees; and green-attack

457   values were the lowest. However, the EVI shows better performance during the entire

458   season (post hoc test for two pairs appeared four times, Table 6), and results are

459   consistent for distinguishing between healthy and susceptible trees. In contrast to the

460   VARI, susceptible and green-attack (excluding Day 194) trees were always showing

461   lower values for the EVI than healthy trees, during the days of significant differences,

462   at least for one pair of classes. The observed patterns may indicate that the EVI could

463   be the best index for the detection of Norway spruce trees that are susceptible to bark

464   beetle infestation and green-attack phases.

465   Interestingly, IPVI and SAVI show the most consistent results in the second

466   half of the study period. Trees with green-attacks have the lowest values. Healthy trees

467   have higher values, and trees with green-attack have the highest values.

468   Therefore, we may be required to use a different set of SVIs, e.g., EVI and

469   VARI vs. IPVI and SAVI, over the course of a growing season as trees are less likely

470   water-stressed in the first half of a growing season than the second half. Similarly,

471   individual wavebands, e.g., Blue, Green, and Red, can be prioritized to differentiate

472   our proposed three classes, healthy, susceptible, and green-attacked trees, in the first

473   and second half of the growing season.

474

475   4.3 Assessment of statistical methods

476   In our previous paper (Trubin et al., 2023), we used Welch's t-test, followed by

477   Linear Discriminant Analysis (LDA) with leave-one-out cross-validation accuracy

478   (LOOCV), in order to examine the overall classification accuracy (CA) and to evaluate

479   the separability between forests that are susceptible to attacks, and healthy forests. The

480   significant results (LDA accuracy greater than 0.7 and p-value for the Welch's t-test

481   less than 0.05) of the separability between forests that are susceptible to attacks, and

482   healthy forests of the previous paper, and the current statistical approach were

483   archived on Day 183 with EVI and VARI. In the current paper, we also found

484   significant results for the separability between forests that are susceptible to attacks

485   and healthy forests on Day 194 (GCI, GRVI, IPVI, MSR, OSAVI, SR), Day 196 (EVI,

486   VARI), and Day 180 (VARI).

487   These additional findings reinforce the robustness of the separability between

488   trees that are susceptible to attack and healthy trees, providing further evidence of the

489   reliability and consistency of the classification accuracy results. The collective

490   findings from our previous and current studies contribute to a comprehensive

491   understanding of the separability dynamics, and highlight the potential of utilising

492   different statistical approaches to evaluate forest health and susceptibility to attacks,

493   using EVI and VARI SVIs.

494

495   4.4 Spectral separation between 3 groups of trees in relation to the mechanism

496   to bark beetle attack.

497   An important point in the present study, is that our results (Figures 6 and 7)

498   show certain spectral separations in single wavebands or vegetation indices, between

499   susceptible and green-attacked forest areas, only since July. We can see the seasonal

500   switch in the green waveband (Figure 6). In May, susceptible and green-attacked trees

501   exhibit higher reflectance compared to healthy trees. However, in July, there is no

502   statistical difference between healthy and susceptible trees. Green- attacked trees still

503   show higher reflectance than susceptible trees. Stressed trees should show higher

504   reflectance than healthy trees in the visible part of the spectrum (Carter and Knapp,

505   2001). In the Red waveband, there is no statistically significant difference between

506   green-attacked and healthy trees. However, susceptible trees have lower reflectance,

507   and this difference is statistically significant.

508   The EVI spectral vegetation index shows consistently lower values for

509   susceptible trees, rather than the healthy trees, during the whole study period (Figure

510   7). There are no statistical differences between susceptible and green-attacked trees

511   until the beginning of June. However, in June, green-attacked trees showed statistically

512   significant higher values.

513   In the first half of the study period, no differences in spectral signatures

514   between susceptible and green-attacked trees were observed, as described by Huo et al.

515   (2021). However, spectral differences between healthy and susceptible trees were

516   observed prior to the bark beetle attacks, as also noted by Huo et al. (2021) and Trubin

517   et al. (2023). A similar pattern, spectral differences between healthy trees and trees

518   that were attacked later, were also shown by Minařík and Langhammer (2016) and

519   Abdullah et al. (2019). Lausch et al. (2013) have shown these differences in the year

520   before attacks occurred.

521   The spectral difference existing before attacks may be related to acute thermal

522   stress of fresh forest edges (Kautz et al., 2013) or drought stress (Netherer et al., 2014),

523   which predispose trees to bark beetle attacks. Another point is a temporal and spatial

524   autocorrelation between current and previous bark beetle attacks (Aukema et al., 2006;

525   Aukema et al., 2008; Wulder et al., 2009; Simard et al., 2011; Kamińska, 2022). It

526   means that the newly attacked trees in our study area should be located near clearcut

527   areas caused by salvage cutting in the previous or current year. Forest edges also show

528   spectral signatures that are different to those in forest interiors (Buras et al., 2018).

529   It seems that abiotic stress related to bark beetle attack, and physiological

530   processes related to initial bark beetle infestation in the first half of vegetation season,

531   affect the spectral signatures of trees in similar ways, especially in studied spectral

532   ranges, or where the effect of bark beetle attack on leaf spectral reflectance has a

533   delayed effect. According to Abdullah et al. (2019), the earliest period in which the

534   spectral difference between infested and healthy trees can be visible is in the

535   differences in spectral signatures from mid-June to the beginning of July.

536   The switch between 'green reflectance' and 'no difference in spectral

537   reflectance' between healthy and susceptible trees in July (Figure 6) and, partially, also

538   the pattern in the Red waveband, can also be explained by the mechanism of host

539   selection. *I. typographus*, the first target, at the beginning of the season, represents

540   physiologically weak trees. Later, by a pheromone-based switching mechanism,

541   relatively healthy trees can be attacked (Korolyova et al., 2022).

542

543   4.5. Limitations of the study

544   In line with the limitations highlighted in our previous study (Trubin et al.,

545   2023), there are certain constraints and considerations that should be acknowledged in

546   relation to the present study. The spectral resolution was limited by the choice of the

547   sensor with 4 bands, due to the year of our observation, and it is preferable to use

548   datasets with Red Edge (which could be achieved with the PlanetScope products of the

549   3rd generation sensors, known as SuperDove or PSB.SDafter) and SWIR (which could

550   be achieved with the Sentinel-2, with coarser spatial resolution) bands. Huo et al.

551   (2023) show that the Red Edge waveband has good potential for distinguishing

552   between healthy and green-attacked trees. The additional coefficients in vegetation

553   indices like PVI, TSAVI, and WDRVI, which are unrelated to band values, were set as

554   recommended default values due to limitations in GIS data collection campaigns, but

555   more precise ground truth data, including these parameters, could enhance the

556   performance of the indices. However, Dalponte et al. (2023) achieved similar results in

557   their research, as we did in the present study with the SuperDove data. Significant

558   improvement could, possibly, be achieved with the use of the SWIR waveband, and

559   also by the possible use of the NDRS vegetation index of Huo et al. (2021).

560   Weekly identification of ground truth data revealed the locations of all bark

561   beetle infestations; however, the cause of the infestations remains undetermined, with

562   each infestation area potentially being triggered by unharvested internal and/or

563   neighbouring trees from 2019.

564   Transitioning to an individual tree level has the potential to enhance the

565   accuracy of detection of the separability between classes, but requires additional data

566   collection (such as high-resolution airborne LiDAR data) and preprocessing, geometric

567   correction, fusion, and validation, to ensure compatibility and accurate alignment

568   (Dalponte et al., 2023).

569   4.6 Management implications

570   We can expect relatively large bark beetle outbreaks in extensive areas in the

571   future (Hlásny et al., 2021). Airborne detection encounters inherent difficulties in

572   achieving precise timing(s) for aircraft flights. The need for a substantial number of

573   images adds to the complexity of image processing, including tasks like

574   georeferencing, mosaicing, and absolute reflectance correction. Consequently, this also

575   increases the associated costs. Additionally, since the spectral conditions often differ

576   from one scene to another, normalisation becomes necessary, in order to ensure

577   consistency across images. However, this normalisation process reduces the overall

578   variability of spectral values, which in turn affects the effectiveness of detection

579   algorithms (Wulder et al., 2009). Consequently, the combination of local field surveys

580   and phenology models can serve as a valuable strategy to determine the most suitable

581   timing for conducting airborne sensing activities (Bárta et al., 2022). The timely

582   generation of image processing and information regarding green-attack is crucial, as it

583   needs to be swiftly provided to forest managers. Otherwise, if the information is not

584   provided promptly, forest managers may (inaccurately) continue relying on existing

585   field surveys (Kautz et al., 2022). An important point is the detection delay of remote

586   sensing methods (Marvasti-Zadeh et al., 2023). Terrestrial methods can detect bark

587   beetle attached trees almost immediately (Kautz et al., 2022, Vošvrdová et al., 2023).

588   Detection delay, in case of the use of remote sensing methods for the detection of bark

589   beetle attack, can be 23 days (Barta et al. 2022).

590   In order to detect bark beetle attacks in large areas, the use of satellite data with

591   a high frequency of scanning, such as PlanetScope products would, possibly, be the

592   best approach (Zahibi et al., 2021). The possibility to detect predisposition could,

593   possibly, be an advantage in the case where we can use the detection in the bark beetle

594   attack prediction model, involving spatial autocorrelation of bark beetle attack

595   (Ďuračiová et al., 2020). Optimally, it should be an online web map application

596   suggesting to foresters to physically detect bark beetle-attacked trees. Field detection

597   can be further enhanced by the use of the aforementioned sniffer dogs (Vošvrdová et

598   al., 2023).

599   Huo et al. (2023) assume that drone imagery with better spatial resolution

600   should be a better methodology in early attack detection than satellite imagery.

601   However, the differences are probably not so large. The main issue is the necessity for

602   covering the whole area of the bark beetle outbreak, and arranging the early removal

603   of attacked trees in all areas. Otherwise, we could have a mosaic of areas with a

604   different system of management. Such a situation would cause extensive additional

605   damage in buffer zones (Mezei et al., 2017).

606   **5 CONCLUSIONS**

607   The findings of this study provide insights into the separability between

608   healthy, susceptible, and green-attacked trees using PlanetScope imagery and spectral

609   analysis. The Green and Red wavebands emerged as promising indicators for

610   distinguishing between these three categories. Green-attacked trees had higher

611   reflectance than healthy trees in the second half of the season. Towards the end of the

612   study period, the Red waveband showed significant differences, with susceptible trees

613   displaying lower reflectance compared to healthy trees.

614   The observed spectral differences between healthy and susceptible trees before

615   bark beetle attacks suggest the presence of abiotic stress and physiological processes

616   related to initial infestation. It is likely that physiologically weak trees, which exhibit

617   higher reflectance in the Green waveband, are initially targeted by the bark beetles.

618   However, as the infestation progresses, the bark beetles employ a host selection

619   mechanism that enables them to also attack relatively healthy trees. This mechanism

620   may explain the switch in green reflectance, and the absence of spectral differences

621   between healthy and susceptible trees in July.

622   Furthermore, the findings underscore the importance of considering multiple

623   wavebands and spectral indices. The EVI and VARI spectral vegetation indices

624   demonstrated potential in detecting trees that are susceptible to bark beetle infestation

625   and green-attack phases. The consistently lower values of EVI for susceptible trees

626   throughout the study period suggest a spectral signature that is associated with their

627   predisposition to infestation.

628   These insights into the spectral separability between healthy, susceptible, and

629   green-attacked trees contribute to our understanding of the dynamics of bark beetle

630   infestations, and the potential influence of the predisposition factors. Further research

631   is needed to refine and validate these findings, enhance the accuracy of detection

632   methods, and gain a deeper understanding of the underlying mechanisms behind the

633   predisposition.

634   To optimize early detection of bark beetle-attacked trees, an integrated system

635   employing high-resolution satellite platforms like PlanetScope, equipped with sensors

636   finely tuned to the Green and Red wavebands and capable of computing indices such

637   as EVI and VARI, is recommended for its precision in capturing the spectral

638   signatures indicative of tree susceptibility and early infestation stages with high spatial

639   and temporal resolution.

640

650

REFERENCES

Abdollahnejad, A., and Panagiotidis, D. (2020). Tree species classification and health status assessment for a mixed broadleaf-conifer forest with UAS multispectral imaging. Remote Sens. 12:3722. doi: 10.3390/rs12223722

Abdullah, H., Darvishzadeh, R., Skidmore, A. K., Groen, T. A., and Heurich, M. (2018). European spruce bark beetle (Ips typographus, L.) green attack affects foliar reflectance and biochemical properties. International Journal of Applied Earth Observation and Geoinformation 64, 199–209. doi: 10.1016/j.jag.2017.09.009.

Abdullah, H., Skidmore, A. K., Darvishzadeh, R., and Heurich, M. (2019a). Sentinel-2 accurately maps green-attack stage of European spruce bark beetle (Ips typographus. L.) compared with Landsat-8. Remote Sens. Ecol. Conserv. 5, 87–106. doi: 10.1002/rse2.93

Abdullah, H., Skidmore, A. K., Darvishzadeh, R., and Heurich, M. (2019b). Timing of red-edge and shortwave infrared reflectance critical for early stress detection induced by bark beetle (Ips typographus, L.) attack. Int. J. Appl. Earth Observ. Geoinform. 82, 101900. doi: 10.1016/j.jag.2019.101900

Ali, A. M., Abdullah, H., Darvishzadeh, R., Skidmore, A. K., Heurich, M., Roeoesli, C., et al., (2021). Canopy chlorophyll content retrieved from time series remote sensing data as a proxy for detecting bark beetle infestation. Remote Sens. Appl. Soc. Envi. 22:100524.

671   Allen, C. D., Macalady, A. K., Chenchouni, H., Bachelet, D., McDowell, N.,

672   Vennetier, M., et al., (2010). A global overview of drought and heat-induced tree

673   mortality reveals emerging climate change risks for forests. For. Ecol. Manag. 259,

674   660–684. doi: 10.1016/j.foreco.2009.09.001

675   Aukema, B. H., Carroll, A. L., Zheng, Y., Zhu, J., Raffa, K. F., Moore, R. D., et

676   al., (2008). Movement of outbreak populations of mountain pine beetle: Influences of

677   spatiotemporal patterns and climate. Ecography 31, 348–358.

678   Aukema, B. H., Carroll, A. L., Zhu, J., Raffa, K. F., Sickley, T., and Taylor, S.

679   W. (2006). Landscape level analysis of mountain pine beetle in British Columbia,

680   Canada: Spatiotemporal development and spatial synchrony within the present out-

681   break. Ecography 29, 427–441.

682   Bače, R., Svoboda, M., Janda, P., Morrissey, R. C., Wild, J., Clear, J. L., et al.,

683   (2015). Legacy of pre-disturbance spatial pattern determines early structural diversity

684   following severe disturbance in montane spruce forests. PLoS One 10:e0139214. doi:

685   10.1371/journal.pone.0139214

686   Baret, F., and Guyot, G. (1991). Potentials and limits of vegetation indices for

687   LAI and APAR assessment. Remote Sens. Environ. 35, 161–173.

688   Bárta, V., Hanuš, J., Dobrovolný, L., and Homolová, L. (2022). Comparison of

689   field survey and remote sensing techniques for detection of bark beetle-infested trees.

690   Forest Ecology and Management 506, 119984. doi: 10.1016/j.foreco.2021.119984.

691   Bentz, B. J., and Jönsson, A. M. (2015). "Modeling bark beetle responses to

692   climate change," in Bark beetles, eds F. E. Vega and R. W. Hofstetter (London:

693   Elsevier), 533–553. doi: 10.1016/B978-0-12-417156-5.00013-7

694   Bentz, B. J., Régnière, J., Fettig, C. J., Hansen, E. M., Hayes, J. L., Hicke, J. A.,

695   et al., (2010). Climate change and bark beetles of the western United States and

696   Canada: Direct and indirect effects. BioScience 60, 602–613.

697   Birth, G., and McVey, G. (1968). Measuring the color of growing turf with a

698   reflectance spectrophotometer. Agron. J. 60, 640–643.

699   Blackburn, G. A. (1998). Spectral indices for estimating photosynthetic

700   pigment concentrations: A test using senescent tree leaves. Int. J. Remote Sens. 19,

701   657–675. doi: 10.1080/014311698215919

702   Blackburn, G. A. (2006). Hyperspectral remote sensing of plant pigments. J.

703   Exp. Bot. 58, 855–867. doi: 10.1093/jxb/erl123

704   Brovkina, O., Cienciala, E., Surový, P., and Janata, P. (2018). Unmanned aerial

705   vehicles (UAV) for assessment of qualitative classification of Norway spruce in

706   temperate forest stands. Geospatial Inform. Sci. 21, 12–20. doi:

707   10.1080/10095020.2017.1416994

708   Buras, A., Schunk, C., Zeiträg, C., Herrmann, C., Kaiser, L., Lemme, H., et al.

709   (2018). Are Scots pine forest edges particularly prone to drought-induced mortality?

710   Environ. Res. Lett. 13, 025001. doi: 10.1088/1748-9326/aaa0b4.

711   Carter, G. A., and Knapp, A. K. (2001). Leaf optical properties in higher plants:

712   linking spectral characteristics to stress and chlorophyll concentration. Am. J. Bot. 88,

713   677–684. doi: 10.2307/2657068.

714   Chen, J. (1996). Evaluation of vegetation indices and modified simple ratio for

715   boreal applications. Can. J. Remote Sens. 22, 229–242.

716   Christiansen, E., and Bakke, A. (1988). "The spruce bark beetle of Eurasia," in

717   Dynamics of forest insect populations, ed. A. A. Berryman (Boston, MA: Springer

718   US), 479–503. doi: 10.1007/978-1-4899-0789-9_23

719   Colombari, F., Schroeder, M. L., Battisti, A., and Faccoli, M. (2013). Spatio-

720   temporal dynamics of an Ips acuminatus outbreak and implications for management.

721   Agric. For. Entomol. 15, 34–42. doi: 10.1111/j.1461-9563.2012.00589.x

722   Crippen, R. (1990). Calculating the vegetation index faster. Remote Sens.

723   Environ. 34, 71–73.

724   Dalponte, M., Cetto, R., Marinelli, D., Andreatta, D., Salvadori, C., Pirotti, F.,

725   et al. (2023). Spectral separability of bark beetle infestation stages: A single-tree time-

726   series analysis using Planet imagery. Ecological Indicators 153, 110349. doi:

727   10.1016/j.ecolind.2023.110349.

728   DeRose, R. J., Bentz, B. J., Long, J. N., and Shaw, J. D. (2013). Effect of

729   increasing temperatures on the distribution of spruce beetle in Engelmann spruce

730   forests of the Interior West USA. For. Ecol. Manag. 308, 198–206. doi:

731   10.1016/j.foreco.2013.07.061

732   Duračiová, R., Muňko, M., Barka, I., Koreň, M., Resnerová, K., Holuša, J., et

733   al. (2020). A bark beetle infestation predictive model based on satellite data in the

734   frame of decision support system TANABBO. iForest 13, 215–223. doi:

735   10.3832/ifor3271-013.

736   Fettig, C. J., Klepzig, K. D., Billings, R. F., Munson, A. S., Nebeker, T. E.,

737   Negrón, J. F., et al., (2007). The effectiveness of vegetation management practices for

738   prevention and control of bark beetle infestations in coniferous forests of the western

739   and southern United States. For. Ecol. Manag. 238, 24–53.

740   Gao, B.-C. (1995). "Normalized difference water index for remote sensing of

741   vegetation liquid water from space," in Proceedings of the SPIE, eds M. R. Descour, J.

742   M. Mooney, D. L. Perry, and L. R. Illing (Orlando, FL), 225. doi: 10.1117/12.210877

743   Gely, C., Laurance, S. G. W., and Stork, N. E. (2020). How do herbivorous

744   insects respond to drought stress in trees? Biol. Rev. 95, 434–448. doi:

745   10.1111/brv.12571

746   Gitelson, A. A. (2004). Wide dynamic range vegetation index for remote

747   quantification of biophysical characteristics of vegetation. J. Plant Physiol. 161, 165–

748   173. doi: 10.1078/0176-1617-01176

749   Gitelson, A. A., Kaufman, Y. J., and Merzlyak, M. N. (1996). Use of a green

750   channel in remote sensing of global vegetation from EOS-MODIS. Remote Sens.

751   Environ. 58, 289–298. doi: 10.1016/S0034-4257(96)00072-7

752   Gitelson, A., Gritz, Y., and Merzlyak, M. (2003). Relationships between leaf

753   chlorophyll content and spectral reflectance and algorithms for non-destructive

754   chlorophyll assessment in higher plant leaves. J. Plant Physiol. 160, 271–282. doi:

755   10.1078/0176-1617-00887

756   Gitelson, A., Stärk, R. F., Grits, U., Rundquist, D. C., Kaufman, Y. J., and

757   Derry, D. (2002). Vegetation and soil lines in visible spectral space: A concept and

758   technique for remote estimation of vegetation fraction. Int. J. Remote Sens. 23, 2537–

759   2562.

760   Goel, N., and Qin, W. (1994). Influences of canopy architecture on

761   relationships between various vegetation indices and LAI and Fpar: A computer

762   simulation. Remote Sens. Rev. 10, 309–347.

763   Grizonnet, M., Michel, J., Poughon, V., Inglada, J., Savinaud, M., and Cresson,

764   R. (2017). Orfeo ToolBox: Open source processing of remote sensing images. Open

765   Geospatial Data Softw. Stand. 2:15. doi: 10.1186/s40965-017-0031-6

766   Hastie, T., Tibshirani, R., and Friedman, J. H. (2009). The elements of

767   statistical learning: Data mining, inference, and prediction, 2nd Edn. New York, NY:

768   Springer.

769   Havašová, M., Ferenčík, J., and Jakuš, R. (2017). Interactions between

770   windthrow, bark beetles and forest management in the TATRA national parks. For.

771   Ecol. Manag. 391, 349–361. doi: 10.1016/j.foreco.2017.01.009

772   Hlásny, T., Barka, I., Merganičová, K., Køístek, Š, Modlinger, R., Turčáni, M.,

773   et al., (2022). A new framework for prognosing forest resources under intensified

774   disturbance impacts: Case of the Czech Republic. For. Ecol. Manag. 523:120483. doi:

775   10.1016/j.foreco.2022.120483

776   Hlásny, T., Zajíčková, L., Turčáni, M., Holuša, J., and Sitková, Z. (2011).

777 Geographical variability of spruce bark beetle development under climate change in

778 the Czech Republic. J. For. Sci. 57, 242–249. doi: 10.17221/104/2010-JFS

779   Hlásny, T., Zimová, S., Merganičová, K., Štěpánek, P., Modlinger, R., and

780 Turčáni, M. (2021). Devastating outbreak of bark beetles in the Czech Republic:

781 Drivers, impacts, and management implications. For. Ecol. Manag. 490:119075. doi:

782 10.1016/j.foreco.2021.119075

783   Hlásny, T., König, L., Krokene, P., Lindner, M., Montagné-Huck, C., Müller,

784 J., et al. (2021). Bark Beetle Outbreaks in Europe: State of Knowledge and Ways

785 Forward for Management. Curr Forestry Rep 7, 138–165. doi: 10.1007/s40725-021-

786 00142-x.

787   Huete, A. (1988). A soil-adjusted vegetation index (SAVI). Remote Sens.

788 Environ. 25, 295–309.

789   Huete, A., Didan, K., Miura, T., Rodriguez, E. P., Gao, X., and Ferreira, L. G.

790 (2002). Overview of the radiometric and biophysical performance of the MODIS

791 vegetation indices. Remote Sens. Environ. 83, 195–213.

792   Huo, L., Persson, H. J., and Lindberg, E. (2021). Early detection of forest stress

793 from European spruce bark beetle attack, and a new vegetation index: Normalized

794 distance red & SWIR (NDRS). Remote Sens. Environ. 255:112240. doi:

795 10.1016/j.rse.2020.112240

796   Huo, L., Lindberg, E., Bohlin, J., and Persson, H. J. (2023). Assessing the

797 detectability of European spruce bark beetle green attack in multispectral drone images

798   with high spatial- and temporal resolutions. Remote Sensing of Environment 287,

799   113484. doi: 10.1016/j.rse.2023.113484.

800   Immitzer, M., Vuolo, F., and Atzberger, C. (2016). First experience with

801   Sentinel-2 data for crop and tree species classifications in central Europe. Remote

802   Sens. 8:166. doi: 10.3390/rs8030166

803   Jactel, H., Petit, J., Desprez-Loustau, M.-L., Delzon, S., Piou, D., Battisti, A., et

804   al., (2012). Drought effects on damage by forest insects and pathogens: A meta-

805   analysis. Glob. Change Biol. 18, 267–276. doi: 10.1111/j.1365-2486.2011.02512.x

806   Jakuš, R., Zajíčkova, L., Cudlín, P., Blaženec, M., Turčani, M., Ježík, M., et al.,

807   (2011). Landscape-scale Ips typographus attack dynamics: From monitoring plots to

808   GIS-based disturbance models. iForest 4, 256–261. doi: 10.3832/ifor0589-004

809   Kamińska, A. (2022). Spatial autocorrelation based on remote sensing data in

810   monitoring of Norway spruce dieback caused by the European spruce bark beetle

811   Ips typographus L. in the Białowieża Forest. Sylwan 166 (11): 719-732.

812   doi: 10.26202/SYLWAN.2022072.

813   Karkauskaite, P., Tagesson, T., and Fensholt, R. (2017). Evaluation of the plant

814   phenology index (PPI), NDVI and EVI for start-of-season trend analysis of the

815   Northern Hemisphere boreal zone. Remote Sens. 9:485. doi: 10.3390/rs9050485

816   Kärvemo, S., Van Boeckel, T. P., Gilbert, M., Grégoire, J.-C., and Schroeder,

817   M. (2014). Large-scale risk mapping of an eruptive bark beetle – Importance of forest

818   susceptibility and beetle pressure. For. Ecol. Manag. 318, 158–166. doi:

819   10.1016/j.foreco.2014.01.025

820   Kautz, M., Schopf, R., and Ohser, J. (2013). The "sun-effect": microclimatic

821 alterations predispose forest edges to bark beetle infestations. Eur J Forest Res 132,

822 453–465. doi: 10.1007/s10342-013-0685-2.

823   Keeling, C. I. (2016). "Bark beetle research in the postgenomic Era," in

824 Advances in Insect physiology, Vol. 50, eds T. Claus and G. J. Blomquist (Cambridge,

825 MA: Academic Press), 265–293.

826   Kim, Y. (2013). Drought and elevation effects on MODIS vegetation indices in

827 northern Arizona ecosystems. Int. J. Remote Sens. 34, 4889–4899. doi:

828 10.1080/2150704X.2013.781700

829   Klouček, T., Komárek, J., Surový, P., Hrach, K., Janata, P., and Vašíček, B.

830 (2019). The use of UAV mounted sensors for precise detection of bark beetle

831 infestation. Remote Sens. 11:1561. doi: 10.3390/rs11131561

832   Komonen, A., Schroeder, L. M., and Weslien, J. (2011). Ips typographus

833 population development after a severe storm in a nature reserve in southern Sweden:

834 Ips typographus after storm disturbance. J. Appl. Entomol. 135, 132–141. doi:

835 10.1111/j.1439-0418.2010.01520.x

836   Koontz, M. J., Latimer, A. M., Mortenson, L. A., Fettig, C. J., and North, M. P.

837 (2021). Cross-scale interaction of host tree size and climatic water deficit governs bark

838 beetle-induced tree mortality. Nat. Commun. 12:129. doi: 10.1038/s41467-020-20455-

839 y

840   Korolyova, N., Buechling, A., Lieutier, F., Yart, A., Cudlín, P., Turčáni, M., et

841 al. (2022). Primary and secondary host selection by Ips typographus depends on

842   Norway spruce crown characteristics and phenolic-based defenses. Plant Science 321,

843   111319. doi: 10.1016/j.plantsci.2022.111319.

844   Krokene, P. (2015). "Conifer defense and resistance to bark beetles," in Bark

845   beetles, eds F. E. Vega and R. W. Hofstetter (Amsterdam: Elsevier), 177–207. doi:

846   10.1016/B978-0-12-417156-5.00005-8

847   Lausch, A., Fahse, L., and Heurich, M. (2011). Factors affecting the spatio-

848   temporal dispersion of Ips typographus (L.) in Bavarian Forest National Park: A long-

849   term quantitative landscape-level analysis. For. Ecol. Manag. 261, 233–245. doi:

850   10.1016/j.foreco.2010.10.012

851   Lausch, A., Heurich, M., Gordalla, D., Dobner, H.-J., Gwillym-Margianto, S.,

852   and Salbach, C. (2013). Forecasting potential bark beetle outbreaks based on spruce

853   forest vitality using hyperspectral remote-sensing techniques at different scales. Forest

854   Ecology and Management 308, 76–89. doi: 10.1016/j.foreco.2013.07.043.

855   Lawley, V., Lewis, M., Clarke, K., and Ostendorf, B. (2016). Site-based and

856   remote sensing methods for monitoring indicators of vegetation condition: An

857   Australian review. Ecol. Indic. 60, 1273–1283. doi: 10.1016/j.ecolind.2015.03.021

858   Lindner, M., Maroschek, M., Netherer, S., Kremer, A., Barbati, A., Garcia-

859   Gonzalo, J., et al., (2010). Climate change impacts, adaptive capacity, and

860   vulnerability of European forest ecosystems. For. Ecol. Manag. 259, 698–709. doi:

861   10.1016/j.foreco.2009.09.023

862   Long, J. A., and Lawrence, R. L. (2016). Mapping percent tree mortality due to

863   mountain pine beetle damage. For. Sci. 62, 392–402. doi: 10.5849/forsci.15-046

864   Marini, L., Lindelöw, Å, Jönsson, A. M., Wulff, S., and Schroeder, L. M.

865   (2013). Population dynamics of the spruce bark beetle: A long-term study. Oikos 122,

866   1768–1776. doi: 10.1111/j.1600-0706.2013.00431.x

867   Marini, L., Økland, B., Jönsson, A. M., Bentz, B., Carroll, A., Forster, B., et al.,

868   (2017). Climate drivers of bark beetle outbreak dynamics in Norway spruce forests.

869   Ecography 40, 1426–1435. doi: 10.1111/ecog.02769

870   Marvasti-Zadeh, S. M., Goodsman, D., Ray, N., and Erbilgin, N. (2024). Early

871   Detection of Bark Beetle Attack Using Remote Sensing and Machine Learning: A

872   Review. ACM Comput. Surv. 56, 1–40. doi: 10.1145/3625387.

873   McDowell, N., Pockman, W. T., Allen, C. D., Breshears, D. D., Cobb, N.,

874   Kolb, T., et al., (2008). Mechanisms of plant survival and mortality during drought:

875   Why do some plants survive while others succumb to drought? New Phytol. 178, 719–

876   739. doi: 10.1111/j.1469-8137.2008.02436.x

877   Meddens, A. J. H., and Hicke, J. A. (2014). Spatial and temporal patterns of

878   Landsat-based detection of tree mortality caused by a mountain pine beetle outbreak in

879   Colorado USA. For. Ecol. Manag. 322, 78–88. doi: 10.1016/j.foreco.2014.02.037

880   Meddens, A. J. H., Hicke, J. A., Macalady, A. K., Buotte, P. C., Cowles, T. R.,

881   and Allen, C. D. (2015). Patterns and causes of observed piñon pine mortality in the

882   southwestern United States. New Phytol. 206, 91–97. doi: 10.1111/nph.13193

883   Meddens, A. J. H., Hicke, J. A., Vierling, L. A., and Hudak, A. T. (2013).

884   Evaluating methods to detect bark beetle-caused tree mortality using single-date and

885   multi-date Landsat imagery. Remote Sens. Environ. 132, 49–58. doi:

886   10.1016/j.rse.2013.01.002

887   Mezei, P., Jakuš, R., Pennerstorfer, J., Havašová, M., Škvarenina, J., Ferenčík,

888   J., et al., (2017). Storms, temperature maxima and the Eurasian spruce bark beetle Ips

889   typographus—An infernal trio in Norway spruce forests of the Central European High

890   Tatra Mountains. Agric. For. Meteorol. 242, 85–95. doi:

891   10.1016/j.agrformet.2017.04.004

892   Minařík, R., and Langhammer, J. (2016). Use of a multispectral uav

893   photogrammetry for detection and tracking of forest disturbance dynamics. Int. Arch.

894   Photogramm. Remote Sens. Spatial Inf. Sci. XLI-B 8, 711–718. doi:

895   10.5194/isprsarchives-XLI-B8-711-2016

896   Mullen, K. E. (2016). Early detection of mountain pine beetle damage in

897   ponderosa pine forests of the black hills using hyperspectral and worldview-2 data.

898   Master's thesis. Mankato, MN: Minnesota State University.

899   Mullen, K., Yuan, F., and Mitchell, M. (2018). The mountain pine beetle

900   epidemic in the black hills, South Dakota: The consequences of long term fire policy,

901   climate change and the use of remote sensing to enhance mitigation. JGG 10:69. doi:

902   10.5539/jgg.v10n1p69

903   Netherer, S., Kandasamy, D., Jirosová, A., Blanka, K., Schebeck, M., and

904   Schlyter, F. (2021). Interactions among Norway spruce, the bark beetle Ips

905   typographus and its fungal symbionts in times of drought. J. Pest Sci. 94, 591–614.

906   doi: 10.1007/s10340-021-01341-y

907   Netherer, S., Matthews, B., Katzensteiner, K., Blackwell, E., Henschke, P.,
908   Hietz, P., et al., (2015). Do water-limiting conditions predispose Norway spruce to
909   bark beetle attack? New Phytol. 205, 1128–1141. doi: 10.1111/nph.13166

910   Netherer, S., Panassiti, B., Pennerstorfer, J., and Matthews, B. (2019). Acute
911   drought is an important driver of bark beetle infestation in Austrian Norway spruce
912   stands. Front. For. Glob. Change 2:39. doi: 10.3389/ffgc.2019.00039

913   Niemann, K. O., Quinn, G., Stephen, R., Visintini, F., and Parton, D. (2015).
914   Hyperspectral remote sensing of mountain pine beetle with an emphasis on previsual
915   assessment. Can. J. Remote Sens. 41, 191–202. doi: 10.1080/07038992.2015.1065707

916   Öhrn, P., Langstrom, B., LindelÖw, A., and Bjrklund, N. (2014). Seasonal
917   flight patterns of Ips typographus in southern Sweden and thermal sums required for
918   emergence. Agric. For. Entomol. 16, 1–23.

919   Ortiz, S., Breidenbach, J., and Kändler, G. (2013). Early detection of bark
920   beetle green attack using terraSAR-X and rapideye data. Remote Sens. 5, 1912–1931.
921   doi: 10.3390/rs5041912

922   Özçelik, M. S., Tomášková, I., Surový, P., and Modlinger, R. (2022). Effect of
923   forest edge cutting on transpiration rate in Picea abies (L.) H. Karst. For. 13:1238. doi:
924   10.3390/f13081238

925   Pedregosa, F., Varoquaux, G., Gramfort, A., Michel, V., Thirion, B., Grisel, O.,
926   et al., (2011). Scikit-learn: Machine learning in python. J. Mach. Learn. Res. 12, 2825–
927   2830.

928   Pinty, B., and Verstraete, M. (1992). GEMI: A non-linear index to monitor

929   global vegetation from satellites. Vegetation 101, 15–20.

930   Pirtskhalava-Karpova, N., Trubin, A., Karpov, A., and Jakuš, R. (2024).

931   Drought initialised bark beetle outbreak in Central Europe: Meteorological factors and

932   infestation dynamic. Forest Ecology and Management 554, 121666. doi:

933   10.1016/j.foreco.2023.121666.Planet Labs, Inc (2022). Planet imagery product

934   specifications. San Francisco, CA: Planet Labs, Inc.

935   QGIS Development Team (2009). QGIS geographic information system. Open

936   source geospatial foundation. Pittsburgh, PA: Q Development Team.

937   Qi, J., Chehbouni, A., Huete, A., Kerr, Y., and Sorooshian, S. (1994). A

938   modified soil adjusted vegetation index. Remote Sens. Environ. 48, 119–126.

939   Raffa, K. F. (1988). "The mountain pine beetle in western North America," in

940   Dynamics of forest insect populations: Patterns, causes, and implications, ed. A. A.

941   Berryman (New York, NY: Plenum), 556–576.

942   Raffa, K. F., and Berryman, A. A. (1983). The role of host plant resistance in

943   the colonization behavior and ecology of bark beetles (Coleoptera: Scolytidae). Ecol.

944   Monogr. 53, 27–49.

945   Raffa, K. F., Aukema, B. H., Bentz, B. J., Carroll, A. L., Hicke, J. A., Turner,

946   M. G., et al., (2008). Crossscale drivers of natural disturbances prone to anthropogenic

947   amplification: The dynamics of bark beetle eruptions. Bioscience 58, 501–517.

948   Raffa, K. F., Grégoire, J.-C., and Staffan Lindgren, B. (2015). "Natural history

949   and ecology of bark beetles," in Bark beetles, eds F. E. Vega and R. W. Hofstetter

950   (San Diego, CA: Elsevier), 1–40. doi: 10.1016/B978-0-12-417156-5.00001-0

951   Rautiainen, M., Lukeš, P., Homolová, L., Hovi, A., Pisek, J., and Mõttus, M.

952   (2018). Spectral properties of coniferous forests: A review of in situ and laboratory

953   measurements. Remote Sens. 10:207. doi: 10.3390/rs10020207

954   Remeš, J. (2017). "The university forest enterprise in Kostelec nad Černými

955   Lesy – a basis for practical education and research at the Faculty of forestry and wood

956   sciences in Prague," in Proceedings of the Forests for university education: Examples

957   and experiences – SILVA network conference, Faculty of forestry and wood sciences,

958   Czech university of live sciences, Prague, Jun 26th – 28th, 2017, Technische

959   Universität Dresden and Sächsische Landesbibliotek, Dresden, eds P. Schmidt, S.

960   Lewark, J. Remeš, and N. Weber (Prague), 17–22.

961   Richardson, A. J., and Wiegand, C. L. (1977). Distinguishing vegetation from

962   soil background information. Photogram. Eng. Remote Sens. 43, 1541–1552.

963   Rondeaux, G., Steven, M., and Baret, F. (1996). Optimization of soil-adjusted

964   vegetation indices. Remote Sens. Environ. 55, 95–107.

965   Roujean, J., and Breon, F. (1995). Estimating PAR absorbed by vegetation from

966   bidirectional reflectance measurements. Remote Sens. Environ. 51, 375–384.

967   Rouse, J., Haas, R., Schell, J., and Deering, D. (1973). "Monitoring vegetation

968   systems in the great plains with ERTS," in Proceedings of the 3rd ERTS Symposium,

969   NASA, (Washington, DC), 309–317.

970   Seabold, S., & Perktold, J. (2010). "statsmodels: Econometric and statistical

971   modeling with Python." In 9th Python in Science Conference.

972   Seidel, H., Schunk, C., Matiu, M., and Menzel, A. (2016). Diverging drought

973   resistance of scots pine provenances revealed by infrared thermography. Front. Plant

974   Sci. 7:1247. doi: 10.3389/fpls.2016.01247

975   Senf, C., Pflugmacher, D., Wulder, M. A., and Hostert, P. (2015).

976   Characterizing spectral–temporal patterns of defoliator and bark beetle disturbances

977   using Landsat time series. Remote Sens. Environ. 170, 166–177. doi:

978   10.1016/j.rse.2015.09.019

979   Simard, M., Powell, E. N., Raffa, K. F., and Turner, M. G. (2012). What

980   explains landscape patterns of bark beetle outbreaks in Greater Yellowstone? Glob.

981   Ecol. Biogeogr. 21, 556–567.

982   Sripada, R. (2005). Determining in-season nitrogen requirements for corn using

983   aerial color-infrared photography. Ph.D. dissertation. Raleigh, NC: North Carolina

984   State University.

985   Sripada, R., Heiniger, R. W., White, J. G., and Meijer, A. D. (2006). Aerial

986   color infrared photography for determining early in-season nitrogen requirements in

987   corn. Agron. J. 98, 968–977.

988   Stereńczak, K., Mielcarek, M., Modzelewska, A., Kraszewski, B., Fassnacht, F.

989   E., and Hilszczański, J. (2019). Intra-annual Ips typographus outbreak monitoring

990   using a multi-temporal GIS analysis based on hyperspectral and ALS data in the

991   Białowieża Forests. For. Ecol. Manag. 442, 105–116. doi: 10.1016/j.foreco.2019.03.064

993   Stříbrská, B., Hradecký, J., Čepl, J., Tomášková, I., Jakuš, R., Modlinger, R., et al., (2022). Forest margins provide favourable microclimatic niches to swarming bark beetles, but Norway spruce trees were not attacked by Ips typographus shortly after edge creation in a field experiment. Remote Sens. Environ. 506:119950. doi: 10.1016/j.foreco.2021.119950

998   Terpilovskii, Maxim. (2019). scikit-posthocs: Pairwise multiple comparison tests in Python. Journal of Open Source Software. 4. 1169. 10.21105/joss.01169.

1000   Tolasz, R., Míková, T., Valeriánová, A., and Voženílek, V. (eds) (2007). Climate atlas of Czechia, 1st Edn. Prague: Olomouc: Czech Hydrometeorological Institute, Palackého University, 255.

1003   Trubin, A., Kozhoridze, G., Zabihi, K., Modlinger, R., Singh, V. V., Surový, P., Jakuš, R. (2023). Detection of susceptible Norway spruce to bark beetle attack using PlanetScope multispectral imagery. Front. For. Glob. Change 6, 1130721. doi: 10.3389/ffgc.2023.1130721.

1007   Tucker, C. (1979). Red and photographic infrared linear combinations for monitoring vegetation. Remote Sens. Environ. 8, 127–150.

1009   Vacchiano, G., Garbarino, M., Borgogno Mondino, E., and Motta, R. (2012). Evidences of drought stress as a predisposing factor to Scots pine decline in Valle d'Aosta (Italy). Eur. J. For. Res. 131, 989–1000. doi: 10.1007/s10342-011-0570-9

1012   Väisänen, R., and Heliövaara, K. (1994). Assessment of insect occurrence in

1013   boreal forests based on satellite imagery and field measurements. Acta For. Fenn.

1014   243:7505. doi: 10.14214/aff.7505

1015   Van Rossum, G., and Drake, F. L. (2010). The Python language reference.

1016   Release 3.0.1 [Repr.]. Hampton, NH: Python Software Foundation.

1017   Virtanen, P., Gommers, R., Oliphant, T. E., Haberland, M., Reddy, T.,

1018   Cournapeau, D., et al., (2020). SciPy 1.0: Fundamental algorithms for scientific

1019   computing in Python. Nat. Methods 17, 261–272. doi: 10.1038/s41592-019-0686-2

1020   Vošvrdová, N., Johansson, A., Turčáni, M., Jakuš, R., Tyšer, D., Schlyter, F., et

1021   al., (2023). Dogs trained to recognise a bark beetle pheromone locate recently attacked

1022   spruces better than human experts. For. Ecol. Manag. 528:120626. doi:

1023   10.1016/j.foreco.2022.120626

1024   Wallin, K. F., and Raffa, K. (2004). Feedback between individual host selection

1025   behavior and population dynamics in an eruptive herbivore. Ecol. Monogr. 74, 101–

1026   116.

1027   Weed, A. S., Ayres, M. P., and Hicke, J. A. (2013). Consequences of climate

1028   change for biotic disturbances in North American forests. Ecol. Monogr. 83, 441–470.

1029   doi: 10.1890/13-0160.1

1030   Wei, M., Jiao, L., Zhang, P., Wu, X., Xue, R., and Du, D. (2023). Spatio-

1031   temporal diversity in the link between tree radial growth and remote sensing

1032   vegetation index of qinghai spruce on the northeastern margin of the tibetan plateau.

1033   Forests 14:260. doi: 10.3390/f14020260

1034   Wermelinger, B. (2004). Ecology and management of the spruce bark beetle Ips

1035   typographus—a review of recent research. For. Ecol. Manag. 202, 67–82. doi:

1036   10.1016/j.foreco.2004.07.018

1037   White, J. C., Coops, N. C., Hilker, T., Wulder, M. A., and Carroll, A. L. (2007).

1038   Detecting mountain pine beetle red attack damage with EO-1 Hyperion moisture

1039   indices. Int. J. Remote Sens. 28, 2111–2121. doi: 10.1080/01431160600944028

1040   Yang, H., Yang, X., Zhang, Y., Heskel, M. A., Lu, X., Munger, J. W., et al.,

1041   (2017). Chlorophyll fluorescence tracks seasonal variations of photosynthesis from

1042   leaf to canopy in a temperate forest. Glob. Change Biol. 23, 2874–2886. doi:

1043   10.1111/gcb.13590

1044   Yang, S. (2019). Detecting bark beetle damage with Sentinel-2 multi-temporal

1045   data in Sweden. Master's thesis. Lund: Lund University.

1046   Zabihi, K., Surovy, P., Trubin, A., Singh, V. V., and Jakuš, R. (2021b). A

1047   review of major factors influencing the accuracy of mapping green-attack stage of bark

1048   beetle infestations using satellite imagery: Prospects to avoid data redundancy. Remote

1049   Sens. Appl. 24:100638. doi: 10.1016/j.rsase.2021.100638

1050   Zabihi, K., Huettmann, F., and Young, B. (2021a). Predicting multi-species

1051   bark beetle (Coleoptera: Curculionidae: Scolytinae) occurrence in Alaska: First use of

1052   open access big data mining and open source GIS to provide robust inference and a

1053   role model for progress in forest conservation. Biodiv. Inf. 16, 1–19. doi:

1054   10.17161/bi.v16i1.14758

1055   Zeppenfeld, T., Svoboda, M., DeRose, R. J., Heurich, M., Müller, J., Čížková,

1056   P., et al., (2015). Response of mountain Picea abies forests to stand-replacing bark

1057   beetle outbreaks: Neighbourhood effects lead to self-replacement. J. Appl. Ecol. 52,

1058   1402–1411. doi: 10.1111/1365-2664.12504

Supplementary material

Supplementary table 1 | Day number and corresponding dates of the Planet images utilized in 2020. Imagery captured before May 18 and after July 14 were excluded during the later stage of analyses due to the low sample size in one of the classes.

#	2020	Date
1	93	April 2, 2020
2	100	April 9, 2020
3	108	April 17, 2020
4	114	April 23, 2020
5	129	May 8, 2020
6	139	May 18, 2020
7	153	June 1, 2020
8	180	June 28, 2020
9	183	July 1, 2020
10	194	July 12, 2020
11	196	July 14, 2020
12	204	July 22, 2020
13	214	August 1, 2020
14	218	August 5, 2020
15	226	August 13, 2020
16	229	August 16, 2020

Supplementary table 2 | Normality test results using Shapiro-Wilk W test:
P-values for each class and day, using individual bands.

Band	Day	Healthy	Susceptible	Green attack
Blue	139	0.571558177	0.045561921	0.074746802
	153	0.001461527	0.23313874	0.11675977
	180	1.43E-16	0.949291706	0.000567416
	183	0.131985798	0.026162921	0.85139513
	194	1.77E-05	0.04050941	0.033069607
	196	0.131985798	0.099250175	0.47949037
Green	139	0.549032748	0.359176815	0.065942056
	153	0.562062681	0.355298609	0.667787313
	180	1.55E-16	0.831372023	0.109469414
	183	2.43E-05	0.023698358	0.012739294
	194	2.32E-05	0.062834479	0.007477043
	196	2.43E-05	0.024715327	0.005485932
Red	139	0.337320924	0.316230565	0.043953005
	153	0.15338318	0.974345088	0.807996035
	180	9.50E-17	0.497832894	0.01433232
	183	3.05E-05	0.009566276	0.009102435
	194	0.001538837	0.002532137	1.25E-05
	196	3.05E-05	0.015111554	0.003155117
NIR	139	0.073019862	0.523856223	0.100783497
	153	0.006787768	0.281152517	0.958840311
	180	2.63E-12	0.634528756	0.223738134
	183	0.380494624	0.867751539	0.124060914
	194	0.019461125	0.331248373	0.109592035
	196	0.380494624	0.553638577	0.251807094

Supplementary table 3 | Homogeneity of variances test results using Levene test:
P-values for each day, using individual bands.

Band	Day	p-value
Blue	139	4.57E-07
	153	1.06E-06
	180	0.726388734
	183	0.889696205
	194	0.306923828
	196	0.906835937
Green	139	4.90E-07
	153	0.28331022
	180	0.666498674
	183	0.004641489
	194	0.054842745
	196	0.00092536
Red	139	1.48E-06
	153	0.002129506
	180	0.706581946
	183	0.007425201
	194	0.011408946
	196	0.00140756
NIR	139	0.024497864
	153	0.613262335
	180	0.353725786
	183	0.85934646
	194	0.369464161
	196	0.77068533

Supplementary table 4 | Normality test results using Shapiro-Wilk W test:
P-values for each class and day, using different spectral vegetation indices.

SVI	Date	Healthy	Susceptible	Green attack
DVI	139	0.026619174	0.590636253	0.024212651
	153	0.010454412	0.326360494	0.966519594
	180	6.42E-06	0.571104646	0.102542639
	183	0.076487482	0.722168088	0.059257559
	194	0.056853335	0.286667764	0.121066563
	196	0.076487482	0.504210353	0.108256012
EVI	139	0.258673608	0.00036954	0.251695096
	153	0.240178481	0.010032518	0.099430501
	180	8.70E-10	0.427261293	0.009620276
	183	0.657138824	0.009661673	0.981076539
	194	0.002592299	0.041678771	0.283092052
	196	0.657138824	0.033635102	0.92935282
GCI	139	0.232403174	0.122342654	0.662403166
	153	1.60E-05	0.051104404	0.165722504
	180	7.82E-09	0.283169597	0.000367545
	183	0.006451089	0.928213954	0.002342299
	194	0.286889434	0.93195194	0.003147005
	196	0.006451089	0.758946896	0.001557304
GDVI	139	0.02373339	0.624701381	0.015886648
	153	0.002109102	0.258394122	0.914086103
	180	0.000429861	0.454879642	0.066491663
	183	0.038086943	0.786596417	0.071856543
	194	0.061836924	0.300533623	0.106627718
	196	0.038086943	0.576191008	0.14763625
GEMI	139	0.000488652	0.695830584	0.051378205
	153	0.000440945	0.050488383	0.71341455
	180	5.15E-06	0.293138564	0.006862936
	183	0.00188005	0.627306998	0.013534959
	194	1.44E-05	0.289763868	0.033817336
	196	0.00188005	0.404191196	0.055339403
GNDVI	139	0.015678739	0.327255785	0.878314495
	153	0.016752031	0.54294914	0.146265507
	180	4.96E-14	0.659560561	0.003402534
	183	0.006734798	0.491093516	0.010527485
	194	0.439264476	0.200047553	0.30170539
	196	0.006734798	0.17313306	0.008979202
GOSAVI	139	0.015709789	0.327158749	0.878696799
	153	0.016727844	0.542970598	0.146277308
	180	4.97E-14	0.659470618	0.003407296
	183	0.006748586	0.491230756	0.010537285
	194	0.439147651	0.200104594	0.30177775
	196	0.006748586	0.17324172	0.008987094

	139	0.232410878	0.12233381	0.662403166
	153	1.60E-05	0.051104404	0.165723547
	180	7.82E-09	0.283169597	0.000367543
	183	0.006451089	0.928217232	0.002342299
	194	0.28690064	0.93194896	0.003147037
GRVI	196	0.006451089	0.758947015	0.001557304
	139	0.015773663	0.326962382	0.879494429
	153	0.016681265	0.543071389	0.146299258
	180	4.98E-14	0.659242034	0.003417297
	183	0.006777999	0.491517961	0.010558328
	194	0.43888846	0.200227082	0.301927239
GSAVI	196	0.006777999	0.173463821	0.009004026
	139	0.019716784	0.604304075	0.154236123
	153	0.041448966	0.035186008	0.319314241
	180	4.20E-15	0.378483921	0.006684294
	183	0.000832334	0.228841051	0.004281236
	194	0.047899295	0.007129219	0.208460778
IPVI	196	0.000832334	0.050552499	0.004763432
	139	0.027074603	0.830852032	0.325108796
	153	0.00566523	0.001276142	0.009203746
	180	2.24E-15	0.8138358	0.000610064
	183	0.004439739	0.151333272	0.021067763
	194	0.007663554	0.008136318	0.521788061
MSAVI	196	0.004439739	0.184935153	0.062761679
	139	0.316954553	0.600068212	0.120123059
	153	0.002055708	0.001569665	0.581651509
	180	7.55E-11	0.284012556	0.001945555
	183	0.001755075	0.76821208	0.001447818
	194	0.014418311	0.386554956	0.01706011
MSR	196	0.001755075	0.313570201	0.001344494
	139	0.090583868	0.710776091	0.306531221
	153	0.002302207	0.000686767	0.009653499
	180	1.96E-14	0.802382886	0.002020447
	183	0.004351516	0.138928592	0.016330287
	194	0.020136172	0.009841945	0.558378994
NDVI	196	0.004351516	0.170629233	0.047532894
	139	0.015679002	0.327260166	0.878319263
	153	0.016751364	0.542936921	0.146265507
	180	4.96E-14	0.659560561	0.003402534
	183	0.006734798	0.491089016	0.010527419
	194	0.439285576	0.200047553	0.30170539
NDWI	196	0.006734798	0.173133925	0.00897907
	139	0.037362326	0.072571747	0.000538301
	153	0.341914386	0.955720067	0.096468702
	180	4.63E-07	0.637118638	0.177006602
	183	0.105749682	0.580803216	0.106851257
	194	0.056326162	8.61E-05	0.588697731

NLI	196	0.105749682	0.135481969	0.137023509
	139	0.019736284	0.604002535	0.154355809
	153	0.041502383	0.035212401	0.319861323
	180	4.20E-15	0.378215641	0.006693599
	183	0.000834577	0.229118049	0.00428624
	194	0.047974497	0.007130565	0.208365232
OSAVI	196	0.000834577	0.050604489	0.004767759
	139	0.041500147	0.523062706	0.057605408
	153	0.007420359	0.225789547	0.983492315
	180	9.74E-11	0.575727403	0.126388669
	183	0.249560609	0.849588156	0.101108916
	194	0.021784615	0.354060322	0.101087809
PVI	196	0.249560609	0.601140916	0.222554252
	139	0.079376929	0.384983987	0.005958814
	153	0.047787331	0.518702209	0.962099075
	180	0.079349868	0.664864242	0.025423851
	183	0.108190812	0.848788142	0.047465183
	194	0.871610045	0.068283111	0.165035322
RDVI	196	0.108190812	0.660367846	0.135529682
	139	0.090361312	0.71068728	0.306096524
	153	0.002300156	0.000686537	0.009620148
	180	1.96E-14	0.8026613	0.002020321
	183	0.004340342	0.139584467	0.016324617
	194	0.020204389	0.009811868	0.559378982
SAVI	196	0.004340342	0.171681225	0.047558051
	139	0.415124953	0.38476181	0.103506252
	153	0.00043646	0.000446312	0.608055174
	180	7.04E-09	0.216098189	0.000701527
	183	0.001872124	0.891575098	0.000926242
	194	0.006872626	0.733020782	0.004614815
SR	196	0.001872124	0.494847447	0.000791305
	139	0.190339386	0.589342713	0.287172467
	153	0.001081442	0.000422327	0.009737883
	180	1.19E-13	0.788262963	0.004808481
	183	0.004184213	0.132041126	0.0132882
	194	0.04231048	0.01106848	0.566079736
TSAVI	196	0.004184213	0.166041628	0.037953157
	139	0.339646518	0.043608479	0.378246039
	153	1.70E-06	4.08E-06	0.043168273
	180	1.77E-07	0.242500514	0.079029322
	183	0.01721666	0.07335484	0.401809573
	194	0.022019593	0.192349762	0.630911052
VARI	196	0.01721666	0.229611576	0.0799881
	139	0.004786405	0.647272348	0.284608662
	153	0.00059276	0.299163461	0.99961561
	180	1.72E-13	0.454040766	0.091265246
	183	0.01018656	0.536944032	0.041954733

	194	3.08E-05	0.335952431	0.066110164
WDRVI	196	0.01018656	0.251641005	0.120914258

Supplementary table 5 | Homogeneity of variances test results using Levene test:
P-values for each day, using different spectral vegetation indices.

	139	153	180	183	194	196
DVI	0.188835052	0.806442703	0.160182291	0.965010968	0.302528612	0.834433499
EVI	0.054574925	0.000234224	0.093534578	0.319249023	0.037792704	0.040642904
GCI	0.090984657	0.064355221	0.638463871	0.120514809	0.005046034	0.09241796
GDVI	0.216380514	0.591224754	0.180521331	0.981944674	0.15511169	0.864656952
GEMI	0.477879913	0.744040509	0.167767561	0.94498846	0.10628429	0.873564415
GNDVI	0.050986514	0.0047734	0.660162785	0.092501165	0.038162148	0.048676895
GOSAVI	0.051049724	0.004781955	0.660162151	0.092574429	0.038178411	0.048727301
GRVI	0.090984657	0.064355221	0.638463871	0.120514809	0.005046034	0.09241796
GSAVI	0.051184319	0.004800252	0.66016061	0.092730039	0.038212758	0.048834516
IPVI	0.039948588	0.411757211	0.705819497	0.050071454	0.923882466	0.020916954
MSAVI	0.006382985	0.006477768	0.612143923	0.561806828	0.101812124	0.689325
MSR	0.08160143	0.335903391	0.606041052	0.07435999	0.533705962	0.03941057
NDVI	0.006965723	0.006936448	0.494179976	0.508519687	0.078647001	0.660773283
NDWI	0.050986514	0.0047734	0.660162785	0.092501165	0.038162148	0.048676895
NLI	0.395922071	0.952364385	0.296580979	0.277803639	0.717041237	0.206690422
OSAVI	0.039997295	0.412103822	0.705779794	0.05010508	0.923768609	0.02093433
PVI	0.058330605	0.694757829	0.294398465	0.882785019	0.254649043	0.7628799
RDVI	0.393949869	0.860291685	0.081530465	0.937884462	0.369870136	0.990982039
SAVI	0.007056062	0.006977267	0.494214011	0.508514588	0.078448157	0.661716295
SR	0.108891207	0.317510068	0.556383477	0.090667462	0.365104866	0.052798129
TSAVI	0.008394781	0.007625898	0.415165813	0.466266784	0.061675169	0.643474982
VARI	0.001151481	0.014597618	0.027595423	0.092427397	0.524397084	0.395182715
WDRVI	0.072684347	0.70336804	0.457737667	0.922074144	0.393331438	0.825708281

Supplementary table 6 | Spectral Vegetation Indices (SVIs), their acronyms, equations, and publishers, used to detect trees susceptible to bark beetle attack.

Spectral Vegetation Index	Acronym	Equation	Reference
Difference Vegetation Index	DVI	$NIR - R$	Tucker, 1979
Enhanced Vegetation Index	EVI	$2.5 * \dfrac{(NIR - R)}{(NIR + 6 * R - 7.5 * B + 1)}$	Huete et al., 2002
Green Chlorophyll Index	GCI	$\left(\dfrac{NIR}{G}\right) - 1$	Gitelson et al., 2003
Green Difference Vegetation Index	GDVI	$NIR - G$	Sripada et al., 2005
Global Environmental Monitoring Index	GEMI	$eta * (1 - 0.25 * eta) - \dfrac{R - 0.125}{1 - R}$ $eta = \dfrac{2(NIR^2 - R^2) + 1.5 * NIR + 0.5 * R}{NIR + R + 0.5}$	Pinty and Verstraete, 1992
Green Normalized Difference Vegetation Index	GNDVI	$\dfrac{NIR - G}{NIR + G}$	Gitelson et al., 1996
Green Optimized Soil Adjusted Vegetation Index	GOSAVI	$\dfrac{NIR - G}{NIR + G + 0.16}$	Sripada et al., 2005

Green Ratio Vegetation Index	GRVI	$\dfrac{NIR}{G}$	Sripada et al., 2006
Green Soil Adjusted Vegetation Index	GSAVI	$1.5 * \dfrac{(NIR - G)}{(NIR + G + 0.5)}$	Sripada et al., 2005
Infrared Percentage Vegetation Index	IPVI	$\dfrac{NIR}{NIR + R}$	Crippen, 1990
Modified Soil Adjusted Vegetation Index	MSAVI2	$\dfrac{2 * NIR + 1 - \sqrt{(2 * NIR + 1)^2 - 8(NIR - R)}}{2}$	Qi et al., 1994
Modified Simple Ratio	MSR	$\dfrac{\left(\dfrac{NIR}{R}\right) - 1}{\left(\sqrt{\dfrac{NIR}{R}}\right) + 1}$	Chen, 1996
Normalized Difference Vegetation Index	NDVI	$\dfrac{NIR - R}{NIR + R}$	Rouse et al., 1974
Normalized Difference Water Index	NDWI	$\dfrac{G - NIR}{G + NIR}$	Gao, 1995

Non-Linear Index	NLI	$\dfrac{NIR^2 - R}{NIR^2 + R}$	Goel and Qin, 1994
Optimized Soil Adjusted Vegetation Index	OSAVI	$\dfrac{NIR - R}{NIR + R + 0.16}$	Rondeaux et al., 1996
Perpendicular Vegetation Index	PVI	$\dfrac{NIR - a*R - b}{\sqrt{(1 + a^2)}}$ a—slope of the soil line, b—gradient of the soil line	Richardson and Wiegard, 1977
Renormalized Difference Vegetation Index	RDVI	$\dfrac{NIR - R}{\sqrt{NIR + R}}$	Roujean and Breon, 1995
Soil Adjusted Vegetation Index	SAVI	$\dfrac{1.5*(NIR - R)}{(NIR + R + 0.5)}$	Huete, 1988
Simple Ratio	SR	$\dfrac{NIR}{R}$	Birth and McVey, 1968
Transformed Soil Adjusted Vegetation Index	TSAVI	$\dfrac{(s*(NIR - s*R - a))}{(a*NIR + R - a*s + X*(1 + s^2))}$ s—a slope of the soil line, a — the soil line intercept, X - the adjustment factor that is set to minimize soil noise.	Baret and Guyot, 1991

Visible Atmospherically Resistant Index	VARI	$\dfrac{G - R}{G + R - B}$	Gitelson et al., 2002
Wide Dynamic Range Vegetation Index	WDRVI	$\dfrac{(a * NIR - R)}{(a * NIR + R)}$ a - the weighting coefficient	Gitelson et al., 1996

3.2 Tree mortality

3.2.1 Northernmost European spruce bark beetle *Ips typographus* outbreak: Modelling tree mortality using remote sensing and climate data

Authors' contributions

Aleksei Trubin: Formal analysis, Methodology, Data curation, Visualization, Writing – original draft, Writing – review & editing. Pavel Mezei: Formal analysis, Conceptualization, Methodology, Visualization, Writing – original draft, Writing – review & editing. Khodabakhsh Zabihi: Writing – review & editing. Peter Surový: Writing – review & editing. Rastislav Jakuš: Conceptualization, Funding acquisition, Investigation, Methodology, Project administration, Writing – review & editing.

Extended summary

Introduction

Worldwide forests are becoming increasingly susceptible to dieback, largely due to heat and drought stress, with these conditions often encouraging the development of destructive forest insect species (Allen et al., 2010, DeRose et al., 2013, Kolb et al., 2016, McDowell et al., 2008, White, 2015). European spruce forests are particularly vulnerable, with drought and wind being the leading abiotic stressors (Kärvemo et al., 2014, Komonen et al., 2011, Marini et al., 2017). While the physiological mechanisms of drought survival in conifers are not well understood (McDowell et al., 2008), it's known that species adapted to fluctuating water conditions are more susceptible to bark beetle attacks in conditions of severe and constant water shortages (Netherer et al., 2015, Wermelinger, 2004). Climate change, resulting in increasing droughts and higher temperatures, is seen as a major factor for bark beetle outbreaks, which directly affect insect population dynamics and indirectly impact host plant growth and defence (Romashkin et al., 2020, Schroeder and Dalin, 2017). The Eurasian spruce bark beetle, *I. typographus*, has become a significant pest, causing considerable damage to coniferous forests in the Northern Hemisphere (Raffa et al., 2015). The intensification of these outbreaks is connected to latitude (Maslov, 2010, Romashkin et al., 2020) in the European part of Russia, causing mass forest dieback. This study aims to determine the most influential predictive variables such as temperature, precipitation, and previous-year damage to explain annual tree-cover loss, understand their effects, and establish whether factors related to tree mortality in the northern border of spruce occurrence differ from those in lower latitudes.

Materials and methods

This study investigates tree mortality in the Dvinsko-Pinegskiy reserve in the Arkhangelsk region, Russia, where Siberian spruce dominates the preserved taiga ecosystem. Annual tree cover loss data from 2001-2014 and meteorological variables from the Sura station were used to understand the effect of climate on bark beetle outbreaks, a key factor in tree mortality. Particular focus was on the April-June bark beetle season, considering factors such as average monthly temperature, precipitation, and the Selyaninov hydrothermal coefficient for moisture assessment. Using linear regression to analyze tree loss and explanatory variables, multiple models were constructed based on factors known to impact bark beetle population dynamics, with the most suitable model selected using the Akaike information criterion (AIC)

and Akaike weights. Further analyses were performed using the autocorrelation function (ACF) and cross-correlation functions (CCF), with all calculations conducted in R software.

Results

The total tree cover loss in the Dvinsko-Pinegskiy reserve from 2001 to 2014 was 160 km², with varying mortality rates across years. Autocorrelation analysis showed no patterns in tree mortality rates between consecutive years. Linear regression was applied to explore the relationship between tree mortality and meteorological variables, such as different monthly and yearly average air temperatures, precipitation, and total solar radiation. The most suitable model indicated that the average annual air temperature of the previous year had a positive effect on tree mortality, while June temperatures had a negative effect. Other models, although less parsimonious, suggested that variations in monthly or yearly temperatures and June precipitation could also have significant explanatory power regarding tree loss changes.

Discussion

This study investigated the complex interplay between temperature, bark beetle population dynamics, and host tree physiology in the Arkhangelsk region's forests. The results show a nuanced relationship where tree loss decreased slightly with an increase in June temperatures but increased during years with overall higher temperatures. Despite some limitations, including reliance on a single meteorological station's data, the findings highlight the influence of temperature on bark beetle-caused tree mortality. The most significant factors were found to be the average June temperature and the previous year's temperatures. The study also suggests that high temperatures during dry summers and the duration of solar radiation play pivotal roles in bark beetle population dynamics. Moreover, increased temperatures can enhance tree defences, and drought stress can significantly affect spruce trees' susceptibility to infestations. With climate change, the threat of drought-induced bark beetle outbreaks may escalate, potentially affecting northern Russian forests where such outbreaks are currently not significant. This emphasizes the need for urgent protective measures against such future disturbances.

Conclusions

This research concluded that the temperature of the current and preceding years is a critical determinant of tree mortality from bark beetle outbreaks in the Arkhangelsk region. Other significant factors include the duration of solar radiation in April and May and June

precipitation. The study suggests that two groups of variables may influence these outbreaks. The first group links rising temperature sums to increased bark beetle aggressiveness, while the second ties drought to reduced spruce defence abilities. However, the flight behaviour of *I. typographus* and its other biological aspects at high latitudes, as well as their correlation with climatic changes, are not entirely understood and warrant further research.
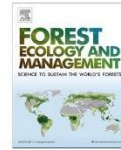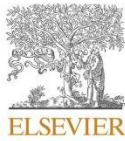
Northernmost European spruce bark beetle *Ips typographus* outbreak: Modelling tree mortality using remote sensing and climate data

Aleksei Trubin [a], Pavel Mezei [b,c,d,*], Khodabakhsh Zabihi [a], Peter Surový [a], Rastislav Jakuš [a,b]

[a] Faculty of Forestry and Wood Sciences, Czech University of Life Sciences in Prague, 16500 Kamycká 129, Suchdol, Prague 6, Czech Republic
[b] Institute of Forest Ecology, Slovak Academy of Sciences, Štúrova 2, 960 53 Zvolen, Slovakia
[c] Faculty of Forestry, Technical University in Zvolen, T.G.Masaryka 24, 960 53 Zvolen, Slovak Republic
[d] Department of Ecosystem and Conservation Sciences, University of Montana, Missoula, MT, United States

ABSTRACT

Acute or chronic drought stress caused by climate change can contribute to the weakening of forest ecosystems and lead to extensive bark beetle infestations. Siberian spruce (*Picea obovata* Ledeb.) forests of the Dvinsko-Pinegskiy, a natural reserve in the Arkhangelsk region, Russia, have been subject to unprecedented tree cover loss caused by the Eurasian spruce bark beetle (*Ips typographus* L.) in the last two decades. This is the first recorded case of such an extensive outbreak of *Ips typographus* occurring at higher latitudes. We used remote sensing and climate data to model and compute annual tree-loss change due to natural factors, with a focus on bark beetle outbreaks, over a 14-year period (2001–2014). Using linear regression models, we found a combination of average annual temperature and precipitation, temperature and precipitation in June, to be the most important drivers of annual tree-loss.

1. Introduction

Forests worldwide are becoming increasingly vulnerable to dieback caused by heat- and drought-induced physiological stress, which is often associated with enhanced development of forest insect pest species (Allen et al., 2010; DeRose et al., 2013; Kolb et al., 2016; Mcdowell et al., 2008; White, 2015). Drought and wind are generally recognized as the two most important abiotic factors affecting the condition of spruce forests in Europe (Kärvemo et al., 2014; Komonen et al., 2011; Marini et al., 2017). In accordance with Manion's theory, the decline of spruce forests is a result of predisposing factors, such as low soil pH, nutrient deficiency, and water deficit, and factors that directly kill trees. For example, trees in areas of drought have their limited water supply further reduced by roots breaking in the drying soil, imposing additional stress on the trees (Holuša and Liška, 2002).

The physiological mechanisms underlying drought survival and mortality in conifers are poorly understood (Mcdowell et al., 2008). Conifers vary greatly in their ability to cope with drought, but species adapted to highly variable water regimes are predisposed to bark beetles attacks under conditions of extreme and constant water deficits (Christiansen et al., 1987; Miller and Keen, 1960; Worrell, 1983). The combination of increasingly frequent droughts and higher temperatures is considered to be an important predisposing factor for bark beetle outbreaks, directly affecting insect population dynamics and indirectly altering host plant growth and defence (Bentz and Jönsson, 2015; Hart et al., 2017; Jactel et al., 2012; Meddens et al., 2015; Raffa et al., 2015; Weed et al., 2013). For example, severe droughts combined with warm temperatures can reduce the water supply to trees and increase their susceptibility to *Ips typographus* L. attacks (Netherer et al., 2015; Wermelinger, 2004). Moderate drought can result in increases of plant chemical defences, whereas long, severe drought events can result in decreases in defence compounds (Gely et al., 2020). In wind-damaged areas, windblown trees exposed to high temperatures or solar radiation may be not suitable for bark beetle attacks (Hrošso et al., 2020).

The European spruce bark beetle, *I. typographus*, is one of the most economically important forest pests in Eurasia (Wermelinger, 2004), causing severe damage to coniferous forests in the Northern Hemisphere (Raffa et al., 2015). Despite their essential role in forest regeneration and succession in conifer-dominated forest ecosystems in the Northern Hemisphere (Bače et al., 2015; Winter et al., 2015; Zeppenfeld et al., 2015), recent outbreaks of bark beetles have noticeably exceeded previously documented frequencies and impacts (Winter et al., 2015). Climate change may cause *I. typographus* to develop additional generations per year and facilitate mass outbreaks further north than

132

previously observed (Romashkin et al., 2020; Schroeder and Dalin, 2017).

In the European part of Russia, the intensity of bark beetle outbreaks, in particular *I. typographus*, are related to latitude (Maslov, 2010; Romashkin et al., 2020). Based on the occurrence of bark outbreaks since 1993 in the European territory of the Russian Federation and neighbouring countries, Maslov (2010) has suggested a division into classes of bark beetle-driven mass-mortality and micro-hotspots on a landscape level. In particular; the interfluve of Northern Dvina and Pinega (marked III on Fig. 1) is also driven by climate and the older age classes of the tree stands. Tree mortality in the Moscow region was most intense from 2011 to 2013 and the bark beetle damage on 74,000 ha of forest land was classified as epidemic, but even from 2013 to 2015 micro-hotspots continued to appear.

The mass forest dieback in the Arkhangelsk region, which has been observed since 1997, has attracted the most attention and is likely the most extensive natural disturbance in Russia. From the beginning of 2004 to the end of 2005, the area of spruce forest mortality increased by about 50% and is estimated today at more than 2 million hectares (Zhigunov et al., 2007). According to Romashkin et al. (2020); there was a notable increase in temperature sums for *I. typographus* development in the Northern part of European Russia after the year 2000 and it has been hypothesized that with increasing summer temperatures, the frequency and number of recorded outbreaks increased.

Publicly available disturbances database – Global Forest Watch (Hansen et al., 2013) provides annual tree cover percentage, gain, and loss from 2000 to 2019 on a global scale at 30 m spatial resolution. In this study, we present a an approach that demonstrates high resolution global maps of forest cover change from Hansen et al. (2013) to acquire annual forest loss change maps over the period 2000–2019 for the reserve studied.

We based our study on the assumption that seasonal temperature and precipitation conditions that affect bark beetle development and the stress level of the host trees play an important role in tree cover loss due to infestations caused by *I. typographus* in the Dvinsko-Pinegskiy reserve.

The objectives of this study were to: (1) determine what combinations of predictive variables, such as temperature, precipitation, and previous-year damage, best explain the annual tree-cover loss, (2) understand possible effects of the selected variables, by the most-parsimonious model, on annual changes of tree loss, and (3) determine whether factors connected to tree mortality in the northern border of spruce occurrence are different than factors in lower latitudes (by using variables related to solar radiation).

2. Material and methods

2.1. Study area

The present study was conducted in the area between the Northern Dvina and Pinega rivers in the Dvinsko-Pinegskiy reserve, Arkhangelsk region, Russian Federation, located in five forestry divisions (Fig. 2), between 62°30′ and 64°00′ N and 42°00′ W to 46°00′ E. The whole outbreak area of the site is approximately 1,045,000 ha. Dvinsko-Pinegskiy is a state natural reserve of regional significance, established on October 1, 2019. The study site is a highly preserved taiga area with no significant traces of anthropogenic impacts. Forest management and logging activities are fully restricted by the regime of the reserve, with no logging activities taking place during both the entire 20th century and the study period. The reserve was established for the preservation of natural ecosystems that have not been exposed to anthropogenic impacts to maintain their biological diversity and serves as a habitat to rare and endangered species of plants, animals, and other organisms (Government of the Arkhangelsk Region, 2019).

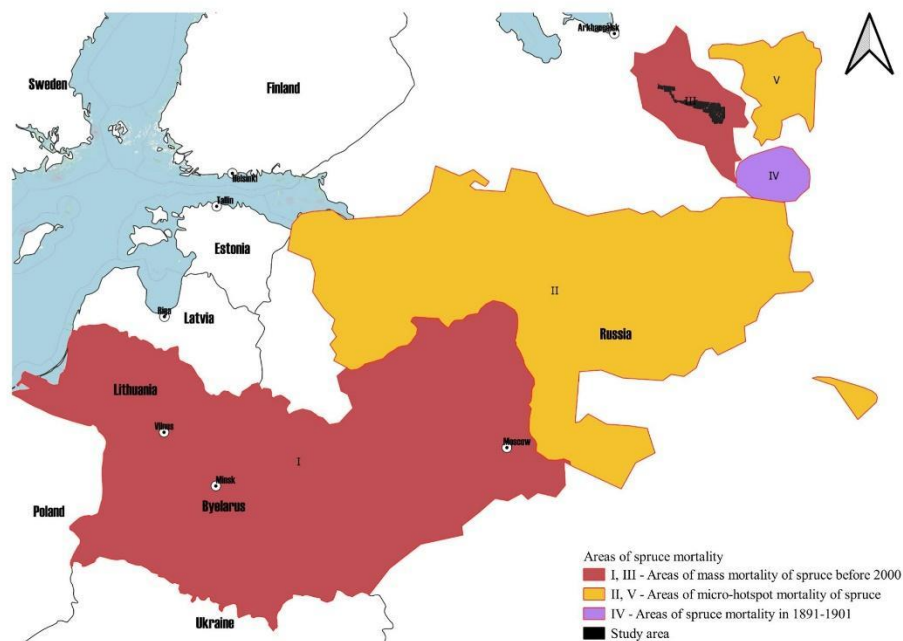The total area of the studied reserve (study area) is 300,420 ha.

Fig. 1. Areas of drought-driven spruce tree mortality in 1993–2005. adapted from Maslov (2010)
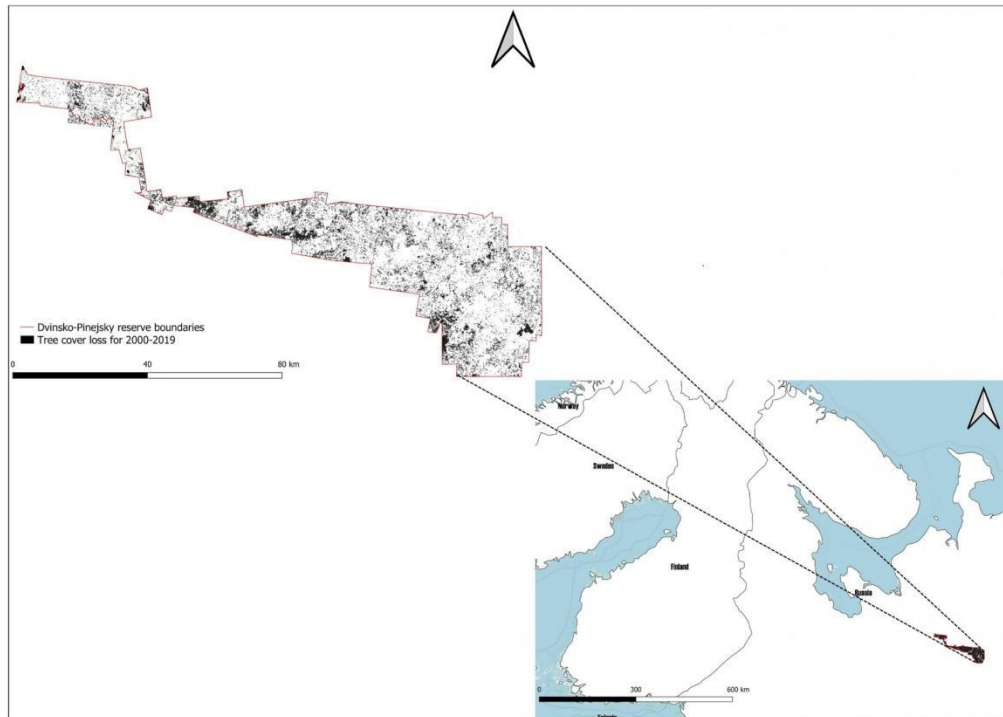
Fig. 2. Study area located in the Dvinsko-Pinegskiy reserve, Arkhangelsk region, Russian Federation. Tree cover loss from 2000 to 2019 is marked in black.

According to forest inventory data, the area has over 90% forest cover and approximately 5% swamp cover, with the remaining area covered by water bodies, hayfields, roads, and glades. The dominant forest-forming species in the area is Siberian spruce (pure forms of Siberian spruce *Picea obovata* Ledeb. and hybrid forms of spruce *P. obovata ×ic fennica* with predominance of Siberian spruce that covers 82.3% of the forested area (Procjuk et al., 2019; Zagidullina and Mirin, 2013).

The spruce stands of the Northern Dvina and Pinega rivers are mostly in older age categories with one dominant generation, all of which have a post-fire origin. Spruce stands of different ages are rare. The dieback of spruce stands is associated with older ages (180–200 years and more) and occurs naturally to renew the taiga forests in a pyrogenic way. The phenomena of higher-age spruce stand degradations are natural and last for many centuries, repeating themselves periodically (Nevolin et al., 2007).

The structure and dynamics of the studied primeval forest landscape are driven by the combined impact of small-scale spruce mortality and infrequent episodes of patchy, intermediate severity and large-scale disturbances (Khakimulina et al., 2016; Kuuluvainen et al., 2014; Nevolin et al., 2005). The main natural disturbances are windthrows and insect outbreaks (Aakala et al., 2011; Aakala et al., 2009; Khakimulina et al., 2016; Nevolin et al., 2007). Forest susceptibility to these agents is usually mediated by summer droughts (Aakala and Kuuluvainen, 2011). Fires are also an important disturbance factor in forests of this region (Nevolin et al., 2005), yet the return intervals appear to be quite long (Khakimulina et al., 2016; Nevolin et al., 2005). The tree mortality episode observed since 1999 is associated with an outbreak of European spruce bark beetle *Ips typographus* (Khakimulina et al., 2016; Nevolin et al., 2005). Drought stress, especially the extremely dry year of 1997

(Nevolin et al., 2005) was likely an inciting factor for the recent bark beetle outbreak (Aakala and Kuuluvainen, 2011; Allen et al., 2010; Khakimulina et al., 2016; Kuuluvainen et al., 2014). The second inciting factor was likely intensive breakage of treetops by snow in the winter of 2001–2002 (Nevolin et al., 2005).

2.2. Annual Norway spruce tree cover loss acquisition

We used the annual tree cover loss (*sensu* Marini et al., 2013) maps from 2001 to 2014 derived from Global Forest Watch data (http://www.globalforestwatch.org/, (Hansen et al., 2013), based on time-series analysis of Landsat imagery, to create annual maps from 2001 to 2019 at $30 \times 30 \text{ m}^2$ spatial resolution. These maps are a set of vectorized data from the original $10 \times 10°$ granules raster layer, cut by the polygon of the reserve's boundaries. Vectorization was performed in the QGIS (Version 3.16) environment, using the GDAL polygonise utility plugin (Version 3.1.4). The area of the polygons for each year were calculated with a field calculator in QGIS.

For the actual assessment, we used a tree cover loss dataset for 2001–2014 for homogeneity of the algorithm used for the assessment of the time-series analysis of Landsat images, which was changed in Version 1.7 (Ceccherini et al., 2020), as well as information from the Arkhangelsk Region Forest Protection Centre data that the massive tree mortality process in the study area had stopped. The information from the Forest Protection Centre was confirmed with the dataset from (Hansen et al., 2013).

3

134

2.3. Meteorological variables

To understand the effects of climate on bark beetle epidemics and subsequent tree mortality, we obtained meteorological data previously identified as important for insect populations (Faccoli, 2009; Marini et al., 2013) comprising temperature, precipitation, and three different indices (JJA, Selyaninov, and DJF, for explanations, see Table 1). We introduced a new variable which we hypothesized may influence tree mortality because of its effect on bark beetle population dynamics - the total monthly duration of solar radiation.

Meteorological data were acquired for the years 2001–2014 from the Sura meteorological station (Platform ID 22676, Latitude 63.58 Longitude 45.63) of the Roshydromet network from specialized arrays for climate research. Data sampling was provided by Web-technology Aisori (Veselov et al., 2000).

We consider the temporal window of April-June as the main season for bark beetles in our study area; outside this period, temperatures are frequently beyond the developmental threshold of *I. typographus* populations. We collected data on average monthly temperature and precipitation (April-June), as well as the Selyaninov coefficient. To assess moisture during the growing season, the Selyaninov hydrothermal coefficient (K) is calculated according to the formula: $K = R*10/\sum t$, where R is the sum of precipitation in mm for the period with the temperatures higher than 10 °C and t is the temperatures in degrees Celsius for the same time. According to the handbook Methods for Monitoring Forest Pests and Diseases (Tuzova, 2004), the values of Selyaninov's hydrothermal coefficient for the growing season indicate the following conditions: 2 = excessive moisture; 1.5 = adequate moisture; 1.0 = on the verge of drought, and 0.5 = severe drought. Our newly introduced variable, duration of solar radiation, was used as the total monthly duration of solar radiation from April to June.

Table 1
Variables used in the study of changes in tree cover loss. Meteorological data were collected from the nearest weather station to the study area for the 2001–2014 period.

Name in model	Variable
TCL	Tree cover loss in a given year
TLC	Tree loss change in a given year
AveTempYear	Average yearly air temperature in a given year
AveTempYear(t-1)	Average yearly air temperature in the previous year
AvePrecYear	Average yearly adjusted precipitation in a given year
AprT	April average monthly air temperature in a given year*
MayT	May average monthly air temperature in a given year
JuneT	June average monthly air temperature in a given year
AprP	April amount of adjusted precipitation in a given year*
MayP	May amount of adjusted precipitation in a given year*
JuneP	June amount of adjusted precipitation in a given year*
Selyaninov	Selyaninov hydrothermal coefficient in a given year
Selyaninov(t-1)	Selyaninov hydrothermal coefficient in the previous year
DJF	December, January, and February average air temperature in a given year
DJF(t-1)	December, January, and February average air temperature in the previous year
JJA	June, July, and August average air temperature in a given year
JJA(t-1)	June, July, and August average air temperature in the previous year
S_Apr	April monthly total duration of solar radiation in a given year
S_May	May monthly total duration of solar radiation in a given year
S_June	June monthly total duration of solar radiation in a given year
S_Apr(t-1)	April monthly total duration of solar radiation in the previous year
S_May(t-1)	May monthly total duration of solar radiation in the previous year
S_June(t-1)	June monthly total duration of solar radiation in the previous year

* The monthly precipitation amount after elimination of systematic errors of gauge instruments.

2.4. Statistical analyses and model selection

Before the analysis, data were checked for outliers and collinearity. During data exploration, we plotted the response variable with each covariate to check the relationship between them. Based on the data exploration, the relationship between tree loss and explanatory variables was analysed using linear regression (Zuur et al., 2010). A set of *a priori* models (Dochtermann and Jenkins, 2011; Rosen, 2016) was selected prior to analysis (Table 2) in order to test which model would best explain the infestation of trees by *I. typographus*. These models were constructed using previously known variables identified as important for bark beetle population dynamics, mainly climatic variables. The information-theory (I-T) approach was used to assess competing models. Models were ranked according to the Akaike information criterion (AIC); the most parsimonious model was selected based on the lowest AIC value. We also calculated Akaike weights to arrange candidate models in order of parsimony, where Akaike weight is a number from 0 to 1, providing a measure of the relative likelihood of each model, given the data and candidate model set (Burnham et al., 2011).

Total tree mortality (km^2 per year) was used as the response variable. As some of the variables were highly correlated, we used the threshold of $r = 0.7$ to select variables. We tested the correlation between changes in annual tree cover losses in a particular year and changes in annual tree cover losses in previous years by calculating the autocorrelation function (ACF). We assessed also the cross-correlation functions (CCF) of the predictor time series and variables in the best model. Because we used previous year tree mortality as an explanatory variable in our analysis, the sample size changed from 14 (2001–2014) to 13 years (2002–2014). All calculations and statistical analysis were conducted in R (Version 3.6.1) in RStudio Version 1.3.1093 (R Development Core Team 2018).

3. Results

3.1. Tree cover loss due to disturbance events

Total tree cover loss, considering all 14 years from 2001 to 2014, amounted to 160 km^2 (Fig. 3). Tree mortality was above zero for all years, with the lowest mortality of 3.37 km^2 in 2013.

Table 2
Proposed models to study annual changes of tree cover loss for a 14-year period.

Model	Variables
1	Annual tree cover loss change = JuneT + AveTempYear(t-1) + Ɛ
2	Annual tree cover loss change = AveTempYear + JuneP + Ɛ
3	Annual tree cover loss change = JuneT + AveTempYear + AveTempYear(t-1) + Ɛ
4	Annual tree cover loss change = AveTempYear(t-1) + AveTempYear + JuneT + JuneP + Ɛ
5	Annual tree cover loss change = DJF + AveTempYear + Ɛ
6	Annual tree cover loss change = AveTempYear + Ɛ
7	Annual tree cover loss change = JuneT + DJF + AveTempYear(t-1) + Ɛ
8	Annual tree cover loss change = JuneT + AveTempYear(t-1) + MayT + Ɛ
9	Annual tree cover loss change = AveTempYear + JuneT + Ɛ
10	Annual tree cover loss change = JuneT + AprT + AveTempYear(t-1) + Ɛ
11	Annual tree cover loss change = JuneT + JJA + AveTempYear(t-1) + Ɛ
12	Annual tree cover loss change = AveTempYear + JuneT + DJF + JuneP + Ɛ
13	Annual tree cover loss change = AveTempYear + S_June + Ɛ
14	Annual tree cover loss change = AveTempYear + AveTempYear(t-1) + DJF + JuneP + Ɛ
15	Annual tree cover loss change = S_June + S_May(t-1) + Ɛ
16	Annual tree cover loss change = AveTempYear + AveTempYear(t-1) + Ɛ
17	Annual tree cover loss change = AveTempYear + S_Apr + Ɛ

Notes: Annual tree cover loss change is the yearly change in the area of damage sensu (Marini et al., 2013); For the explanation of variables used, we refer to Table 1. Ɛ is random error.
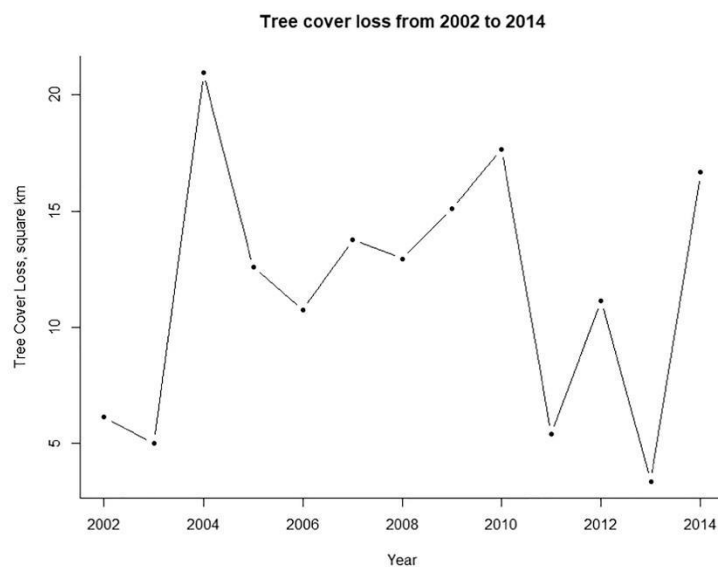
Tree cover loss from 2002 to 2014

Fig. 3. Annual tree cover loss (km^2) of *Picea obovata* caused by *I. typographus*.

3.2. Annual tree loss change

We tested the data on tree mortality throughout our study period for autocorrelation; the ACF function did not reveal trends between tree mortality caused by *I. typographus* in a given year and the previous year. The CCF also did not show any patterns. Linear regression was used to further investigate the relationships between tree mortality and meteorological variables, including average annual air temperature in a given and the previous year; December, January, and February average air temperatures in a given year; June, July, and August average air temperatures in a given year; April, May, and June average air temperatures in a given year; June adjusted precipitation in a given year; April, May, and June total duration of solar radiation in a given year. The *a priori* set of competing models that differ by a combination of predictor variables is given in Table 2.

The most parsimonious model according to AICc was Model 1 (Table 3). Our model revealed that June average air temperature in a given year (*JuneT*) and average annual air temperature in the last year (*L_AveTempYear*) had an effect on tree loss change from 2001 to 2014 (Table 4 and Fig. 4). Higher previous year temperatures had a positive effect on tree mortality, i.e. the higher were the temperatures the higher were tree losses. On the other hand, June temperatures had a negative effect on tree loss, higher June temperatures resulted in less tree loss. Based on the results gained from Model 1, the course of the annual tree mortality and the daily maximum air temperature sums from the previous year is illustrated in Fig. 5.

The rest of the explanatory variables (Table 1) were not included in the most parsimonious models, although according to ΔAIC, *Model 2* and *Model 3* can also have strong explanatory power, because of their ΔAIC < 2. These two models contain variables related to average monthly or yearly temperatures and June precipitation. The rest of the models tested, in the range of ΔAIC 2–7, may have biological meaning, although they are not considered the most parsimonial in our study period and area. These models represent different combinations of various temperatures and underscore the effect of temperature on tree loss change, although they have a much smaller probability of being the best model

Table 3

Akaike's information criterion (AICc) values for a small sample dataset, ΔAIC values and Akaike weights (AIC weight) for the competing models are listed in Table 1. The model with the lowest ΔAIC is the most parsimonious, given the data. Models with ΔAIC < 2 may be considered as good as the best, while models in the ΔAIC range of 2–7 are also plausible. The AIC weight is a value between 0 and 1, with the sum of all models in the candidate set being 1. This weight can be considered the probability that a given model is the best-approximating model.

Model	AICc	ΔAIC	AIC weight
1	33.23052	0.0000000	0.187543982
2	33.54445	0.3139293	0.160300273
3	34.26863	1.0381106	0.111604134
4	36.45356	3.2230384	0.037430811
5	36.72677	3.4962544	0.03265135
6	37.94086	4.7103427	0.017793657
7	38.47268	5.2421605	0.013638997
8	38.55823	5.3277082	0.013067906
9	38.62106	5.3905444	0.01266372
10	38.71484	5.4843209	0.012083646
11	38.74466	5.514145	0.011904791
12	38.85633	5.6258154	0.011258301
13	39.13043	5.8999067	0.009816455
14	39.64515	6.4146355	0.007588968
15	40.1558	6.925283	0.005878913
16	40.17695	6.9464299	0.00581708
17	40.28942	7.0588963	0.005498994

(AIC weight). For example, models 12 and 14 comprises June precipitations, model 13, 15 and 17 comprises solar radiation.

4. Discussion

In recent decades, forests of the Arkhangelsk region have been subjected to large-scale bark beetle outbreaks. Our study examined bark beetle infestations in an area where no sanitary or salvage logging was applied from 2001 to 2014. A total of 160 km^2 of forests was lost during the study period, mainly due to the *I. typographus* outbreak. This is one of

136

Table 4

Linear model equation estimating the alteration in *Picea obovata* annual tree loss change (see Eq. 1) by *I. typographus* as a function of the temperature in June (JuneT) in the given year and the previous-year average temperature by year (L. AveTempYear) from 2001 to 2014 in the Dvinsko-Pinegskiy reserve, Arkhangelsk region, Russian Federation.

Parameter	Estimate	p-value	Model values
Intercept	3.2972	0.0154 *	
JuneT	−0.2911	0.0093 **	Adjusted R-squared: 0.4856
L_AveTempYear	0.56911	0.0167 *	

the first studies on the effects of temperature on host tree mortality and their natural bark beetles in the European region of Russia. The natural process of the active phase of the tree mortality finished in 2014, as well as above mentioned change in the algorithm of the Global Forest Watch data (Hansen et al., 2013).

Our results show that the dynamic of bark beetle-induced tree mortality was mainly associated with temperature. We found that tree-loss changes slightly decreased with increasing temperature in June

while tree-loss increased after years with higher temperatures (Table 4). Similarly, a decrease in aggressive bark beetle population density with increased temperature was found by Wermelinger et al. (2021). Temperatures were used in modelling future bark beetle populations by Berec et al. (2013).

The contradicting results suggest that tree mortality by bark beetles depends not only on bark beetle population dynamics but also on the physiological status of host trees. These relationships are often non-linear, and both very high and low rates of temperature can slow down insect development (Wermelinger and Seifert, 1998). A study conducted in the Bohemian Forest showed that if the climate is projected to continue to change in the future, the number of extreme events will also change, and we, therefore, may expect only a small change in the development time of beetles (Berec et al., 2013).

4.1. Limitations of the study

We assume that almost all tree mortality in the period of bark beetle outbreak was related to bark beetle attacks. Some tree mortality may be
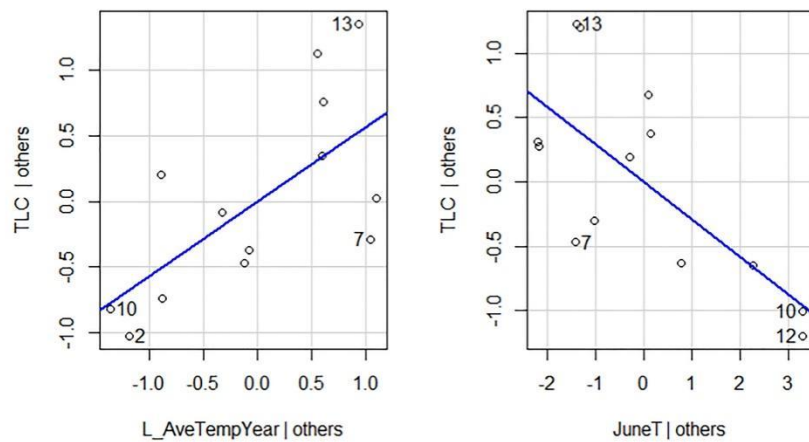
Fig. 4. The result of fitting the most parsimonious model (Tab.4) for the relation between the annual tree cover loss change and average temperatures in the previous year (L_AveTempYear) and average June temperatures (JuneT) in a 14-year study in the Dvinsko-Pinegskiy reserve, Arkhangelsk region, Russian Federation. The graphs show the association between the predictor variable and the response variable while holding the value of all other predictor variables constant.
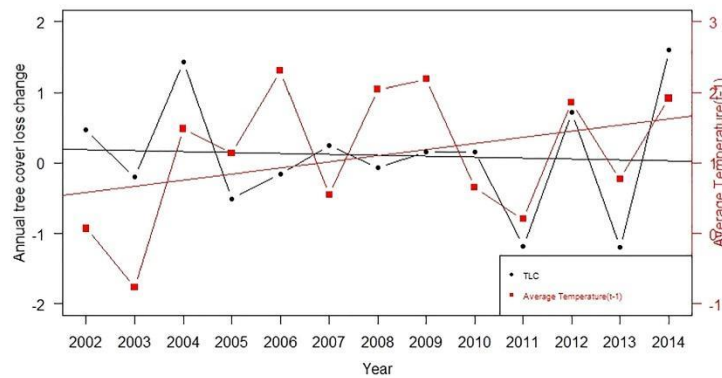
Fig. 5. Time series of yearly tree cover loss change in *P. abies* caused by *I. typographus* and average temperatures in the previous year and their linear trends.

caused by wind damage or by fires; however, there were no records of forest fire activity in the area. We have excluded values of tree mortality after 2014 from the dataset due to a change in the algorithm of Global Forest Watch (Ceccherini et al., 2020). One limitation is that we used only one meteorological station in the study area, despite the relatively large size of the study area. No stand volume data were used in the study and only publicly available data with a spatial resolution of approximately 30 m per pixel were used. For the study area of 350,000 ha, we consider such spatial resolution satisfactory.

During the modelling process, we also tested combinations of generalized additive models (GAM) models in order to investigate the relationships between tree mortality and meteorological variables more correctly, based on expectations of non-linear relationships between tree mortality and temperature, discovered before (Mezei et al., 2017). The best GAM model of the set remained the same as it was during LM modelling, with a negative coefficient for June's temperature in a given year with linear graphical representation.

4.2. Factors influencing bark beetle population

Our results show that the bark beetle-caused tree mortality was mainly related to the average June temperature and the previous year's temperatures. In our best model (Table 4), the annual changes of tree cover loss were dependent on the average temperature in June and the average temperature in the previous year.

Temperature is generally related to insect development; usually, the higher the temperature the higher the developmental rate of bark beetle offspring under the bark, but only to a limited extend. There is an upper-temperature developmental threshold (Baier et al., 2007; Wermelinger and Seifert, 1998). Most studies have shown positive relationships between summer temperatures and bark beetle populations with some exceptions, e.g., Faccoli (2009), Marini et al. (2013) and Wermelinger et al. (2021). For example, Marini et al. (2013)) found temperature-related variables did not show any effect on *I. typographus* population dynamics; whereas summer rainfall revealed associations with the population dynamics. Similarly, Faccoli (2009) found that spruce mortality caused by bark beetles was negatively associated with precipitation from March to July; and temperature played no role in that association. In another study from Central Europe, tree mortality caused by bark beetles had a bell-shaped curve with lower and upper thresholds of suitable temperature sums (Mezei et al., 2017). The inhibitory effects of extreme high and low temperatures on bark beetles are relatively well-known and have been used in phenological modelling of bark beetles (Baier et al., 2007; Wermelinger and Seifert, 1998).

As with our findings, Nevolin et al. (2005) found high temperatures during dry summers an important factor influencing the bark beetle population dynamic in their study area; with very high summer temperatures likely limiting bark beetle population growth. June may also be the main month of *I. typographus* flight activity in northern Europe (Öhrn et al., 2014). Flight activity of *I. typographus* depends on air temperature as beetles do not fly at air temperatures outside the range of 16.5–30 °C (Lobinger, 1994). Temperatures above 30 °C can also limit bark beetle swarming.

Previous year temperatures, especially temperature for the month of May, were important variables in several of our other models and studies conducted by other researchers (Mezei et al., 2017).

The average temperatures in December, January, February, April, May, and July have also shown some degree of importance. In the case of winter months in eastern European Russia, the effect of warmer winters on *I. typographus* mortality remains controversial. Lower winter temperatures may increase mortality of larvae and pupae overwintering above the snow layer (Romashkin et al., 2020). However, higher temperatures during hibernation and thinner snow cover may increase beetle mortality due to increased metabolic rates (Annila, 1969; Romashkin et al., 2020).

The duration of solar radiation in June was selected as one of the biologically viable variable while the duration of solar radiation in April was an important factor in one model (model no. 17.). Interestingly, the duration of solar radiation in May of the previous year was also noteworthy. *I. typographus* flight behaviour is strongly influenced by light, with a strong preference for sunny conditions (Lobinger and Skatulla, 1996) since this means a longer day for flight and reproductive activity. However, the daily rhythm of *I. typographus* flight in high longitudes has not been studied so far. Longer solar radiation duration should also cause higher increases in temperature sum per day at high latitudes compared to low latitudes, due to the increasing day length towards the north.

4.3. Factors influencing spruce defence abilities and drought stress

A more recent study by Wermelinger et al. 2021) found that increased temperatures led to a decrease in aggressive bark beetles and an improvement in the resin flow of trees. Increased resin flow leads to an improved defence of trees against bark beetle attacks.

After temperature, the June precipitation was an important variable in our study in models 2, 4, 12, and 14 (Table 2). The effect of summer temperatures and precipitation in our study can also be related to the reactions of spruce to drought stress (Aakala and Kuuluvainen, 2011). Certain levels of drought stress decrease spruce defence abilities (Netherer et al., 2015); however, severely drought-stressed trees may survive due to reduced host acceptance (Kolb et al., 2019).

The importance of drought as a factor influencing tree susceptibility is not only in the initialization of the outbreak. Bark beetle population dynamics can be deduced from the diffuse pattern of bark beetle infestations (the size distribution of disturbance patches was strongly weighted toward small ones) on relatively large portions of the study area (Kuuluvainen et al., 2014; Nevolin et al., 2005). This pattern is different from the landscape pattern of wind and bark beetle driven disturbances in the middle European mountains (Havašová et al., 2017; Potterf et al., 2019). One possible explanation for this is that stands on mineral soils appeared to be more influenced by drought than paludified sites (Kuuluvainen et al., 2014). Nevolin et al. (2005) noted that fluctuation of groundwater level is another key factor that influences bark beetle populations.

Recently, extensive *I. typographus* outbreaks have occurred in the southern part of European boreal forests (Jönsson et al., 2012; Marini et al., 2013; Maslov, 2010; Romashkin et al., 2020) when windstorms coincided with periods of temperature extremes causing drought stress on spruce forests. Drought is an important factor predisposing conifers to bark beetle attack in a broad range of geographical locations (Marini et al., 2017; Obladen et al., 2021).

4.4. Longitudinal shift of bark beetle outbreak distribution

Based on Maslov (2010) findings; there is a possibility that bark beetle outbreaks have been shifting towards the northern limit of spruce distribution across the landscape. Blomqvist et al. (2018) stated that *I. typographus* L. abundance and outbreak frequency in Finland have significantly increased during the last decade. However; Romashkin et al. (2020) analysed the latitudinal and longitudinal distribution of *I. typographus* outbreaks in the European part of Russia in the period 1960–2019 and found no statistically significant changes in the average distribution of the outbreaks.

4.5. Management implications

In the warming climate, drought and drought-induced bark beetle outbreaks may become more severe even at the northern limits of a spruce occurrence (Jönsson et al., 2012; Kuuluvainen et al., 2014; Venäläinen et al., 2020). It is likely that infestations will spread towards northern forests in Russia where no bark beetle outbreaks have been reported in significant intensity. Therefore, forest managers and

policymakers need to provide immediate protection measures against future anthropogenic disturbances in the northern forests that otherwise may result in further bark beetle infestations (Zabihi et al., 2021)

5. Summary and conclusions

Our results show that tree mortality caused by the bark beetle outbreak in the Arkhangelsk region was related mainly to temperature in current and previous years. Other factors like June precipitation and April and May duration of solar radiation were also important. The bark beetle outbreak in the study areas was probably influenced by two groups of factors. The first group of factors relates to the increasing temperature sums and connected increase of aggressiveness of bark beetle populations, while the second group of factors relates to drought and a connected decrease of spruce defence abilities. So far, we do not fully understand the *I. typographus* flight behaviour and other biological aspects at high latitudes, as well as their connections with climatic changes, so further study in this area is needed.

CRediT authorship contribution statement

Aleksei Trubin: Formal analysis, Methodology, Data curation, Visualization, Writing – original draft, Writing – review & editing. **Pavel Mezei:** Formal analysis, Conceptualization, Methodology, Visualization, Writing – original draft, Writing – review & editing. **Khodabakhsh Zabihi:** Writing – review & editing. **Peter Surový:** Writing – review & editing. **Rastislav Jakuš:** Conceptualization, Funding acquisition, Investigation, Methodology, Project administration, Writing – review & editing.

Declaration of Competing Interest

The authors declare that they have no known competing financial interests or personal relationships that could have appeared to influence the work reported in this paper.

Acknowledgments

References

Aakala, T., Kuuluvainen, T., 2011. Summer droughts depress radial growth of Picea abies in pristine taiga of the Arkhangelsk province, northwestern Russia. Dendrochronologia 29 (2), 67–75. https://doi.org/10.1016/j.dendro.2010.07.001.

Aakala, T., Kuuluvainen, T., Wallenius, T., Kauhanen, H., 2011. Tree mortality episodes in the intact Picea abies-dominated taiga in the Arkhangelsk region of northern European Russia. J. Veg. Sci. 22, 322–333. https://doi.org/10.1111/j.1654-1103.2010.01253.x.

Aakala, T., Kuuluvainen, T., Wallenius, T., Kauhanen, H., 2009. Contrasting patterns of tree mortality in late successional Picea abies stands in two areas in northern Fennoscandia. J. Veg. Sci. 20, 1016–1026. https://doi.org/10.1111/j.1654-1103.2009.01100.x.

Allen, C.D., Macalady, A.K., Chenchouni, H., Bachelet, D., McDowell, N., Vennetier, M., Kitzberger, T., Rigling, A., Breshears, D.D., Hogg, E.H.(., Gonzalez, P., Fensham, R., Zhang, Z., Castro, J., Demidova, N., Lim, J.-H., Allard, G., Running, S.W., Semerci, A., Cobb, N., 2010. A global overview of drought and heat-induced tree mortality reveals emerging climate change risks for forests. For. Ecol. Manage. 259 (4), 660–684. https://doi.org/10.1016/j.foreco.2009.09.001.

Annila, E., 1969. Influence of temperature upon the development and voltinism of Ips typographus L. (Coleoptera, Scolytidae). Ann. Zool. Fennici 6, 161–208.

Bače, R., Svoboda, M., Janda, P., Morrissey, R.C., Wild, J., Clear, J.L., Čada, V., Donato, D.C., Chen, H.Y.H., 2015. Legacy of Pre-Disturbance Spatial Pattern Determines Early Structural Diversity following Severe Disturbance in Montane Spruce Forests. PLoS One 10 (9), e0139214. https://doi.org/10.1371/journal.pone.013921410.1371/journal.pone.0139214.g00110.1371/journal.pone.0139214.g00210.1371/journal.pone.0139214.g00310.1371/journal.pone.0139214.g00410.1371/journal.pone.0139214.g00510.1371/journal.pone.0139214.g00610.1371/journal.pone.0139214.s00110.1371/journal.pone.0139214.s00210.1371/journal.pone.0139214.s00310.1371/journal.pone.0139214.s00410.1371/journal.pone.0139214.s005.

Baier, P., Pennerstorfer, J., Schopf, A., 2007. PHENIPS—A comprehensive phenology model of Ips typographus (L.) (Col., Scolytinae) as a tool for hazard rating of bark beetle infestation. For. Ecol. Manage. 249 (3), 171–186. https://doi.org/10.1016/j.foreco.2007.05.020.

Bentz, B.J., Jönsson, A.M., 2015. In: Bark Beetles. Elsevier, pp. 533–553. https://doi.org/10.1016/B978-0-12-417156-5.00013-7.

Berec, L., Doležal, P., Hais, M., 2013. Population dynamics of Ips typographus in the Bohemian Forest (Czech Republic): Validation of the phenology model PHENIPS and impacts of climate change. For. Ecol. Manage. 292, 1–9. https://doi.org/10.1016/j.foreco.2012.12.018.

Blomqvist, M., Kosunen, M., Starr, M., Kantola, T., Holopainen, M., Lyytikäinen-Saarenmaa, P., 2018. Modelling the predisposition of Norway spruce to Ips typographus L. infestation by means of environmental factors in southern Finland. Eur. J. For. Res. 137 (5), 675–691. https://doi.org/10.1007/s10342-018-1133-0.

Burnham, K.P., Anderson, D.R., Huyvaert, K.P., 2011. AIC model selection and multimodel inference in behavioral ecology: Some background, observations, and comparisons. Behav. Ecol. Sociobiol. 65 (1), 23–35. https://doi.org/10.1007/s00265-010-1029-6.

Ceccherini, G., Duveiller, G., Grassi, G., Lemoine, G., Avitabile, V., Pilli, R., Cescatti, A., 2020. Abrupt increase in harvested forest area over Europe after 2015. Nature 583 (7814), 72–77. https://doi.org/10.1038/s41586-020-2438-y.

Christiansen, E., Waring, R.H., Berryman, A.A., 1987. Resistance of conifers to bark beetle attack: Searching for general relationships. For. Ecol. Manage. 22 (1-2), 89–106. https://doi.org/10.1016/0378-1127(87)90098-3.

DeRose, R.J., Bentz, B.J., Long, J.N., Shaw, J.D., 2013. Effect of increasing temperatures on the distribution of spruce beetle in Engelmann spruce forests of the Interior West. USA. For. Ecol. Manage. 308, 198–206. https://doi.org/10.1016/j.foreco.2013.07.061.

Dochtermann, N.A., Jenkins, S.H., 2011. Developing multiple hypotheses in behavioral ecology. Behav. Ecol. Sociobiol. 65 (1), 37–45. https://doi.org/10.1007/s00265-010-1039-4.

Faccoli, M., 2009. Effect of weather on Ips typographus (Coleoptera Curculionidae) phenology, voltinism, and associated spruce mortality in the southeastern Alps. Environ. Entomol. 38 (2), 307–316.

Gely, C., Laurance, S.G.W., Stork, N.E., 2020. How do herbivorous insects respond to drought stress in trees? Biol. Rev. 95 (2), 434–448. https://doi.org/10.1111/brv.v95.210.1111/brv.12571.

Hansen, M.C., Potapov, P.V., Moore, R., Hancher, M., Turubanova, S.A., Tyukavina, A., Thau, D., Stehman, S.V., Goetz, S.J., Loveland, T.R., Kommareddy, A., Egorov, A., Chini, L., Justice, C.O., Townshend, J.R.G., 2013. High-Resolution Global Maps of 21st-Century Forest Cover Change. Science (80-. 342 (6160), 850–853. https://doi.org/10.1126/science:1244693.

Hart, S.J., Veblen, T.T., Schneider, D., Molotch, N.P., 2017. Summer and winter drought drive the initiation and spread of spruce beetle outbreak. Ecology 98 (10), 2698–2707. https://doi.org/10.1002/ecy.2017.98.issue-1010.1002/ecy.1963.

Havašová, M., Ferenčík, J., Jakuš, R., 2017. Interactions between windthrow, bark beetles and forest management in the Tatra national parks. In press. For. Ecol. Manage. 391, 649–1361. https://doi.org/10.1016/j.foreco.2017.01.009.

Holuša, J., Liška, J., 2002. HYPOTÉZA CHŘADNUTÍ A ODUMÍRÁNÍ SMRKOVÝCH POROSTŮ VE SLEZSKU * (ČESKÁ REPUBLIKA) Hypothesis of spruce forests decline and dying in Silesia (Czech Republic). Zprávy Lesn. výskumu 47, 9–15.

Hrošo, B., Mezei, P., Potterf, M., Majdák, A., Blaženec, M., Korolyova, N., Jakuš, R., 2020. Drivers of Spruce Bark Beetle (Ips typographus) Infestations on Downed Trees after Severe Windthrow. Forests 11, 1290. https://doi.org/10.3390/f11121290.

Jactel, H., Petit, J., Desprez-Loustau, M.-L., Delzon, S., Piou, D., Battisti, A., Koricheva, J., 2012. Drought effects on damage by forest insects and pathogens: A meta-analysis. Glob. Chang. Biol. 18 (1), 267–276. https://doi.org/10.1111/j.1365-2486.2011.02512.x.

Jönsson, A.M., Schroeder, L.M., Lagergren, F., Anderbrant, O., Smith, B., 2012. Guess the impact of Ips typographus—An ecosystem modelling approach for simulating spruce bark beetle outbreaks. Agric. For. Meteorol. 166–167, 188–200. https://doi.org/10.1016/j.agrformet.2012.07.012.

Kärvemo, S., Rogell, B., Schroeder, M., 2014. Dynamics of spruce bark beetle infestation spots: Importance of local population size and landscape characteristics after a storm disturbance. For. Ecol. Manage. 334, 232–240. https://doi.org/10.1016/j.foreco.2014.09.011.

Khakimulina, T., Fraver, S., Drobyshev, I., Nakashizuka, T., 2016. Mixed-severity natural disturbance regime dominates in an old-growth Norway spruce forest of northwest Russia. J. Veg. Sci. 27 (2), 400–413. https://doi.org/10.1111/jvs.12351.

Kolb, T., Keefover-Ring, K., Burr, S.J., Hofstetter, R., Gaylord, M., Raffa, K.F., 2019. Drought-Mediated Changes in Tree Physiological Processes Weaken Tree Defenses to Bark Beetle Attack. J. Chem. Ecol. 45 (10), 888–900. https://doi.org/10.1007/s10886-019-01105-0.

Kolb, T.E., Fettig, C.J., Ayres, M.P., Bentz, B.J., Hicke, J.A., Mathiasen, R., Stewart, J.E., Weed, A.S., 2016. Observed and anticipated impacts of drought on forest insects and diseases in the United States. For. Ecol. Manage. 380, 321–334. https://doi.org/10.1016/j.foreco.2016.04.051.

8

Komonen, A., Schroeder, M.L., Weslien, J., 2011. Ips typographus population development after a severe storm in a nature reserve in southern Sweden. J. Appl. Entomol. 135, 132–141. https://doi.org/10.1111/j.1439-0418.2010.01520.x.

Kuuluvainen, T., Wallenius, T.H., Kauhanen, H., Aakala, T., Mikkola, K., Demidova, N., Ogibin, B., 2014. Episodic, patchy disturbances characterize an old-growth Picea abies dominated forest landscape in northeastern Europe. For. Ecol. Manage. 320, 96–103. https://doi.org/10.1016/j.foreco.2014.02.024.

Lobinger, G., 1994. Die Lufttemperatur als limitierender Faktor für die Schwärmaktivität zweier rindenbrütender Fichtenborkenkäferarten, Ips typographus L. und Pityogenes chalcographus L. (Col., Scolytidae). Anzeiger Für Schädlingskunde Pflanzenschutz Umweltschutz 67 (1), 14–17. https://doi.org/10.1007/BF01906563.

Lobinger, G., Skatulla, U., 1996. Untersuchungen zum einfluß von sonnenlicht auf das schwärmverhalten von borkenkäfernInfluencing the flight behaviour of bark beetles by light conditions. Anzeiger für Schadlingskd. 69 (8), 183–185. https://doi.org/10.1007/BF01908442.

Marini, L., Lindelöw, Å., Jönsson, A.M., Wulff, S., Schroeder, L.M., 2013. Population dynamics of the spruce bark beetle: A long-term study. Oikos 122 (12), 1768–1776. https://doi.org/10.1111/more.2013.122.issue-1210.1111/j.1600-0706.2013.00431.x.

Marini, L., Økland, B., Jönsson, A.M., Bentz, B., Carroll, A., Forster, B., Grégoire, J.-C., Hurling, R., Nageleisen, L.M., Netherer, S., Ravn, H.P., Weed, A., Schroeder, M., 2017. Climate drivers of bark beetle outbreak dynamics in Norway spruce forests. Ecography (Cop.) 40 (12), 1426–1435. https://doi.org/10.1111/ecog.2017.v40.i1210.1111/ecog.02769.

Maslov, A.D., 2010. Короед типограф и усыхание еловых лесов [Bark beetle and the decay of spruce forests]. ВНИИЛМ 138.

Mcdowell, N., Pockman, W.T., Allen, C.D., Breshears, D.D., Cobb, N., Kolb, T., Plaut, J., Sperry, J., West, A., Williams, D.G., Yepez, E.A., Mcdowell, N., Pockman, W.T., Allen, C.D., David, D., Mcdowell, N., Cobb, N., Kolb, T., Plaut, J., Sperry, J., 2008. Mechanisms of Plant Survival and Mortality during Drought : Why Do Some Plants Survive while Others Succumb to Drought ? Published by : Wiley on behalf of the New Phytologist Trust Stable URL : http://www.jstor.org/stable/30149305 REFERENCES Linked refere 178, 719–739.

Meddens, A.J.H., Hicke, J.A., Macalady, A.K., Buotte, P.C., Cowles, T.R., Allen, C.D., 2015. Patterns and causes of observed piñon pine mortality in the southwestern United States. New Phytol. 206 (1), 91–97. https://doi.org/10.1111/nph.2015.206.issue-110.1111/nph.13193.

Mezei, P., Jakuš, R., Pennerstorfer, J., Havašová, M., Škvarenina, J., Ferenčík, J., Slivinský, J., Bičárová, S., Bilčík, D., Blaženec, M., Netherer, S., 2017. Storms, temperature maxima and the Eurasian spruce bark beetle Ips typographus—An infernal trio in Norway spruce forests of the Central European High Tatra Mountains. Agric. For. Meteorol. 242, 85–95. https://doi.org/10.1016/j.agrformet.2017.04.004.

Miller, J.M., Keen, F.P., 1960. Biology and control of the western pine beetle: a summary of the first fifty years of research (No. 800). US Department of Agriculture.

Netherer, S., Matthews, B., Katzensteiner, K., Blackwell, E., Henschke, P., Hietz, P., Pennerstorfer, J., Rosner, S., Kikuta, S., Schume, H., Schopf, A., 2015. Do water-limiting conditions predispose Norway spruce to bark beetle attack? New Phytol. 205, 1128–1141. https://doi.org/10.1111/nph.13166.

Nevolin, O.A., Gritsynin, A.N., Torkhov, S.V., 2005. On Decay and Downfall of Over-mature Spruce Forests in Beresnik Forestry Unit of Arkhangelsk Region. Лесной Журнал 6.

Nevolin, O.A., Tretiyakov, S.V., Torkhov, S.V., 2007. К истории об усыхании еловых лесов в Междуречье Северной Двины и Пинеги [Towards a history of spruce forest decline in the Northern Dvina-Pinega interfluve]. Лесной вестник / For. Bull. 5, 65–74.

Obladen, N., Dechering, P., Skiadaresis, G., Tegel, W., Keßler, J., Höllerl, S., Kaps, S., Hertel, M., Dulamsuren, C., Seifert, T., Hirsch, M., Seim, A., 2021. Tree mortality of European beech and Norway spruce induced by 2018–2019 hot droughts in central Germany. Agric. For. Meteorol. 307, 108482. https://doi.org/10.1016/j.agrformet.2021.108482.

Öhrn, P., Långström, B., Lindelöw, Å., Björklund, N., 2014. Seasonal flight patterns of Ips typographus in southern Sweden. Agric. For. Entomol. 16, 147–157. https://doi.org/10.1111/afe.12044.

Potterf, M., Nikolov, C., Kočická, E., Ferenčík, J., Mezei, P., Jakuš, R., 2019. Landscape-level spread of beetle infestations from windthrown- and beetle-killed trees in the non-intervention zone of the Tatra National Park, Slovakia (Central Europe). For. Ecol. Manage. 432, 489–500. https://doi.org/10.1016/j.foreco.2018.09.050.

Procjuk, N.V., Kopytov, A.A., Andriyanov, V.V., Gvozdetskaya, E.V., Alekseeva, A.A., 2019. Материалы коМплексного экологического обследования участков территории, обосновывающих придание правового статуса особо охраняеМой природной территории регионального значения – государственного природного ландшафтного заказника «Двинско-ПинеЖский» [Materi. Arkhangelsk Obl. State Budg. Inst. Nat. Manag. Environ. Prot, Centre, Arkhangelsk (in Russ.

Raffa, K.F., Gregoire, J., Lindgren, B.S., Gre, J., 2015. Natural History and Ecology of Bark Beetles, in: Vega, F.E., Hofstetter, R.W. (Eds.), Bark Beetles: Biology and Ecology of Native and Invasive Species. Academic Press, pp. 1–40. https://doi.org/10.1016/B978-0-12-417156-5.00001-0.

Romashkin, I., Neuvonen, S., Tikkanen, O.-P., 2020. Northward shift in temperature sum isoclines may favour Ips typographus outbreaks in European Russia. Agric. For. Entomol. 22 (3), 238–249. https://doi.org/10.1111/afe.v22.310.1111/afe.12377.

Rosen, J., 2016. A forest of hypotheses. Nature 536, 239–241.

Schroeder, M., Dalin, P., 2017. Differences in photoperiod-induced diapause plasticity among different populations of the bark beetle Ips typographus and its predator Thanasimus formicarius. Agric. For. Entomol. 19 (2), 146–153. https://doi.org/10.1111/afe.2017.19.issue-210.1111/afe.12189.

Tuzova, V., 2004. Methods for monitoring forest pests and diseases. VNIILM, Moscow.

Venäläinen, A., Lehtonen, I., Laapas, M., Ruosteenoja, K., Tikkanen, O.-P., Viiri, H., Ikonen, V.-P., Peltola, H., 2020. Climate change induces multiple risks to boreal forests and forestry in Finland: A literature review. Glob. Chang. Biol. 26 (8), 4178–4196. https://doi.org/10.1111/gcb.v26.810.1111/gcb.15183.

Veselov, V.M., Pribylskaya, I.R., Mirzeabasov, O., 2000. Специализированные Массивы для климатических исследований ВНИИГМИ МЦД [Specialised arrays for climate research VNIIGMI MDC]. http://aisori m.meteo.ru/waisori/.

Weed, A.S., Ayres, M.P., Hicke, J.A., 2013. Consequences of climate change for biotic disturbances in North American forests. Ecol. Monogr. 83 (4), 441–470. https://doi.org/10.1890/13-0160.1.

Wermelinger, B., 2004. Ecology and management of the spruce bark beetle Ips typographus—a review of recent research. For. Ecol. Manage. 202 (1-3), 67–82. https://doi.org/10.1016/j.foreco.2004.07.018.

Wermelinger, B., Rigling, A., Mathis, D.S., Kenis, M., Gossner, M.M., 2021. Climate Change Effects on Trophic Interactions of Bark Beetles in Inner Alpine Scots Pine Forests.

Wermelinger, B., Seifert, M., 1998. Analysis of the temperature dependent development of the spruce bark beetle Ips typographus (L)(Col., Scolytidae). J. Appl. Entomol. 122, 185–191. https://doi.org/10.1111/j.1439-0418.1998.tb01482.x.

White, T.C.R., 2015. Are outbreaks of cambium-feeding beetles generated by nutritionally enhanced phloem of drought-stressed trees? J. Appl. Entomol. 139, 567–578. https://doi.org/10.1111/jen.12195.

Winter, M.-B., Baier, R., Ammer, C., 2015. Regeneration dynamics and resilience of unmanaged mountain forests in the Northern Limestone Alps following bark beetle-induced spruce dieback. Eur. J. For. Res. 134 (6), 949–968. https://doi.org/10.1007/s10342-015-0901-3.

Worrell, R., 1983. Damage by the spruce bark beetle in south Norway 1970-80: a survey and factors affecting its occurrence.

Zabihi, K., Huettmann, F., Young, B.D., 2021. Predicting Multi-Species Bark Beetle (Coleoptera: Curculionidae: Scolytinae) Occurrence in Alaska: Open Access Big Gis Data Mining To Provide Robust Inference. Biodivers. Informatics 16, 1.

Zagidullina, A., Mirin, D.M., 2013. Physical–geographical characteristics of the watershed between Northern Dvina and Pinega rivers, in: Landscape and Biodiversity in the Watershed of Northern Dvina and Pinega, St. Petersburg (in Russian). p. 116.

Zeppenfeld, T., Svoboda, M., DeRose, R.J., Heurich, M., Müller, J., Čížková, P., Starý, M., Bače, R., Donato, D.C., Bugmann, H., 2015. Response of mountain Picea abies forests to stand-replacing bark beetle outbreaks: neighbourhood effects lead to self-replacement. J. Appl. Ecol. 52 (5), 1402–1411. https://doi.org/10.1111/1365-2664.12504.

Zhigunov, A.V., Semakova, T.A., Shabunin, D.A., 2007. Массовое усыхание лесов на Северо-Западе России [Mass decline of forests at North-West of Russia]., in: Forest Biology Research in the North-West of the Russian Taiga Zone: Results and Perspectives. In: Forest Research Institute of Karelian Research Center of the Russian Academy of Sciences, pp. 42–52.

Zuur, A.F., Ieno, E.N., Elphick, C.S., 2010. A protocol for data exploration to avoid common statistical problems. Methods Ecol. Evol. 1, 3–14. https://doi.org/10.1111/j.2041-210X.2009.00001.x.

140

3.2.2 Drought initialised bark beetle outbreak in Central Europe: Meteorological factors and infestation dynamic

Authors' contributions

Nana Pirtskhalava-Karpova: Investigation, Formal analysis, Conceptualization, Methodology, Writing – original draft, Writing – review & editing. Aleksei Trubin: Formal analysis, Conceptualization, Methodology, Visualization, Writing – original draft, Writing – review & editing. Aleksandr Karpov: Methodology, Data curation, Data collection, Visualization, Writing – original draft, Writing – review & editing. Rastislav Jakuš: Conceptualization, Funding acquisition, Methodology, Project administration, Writing – original draft, Writing – review & editing.

Extended summary

Introduction

The Eurasian spruce bark beetle (*Ips typographus* L.), a destructive pest, thrives in weakened trees under climate-induced stress. Climate change, marked by extreme events like storms and droughts, creates ideal conditions for these beetles, leading to significant outbreaks (Raffa et al., 2008; Jönsson et al., 2012; Mezei et al., 2014; Bentz and Jönsson, 2015). Rising temperatures enhance beetle activity and reproduction, while drought weakens tree defences, fueling infestations (Huang et al., 2020; Hlásny et al., 2021; Netherer et al., 2021). This has been evidenced by correlations between increased temperatures, prolonged droughts, and severe beetle outbreaks across Europe (Nowakowska et al., 2020; Abdollahnejad et al., 2021; Korolyova et al., 2022). Key studies highlight the role of specific climatic factors like June temperatures, annual precipitation, and summer drought in influencing these outbreaks (Seidl et al., 2011; Mezei et al., 2017; Trubin et al., 2022). The Czech Republic, particularly affected by these outbreaks, witnessed a major one in the 1990s and a catastrophic event following the 2018 drought, leading to widespread forest damage (Knížek and Liska, 2020; Korolyova et al., 2022; Hlásny et al., 2021). Our study leverages the Global Forest Watch database to analyze the relationship between meteorological variables and bark beetle outbreaks in the Czech Republic. Using data from 2000 to 2022, we focus on annual forest loss patterns, particularly in the Kostelec nad Černými Lesy area. Prior research has shown the importance of tree characteristics and environmental factors like solar radiation and elevation in beetle infestation patterns (Jakuš et al., 2003; Mezei et al., 2014; Potterf et al., 2019; Kärvemo et al., 2023). This study aims to identify meteorological variables influencing annual tree cover loss, spot initiation, and spreading, and to assess how these factors affect bark beetle outbreak patterns. We hypothesize that temperature and precipitation conditions significantly impact bark beetle development, flight activity, and host tree stress, thereby shaping the spatial dynamics of outbreaks.

Materials and methods

Our study focused on the School Forest Enterprise area near Kostelec nad Černými Lesy in the Czech Republic's Central Bohemian region, covering about 5700 ha of forest land. To assess tree cover loss, we utilized the Global Forest Change dataset with Landsat images from 2011 to 2022, refining this data with a spruce forest mask based on forest management

data. Bark beetle spot initialisation and growth were analyzed by distinguishing new infestations from expansions of existing ones, using a 30-metre rule for identification. Meteorological data was sourced from a weather station in Ondřejov, near the study area. Statistical analyses were conducted using Generalised Additive Models (GAMs) and Ridge regression, focusing on the initialisation and spread of bark beetle spots and tree mortality. Models were selected based on the Akaike information criterion and Root Mean Square Error, respectively. Our study employed various variables, including tree cover loss changes and weather parameters, processed through Python with pandas, matplotlib, and scikit-learn libraries.

Results

In our 10-year study, total tree cover loss reached 845.4 ha, largely due to a bark beetle outbreak initiated by a decrease in precipitation and a rise in average temperature in 2018. The peak of this loss occurred in 2020. Our analysis showed that initial spot areas were most extensive during the early and epidemic phases, with a significant reduction in tree loss rates and an increase in spot spread area post-peak. By 2022, the outbreak entered the post-epidemic phase, yet tree cover loss hadn't returned to pre-outbreak levels. For bark beetle spot initialisation, the GAM regression pinpointed the previous year's April solar radiation sum and August wind speed as influential factors in tree loss. Ridge regression identified the current year's May air temperature, the previous year's average precipitation, and the current year's June wind speed as significant variables. In the case of bark beetle spot spreading, GAM regression indicated the current year's average air temperature and the previous year's June wind speed as crucial factors. Ridge regression, however, highlighted the previous year's average yearly precipitation and solar radiation sum in April and June as key variables. In the case of Annual tree loss change, the GAM regression revealed that the June and September solar radiation sum in the current year significantly influenced tree loss. Ridge regression showed that the previous year's average yearly precipitation, the current year's May precipitation, and May wind speed were significant factors. These findings underscore the complex interplay of meteorological conditions in influencing bark beetle activity and subsequent tree cover loss.

Discussion

In the current investigation of forest dynamics within a 5700 ha area, a substantial 15% forest loss was attributed primarily to an *I. typographus* outbreak, catalyzed by the severe drought conditions of 2018. It is important to note that this study operates under the assumption that the majority of tree mortality during the outbreak period was a direct result of bark beetle activity, albeit acknowledging some contribution from wind damage. Also, the limitation of this research stems from its dependence on a single meteorological station to represent the entire study area, coupled with the utilization of version 1.10 of Global Forest Watch data, whose accuracy was criticized (Ceccherini et al., 2020). Despite these constraints, the study's findings offer meaningful insights into the dynamics of bark beetle outbreaks, particularly in relation to meteorological conditions. The results of regression analyses identified several key factors influencing the initiation and spread of bark beetle spots. The initiation phase was predominantly affected by the previous year's April solar radiation duration and June wind speed, while the spreading phase was most influenced by the current year's average air temperature, along with the previous year's average yearly precipitation. Additionally, the April duration of solar radiation in the previous year emerged as a significant factor. These findings align with existing literature on the subject and contribute to a deeper understanding of bark beetle behaviour in response to climatic variables. In terms of practical implications, the insights derived from this study are particularly relevant for the development of predictive models for spruce bark beetle outbreaks. Understanding the climatic triggers and patterns of outbreak development is crucial for forest management, especially in the context of climate change and its impact on forestry economics. This research, conducted in the relatively flat terrains of Czech forests, provides valuable data that could enhance forest management strategies in Central Europe and other regions with similar ecological characteristics.

Conclusions

The 2018 bark beetle outbreak, triggered by severe drought, led to notable tree cover loss through the initialization and spread of beetle spots, influenced by distinct meteorological factors. Initially, spot initialisation was the key process, closely linked to April's solar radiation from the previous year. As the infestation advanced, spot spreading became more significant, influenced by the current year's average air temperature. Overall, the change in annual tree loss was primarily driven by solar radiation in June and September, as well as the previous year's average precipitation (using ridge regression) emerging as a significant factor.

Drought initialised bark beetle outbreak in Central Europe: Meteorological factors and infestation dynamic

Nana Pirtskhalava-Karpova [a],[*], Aleksei Trubin [a], Aleksandr Karpov [a], Rastislav Jakuš [a],[b]

[a] Faculty of Forestry and Wood Sciences, Czech University of Life Sciences in Prague, Kamycká 129, Suchdol, 16500 Prague 6, Czech Republic
[b] Institute of Forest Ecology, Slovak Academy of Sciences, Štúrova 2, 960 53 Zvolen, Slovakia

ABSTRACT

Extreme events, such as extreme droughts and intense temperatures, have become more frequent and severe, contributing to increased mortality rates in Norway spruce (*Picea abies*) due to bark beetle attacks. In particular, the most devastating outbreak of the spruce bark beetle in Central Europe began after the extreme drought year of 2018. This drought event also corresponds to the peak of the outbreak of the Eurasian spruce bark beetle (*Ips typographus* L.) in the study area - the School Forest Enterprise in the area surrounding the town of Kostelec nad Černými Lesy (Czech Republic). The study covers the period from 2012 to 2022, when there was a significant tree cover loss of 845.4 ha (15% of the spruce dominated area) that was caused by bark beetle. The primary objectives of the study were to identify the key meteorological variables affecting annual tree cover loss, bark beetle damage spot initiation, and spreading. We used the Global Forest Change dataset and meteorological data from the nearest weather station. The predictor variables were modelled in two ways: Generalised Additive Models (GAMs) regression and ridge regression. The study found that different climatic variables influenced the initialisation and spreading of bark beetle infestations. The most important climatic factor for initialisation is the duration of solar radiation in April of the previous year. The average annual air temperature in the current year plays an important role in the spreading of bark beetle spots. The higher area of spot initialisation occurred in the initial beetle outbreak phase, while the area of spreading of bark beetle spots started to increase at the peak, and was higher in later phases. Regarding annual tree cover loss, the most important factors are the duration of solar radiation in June and September of the current year, as well as the average annual precipitation of the previous year.

1. Introduction

The Eurasian spruce bark beetle (*Ips typographus L.*) is a destructive insect that attacks weakened, stressed trees in endemic-level conditions. Climate change is leading to an increase in extreme events. Storm winds lead to windfall and windthrow, while low precipitation induces severe drought. These conditions result in fallen and weakened trees, thereby providing perfect breeding conditions for bark beetles (Raffa et al., 2008; Jönsson et al., 2012; Mezei et al., 2014; Bentz et al., 2015).

Climate change significantly impacts the reproduction rate of the Eurasian spruce bark beetle and the resistance of spruce forests to bark beetle outbreaks in Europe. Rising temperatures stimulate the beetle's activity and oviposition rate, thus accelerating the development from larva to adult, and facilitating multiple generations within a year (Wermelinger, 2004; Jönsson et al., 2012; Bentz et al., 2015). Both

reduced precipitation and intensified droughts, often exacerbated by gale winds, induce water stress in trees, weakening their defences against infestations (Huang et al., 2020; Hlásny et al., 2021; Netherer et al., 2021). This combination of conditions creates an ideal environment for beetle outbreaks. Numerous studies indicate the influence of increasing temperature, its frequency, and prolonged periods of drought on the devastating consequences of Eurasian spruce bark beetle outbreaks (Nowakowska et al., 2020; Abdollahnejad et al., 2021; Korolyova et al., 2022).

These studies identified the mean June temperature of the current year, the sum of daily maximum temperatures of the previous year, temperatures in May-June for both the previous and current years, and the mean annual temperature of the previous year (Seidl et al., 2011; Mezei et al., 2017; Trubin et al., 2022). Precipitation in March-July of the previous year and the summer precipitation sum of the current and

145

previous year were also found to be important climatic factors influencing outbreak development (Faccoli, 2009; Seidl et al., 2011; Marini et al., 2012, 2017). This growing vulnerability of spruce forests to bark beetle infestations underscores the escalating problem confronted by Europe, particularly the Czech Republic.

The Czech Republic has experienced multiple outbreaks of the spruce bark beetle over the years (Knížek, 2021). Notably, there was a major outbreak during the 1990 s when extensive damage occurred across vast forested areas in the Bohemia and Moravia regions (Knížek and Liška, 2020; Korolyova et al., 2022). The most recent outbreak in the Czech Republic started after the extreme drought year of 2018. The outbreak was predominantly driven by climatic factors, and stands as the most catastrophic spruce bark beetle outbreak in Central Europe, eclipsing records observed over the previous two centuries (Hlásny et al., 2021). More frequent and severe extreme events, such as drastic droughts and intense heat, create favourable conditions for the spread of the bark beetle. A significant shift in climatic conditions is observed in the Czech Republic, leading to an escalating trend in mortality rates for most forest tree species, including spruce (Hlásny et al., 2022). To predict the effect of natural factors on bark beetle outbreaks in the Czech Republic, it's crucial to understand the specific climatic characteristics that influence trends. For this purpose, the Global Forest Watch database was used to analyse the relationship between meteorological variables and bark beetle outbreaks.

The Global Forest Watch database, which provides comprehensive data on annual tree cover percentage, gain, and loss from 2000 to 2022 at a spatial resolution of 30 m, serves as the basis for our study (Hansen et al., 2013). Leveraging this database, we integrated high-resolution global maps of forest cover change to acquire annual forest loss maps from 2011 to 2022 for the study area. We used spatial analysis to understand the complex relationships within the ecosystem, focusing in particular on patterns of bark beetle infestations. Previous studies have examined the spatial distribution of bark beetle spot initialisation and spreading, initiation, and severity of infestations (Jakuš et al., 2003; Mezei et al., 2014; Potterf et al., 2019; Kärvemo et al., 2023).

Potterf et al. (2019) recently discovered that the number of initialisation spots is highest during the initiation phase of an outbreak, followed by a gradual decrease as the outbreak progresses to the decline phase. It was also found that during the initiation phase, host characteristics, such as diameter at breast height of trees, have the most pronounced effects and significantly influence the creation of new initialisation sites. This is consistent with the idea that specific host tree characteristics play an important role in the early stages of an outbreak, as also suggested by Mezei et al. (2014). As the outbreak developed, environmental factors such as solar radiation and elevation became increasingly influential. Mezei et al. (2014) also reported that these factors have a constant influence throughout the outbreak, affecting the growth of beetle populations, and thus their ability to colonise new areas.

This study focuses on patterns of spot initialisation and spreading in relation to meteorological factors. Our study was based on the assumption that seasonal temperature and precipitation conditions, which influence bark beetle development and flight activity and host tree stress levels, have a significant role in determining tree cover loss and the spatial pattern of outbreaks. In this study, we analysed the *I. typographus* outbreak in the area surrounding the town of Kostelec nad Černými Lesy.

The objectives of this study included the following: (1) identifying combinations of meteorological predictor variables, such as temperature, precipitation, solar radiation, and wind, that best explain the annual tree-cover loss change, (2) initialisation of spot area, (3) spreading of spot area, and (4) examining the possible effects of the selected variables, as determined by the most parsimonious models, on the annual changes in tree loss and bark beetle spread patterns.

2. Material and methods

2.1. Study area

The study area is located within the School Forest Enterprise (ŠLP) area surrounding the town of Kostelec nad Černými Lesy, in the Central Bohemian region of the Czech Republic (Fig. 1). The ŠLP oversees approximately 5700 ha of forest land and it is managed by the Czech University of Life Sciences Prague (CZU). The forest area is located on the border of the lowland of Polabí in the north, which is a part of the Česká křídová tabule (a geomorphological subprovince). The majority of the forests are located within the natural forest region Středočeská pahorkatina (Central Bohemia Uplands), while a small portion in the north belongs to the natural forest region Polabí (Central Bohemia Lowlands). The elevation of the study area varies between 300 and 527 m (Remeš, 2019).

The region has an average annual temperature ranging from 7.0 to 7.5 °C and experiences mild winters. The average annual precipitation is 650 mm, and the vegetation season lasts approximately 150 to 160 days (Podrázský et al., 2009; Remeš, 2019; D'Andrea et al., 2023; Trubin et al., 2023 a,b). The most prominent tree species that are present in the area are Norway spruce (*Picea abies*) (49.7%), Scots pine (*Pinus sylvestris*) (18.1%), European beech (*Fagus sylvatica*) (11.6%), and oak species (*genera Quercus*) (8.8%). Tree cover loss in the study area was caused mostly by wind damage and regular silvicultural activities until the drought of 2018. The drought conditions initiated a subsequent bark beetle outbreak, which became the main cause of mortality in Norway spruce-dominated forest areas.

2.2. Annual Norway spruce tree cover loss, area of initialisation, and growing spots acquisition

We used the gross forest cover loss (lossyear) layers derived from the Global Forest Change dataset Version 1.10 (Hansen et al., 2013). These maps were produced using a time-series analysis of Landsat satellite images, allowing us to generate annual maps from 2011 to 2022, with an approximate spatial resolution of 30 by 30 m. Each year's layers have been converted into vector format from the original raster layers, which were composed of 10 × 10 degree tiles. Additionally, these vector layers were clipped to fit the spruce forest mask boundaries (based on forest management data) of the area under study. Using forest inventory data from 2011, we constructed a spruce forest mask based on the criteria of units containing over 10% of Norway spruce aged more than 25 years. Combining this mask with the Global Forest Change dataset, we delineate alterations in spruce forest cover from 2011 to 2022 with increased precision.

Our study includes the calculation of the area of the bark beetle spot initialisation and spot growth. Spots initialisation was defined as a new infestation in undisturbed forests, and spot growth as infestations adjacent to spots from the previous year (Coulson et al., 1985; Havašová et al., 2017). We used the rule for identifying initialisation spots as an infestation if they were more than 30 m (one pixel) away from the previous year's infestation, while spots within this 30-metre distance were recognised as growth spots. The distance from the previous to the current year's spots infestation was measured by the dispersal distances as the nearest edge-to-edge distance, using the 'generate near table' distances tool in ArcGIS v. 10.6 (Esri, 2017). We created a 500-metre buffer around the perimeter of the study area, and filled this buffer with data from the CORINE land cover dataset (EEA, European Environment Agency), which provided coniferous forest boundary data from 2012. This dataset served as an additional forest mask, and was used to minimise potential inaccuracies in the identification of initialisation and growing spots along the study area. This approach improved the accuracy of initiation and growth spot determination along the boundaries of the study area.
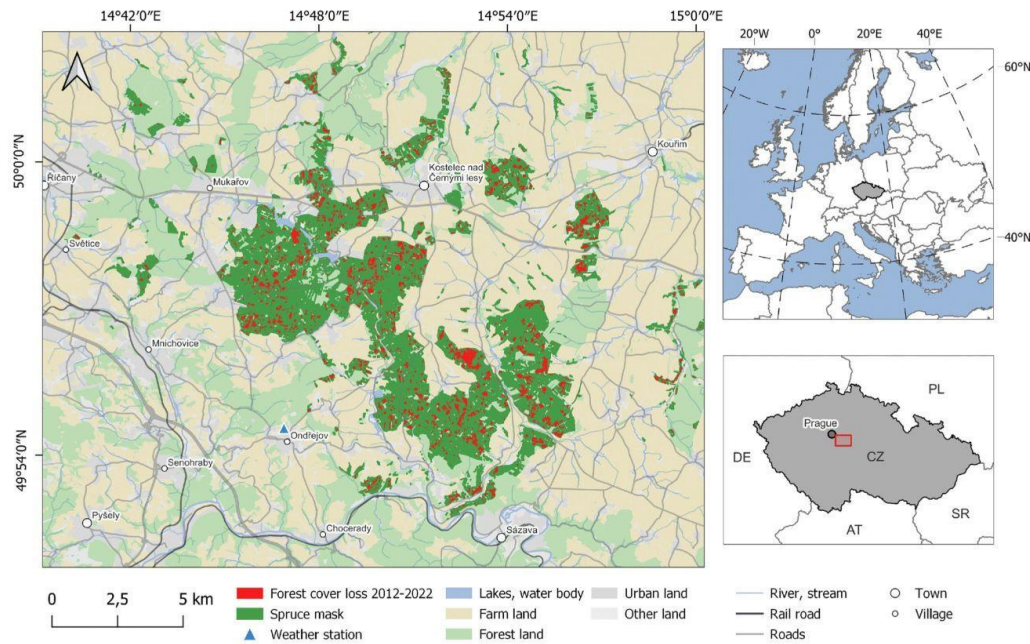
2

Fig. 1. Study area: School Forest Enterprise surrounding Kostelec nad Černými Lesy. The map of the study area shows the main layers of the spruce mask in green, the forest cover loss from 2011 to 2022 in red, the location of the weather station as a blue triangle and topographical data to understand the location of the study area.

2.3. Meteorological variables

The weather station is located in the village of Ondřejov (id P3ONDR01, ČHMÚ) at an elevation of 491 m above sea level, approximately 1 km from the nearest edge and 7 km from the centre of our study area.

2.4. Statistical analyses and model selection

Before the analysis, the data were checked for outliers and collinearity. During data exploration, we plotted the response variable with each covariate to check the relationship between them. Based on the data exploration, the relationship between tree loss and the explanatory variables was analysed using Generalised Additive Models (GAMs) and Ridge regression. A set of a priori models (Dochtermann and Jenkins, 2011; Rosen, 2016) were selected prior to analysis (Tables 2, 4, 5, 7, 8, 10) in order to test which model would best explain the initialisation and spreading of spots, and infestation of trees by *I. typographus*. These models were constructed using previously known variables that were identified as important for bark beetle population dynamics, mainly climatic variables and this is consistent with previous work from Trubin et al. (2022) and Mezei et al., (2014, 2017).

For the GAMs, the Information-Theoretic (I-T) approach was used to assess competing models. Models were ranked according to the Akaike information criterion (AIC) for a small sample dataset. The delta AIC (ΔAIC) represents the difference in the AIC between a given model and the best-performing model in a set of candidate models; the most parsimonious model was selected based on the lowest ΔAIC value. Models with ΔAIC< 2 can be considered as good as the best, while models in the ΔAIC range of 2–7 are also plausible. We also calculated Akaike weights to arrange candidate models in order of parsimony,

where the Akaike weight is a number from 0 to 1, thus providing a measure of the relative likelihood of each model, given the data and the candidate model set. This weight can be considered the probability that a given model is the best-approximating model (Burnham et al., 2011).

For ridge regression, the error-based evaluation method was applied in order to scrutinise competing models. Models were compared using the Root Mean Square Error (RMSE) criteria; the best fitting model was chosen based on the smallest RMSE value. The alpha parameter serves as a regularisation term that penalises large coefficients in the model, thereby mitigating the risk of overfitting the training data. A higher value of alpha increases the strength of the regularisation, pushing the model towards simplicity, while a lower value makes the model more flexible, but susceptible to capturing noise.

We used Annual bark beetle spots initialisation (ha), Annual bark beetle spots spreading (ha), and Annual tree loss change (TLC, the natural logarithm of the ratio between tree mortality in the current year and tree mortality in the previous year) as the response variables.

$$TLC = \ln(\frac{TCL}{TCL(t-1)}) \qquad (1)$$

where ln is the natural logarithm, *TCL* is the Tree cover loss in the current year, $TCL(t-1)$ is the Tree cover loss in a previous year.

As some of the variables were highly correlated, we used the threshold of r = 0.7 to select variables. We tested the correlation between changes in annual tree cover losses in a particular year, and changes in annual tree cover losses in previous years, by calculating the autocorrelation function (ACF). We also assessed the cross-correlation functions (CCFs) of the predictor time series and variables in the best model. Because we used the previous year's tree mortality as an explanatory variable in our analysis, the sample size changed from 11

3

147

years (2011–2022) to 10 years (2012–2022). All data manipulations, plotting, calculations, and statistical analysis were performed in VSCode 1.73.1 in Jupiter Notebook using Python programming language (ver. 3.11.1; Rossum and Drake, 2010) with pandas 1.5.0, Matplotlib 3.6.0, statsmodels 0.15.0, pygam 0.5.5, scikit-learn 1.3.0.

3. Results

3.1. Tree cover loss due to disturbance events

Total tree cover loss, considering all 10 years from 2012 to 2022, amounted to 845.4 ha (Fig. 2). The trigger for the bark beetle outbreak was a dramatic reduction in annual precipitation of around 250 mm, and an increase in average annual temperature of 2 °C in 2018 (Fig. 3). The amount of tree cover loss peaked in 2020, marking the culmination of the bark beetle outbreak. The spot initialisation area was at the maximum from the incipient to the epidemic phase of the bark beetle outbreak. After the peak in tree loss, there was a significant decrease in tree loss rates and an increase in the area of spot spread. The bark beetle outbreak is in the post-epidemic phase in 2022, but annual tree cover loss has not yet reached pre-outbreak levels (Fig. 2). We also hypothesise that the decrease in tree cover loss observed in 2018 was influenced by the relatively cold, wet conditions experienced in 2017.

3.2. Bark beetle spot initialisation

We tested the data on tree mortality in bark beetle spot initialisation throughout our study period for autocorrelation; the ACF function did not reveal trends between tree mortality in bark beetle spot initialisation caused by *I. typographus*.

3.2.1. Generalised additive models regression

GAM regression was used to further investigate the relationships between tree mortality in bark beetle spot initialisation and meteorological variables (Table 1). The a priori set of competing models that differ by a combination of predictor variables is given in Table 2.

As per the Akaike's information criterion, Model 1 emerged as the most significant (see Table 2). Insights extracted from our model (Table 3), suggest that the April sum duration of solar radiation in the previous year, along with the August wind speed in the previous year, played a role in shaping the changes in tree loss from 2012 to 2022 (Fig. 3). An increase in any of the aforementioned variables corresponds to an escalation in tree loss.

3.2.2. Ridge regression

Ridge regression was used to further investigate the relationships between tree mortality in bark beetle spots initialisation and meteorological variables (Table 1). The a priori set of competing models that differ by a combination of predictor variables is given in Table 4.

Model 1 emerged as the most significant model (Table 4). Insights extracted from our model (Table 4) suggest that the May average monthly air temperature in the current year, Average yearly precipitation in the previous year, and June wind speed in the current year, played a role in shaping the changes in tree loss from 2012 to 2022 (Fig. S1).

3.3. Bark beetle spot spreading

We tested the data on tree mortality in conditions of bark beetle spots spreading throughout our study period for autocorrelation; the ACF function did not reveal the trends between tree mortality caused by *I. typographus*.

3.3.1. Generalised additive models regression

GAM regression was used to further investigate the relationships between tree mortality in conditions of bark beetle spot spreading and meteorological variables (Table 1). The a priori set of competing models that differ by a combination of predictor variables is given in Table 5.

As per the Akaike's information criterion, Model 1 emerged as the most significant (Table 5). Insights extracted from our model (Table 6), suggest that the Average yearly air temperature in the current year, along with the June wind speed in the previous year, played a role in shaping the changes in tree loss from 2012 to 2022 (Fig. 4). An increase in any of the aforementioned variables corresponded to an escalation in tree loss.

In the analysis of the bark beetle spots spreading area, we identified one more model that exhibited a ΔAIC of less than 7, indicating a substantial level of support relative to the best model. This model contained one variable - the April wind speed in the current year (AprW).

The remaining explanatory variables, as detailed in Table 1, did not find a place in the most parsimonious models; however, they might possess biological significance, despite not being deemed optimal within the temporal and spatial confines of our study. The models in question are constituted of an assortment of different combinations involving temperature, wind speed, and precipitation. This highlights the role that temperature, wind, and precipitation play in influencing alterations in tree loss, even though these models carry a considerably diminished likelihood of being the best fit, as indicated by their AIC weights.
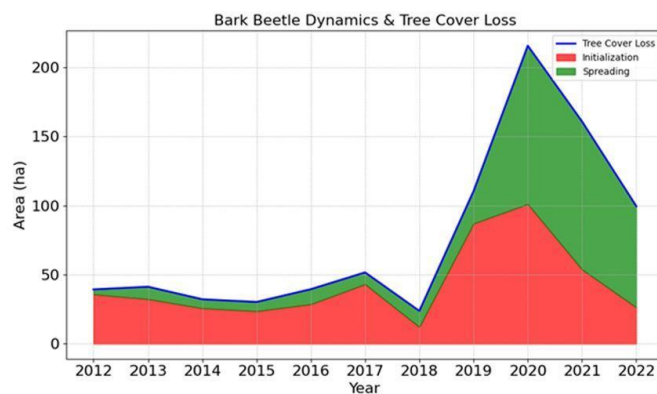

Fig. 2. Annual bark beetle spot initialisation, spreading, and tree cover loss (ha) of *Picea abies* caused by *Ips typographus*.
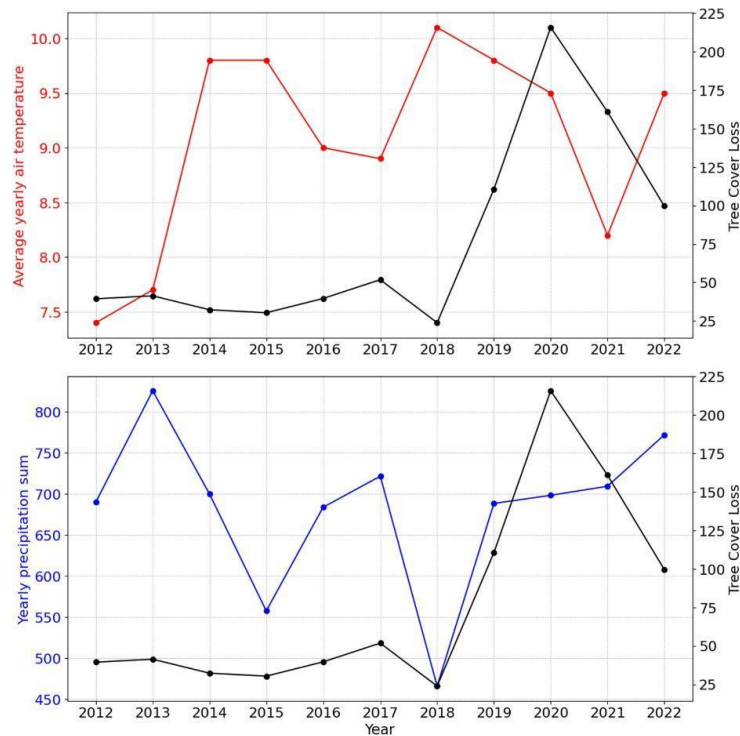
4

Fig. 3. Tree cover loss of *Picea abies* caused by *Ips typographus* from 2012 to 2022, with average yearly air temperature (red) and yearly precipitation sum (blue) in the current year.

3.3.2. Ridge regression

Ridge regression was used to further investigate the relationships between the spot spreading and meteorological variables (Table 1). The a priori set of competing models that differ by a combination of predictor variables is given in Table 7.

Model 1 emerged as the most significant model (Table 7). Insights extracted from our model, suggest that the Average yearly precipitation in the previous year, the sum duration of solar radiation in the previous year in April and June, played a role in shaping the changes in tree loss from 2012 to 2022 (Fig. S2).

3.4. Annual tree loss change

Throughout our study, we tested the data on tree mortality period for autocorrelation; the ACF function did not reveal trends between tree mortality caused by *I. typographus* in the current year and the previous year.

3.4.1. Generalised additive models regression

GAM regression was used to further investigate the relationships between tree mortality and meteorological variables (Table 1). The a priori set of competing models that differ by a combination of predictor variables is given in Table 8.

Based on Akaike's information criterion, Model 1 emerged as the most parsimonious model (Table 8). The insights gleaned from our model (Table 9) indicate that the June sum duration of solar radiation in the current year, and September sum duration of solar radiation in the

current year, exerted an influence on the changes in tree loss from 2012 to 2022 (Fig. 5). Both higher June and September sum duration of solar radiation in a current year resulted in more tree loss.

In the analysis of the annual tree loss change, we identified a total of 102 models (Table S1) that exhibited a ΔAIC of less than 7, indicating a substantial level of support relative to the best model. Each of these models incorporated two explanatory variables. When assessing the prevalence of variables within these models, April wind speed in the current year (AprW) emerged as the most recurrent, featuring 20 models. This was followed by September sum duration of solar radiation in the current year (SepS), which was present in 16 models. September sum duration of solar radiation in the previous year (SepS(t-1)) was included in each of the fifteen models. There was also June sum duration of solar radiation in the current year (JunS) included in 13 models; December, January, and February average air temperature in the current year (DJF) in 12 models; and June sum duration of solar radiation in the previous year (JunS(t-1)); June wind speed in the current year (JunW) in 9 models; April wind speed in the previous year (AprW(t-1)) in 8 models; April sum duration of solar radiation in the previous year (AprS(t-1)), December, January, and February average air temperature in the previous year (DJF(t-1)), June amount of precipitation in the current year (JunP), and July amount of precipitation in the current year (JulP) in 7 models. The sorting of these variables, from the most frequently used to the least, provides insights into their relative importance in the models, based on the criterion that we applied.

The remaining explanatory variables (detailed in Table 1), did not find a place in the most parsimonious models; however, they might

5

Table 1

Variables used in the study of changes in tree cover loss. Meteorological data were collected from Ondřejov weather station, adjacent to the study area, for the 2012–2022 period.

Name in model	Variable	Unit of measure
TCL	Tree cover loss in the current year	Hectares
TLC	Tree loss change in the current year	
AveTempYear	Average yearly air temperature in the current year	degrees Celsius
AveTempYear (t-1)	Average yearly air temperature in the previous year	degrees Celsius
AprT	April average monthly air temperature in the current year	degrees Celsius
MayT	May average monthly air temperature in the current year	degrees Celsius
JunT	June average monthly air temperature in the current year	degrees Celsius
JulT	July average monthly air temperature in the current year	degrees Celsius
AugT	August average monthly air temperature in the current year	degrees Celsius
SepT	September average monthly air temperature in the current year	degrees Celsius
AvePrecYear	Average yearly precipitation in the current year	millimetres
AvePrecYear(t-1)	Average yearly precipitation in the previous year	millimetres
AprP	April amount of precipitation in the current year	millimetres
MayP	May amount of precipitation in the current year	millimetres
JunP	June amount of precipitation in the current year	millimetres
JulP	July amount of precipitation in the current year	millimetres
AugP	August amount of precipitation in the current year	millimetres
SepP	September amount of precipitation in the current year	millimetres
AprS	April sum of duration of solar radiation in the current year	hours
MayS	May sum of duration of solar radiation in the current year	hours
JunS	June sum of duration of solar radiation in the current year	hours
JulS	July sum of duration of solar radiation in the current year	hours
AugS	August sum of duration of solar radiation in the current year	hours
SepS	September sum of duration of solar radiation in the current year	hours
AprS(t-1)	April sum of duration of solar radiation in the previous year	hours
MayS(t-1)	May sum of duration of solar radiation in the previous year	hours
JunS(t-1)	June sum of duration of solar radiation in the previous year	hours
JulS(t-1)	July sum of duration of solar radiation in the previous year	hours
AugS(t-1)	August sum of duration of solar radiation in the previous year	hours
SepS(t-1)	September sum of duration of solar radiation in the previous year	hours
DJF	December, January, and February average air temperature in the current year	degrees Celsius
DJF(t-1)	December, January, and February average air temperature in the previous year	degrees Celsius
JJA	June, July, and August average air temperature in the current year	degrees Celsius
JJA(t-1)	June, July, and August average air temperature in the previous year	degrees Celsius
AprW	April wind speed in the current year	metres per second
MayW	May wind speed in the current year	metres per second

Table 1 (*continued*)

Name in model	Variable	Unit of measure
JunW	June wind speed in the current year	metres per second
JulW	July wind speed in the current year	metres per second
AugW	August wind speed in the current year	metres per second
SepW	September wind speed in the current year	metres per second
AprW(t-1)	April wind speed in the previous year	metres per second
MayW(t-1)	May wind speed in the previous year	metres per second
JunW(t-1)	June wind speed in the previous year	metres per second
JulW(t-1)	July wind speed in the previous year	metres per second
AugW(t-1)	August wind speed in the previous year	metres per second
SepW(t-1)	September wind speed in the previous year	metres per second
AveWindYear	Average yearly wind speed in the current year	metres per second
AveWindYear(t-1)	Average yearly wind speed in the previous year	metres per second

Table 2

Proposed three best GAM regression models used to study annual bark beetle spots initialisation for a 10-year period.

Model	Combination	AIC	ΔAIC	AIC weight
1	INIT = s(AprS(t-1)) + s(AugW(t-1)) + ε	74.25664	0	0.950966
2	INIT = s(AprS(t-1)) + ε	80.19412	5.93748	0.048849
3	INIT = s(MayT) + s(AprS(t-1)) + ε	93.47902	19.22238	6.37E-05

Notes: For the explanation of variables used, refer to Table 1. All models include an intercept. ε is a random error.

possess biological significance, despite not being deemed optimal within the temporal and spatial confines of our study. The models in question are constituted of an assortment of different combinations involving temperature, wind speed, and precipitation. This highlights the role that temperature, wind, and precipitation play in influencing alterations in tree loss, even though these models carry a considerably diminished likelihood of being the best fit, as indicated by their AIC weights.

3.4.2. *Ridge regression*

Ridge regression was used to further investigate the relationships between annual tree loss change and meteorological variables (Table 1). The a priori set of competing models that differ by a combination of predictor variables is given in Table 10.

Model 1 emerged as the most significant model (Table 10). Insights extracted from our model, suggest that the Average yearly precipitation in the previous year, the May amount of precipitation in the current year, and the May wind speed in the current year, played a role in shaping the changes in tree loss from 2012 to 2022 (Fig. S3).

4. Discussion

During the study period, we observed a forest loss of nearly 15% within the 5700 ha study area, mainly due to an *I. typographus* outbreak. The bark beetle outbreak was triggered by the drought in 2018. GAM and ridge regression were used to model the predictor variables. The selection of the best GAM was based on the Akaike Information Criterion (AIC) value, AIC weight and ΔAIC, while the ridge regression models

150

Table 3

GAM model equation estimating the variation in annual bark beetle spots initialisation of *I. typographus* as a function of April sum of duration of solar radiation in the current year and August wind speed in the previous year, over the period of 2012 to 2022 within the study area.

Parameter	Estimate	p-value	Model values
Intercept	-83.39317961915626	0.560759915547079	Adjusted R-squared: 1.0000088409108
AprS(t-1)	0.3198121836687413	0.08296271101229276	
AugW(t-1)	38.5290344215266	0.6927743030810429	

Table 4

Proposed 10 best models to study bark beetle spots initialisation for a 10-year period using ridge regression.

Model	Variables	Alpha	RMSE
1	INIT = b0 + b1 * MayT + b2 * AvePrecYear(t-1) + b3 * JunW + ε	0.1	21.55238
2	INIT = b0 + b1 * MayT + b2 * AvePrecYear(t-1) + b3 * JunW + ε	0.5	22.60772
3	INIT = b0 + b1 * MayT + b2 * AugP + b3 * JJA(t-1) + ε	0.1	23.10516
4	INIT = b0 + b1 * MayT + b2 * MayS + b3 * JJA(t-1) + ε	0.1	23.16889
5	INIT = b0 + b1 * MayT + b2 * MayS + b3 * JJA(t-1) + ε	0.5	23.32635
6	INIT = b0 + b1 * MayT + b2 * AugP + b3 * JJA(t-1) + ε	0.5	23.52982
7	INIT = b0 + b1 * MayT + b2 * MayS + b3 * JJA(t-1) + ε	1	23.61171
8	INIT = b0 + b1 * MayT + b2 * AvePrecYear(t-1) + b3 * JunW + ε	1	23.84964
9	INIT = b0 + b1 * MayT + b2 * AugP + b3 * JJA(t-1) + ε	1	23.90161
10	INIT = b0 + b1 * MayT + b2 * JulS(t-1) + b3 * JJA(t-1) + ε	0.1	23.91198

Notes: For the explanation of variables used, refer to Table 1. All models include an intercept. ε is a random error.

Table 5

Proposed best GAM regression models used to study annual bark beetle spots spreading for a 10-year period.

Model	Combination	AIC	ΔAIC	AIC weight
1	SPREAD = s(AveTempYear) + s(JunW(t-1)) + ε	82.48321	0	0.9102
2	SPREAD = s(AprW) + ε	87.71957	5.236358	0.066386
3	SPREAD = s(AveTempYear) + s(JulW(t-1)) + ε	89.86587	7.382666	0.022699

Notes: For the explanation of variables used, refer to Table 1. All models include an intercept. ε is a random error.

were evaluated using the RMSE value. In the results section, we presented the top three models for GAM, and ten models for ridge regression in order to model bark beetle spots initialisation (Tables 2, 4) and spots spreading (Tables 5, 7). Ten GAM and ten ridge regression models are specified for the annual change in tree loss (Tables 8, 10); nevertheless, 102 GAM models pass the best model selection condition (Table S1). In the following subsections, the variables of the best models for bark beetle initialisation, spreading, and annual change in tree loss were analysed for their biological significance, based on a review of scientific articles from the body of literature.

Table 6

GAM model equation estimating the variation in annual bark beetle spots spreading of *I. typographus* as a function of Average yearly air temperature in the current year and June wind speed in the previous year over the period from 2012 to 2022 within the study area.

Parameter	Estimate	p-value	Model values
Intercept	-203.8065991221044	0.28109334513119316	Adjusted R-squared: 1.00000575664109
AveTempYear	7.428577837285664	0.6139552343349576	
JunW(t-1)	93.30653631670484	0.10290621263503584	

4.1. Limitations of the study

We make the assumption that the tree mortality in the period of the bark beetle outbreak was almost fully related to the bark beetle attacks. Wind damage caused a certain level of tree mortality. The data used in our analysis, version 1.10 of the Global Forest Watch data, differs from the original algorithm, and accuracy has been contested in some research, for example, in the study by Ceccherini et al. (2020). A limitation of our study is the reliance on a single meteorological station with which to represent the study area; although, it is noteworthy that the area in question is relatively compact, thus minimising spatial variations. We used the only publicly available data with a spatial resolution of approximately 30 m per pixel.

Our study is focused on meteorological factors. The role of previous tree mortality or other factors was not analysed.

4.2. Drought initialised bark beetle outbreak

The bark beetle outbreak was initialised by extreme drought in 2018 (Fig. 3). Prior to this year, tree cover loss was caused mostly by wind damage and regular silvicultural operations in the study area. Meteorological conditions since 2019 have remained within historical norms. Later, the outbreak passed all typical stages (progradation, gradation, retrogradation). The course of the outbreak and proportion of spot initialisation and spreading had similar characteristics to those in the case of bark beetle outbreak initialised by the wind in mountainous conditions (Jakuš et al., 2003; Mezei et al., 2017; Potterf et al., 2019). Interestingly, the course of the bark beetle outbreak in our study area differed from that at a relatively low elevation, which was affected by *Armillaria sp.* which was responsible for diseases, and chronic bark beetle outbreak (Jakuš et al., 2001). Furthermore, Kärvemo et al. (2023) indicate that there are distinct variations in the patterns of spruce bark beetle outbreaks resulting from windthrow and drought. The spatial distribution of susceptible trees seems to be the main reason for this difference. There was a greater increase in storm-induced infestations in territories with higher volumes of spruce and in non-forest management forests. Conversely, drought-induced infestations increased in frequency and size with clear-cuts throughout the landscape.

4.3. Factors influencing bark beetle spots initialisation

Spots initialisation was the dominant process before the beginning of the bark beetle outbreak, and in the progradation phase (Fig. 2). This is in agreement with the findings of Jakuš et al. (2003). The bark beetle outbreak started after the drought year of 2018. Almost all of the tree cover loss before 2018 was caused by wind damage or regular forest management operations. Forests in the study area are under the influence of wind-bark beetle disturbance systems (Mezei et al., 2014). The
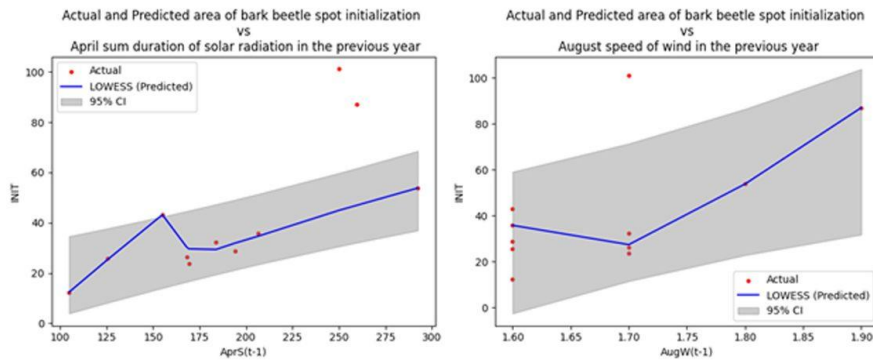
7

Fig. 4. The result of fitting the most parsimonious model (Table 3) for the relation between the bark beetle spots initialisation, April sum duration of solar radiation in the previous year, and the August wind speed in the previous year over a 10-year span in the study area. The graphs illustrate the association between each predictor variable and the response variable with Locally Weighted Scatterplot Smoothing (LOWESS, blue line) with 95% confidence intervals (marked grey) and actual values (red dots).

Table 7
Proposed 10 best models used to study annual bark beetle spots spreading for a 10-year period using ridge regression.

Model	Variables	Alpha	RMSE
1	SPREAD = b0 + b1 * AvePrecYear(t-1) + b2 * AprS(t-1) + b3 * JunS(t-1) + ε	100	21.68994
2	SPREAD = b0 + b1 * AvePrecYear(t-1) + b2 * AprS(t-1) + b3 * JunS(t-1) + ε	50	21.72945
3	SPREAD = b0 + b1 * AvePrecYear(t-1) + b2 * AprS(t-1) + b3 * JunS(t-1) + ε	10	21.76529
4	SPREAD = b0 + b1 * AvePrecYear(t-1) + b2 * AprS(t-1) + b3 * JunS(t-1) + ε	5	21.77004
5	SPREAD = b0 + b1 * AvePrecYear(t-1) + b2 * AprS(t-1) + b3 * JunS(t-1) + ε	1	21.77389
6	SPREAD = b0 + b1 * AvePrecYear(t-1) + b2 * AprS(t-1) + b3 * JunS(t-1) + ε	0.5	21.77437
7	SPREAD = b0 + b1 * AvePrecYear(t-1) + b2 * AprS(t-1) + b3 * JunS(t-1) + ε	0.1	21.77476
8	SPREAD = b0 + b1 * AvePrecYear(t-1) + b2 * AprS(t-1) + b3 * AugW + ε	0.1	26.59901
9	SPREAD = b0 + b1 * AvePrecYear(t-1) + b2 * DJF (t-1) + b3 * JunW(t-1) + ε	0.1	26.99088
10	SPREAD = b0 + b1 * AvePrecYear(t-1) + b2 * AprS(t-1) + b3 * JJA(t-1) + ε	1	27.23683

Notes: For the explanation of variables used, refer to Table 1. All models include an intercept. ε is a random error.

Table 8
Proposed 10 best GAM regression models used to study annual changes of tree cover loss for a 10-year period. All plausible models are presented in Supplementary Materials (Table S1).

Model	Variables	AIC	ΔAIC	AIC weight
1	TLC = s(JunS) + s(SepS) + ε	-12.105	0	0.049177
2	TLC = s(DJF) + s(AprW) + ε	-12.0282	0.076793	0.047325
3	TLC = s(SepS(t-1)) + s(DJF) + ε	-11.8986	0.206414	0.044355
4	TLC = s(AprS(t-1)) + s(AprW) + ε	-11.572	0.533046	0.037672
5	TLC = s(SepS) + s(JulS(t-1)) + ε	-11.3643	0.740738	0.033956
6	TLC = s(JunS(t-1)) + s(SepS(t-1)) + ε	-11.1823	0.922723	0.031002
7	TLC = s(SepS) + s(DJF) + ε	-11.1413	0.96376	0.030373
8	TLC = s(JJA(t-1)) + s(AprW) + ε	-10.9138	1.191198	0.027108
9	TLC = s(MayS) + s(JunS) + ε	-10.8578	1.247222	0.026359
10	TLC = s(DJF(t-1)) + s(AprW(t-1)) + ε	-10.6673	1.437702	0.023965

Notes: Annual tree cover loss change is the yearly change in the area of damage sensu Marini et al. (2013); For the explanation of variables used, refer to Table 1. All models include an intercept. ε is a random error.

Table 9
GAM model equation estimating the variation in annual tree loss change of *Picea abies* by *I. typographus* as a function of the sum duration of solar radiation in June and September in the current year over the period from 2012 to 2022 within the study area.

Parameter	Estimate	p-value	Model values
Intercept	-1.90448710103119	0.3182143402348817	Adjusted R-squared: 1.000005
JunS	0.005618101280442977	0.27095011481516995	
SepS	0.004177419235052129	0.5091506524662619	

areas affected by wind damage and harvesting activities were the initial spots of the bark beetle outbreak. Part of the bark beetle spots were, possibly, also initiated by drought (Netherer et al., 2015).

GAM regression analysis (Tables 2, 3, Fig. 3) has shown that the most important factor influencing spots initialisation was the April duration of solar radiation in the previous year. The second important factor was the June wind speed in the previous year. The results of the ridge regression (Table 4) have shown the current year May temperatures as the most important factor. The wind speed in the previous year was also important.

In the case of spots initialisation, meteorological characteristics from the previous year were important. Mezei et al. (2017) and Trubin et al. (2022) have shown the importance of average temperature in the previous year for predicting tree mortality. Faccoli (2009) has shown the importance of precipitation in the period from March to July of the previous year. Bakke (1992) has reported good correlations of May-June temperatures from the previous year with actual beetle catches in pheromone traps. To the best of our knowledge, above-mentioned works

have tended to ignore the variables that are related to the duration of solar radiation. Trubin et al. (2022) have used the duration of solar radiation; however, it was not an important factor in their analysis. We can assume a certain correlation among the duration of solar radiation, temperature, and rainfall. We can also conclude that our results are in agreement with the previous works. Faccoli (2009) suggests that, generally, a spring drought increases the bark beetle damage in the following year.

Logically, high wind speed is related to wind damage. Wind damage usually predisposes to bark beetle spread in the following years (Marini
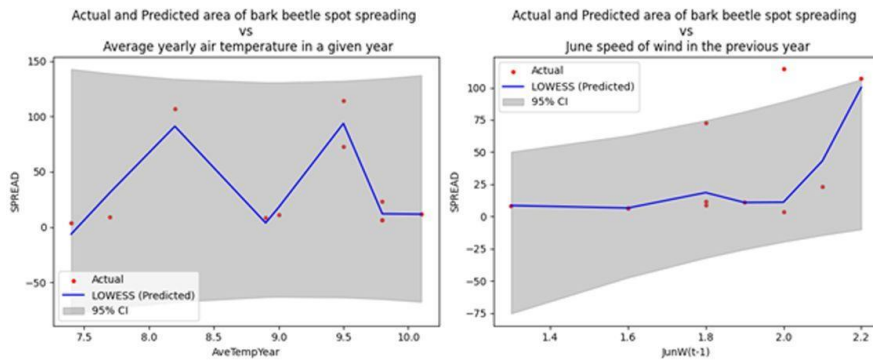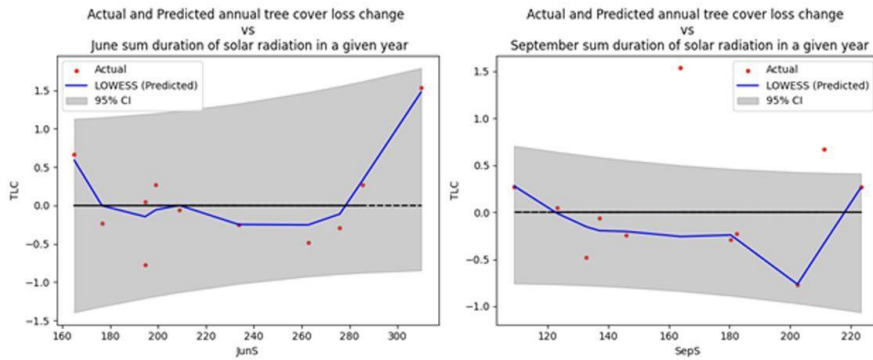
Fig. 5. The result of fitting the most parsimonious model (Table 6) for the relation between the bark beetle spots spreading and Average yearly air temperature in the current year, along with the June wind speed in the previous year over a 10-year span in the study area. The graphs illustrate the association between each predictor variable and the response variable with Locally Weighted Scatterplot Smoothing (LOWESS, blue line) with 95% confidence intervals (marked grey) and actual values (red dots).

Fig. 6. The result of fitting the most parsimonious model (Table 9) for the relation between the annual tree cover loss change and sum duration of solar radiation in the current year in June and September over a 10-year span in the study area. The graphs illustrate the association between each predictor variable and the response variable with Locally Weighted Scatterplot Smoothing (LOWESS, blue line) with 95% confidence intervals (marked grey) and actual values (red dots).

et al., 2017). An important point is that wind damage creates new gaps and fresh forest edges, which predispose the remaining spruce stands to bark beetle attacks (Kautz et al., 2013; Marešová et al., 2020).

Researchers have found that the flight distance of the overwintered generation of spruce bark beetle exceeds the flight distance of subsequent generations. Dolezal et al. (2016) examined flight distances of the spruce bark beetles in the Šumava National Park. They found that the spring overwintered generation had a longer flight distance than the summer generation. A model based on dispersal data suggests that 10% of the overwintered beetles fly more than 55 m in spring, whereas only 4 m was observed for the first filial generation in summer. Similar observations on the increased flight distances of overwintered beetles were made by Furuta et al. (1996). Weslien et al. (1990) found that spring swarming bark beetles had a recapture rate of around 8% in traps located 100 m away. Similar results were found by Lindelöw et al. (2012).

The enhanced migration tendency of the overwintered generation can be attributed to their need to resume direct development post-overwintering, replenish energy reserves, and locate new breeding sites. This behaviour is consistent with many other insect species (Koštál, 2006). Based on these studies, it can be assumed that the first generation of bark beetles has greater influence on the initialisation of infested spots. From a biological point of view, the most important variables for the spring bark beetle population in our study are the temperatures of the previous summer, the winter temperatures of the current year, and the temperatures of April of the current year. In seven of the top ten models, the average air temperature of the summer months of the previous year is a variable in the ridge regression models. Additionally, the top two models include the variable average annual air temperature in the previous year, which might influence the first generation bark beetle population in the following year (Table 4).

4.4. Factors influencing the spreading of bark beetle spots

The spreading of bark beetle spots was a dominant process in the later phases of gradation (Fig. 2). This is also in agreement with the findings of Jakuš et al. (2003). GAM regression analysis (Tables 5, 6, Fig. 4) has shown that the most important factor influencing spot spreading was the average yearly air temperature in the current year. Wind speeds in two summer months (June and July) in previous years were also important factors. Marini et al. (2017) also found a positive effect of current summer temperatures for the rate of timber loss due to

Table 10

Proposed 10 best models used to study annual changes of tree cover loss for a 10-year period using ridge regression. The model with the lowest RMSE is the most parsimonious.

Model	Variables	Alpha	RMSE
1	TLC = b0 + b1 * AvePrecYear(t-1) + b2 * MayP + b3 * MayW + ε	0.1	0.419127
2	TLC = b0 + b1 * AveTempYear + b2 * MayT + b3 * AvePrecYear(t-1) + ε	0.1	0.421982
3	TLC = b0 + b1 * AveTempYear + b2 * MayT + b3 * AvePrecYear(t-1) + ε	0.5	0.425943
4	TLC = b0 + b1 * AveTempYear + b2 * MayT + b3 * AvePrecYear(t-1) + ε	1	0.433299
5	TLC = b0 + b1 * AvePrecYear(t-1) + b2 * MayS + b3 * MayW + ε	0.1	0.450437
6	TLC = b0 + b1 * MayT + b2 * AvePrecYear(t-1) + b3 * JunW(t-1) + ε	0.1	0.456736
7	TLC = b0 + b1 * MayT + b2 * AugS + b3 * JJA(t-1) + ε	0.1	0.459826
8	TLC = b0 + b1 * AvePrecYear(t-1) + b2 * JunP + b3 * MayS + ε	0.1	0.463782
9	TLC = b0 + b1 * AvePrecYear(t-1) + b2 * JunP + b3 * MayS + ε	0.5	0.463785
10	TLC = b0 + b1 * AvePrecYear(t-1) + b2 * JunP + b3 * MayS + ε	1	0.463788

Notes: For the explanation of variables used, refer to Table 1. All models include an intercept. ε is a random error.

I. typographus.

The ridge regression (Table 8) has shown the average yearly precipitation in the previous year as the most important factor. This is in agreement with the results of Marini et al. (2012). The April duration of solar radiation in the previous year was the second important factor in our results.

4.5. Factors influencing annual tree loss change

GAM regression analysis (Tables 8, 9, Fig. 5) has shown that the most important factors influencing the annual tree loss change were the sums of duration of solar radiation in June and September of the current year. Trubin et al. (2022) have also shown the relation of June weather to tree loss change caused by the bark beetle outbreak. The best 102 GAM models (Table S1) include 81 solar radiation duration predictors for the months of the current year and the previous year. The study by Yu et al. (2022) shows that longer periods of solar radiation, particularly in May, are positively correlated with the area infested by pine shoot beetles (*Tomicus spp.*), and they also accelerate beetle flight behaviour. The relationship between the duration of solar radiation often coincides with warm temperatures and drought conditions. According to Lobinger and Skatulla (1996), spruce bark beetles show a strong preference for conditions with high solar activity, which facilitates their flight and reproductive activity; longer durations of solar radiation also contribute to higher daily temperature sums.

The ridge regression (Table 10) has shown the average yearly precipitation in the previous year as the most important factor. This result corresponds to the findings of Faccoli (2009) and Marini et al. (2012) in the south-eastern Italian Alps. Marini et al. (2012) observed that precipitation deficit has a more pronounced effect in mountainous conditions and is related to the upward shifts in the altitudinal outbreak range of bark beetles. Those authors also note a greater susceptibility to climate-induced tree cover loss in sites where spruce is planted on the warmer side of its natural range.

The importance of precipitation is consistent with the comprehensive study of 21 European countries by Seidl et al. (2011), who concluded that a combination of summer and spring precipitation in the current year, together with the average annual temperature of the previous year, was the most predictive marker of the bark beetle outbreaks. This agrees well with our ridge regression models, seven of which include variables

such as the average yearly air temperature, and the amount of precipitation in May and June in the current year. Notably, all of the best ten models included precipitation variables from the previous year, but temperature variables were not consistently included, highlighting the potentially more robust role of precipitation in influencing tree loss. Table S1 in Supplementary Materials shows that the parsimony GAM models include approximately the same number of variables related to temperature (25 predictors) and precipitation variables (21 predictors).

Winter temperatures also play a pivotal role in the life cycle of *I. typographus*, traditionally inducing a state of diapause or dormancy (Faccoli, 2009). Winter temperatures affect the survival of the spruce bark beetle, and winter mortality can reach up to 50% (Biermann, 1977; Faccoli, 2002). Research by Stefkova et al. (2017) suggests that beetles are able to complete their development during the winter, especially at temperatures above zero, contradicting previous assumptions (Lombardero et al., 2000; Faccoli, 2002). These immature stages of the beetle were able to survive and may contribute significantly to spring infestations (Dworschak et al., 2014). This is reflected in the GAM list of best models, which includes models with 19 predictors, using the average temperature of the winter months in the given and previous year.

Several studies, including those by Mezei et al. (2017) and Trubin et al. (2022), have highlighted the relationship between temperature variables — average temperatures of both past and current years and tree cover losses. Higher temperatures not only diminish the resistance of trees to bark beetle infestations but also positively influence bark beetle populations, as noted by Bakke (1992).

Another noteworthy aspect is the role of wind-damaged wood as a driver of increased tree loss by bark beetles. Mezei et al. (2017) and Marini et al. (2017) highlighted the importance of the volume of wind-damaged trees in the previous year as a predictive variable. Our best ridge regression model reflects this, including variables such as May wind speed in the current year, which may be related to the occurrence of gale winds. The GAM models also include 51 variables related to wind speed in a particular month in a given or previous year from the 102 best models (Table S1). This supports the claim of Marini et al. (2017) that a surplus of breeding material allows spruce bark beetles to reproduce, eventually colonising and killing healthy trees, independent of other climatic triggers.

4.6. Practical implementation

In response to the increasing threat of spruce bark beetle outbreaks, particularly in the context of climate change, this finding can improve spruce bark beetle prediction models. Understanding the key climatic factors that can trigger and influence the pattern of outbreak development is crucial for predicting potential mass bark beetle outbreaks. These outbreaks can cause significant economic damage to the forestry sector. By analysing specific climatic variables, such as temperature and precipitation patterns, forest managers can better anticipate and prepare for these events.

This study, conducted in the relatively flat areas of Czech forests, provides valuable insights that can be applied to areas with similar landscape and climatic conditions, mainly in Central Europe. The transferability of these findings to other regions with comparable ecological characteristics could improve forest management strategies on a wider geographical scale.

5. Conclusions

The analysed bark beetle outbreak was initiated by the extremely drought-ridden year of 2018. The tree cover loss in the study area was characterized by the processes of spot initialization and bark beetle spot spreading. Both processes were influenced by different meteorological variables.

Spots initialisation was the dominant process before the beginning of

the bark beetle outbreak, and in the progradation phase. The extension of tree cover loss in this process was strongly related to the total duration of solar radiation in April of the previous year. Bark beetle spots spreading was the dominant process in later phases of outbreak gradation. The most important factor influencing spots spreading was the average yearly air temperature in the current year.

The total Annual Tree Loss Change was driven mainly by the sums of duration of solar radiation in June and in September of the current year. The ridge regression has shown the average yearly precipitation in the previous year as the most important factor.

CRediT authorship contribution statement

Karpov Aleksandr: Writing – review & editing, Writing – original draft, Visualization, Methodology, Data curation. **Jakuš Rastislav:** Writing – review & editing, Writing – original draft, Supervision, Project administration, Methodology, Funding acquisition, Conceptualization. **Pirtskhalava-Karpova Nana:** Writing – review & editing, Writing – original draft, Methodology, Investigation, Formal analysis, Conceptualization. **Trubin Aleksei:** Writing – review & editing, Writing – original draft, Visualization, Methodology, Formal analysis, Data curation, Conceptualization.

Declaration of Competing Interest

The authors declare that they have no known competing financial interests or personal relationships that could have appeared to influence the work reported in this paper.

Data Availability

Data will be made available on request.

Appendix A. Supporting information

Supplementary data associated with this article can be found in the online version at doi:10.1016/j.foreco.2023.121666.

References

Abdollahnejad, A., Panagiotidis, D., Surový, P., Modlinger, R., 2021. Investigating the correlation between multisource remote sensing data for predicting potential spread of *Ips typographus* L. Spots in Healthy Trees. Remote Sens. 13 (23), 4953. https://doi.org/10.3390/rs13234953.

Bakke, A., 1992. Monitoring bark beetle populations: effects of temperature. J. Appl. Ent. 114, 208–211.

Bentz, B.J., Jönsson, A.M., 2015. Modeling Bark Beetle Responses to Climate Change. Bark Beetles. Academic Press, pp. 533–553. https://doi.org/10.1016/B978-0-12-417156-5.00013-7.

Biermann, G., 1977. Hibernation of Ips typographus (L.) in the soil litter (Col., Scolytidae). J. Appl. Entomol. 84, 59–74.

Burnham, K.P., Anderson, D.R., Huyvaert, K.P., 2011. AIC model selection and multimodel inference in behavioral ecology: some background, observations, and comparisons. Behav. Ecol. Sociobiol. 65, 23–35. https://doi.org/10.1007/s00265-010-1029-6.

Ceccherini, G., Duveiller, G., Grassi, G., Lemoine, G., Avitabile, V., Pilli, R., et al., 2020. Abrupt increase in harvested forest area over Europe after 2015. Nature 583, 72–77. https://doi.org/10.1038/s41586-020-2438-y.

Coulson, R.N., Amman, G.D., Dahlsten, D.L., DeMars Jr, C.J., Stephen, F.M., 1985. Forest-bark beetle interactions: bark beetle population dynamics. Integr. Pest Manag. pine Bark. beetle Ecosyst. 61–80.

D'Andrea, G., Šimůnek, V., Pericolo, O., Vacek, Z., Vacek, S., Corleto, R., Olejár, L., Ripullone, F., 2023. Growth Response of Norway Spruce (*Picea abies* [L.] Karst.) in Central Bohemia (Czech Republic) to Climate Change. Forests 14, 1215. https://doi.org/10.3390/f14061215.

Dochtermann, N.A., Jenkins, S.H., 2011. Developing multiple hypotheses in behavioral ecology. Behav. Ecol. Sociobiol. 65, 37–45. https://doi.org/10.1007/s00265-010-1039-4.

Dolezal, P., Okrouhlik, J., Davidkova, M., 2016. Fine fluorescent powder marking study of dispersal in the spruce bark beetle, Ips typographus (Coleoptera: Scolytidae). Eur. J. Entomol. 113 https://doi.org/10.14411/eje.2016.001.

Dworschak, K., Gruppe, A., Schopf, R., 2014. Survivability and post diapause fitness in a scolytid beetle in dependence of overwintering developmental stage and implications for population dynamics. Ecol. Entomol. 39, 519–526.

Esri, 2017. ArcGIS (Version 10.6) [Computer software].

European Environment Agency (EEA), 2012. CORINE Land Cover (CLC) [Data file]. Available from: ⟨https://land.copernicus.eu/pan-european/corine-land-cover⟩.

Faccoli, M., 2002. Winter mortality in sub-corticolous population of Ips typographus (Coleoptera, Scolytidae) and its parasitoids in the south-eastern Alps. Journal of Pest Science, 75, 62–68.

Faccoli, M., 2009. Effect of weather on Ips typographus (Coleoptera: Curculionidae) phenology, voltinism, and associated spruce mortality in the Southeastern Alps. Environ. Entomol. 38, 307–316.

Furuta, K., Iguchi, K., Lawson, S., 1996. Seasonal difference in the abundance of the spruce beetle (*Ips typographus japonicus Niijima*) (Col., Scolytidae) within and outside forest in a bivoltine area. J. Appl. Entomol. 120, 125–129. https://doi.org/10.1111/j.1439-0418.1996.tb01578.x.

Hansen, M.C., Potapov, P.V., Moore, R., Hancher, M., Turubanova, S.A., Tyukavina, A., Thau, D., Stehman, S.V., Goetz, S.J., Loveland, T.R., Kommareddy, A., Egorov, A., Chini, L., Justice, C.O., Townshend, J.R.G., 2013. High-resolution global maps of 21st-century forest cover change. Science 342 (6160), 850–853. https://doi.org/10.1126/science.1244693.

Havašová, M., Ferenčík, J., Jakuš, R., 2017. Interactions between windthrow, bark beetles and forest management in the Tatra national parks. For. Ecol. Manag. 391, 349–361. https://doi.org/10.1016/j.foreco.2017.01.009.

Hlásny, T., Zimová, S., Merganičová, K., Štěpánek, P., Modlinger, R., Turčáni, M., 2021. Devastating outbreak of bark beetles in the Czech Republic: Drivers, impacts, and management implications. For. Ecol. Manag. 490, 119075 https://doi.org/10.1016/j.foreco.2021.119075.

Hlásny, T., Barka, I., Merganičová, K., Køístek, Š., Modlinger, R., Turčáni, M., et al., 2022. A new framework for prognosing forest resources under intensified disturbance impacts: Case of the Czech Republic. For. Ecol. Manag. 523, 120483 https://doi.org/10.1016/j.foreco.2022.120483.

Huang, J., Kautz, M., Trowbridge, A.M., Hammerbacher, A., Raffa, K.F., Adams, H.D., et al., 2020. Tree defence and bark beetles in a drying world: Carbon partitioning, functioning and modelling. N. Phytol. 225, 26–36. https://doi.org/10.1111/nph.16173.

Jakuš, R., 2001. Bark beetle (Coleoptera, Scolytidae) outbreak and system of IPM measures in an area affected by intensive forest decline connected with honey fungus (Armillaria sp.). J. Pest Science 74, 46–51.

Jakuš, R., Grodzki, W., Ježík, M., Jachym, M., 2003. Definition of spatial patterns of bark beetle Ips typographus (L.) outbreak spreading in Tatra Mountains (Central Europe), using GIS. McManus, M.L., Liebhold, A.M. (Eds.), Ecology, Survey and Management of Forest Insect. USDA Forest Northeastern Research Station, Delaware, 25–32.

Jönsson, A.M., Schroeder, L.M., Lagergren, F., Anderbrant, O., Smith, B., 2012. Guess the impact of Ips typographus—an ecosystem modelling approach for simulating spruce bark beetle outbreaks, 188–200 Agric. For. Meteorol. 166–167. https://doi.org/10.1016/j.agrformet.2012.07.012.

Kärvemo, S., Huo, L., Öhrn, P., Lindberg, E., Persson, H.J., 2023. Different triggers, different stories: Bark-beetle infestation patterns after storm and drought-induced outbreaks. For. Ecol. Manag. 545, 121255 https://doi.org/10.1016/j.foreco.2023.121255.

Kautz, M., Schopf, R., Ohser, J., 2013. The "sun-effect": Microclimatic alterations predispose forest edges to bark beetle infestations. Eur. J. For. Res. 132 (3), 453–465. https://doi.org/10.1007/s10342-013-0685-2.

Knížek, M., 2021. Disturbance factors in the Czech Republic forests 2020/2021. Forest protection on calamity clearings. Jíloviste, Czech Republic.

Knížek, M., Liška, J., 2020. Bark beetle outbreak in 2020 and prospects for 2021. Strnady, Jíloviste, Czech Republic.

Korolyova, N., Buechling, A., Ďuračiová, R., Zabihi, K., Turčáni, M., Svoboda, M., Bláha, J., Swarts, K., Poláček, M., Hradecký, J., Červenka, J., Němčák, P., Schlyter, F., Jakuš, R., 2022. The last trees standing: climate modulates tree survival factors during a prolonged bark beetle outbreak in Europe. Agric. . Meteorol. 322, 109025 https://doi.org/10.1016/j.agrformet.2022.109025.

Koštál, V., 2006. Eco-physiological phases of insect diapause. J. Insect Physiol. 52, 113–127.

Lobinger, G., Skatulla, U., 1996. Untersuchungen zum einfluß von sonnenlicht auf das schwarmverhalten von borkenkäfern: influencing the flight behaviour of bark

11

155

beetles by light conditions. Anz. für Schädl. 69 (8), 183–185. https://doi.org/10.1007/BF01908442.

Lombardero, M., Ayres, M.P., Ayres, B., Reeve, J.D., 2000. Cold tolerance of four species of bark beetle (Coleoptera: Scolytidae) in North America. Environ. Entomol. 29, 421–432.

Marešová, J., Majdák, A., Jakuš, R., et al., 2020. The short-term effect of sudden gap creation on tree temperature and volatile composition profiles in a Norway spruce stand. Trees 34, 1397–1409. https://doi.org/10.1007/s00468-020-02010-w.

Marini, L., Ayres, M.P., Battisti, A., et al., 2012. Climate affects severity and altitudinal distribution of outbreaks in an eruptive bark beetle. Clim. Change 115, 327–341. https://doi.org/10.1007/s10584-012-0463-z.

Marini, L., Lindelöw, Å., Jönsson, A.M., Wulff, S., Schroeder, L.M., 2013. Population dynamics of the spruce bark beetle: a long-term study. Oikos 122, 1768–1776. https://doi.org/10.1111/j.1600-0706.2013.00431.x.

Marini, L., Økland, B., Jönsson, A.M., Bentz, B., Carroll, A., Forster, B., Grégoire, J.-C., Hurling, R., Nageleisen, L.M., Netherer, S., Ravn, H.P., Weed, A., Schroeder, M., 2017. Climate drivers of bark beetle outbreak dynamics in Norway spruce forests. Ecography 40, 1426–1435. https://doi.org/10.1111/ecog.02769.

Mezei, P., Grodzki, W., Blaženec, M., Jakuš, R., 2014. Factors influencing the wind–bark beetles' disturbance system in the course of an Ips typographus outbreak in the Tatra Mountains. For. Ecol. Manag. 312, 67–77. https://doi.org/10.1016/j.foreco.2013.10.020.

Mezei, P., Jakus, R., Pennerstorfer, J., Havasova, M., Skvarenina, J., Ferencik, J., et al., 2017. Storms, temperature maxima and the Eurasian spruce bark beetle Ips typographus—an infernal trio in Norway spruce forests of the Central European High Tatra Mountains. Agric. . Meteorol. 242, 85–95. https://doi.org/10.1016/j.agrformet.2017.04.004.

Netherer, S., Matthews, B., Katzensteiner, K., Blackwell, E., Henschke, P., Hietz, P., Pennerstorfer, J., Rosner, S., Kikuta, S., Schume, H., Schopf, A., 2015. Do water-limiting conditions predispose Norway spruce to bark beetle attack? N. Phytol. 205, 1128–1141. https://doi.org/10.1111/nph.13166.

Netherer, S., Kandasamy, D., Jirosová, A., Kalinová, B., Schebeck, M., Schlyter, F., 2021. Interactions among Norway spruce, the bark beetle Ips typographus and its fungal symbionts in times of drought. J. Pest Sci. 94, 591–614. https://doi.org/10.1007/s10340-021-01341-y.

Nowakowska, J.A., Hsiang, T., Patynek, P., Stereńczak, K., Olejarski, I., Oszako, T., 2020. Health assessment and genetic structure of monumental Norway spruce trees during A bark beetle (Ips typographus L.) outbreak in the Białowieża Forest District, Poland. Forests 11 (6), 647. https://doi.org/10.3390/f11060647.

Podrázský, V., Remeš, J., Hart, V., Moser, W.K., 2009. Production and humus form development in forest stands established on agricultural lands - Kostelec nad Černými lesy region. J. . Sci. 55 (7), 299–305. https://doi.org/10.17221/11/2009-JFS.

Potterf, M., Nikolov, C., Kočická, E., Ferenčík, J., Mezei, P., Jakuš, R., 2019. Landscape-level spread of beetle infestations from windthrown- and beetle-killed trees in the non-intervention zone of the Tatra National Park, Slovakia (Central Europe). . Ecol. Manag. 432, 489–500. https://doi.org/10.1016/j.foreco.2018.09.050.

Raffa, K.F., Aukema, B.H., Bentz, B.J., Carroll, A.L., Hicke, J.A., Turner, M.G., 2008. Cross-scale drivers of natural disturbances prone to anthropogenic amplification: the dynamics of bark beetle eruptions, 501–17 BioScience 58 (6). https://doi.org/10.1641/B580607.

Remeš, J., 2019. The University forest enterprise in Kostelec nad Černými Lesy - a basis for practical education and research at the faculty of forestry and wood sciences in Prague. SILVA Network Conference. Faculty of Forestry and Wood Sciences, Czech University of Life Sciences, Prague.

Rosen, J., 2016. A forest of hypotheses. Nature 536, 239–241.

Rossum, G., van, Drake, F.L., 2010. The Python Language Reference. Release 3.0.1 [Repr.]. Python Software Foundation, Hampton, NH.

Seidl, R., Schelhaas, M. J., Lexer, M.J., 2011. Unraveling the drivers of intensifying forest disturbance regimes in Europe. Glob. Change Biol. 17, 2842–2852. https://doi.org/10.1111/j.1365-2486.2011.02452.x.

Stefkova, K., Okrouhlik, J., Dolezal, P., 2017. Development and survival of the spruce bark beetle, Ips typographus (Coleoptera: Curculionidae: Scolytinae) at low temperatures in the laboratory and the field. Eur. J. Entomol. 114, 1–6. https://doi.org/10.14411/eje.2017.001.

Trubin, A., Mezei, P., Zabihi, K., Surový, P., Jakuš, R., 2022. Northernmost European spruce bark beetle Ips typographus outbreak: Modelling tree mortality using remote sensing and climate data. . Ecol. Manag. 505, 119829 https://doi.org/10.1016/j.foreco.2021.119829.

Trubin, A., Kozhoridze, G., Zabihi, K., Modlinger, R., Singh, V.V., Surový, P., Jakuš, R., 2023. A detection of green attack and bark beetle susceptibility in norway spruce trees using planetscope multispectral imagery. Front. Glob. Change.

Trubin, A., Kozhoridze, G., Zabihi, K., Modlinger, R., Singh, V.V., Surový, P., Jakuš, R., 2023. a. Detection of susceptible Norway spruce to bark beetle attack using PlanetScope multispectral imagery. Front. . Glob. Change 6, 1130721. https://doi.org/10.3389/ffgc.2023.1130721.

Wermelinger, B., 2004. Ecology and management of the spruce bark beetle Ips typographus - a review of recent research. . Ecol. Manag. 202, 67–82. https://doi.org/10.1016/j.foreco.2004.07.018.

Weslien, J., Lindelöw, Å., 1990. Recapture of marked spruce bark beetles (Ips typographus) in pheromone traps using area-wide mass trapping. Can. J. For. Res. 20 (11), 1786–1790. https://doi.org/10.1139/x90-238.

Yu, L., Zhan, Z., Zhou, Q., Gao, B., Ren, L., Huang, H., Luo, Y., 2022. Climate drivers of pine shoot beetle outbreak dynamics in Southwest China. Remote Sens. 14 (12), 2728. https://doi.org/10.3390/rs14122728.

156

4. Discussion

4.1 Data collection of forest and climate data

Monitoring forests at risk of bark beetle infestations necessitates the expertise of seasoned professionals, such as foresters and researchers, who are trained to discern subtle changes in the canopy and detect the presence of bark beetle boreholes. Given the high degree of precision required for detection and the often inconspicuous signs of an early-stage attack on the tree, this task presents substantial challenges. These complexities underscore the importance of a skilled workforce in effectively managing the threat of bark beetle infestations, highlighting the need for rigorous training and a nuanced understanding of the early indicators of infestation (Trubin et al., 2023; Hlásny et al., 2019).

Trained detection dogs offer considerable advantages in promptly identifying bark beetle infestations due to their acute sense of smell and their capacity to survey large areas more quickly than humans. Conventional human detection methods require close inspection and are time-consuming, expensive, and not always feasible, often leading to delayed detection. As a result, infestations are typically identified 2-3 months post-infestation in northern Europe, by which time most bark beetles have moved on to infest other trees. The presence of specific beetle pheromone components and other semiochemicals for several weeks after an initial attack makes detection dogs a potentially more effective alternative (Johansson et al., 2019). Dogs trained to recognize bark beetle pheromones are significantly more efficient than human experts in detecting bark beetle infestations, with the ability to locate infested trees up to a distance of 150 meters (Vošvrdová et al., 2023). The use of sniffer dogs, therefore, greatly expands the window for the detection and removal of infested trees, thereby potentially averting the development of larger infestations. These factors underscore the potential of trained detection dogs as a valuable asset in the timely management of bark beetle infestations (Singh et al., 2024).

In the context of rapidly evolving bark beetle infestations, the utility of mobile applications for prompt and accurate data collection regarding emerging hotspots cannot be overstated. These applications provide critical real-time geospatial data, enabling timely and effective responses to unfolding infestation events. As such, the ability to quickly collect, analyze, and act upon data related to infestation hotspots is crucial in the management and mitigation of bark beetle outbreaks, reinforcing the significant role these mobile applications play in contemporary forest health management. There exists a diverse array of platforms

designed to facilitate the collection of data pertaining to emerging hotspots of bark beetle infestations. ArcGIS Field Maps is an all-in-one app that uses data from ArcGIS to deliver easy-to-use maps to the field. It integrates with ArcGIS Online and ArcGIS Enterprise, enabling users to capture and update data in real-time. Its capabilities extend to high-accuracy data collection, tracking the location of mobile workers, and the capacity to perform map viewing, markups, and measurements. Survey123 for ArcGIS is an application geared towards form-centric data collection. This design aspect may be particularly useful for the structured collection and categorization of data regarding different stages and aspects of bark beetle infestations. QField, an open-source application, enables users to transfer their QGIS projects to the field, making it an effective tool for individuals already working with QGIS for their GIS needs. Mappt is a robust, intuitive, and cost-efficient mobile GIS and data collection application. It provides the capacity to gather, view, and scrutinize geospatial data offline or online, thereby making it a valuable tool for real-time data collection and analysis of bark beetle infestations. Fulcrum is a mobile data collection platform that allows for the creation of custom apps for field data collection. Its ability to capture location-specific data renders it particularly useful in the geographical mapping of infestations. Input is another open-source app designed to bring QGIS projects to mobile devices, reinforcing field data collection capabilities for QGIS users. Finally, OpenDataKit (ODK) provides a free and open-source suite of tools that facilitate data collection using Android mobile devices, even in the absence of internet or mobile carrier service. These platforms, each with its unique functionalities and strengths, offer valuable tools for the systematic collection of data related to emerging hotspots of bark beetle infestations. Future research could benefit from utilizing these tools, allowing for more accurate, prompt, and comprehensive data collection and thereby enhancing our understanding and management of bark beetle infestations.

Another critical data source for monitoring both bark beetle activity and tree responses involves sap flow measurements. These are captured through installed sensors, enabling us to track fluctuations in sap flow dynamics. Such data provide key insights into the physiological state of trees, including stress-induced patterns. Climate and meteorological datasets, when analyzed in conjunction with sap flow data, offer a comprehensive understanding of both the environmental conditions and tree behaviors. As such, sap flow monitoring emerges as an indispensable tool in the evaluation and prediction of tree responses to bark beetle infestations, thereby contributing significantly to our holistic understanding of forest health dynamics.

4.2 Data processing

The calculations for the Spectral Vegetation Index (SVI) were conducted using the ArcGIS Image Analysis module (arcpy.ia) and QGIS (QGIS Development Team, 2009) Raster Calculator. These tools, although effective, are primarily suited for single calculations. When multiple SVI calculations are required, particularly with extensive time-series remote sensing datasets, these methods can prove to be highly time-consuming. For efficiency and speed in processing, the application of programming languages, such as Python, can be considered. The use of Python (Van Rossum and Drake, 2010), specifically with the spyndex library (Montero et al., 2023), can facilitate rapid and efficient solutions, allowing for the generation of multiple outputs simultaneously. This has the potential to significantly expedite the computational processes involved in SVI calculations.

4.3 Mortality analysis

In this section, we discuss and compare two studies on bark beetle outbreaks in diverse climatic and geographical settings. The study, conducted in the Dvinsko-Pinegskiy reserve in Russia, examines tree mortality in a largely untouched taiga ecosystem. The second, set in the School Forest Enterprise (ŠLP) near Kostelec nad Černými Lesy in the Czech Republic, focuses on a bark beetle outbreak in a Central European forest landscape. These studies, while centered on the same insect species – the Eurasian spruce bark beetle (*Ips typographus*) – provide insights into how different climatic conditions, forest management practices, and statistical models can influence and explain tree mortality dynamics.

The core of both studies is the analysis of climate variables in relation to bark beetle-induced tree mortality. While both studies emphasize temperature and precipitation, they differ in specific variables and approaches. The Dvinsko-Pinegskiy study highlights the significance of the previous year's temperatures and June temperatures, using linear regression. On the other hand, the Czech study employs Generalised Additive Models (GAMs) and Ridge regression, and using wind speeds in addition to temperature, precipitation and solar radiation. These differences underscore the importance of selecting appropriate climatic variables based on regional climate characteristics when analyzing bark beetle outbreaks.

The geographical setting of each study area plays a crucial role in understanding the differing dynamics of bark beetle outbreaks. The Dvinsko-Pinegskiy reserve, located in a colder, more northerly latitude, experiences distinct climatic conditions compared to the temperate climate of the Czech Republic's ŠLP. This geographic distinction likely influences

the lifecycle and behavior of *Ips typographus*, affecting how climate variables impact tree mortality.

The two areas also differ significantly in their forest management practices and disturbance regimes. The ŠLP area in the Czech Republic has seen active forest management, including sanitary logging in response to bark beetle infestations. In contrast, the Dvinsko-Pinegskiy reserve is a protected area with minimal human intervention, allowing for a more natural progression of forest dynamics and beetle outbreaks. This contrast provides a valuable comparison for understanding how management practices can influence the severity and dynamics of bark beetle outbreaks.

Both studies leverage the Global Forest Watch (GFW) data, highlighting its utility in monitoring forest cover loss and disturbances. The high-resolution, time-series data from GFW allows for precise tracking of tree mortality and forest changes, if a particular type of disturbance is confirmed, making it an indispensable tool for studies focusing on forest health and dynamics.

The findings from these studies have significant implications for forest management, especially in the context of climate change. Understanding the climatic drivers of bark beetle outbreaks and their interaction with forest ecosystems is crucial for developing effective management strategies. The differing methodologies and findings of these studies also highlight the need for further research, particularly in exploring the effects of climate variables on bark beetle dynamics across various geographical settings.

4.4 Limitations of this research

The findings of this thesis predominantly pertain to the susceptibility, green attack, and mortality phases of bark beetle infestations. The red attack phase was not a focal point of this research, given its comprehensive coverage in existing studies (Wulder et al., 2006; Zabihi et al., 2021; Marvasti-Zadeh et al., 2023). Instead, this research placed a greater emphasis on the early stages of infestation, even prior to the outbreak, due to the substantial challenges associated with gaining meaningful insights during these initial stages. The primary constraint in identifying these early stages is establishing a reliable system for ground truth data collection and validation. The process of obtaining accurate and reliable ground truth data for these initial infestation stages can be labor-intensive (Zabihi et al., 2021), which may limit the scope and frequency of such data collection efforts. This has the potential to impact the validation of

models and tools designed for early detection, presenting a notable limitation of the current study.

When dealing with the susceptibility and green attack phases of bark beetle infestations, a key challenge lies in accurately identifying the appropriate vegetation index at the right temporal point. This is a significant limitation given the specific nature and time dependence of such invasions. Additionally, geographical location could have a significant impact on susceptibility. For example, mountainous regions may exhibit unique patterns of infestation, and our understanding of these patterns is currently limited. Thus, the interaction between geographical variables and bark beetle susceptibility remains an area requiring further exploration and constitutes a potential limitation of the current study.

In the case of forest mortality resulting from bark beetle infestations, a major limiting factor lies in leveraging historical data to gain a better understanding of the dynamics of bark beetle spread under varying conditions. Using methods such as Generalized Additive Models (GAM), non-linear models, and Machine Learning (ML) models could potentially reveal significant insights regarding the drivers of forest mortality. However, the application of these complex modelling techniques requires comprehensive and accurately recorded historical data, and the absence or insufficiency of such data could limit the depth and accuracy of these analyses (Pirtskhalava-Karpova et al., 2024). Hence, while these models promise new and meaningful insights, their efficacy is contingent on the availability and quality of historical data, representing a significant limitation in studying forest mortality due to bark beetle infestations.

4.5 Future studies

There is a noticeable deficit in the development of models and platforms specifically tailored towards monitoring bark beetle infestations within the season and making accurate forecasts based on our current knowledge. The existing TANABBO model (Duračiová et al., 2020; Pirtskhalava-Karpova et al., 2024), although effective, leaves room for enhancements and adjustments. For future studies, it would be advantageous to explore the integration of various data sources, including climate variables, bark beetle-related ground truth data, and remote sensing information. The amalgamation of these diverse and rich data types could pave the way for a comprehensive and effective tool. This would significantly aid in the timely

detection of infestations, potentially preventing extensive forest losses. An innovative, data-integrated approach like this has the potential to transform our understanding of bark beetle infestations, enhancing our ability to predict, monitor, and manage these events within a forest management context.

It would be beneficial to explore and test a broader range of spectral indices beyond just vegetation. Investigating soil indices, for instance, might provide valuable insights and further enhance our ability to differentiate between stressed and healthy forests. Once established indices have been thoroughly tested, another promising way of research could be the development of novel indices. These new indices could be tailored to achieve clear separability throughout the vegetation season, with a particular emphasis on its early stages. By evolving and diversifying our approach to spectral indices, we can potentially refine our ability to monitor and respond to forest health and infestation risks in a timely and effective manner.

For the green attack phase of bark beetle infestations, the principal challenge in formulating effective management strategies is the ability to promptly respond to emergent hotspots within the ongoing season. This challenge is further compounded by constraints related to human capacity, and the need for rapid, informed decision-making in the face of an active infestation. A thorough analysis of the dynamics of the previous season's hotspots could provide valuable insights to inform the development of proactive management strategies. However, the time-sensitive nature of this phase and the need for an immediate response present significant obstacles.

4.5.1 Satellites with multi and hyperspectral sensors

With the advent of increasingly advanced satellite systems, researchers are equipped with newer datasets to better comprehend and manage bark beetle infestations. Notably, the emergence of multispectral and hyperspectral satellites offers promising prospects for insightful and detailed data. Hyperspectral satellites, in particular, hold significant potential in providing deeper insights into forest health. Existing systems such as PRISMA and DESIS (Aneece and Thenkabail, 2021; Giacomo et al., 2020; Alonso et al., 2019) are already in operation, offering substantial data resources. Moreover, further advancements are on the horizon, with more systems, such as the European Copernicus Next Generation Hyperspectral Satellite CHIME (Nieke and Rast, 2018), being planned for future deployment. Notably, the

German system EnMAP (Storch et al., 2023) was successfully launched into space on April 1st, 2022, marking a significant milestone in remote sensing capabilities. The forthcoming Global Hyperspectral Observation Satellite (GHOSt, launch date - April 15, 2023) further underlines the dynamic progression in this field. These burgeoning developments in satellite technology offer increasingly refined datasets for the surveillance and management of bark beetle infestations. The implementation of these new technologies can potentially revolutionize our understanding and response to these infestations, thereby marking a pivotal shift in the field of forest health management.

5. Conclusions

The progression of this research underlines several key conclusions and directions for future exploration in the monitoring and management of bark beetle infestations.

Rapid Data Collection and Monitoring: Mobile applications and sensor technology have emerged as vital tools, used by skilled specialists, for prompt and accurate data collection on emerging hotspots of infestation. The use of trained detection dogs also presents a promising alternative for the fast and efficient detection of infestations, amplifying the window of opportunity for effective management.

Integrating Diverse Data Sources: The integration of diverse datasets, such as climate and meteorological data, sap flow measurements, and remote sensing data, can offer a comprehensive understanding of the factors influencing bark beetle infestations and tree responses. The advent of advanced satellite systems, particularly hyperspectral satellites, presents immense potential for detailed and insightful data on forest health.

Focus on Early Detection: While monitoring the green attack phase is important, catching the early symptoms of susceptible trees to future bark beetle attacks is crucial. The development and application of systems based on thresholds of EVI/VARI or new indices could provide timely indications of potential infestations.

Evaluating Mortality Patterns: Yearly mortality data can provide valuable insights into the history and dynamics of infestations. Such data can be transformed into actionable metrics for real-time assessment, aiding in the creation of effective mitigation strategies.

In conclusion, the management of bark beetle infestations is a complex, multi-faceted task that necessitates rapid data collection, integration of diverse data sources, a focus on early detection, and a skilled workforce. The advent of new technologies and methods promises to enhance our understanding and response to these infestations, setting the stage for effective and sustainable forest health management strategies.

6. References

Abdollahnejad, A., Panagiotidis, D., Surový, P., Modlinger, R., 2021. Investigating the Correlation between Multisource Remote Sensing Data for Predicting Potential Spread of Ips typographus L. Spots in Healthy Trees. Remote Sensing 13, 4953. https://doi.org/10.3390/rs13234953

Allen, C.D., Macalady, A.K., Chenchouni, H., Bachelet, D., McDowell, N., Vennetier, M., Kitzberger, T., Rigling, A., Breshears, D.D., Hogg, E.H. (Ted), Gonzalez, P., Fensham, R., Zhang, Z., Castro, J., Demidova, N., Lim, J.-H., Allard, G., Running, S.W., Semerci, A., Cobb, N., 2010. A global overview of drought and heat-induced tree mortality reveals emerging climate change risks for forests. Forest Ecology and Management 259, 660–684. https://doi.org/10.1016/j.foreco.2009.09.001

Alonso, K., Bachmann, M., Burch, K., Carmona, E., Cerra, D., De Los Reyes, R., Dietrich, D., Heiden, U., Hölderlin, A., Ickes, J., Knodt, U., Krutz, D., Lester, H., Müller, R., Pagnutti, M., Reinartz, P., Richter, R., Ryan, R., Sebastian, I., Tegler, M., 2019. Data Products, Quality and Validation of the DLR Earth Sensing Imaging Spectrometer (DESIS). Sensors 19, 4471. https://doi.org/10.3390/s19204471

Aneece, I., Thenkabail, P.S., 2021. DESIS and PRISMA: A study of a new generation of spaceborne hyperspectral sensors in the study of world crops, in: 2021 IEEE International Geoscience and Remote Sensing Symposium IGARSS. Presented at the IGARSS 2021 - 2021 IEEE International Geoscience and Remote Sensing Symposium, IEEE, Brussels, Belgium, pp. 479–479. https://doi.org/10.1109/IGARSS47720.2021.9553718

Bače, R., Svoboda, M., Janda, P., Morrissey, R.C., Wild, J., Clear, J.L., Čada, V., Donato, D.C., 2015. Legacy of Pre-Disturbance Spatial Pattern Determines Early Structural Diversity following Severe Disturbance in Montane Spruce Forests. PLoS ONE 10, e0139214. https://doi.org/10.1371/journal.pone.0139214

Bentz, B.J., Jönsson, A.M., 2015. Modeling Bark Beetle Responses to Climate Change, in: Bark Beetles. Elsevier, pp. 533–553. https://doi.org/10.1016/B978-0-12-417156-5.00013-7

Blomqvist, M., Kosunen, M., Starr, M., Kantola, T., Holopainen, M., Lyytikäinen-Saarenmaa, P., 2018. Modelling the predisposition of Norway spruce to Ips typographus L. infestation by means of environmental factors in southern Finland. Eur J Forest Res 137, 675–691. https://doi.org/10.1007/s10342-018-1133-0

Brůna, J., Wild, J., Svoboda, M., Heurich, M., Müllerová, J., 2013. Impacts and underlying factors of landscape-scale, historical disturbance of mountain forest identified using archival documents. Forest Ecology and Management 305, 294–306. https://doi.org/10.1016/j.foreco.2013.06.017

Ceccherini, G., Duveiller, G., Grassi, G., Lemoine, G., Avitabile, V., Pilli, R., Cescatti, A., 2020. Abrupt increase in harvested forest area over Europe after 2015. Nature 583, 72–77. https://doi.org/10.1038/s41586-020-2438-y

Christiansen, E., Bakke, A., 1988. The Spruce Bark Beetle of Eurasia, in: Berryman, A.A. (Ed.), Dynamics of Forest Insect Populations. Springer US, Boston, MA, pp. 479–503. https://doi.org/10.1007/978-1-4899-0789-9_23

DeRose, R.J., Bentz, B.J., Long, J.N., Shaw, J.D., 2013. Effect of increasing temperatures on the distribution of spruce beetle in Engelmann spruce forests of the Interior West, USA. Forest Ecology and Management 308, 198–206. https://doi.org/10.1016/j.foreco.2013.07.061

Duračiová, R., Muňko, M., Barka, I., Koreň, M., Resnerová, K., Holuša, J., Blaženec, M., Potterf, M., Jakuš, R., 2020. A bark beetle infestation predictive model based on satellite data in the frame of decision support system TANABBO. iForest 13, 215–223. https://doi.org/10.3832/ifor3271-013

Esri. (2023). ArcGIS Image Analysis module (arcpy.ia) [Software]. Available from https://www.esri.com

Gely, C., Laurance, S.G.W., Stork, N.E., 2020. How do herbivorous insects respond to drought stress in trees? Biol Rev 95, 434–448. https://doi.org/10.1111/brv.12571

Georgiev G., Georgieva M., Belilov S., Mirchev P., Deliyanchev S., Mladenov V., Kropov K., Haydarova S. 2023. Early detection of Ips typographus infestations by using Sentinel-2 satellite images in windthrow affected Norway spruce forests in Smolyan region, Bulgaria. Silva Balcanica 23(2): 27-34. https://doi.org/10.3897/silvabalcanica.22.e98314

Giacomo, C., Ettore, L., Rino, L., Rosa, L., Rocchina, G., Girolamo, D.M., Patrizia, S., 2020. The Hyperspectral Prisma Mission in Operations, in: IGARSS 2020 - 2020 IEEE International Geoscience and Remote Sensing Symposium. Presented at the IGARSS 2020 - 2020 IEEE International Geoscience and Remote Sensing Symposium, IEEE, Waikoloa, HI, USA, pp. 3282–3285. https://doi.org/10.1109/IGARSS39084.2020.9323301

Haarsma, R.J., Hazeleger, W., Severijns, C., De Vries, H., Sterl, A., Bintanja, R., Van Oldenborgh, G.J., Van Den Brink, H.W., 2013. More hurricanes to hit western Europe due to global warming. Geophysical Research Letters 40, 1783–1788. https://doi.org/10.1002/grl.50360

Hansen, M.C., Potapov, P.V., Moore, R., Hancher, M., Turubanova, S.A., Tyukavina, A., Thau, D., Stehman, S.V., Goetz, S.J., Loveland, T.R., Kommareddy, A., Egorov, A., Chini, L., Justice, C.O., Townshend, J.R.G., 2013. High-Resolution Global Maps of 21st-Century Forest Cover Change. Science 342, 850–853. https://doi.org/10.1126/science.1244693

Havašová, M., Ferenčík, J., Jakuš, R., 2017. Interactions between windthrow, bark beetles and forest management in the Tatra national parks. Forest Ecology and Management 391, 349–361. https://doi.org/10.1016/j.foreco.2017.01.009

Hlásny, T., König, L., Krokene, P., Lindner, M., Montagné-Huck, C., Müller, J., Qin, H., Raffa, K.F., Schelhaas, M.-J., Svoboda, M., Viiri, H., Seidl, R., 2021. Bark Beetle Outbreaks in Europe: State of Knowledge and Ways Forward for Management. Curr Forestry Rep 7, 138–165. https://doi.org/10.1007/s40725-021-00142-x

Hlásny, T., Krokene, P., Liebhold, A., Montagné-Huck, C., Müller, J., Qin, H., Raffa, K., Schelhaas, M.-J., Seidl, R., Svoboda, M., Viiri, H., European Forest Institute, 2019. Living with bark beetles: impacts, outlook and management options (From Science to Policy), From Science to Policy. European Forest Institute. https://doi.org/10.36333/fs08

Hlásny, T., Zimová, S., Merganičová, K., Štěpánek, P., Modlinger, R., Turčáni, M., 2021. Devastating outbreak of bark beetles in the Czech Republic: Drivers, impacts, and management implications. Forest Ecology and Management 490, 119075. https://doi.org/10.1016/j.foreco.2021.119075

Huang, J., Kautz, M., Trowbridge, A.M., Hammerbacher, A., Raffa, K.F., Adams, H.D., Goodsman, D.W., Xu, C., Meddens, A.J.H., Kandasamy, D., Gershenzon, J., Seidl, R., Hartmann, H., 2020. Tree defence and bark beetles in a drying world: carbon partitioning, functioning and modelling. New Phytologist 225, 26–36. https://doi.org/10.1111/nph.16173

Jactel, H., Koricheva, J., Castagneyrol, B., 2019. Responses of forest insect pests to climate change: not so simple. Current Opinion in Insect Science 35, 103–108. https://doi.org/10.1016/j.cois.2019.07.010

Jactel, H., Petit, J., Desprez-Loustau, M.-L., Delzon, S., Piou, D., Battisti, A., Koricheva, J., 2012. Drought effects on damage by forest insects and pathogens: a meta-analysis. Glob Change Biol 18, 267–276. https://doi.org/10.1111/j.1365-2486.2011.02512.x

Jakuš, R., Grodzki, W., Ježík, M., Jachym, M., 2003. Definition of spatial patterns of bark beetle Ips typographus (L.) outbreak spreading in Tatra Mountains (Central Europe), using GIS. McManus, M.L., Liebhold, A.M. (Eds.), Ecology, Survey and Management of Forest Insect. USDA Forest Northeastern Research Station, Delaware, 25–32.

Jönsson, A.M., Schroeder, L.M., Lagergren, F., Anderbrant, O., Smith, B., 2012. Guess the impact of Ips typographus—An ecosystem modelling approach for simulating spruce bark beetle outbreaks. Agricultural and Forest Meteorology 13.

Johansson, A., Birgersson, G., Schlyter, F., 2019. Using synthetic semiochemicals to train canines to detect bark beetle–infested trees. Annals of Forest Science 76, 58. https://doi.org/10.1007/s13595-019-0841-z

Kärvemo, S., Huo, L., Öhrn, P., Lindberg, E., Persson, H.J., 2023. Different triggers, different stories: Bark-beetle infestation patterns after storm and drought-induced outbreaks. Forest Ecology and Management 545, 121255. https://doi.org/10.1016/j.foreco.2023.121255

Kärvemo, S., Johansson, V., Schroeder, M., Ranius, T., 2016. Local colonization-extinction dynamics of a tree-killing bark beetle during a large-scale outbreak. Ecosphere 7, e01257. https://doi.org/10.1002/ecs2.1257

Kärvemo, S., Rogell, B., Schroeder, M., 2014. Dynamics of spruce bark beetle infestation spots: Importance of local population size and landscape characteristics after a storm

disturbance. Forest Ecology and Management 334, 232–240. https://doi.org/10.1016/j.foreco.2014.09.011

Kärvemo, S., Van Boeckel, T.P., Gilbert, M., Grégoire, J.-C., Schroeder, M., 2014. Large-scale risk mapping of an eruptive bark beetle – Importance of forest susceptibility and beetle pressure. Forest Ecology and Management 318, 158–166. https://doi.org/10.1016/j.foreco.2014.01.025

Knížek, M., Liška, J., 2020. Bark beetle outbreak in 2020 and prospects for 2021. Strnady, Jíloviste, Czech Republic.

Kolb, T.E., Fettig, C.J., Ayres, M.P., Bentz, B.J., Hicke, J.A., Mathiasen, R., Stewart, J.E., Weed, A.S., 2016. Observed and anticipated impacts of drought on forest insects and diseases in the United States. Forest Ecology and Management 380, 321–334. https://doi.org/10.1016/j.foreco.2016.04.051

Komonen, A., Schroeder, L.M., Weslien, J., 2011. *Ips typographus* population development after a severe storm in a nature reserve in southern Sweden. J Applied Entomology 135, 132–141. https://doi.org/10.1111/j.1439-0418.2010.01520.x

Komonen, A., Schroeder, L.M., Weslien, J., 2011. Ips typographus population development after a severe storm in a nature reserve in southern Sweden. J Applied Entomology 135, 132–141. https://doi.org/10.1111/j.1439-0418.2010.01520.x

Korolyova, N., Buechling, A., Ďuračiová, R., Zabihi, K., Turčáni, M., Svoboda, M., Bláha, J., Swarts, K., Poláček, M., Hradecký, J., Červenka, J., Němčák, P., Schlyter, F., Jakuš, R., 2022. The Last Trees Standing: Climate modulates tree survival factors during a prolonged bark beetle outbreak in Europe. Agricultural and Forest Meteorology 322, 109025. https://doi.org/10.1016/j.agrformet.2022.109025

Krokene, P., 2015. Conifer Defense and Resistance to Bark Beetles, in: Bark Beetles. Elsevier, pp. 177–207. https://doi.org/10.1016/B978-0-12-417156-5.00005-8

Lieutier, F., Day, K.R., Battisti, A., Grégoire, J.-C., Evans, H.F. (Eds.), 2004. Bark and Wood Boring Insects in Living Trees in Europe, a Synthesis. Springer Netherlands, Dordrecht. https://doi.org/10.1007/978-1-4020-2241-8

Lindman, L., Ranius, T., Schroeder, M., 2023. Regional climate affects habitat preferences and thermal sums required for development of the Eurasian spruce bark beetle, Ips typographus. Forest Ecology and Management 544, 121216. https://doi.org/10.1016/j.foreco.2023.121216

Marini, L., Lindelöw, Å., Jönsson, A.M., Wulff, S., Schroeder, L.M., 2013. Population dynamics of the spruce bark beetle: a long-term study. Oikos 122, 1768–1776. https://doi.org/10.1111/j.1600-0706.2013.00431.x

Marini, L., Økland, B., Jönsson, A.M., Bentz, B., Carroll, A., Forster, B., Grégoire, J.-C., Hurling, R., Nageleisen, L.M., Netherer, S., Ravn, H.P., Weed, A., Schroeder, M., 2017. Climate drivers of bark beetle outbreak dynamics in Norway spruce forests. Ecography 40, 1426–1435. https://doi.org/10.1111/ecog.02769

Marvasti-Zadeh, S. M., Goodsman, D., Ray, N., and Erbilgin, N. (2023). Early Detection of Bark Beetle Attack Using Remote Sensing and Machine Learning. ACM Comput. Surv., 3625387. doi: 10.1145/3625387.

Maslov, A.D., 2010. Короед-типограф и усыхание еловых лесов [Bark beetle and the decay of spruce forests]. ВНИИЛМ 138.

McDowell, N., Pockman, W.T., Allen, C.D., Breshears, D.D., Cobb, N., Kolb, T., Plaut, J., Sperry, J., West, A., Williams, D.G., Yepez, E.A., 2008. Mechanisms of plant survival and mortality during drought: why do some plants survive while others succumb to drought? New Phytologist 178, 719–739. https://doi.org/10.1111/j.1469-8137.2008.02436.x

Meddens, A.J.H., Hicke, J.A., Macalady, A.K., Buotte, P.C., Cowles, T.R., Allen, C.D., 2015. Patterns and causes of observed piñon pine mortality in the southwestern United States. New Phytol 206, 91–97. https://doi.org/10.1111/nph.13193

Mezei, P., Jakuš, R., Pennerstorfer, J., Havašová, M., Škvarenina, J., Ferenčík, J., Slivinský, J., Bičárová, S., Bilčík, D., Blaženec, M., Netherer, S., 2017. Storms, temperature maxima and the Eurasian spruce bark beetle Ips typographus—An infernal trio in Norway spruce forests of the Central European High Tatra Mountains. Agricultural and Forest Meteorology 242, 85–95. https://doi.org/10.1016/j.agrformet.2017.04.004

Mezei, P., Grodzki, W., Blaženec, M., Jakuš, R., 2014. Factors influencing the wind–bark beetles' disturbance system in the course of an Ips typographus outbreak in the Tatra

Mountains. Forest Ecology and Management 312, 67–77. https://doi.org/10.1016/j.foreco.2013.10.020

Montero, D., Aybar, C., Mahecha, M.D., Martinuzzi, F., Söchting, M., Wieneke, S., 2023. A standardized catalogue of spectral indices to advance the use of remote sensing in Earth system research. Sci Data 10, 197. https://doi.org/10.1038/s41597-023-02096-0

Müller, M., Olsson, P.-O., Eklundh, L., Jamali, S., Ardö, J., 2022. Features predisposing forest to bark beetle outbreaks and their dynamics during drought. Forest Ecology and Management 523, 120480. https://doi.org/10.1016/j.foreco.2022.120480

Netherer, S., Kandasamy, D., Jirosová, A., Kalinová, B., Schebeck, M., Schlyter, F., 2021. Interactions among Norway spruce, the bark beetle Ips typographus and its fungal symbionts in times of drought. J Pest Sci 94, 591–614. https://doi.org/10.1007/s10340-021-01341-y

Netherer, S., Matthews, B., Katzensteiner, K., Blackwell, E., Henschke, P., Hietz, P., Pennerstorfer, J., Rosner, S., Kikuta, S., Schume, H., Schopf, A., 2015. Do water-limiting conditions predispose Norway spruce to bark beetle attack? New Phytologist 205, 1128–1141. https://doi.org/10.1111/nph.13166

Netherer, S., Nopp-Mayr, U., 2005. Predisposition assessment systems (PAS) as supportive tools in forest management—rating of site and stand-related hazards of bark beetle infestation in the High Tatra Mountains as an example for system application and verification. Forest Ecology and Management 207, 99–107. https://doi.org/10.1016/j.foreco.2004.10.020

Nieke, J., Rast, M., 2018. Towards the Copernicus Hyperspectral Imaging Mission For The Environment (CHIME), in: IGARSS 2018 - 2018 IEEE International Geoscience and Remote Sensing Symposium. Presented at the IGARSS 2018 - 2018 IEEE International Geoscience and Remote Sensing Symposium, IEEE, Valencia, pp. 157–159. https://doi.org/10.1109/IGARSS.2018.8518384

Nilsson, C., Stjernquist, I., Bärring, L., Schlyter, P., Jönsson, A.M., Samuelsson, H., 2004. Recorded storm damage in Swedish forests 1901–2000. Forest Ecology and Management 199, 165–173. https://doi.org/10.1016/j.foreco.2004.07.031

Nowakowska, J.A., Hsiang, T., Patynek, P., Stereńczak, K., Olejarski, I., Oszako, T., 2020. Health Assessment and Genetic Structure of Monumental Norway Spruce Trees during A Bark Beetle (Ips typographus L.) Outbreak in the Białowieża Forest District, Poland. Forests 11, 647. https://doi.org/10.3390/f11060647

Økland, B., Berryman, A., 2004. Resource dynamic plays a key role in regional fluctuations of the spruce bark beetles Ips typographus. Agri and Forest Entomology 6, 141–146. https://doi.org/10.1111/j.1461-9555.2004.00214.x

Özçelik, M.S., Tomášková, I., Surový, P., Modlinger, R., 2022. Effect of Forest Edge Cutting on Transpiration Rate in Picea abies (L.) H. Karst. Forests 13, 1238. https://doi.org/10.3390/f13081238

Pasztor, F., Matulla, C., Rammer, W., Lexer, M.J., 2014. Drivers of the bark beetle disturbance regime in Alpine forests in Austria. Forest Ecology and Management 318, 349–358. https://doi.org/10.1016/j.foreco.2014.01.044

Pirtskhalava-Karpova N., Trubin A., Karpov A., Jakuš R. (2024). Drought initialised bark beetle outbreak in Central Europe: Meteorological factors and infestation dynamic. Forest Ecology and Management 554, 121666. https://doi.org/10.1016/j.foreco.2023.121666

Potterf, M., Nikolov, C., Kočická, E., Ferenčík, J., Mezei, P., Jakuš, R., 2019. Landscape-level spread of beetle infestations from windthrown- and beetle-killed trees in the non-intervention zone of the Tatra National Park, Slovakia (Central Europe). Forest Ecology and Management 432, 489–500. https://doi.org/10.1016/j.foreco.2018.09.050

QGIS Development Team (2009). QGIS geographic information system. Open source geospatial foundation. Pittsburgh, PA: Q Development Team.

Raffa, K.F., Grégoire, J.-C., Staffan Lindgren, B., 2015. Natural History and Ecology of Bark Beetles, in: Bark Beetles. Elsevier, pp. 1–40. https://doi.org/10.1016/B978-0-12-417156-5.00001-0

Raffa, K.F., Aukema, B.H., Bentz, B.J., Carroll, A.L., Hicke, J.A., Turner, M.G., Romme, W.H., 2008. Cross-scale Drivers of Natural Disturbances Prone to Anthropogenic Amplification: The Dynamics of Bark Beetle Eruptions. BioScience 58, 501–517. https://doi.org/10.1641/B580607

Romashkin, I., Neuvonen, S., Tikkanen, O., 2020. Northward shift in temperature sum isoclines may favour Ips typographus outbreaks in European Russia. Agr Forest Entomol 22, 238–249. https://doi.org/10.1111/afe.12377

Rossum, G. van, Drake, F.L., 2010. The Python language reference, Release 3.0.1 [Repr.]. ed, Python documentation manual / Guido van Rossum; Fred L. Drake [ed.]. Python Software Foundation, Hampton, NH.

Schroeder, M., Dalin, P., 2017. Differences in photoperiod-induced diapause plasticity among different populations of the bark beetle Ips typographus and its predator Thanasimus formicarius: Diapause plasticity in a bark beetle and predator. Agr Forest Entomol 19, 146–153. https://doi.org/10.1111/afe.12189

Seidl, R., Schelhaas, M., Lexer, M.J., 2011. Unraveling the drivers of intensifying forest disturbance regimes in Europe. Global Change Biology 17, 2842–2852. https://doi.org/10.1111/j.1365-2486.2011.02452.x

Seidl, R., Spies, T.A., Peterson, D.L., Stephens, S.L., Hicke, J.A., 2016. REVIEW: Searching for resilience: addressing the impacts of changing disturbance regimes on forest ecosystem services. Journal of Applied Ecology 53, 120–129. https://doi.org/10.1111/1365-2664.12511

Seidl, R., Thom, D., Kautz, M., Martin-Benito, D., Peltoniemi, M., Vacchiano, G., Wild, J., Ascoli, D., Petr, M., Honkaniemi, J., Lexer, M.J., Trotsiuk, V., Mairota, P., Svoboda, M., Fabrika, M., Nagel, T.A., Reyer, C.P.O., 2017. Forest disturbances under climate change. Nature Clim Change 7, 395–402. https://doi.org/10.1038/nclimate3303

Singh V.; Naseer A.; Mogilicherla K.; Trubin A.; Zabihi K.; Roy A.; Jakuš R.; Erbilgin N., 2024.Understanding Bark Beetle Outbreaks: Exploring the Impact of Changing Temperature Regimes, Droughts, Forest Structure, and Prospects for Future Forest Pest Management. Reviews in Environmental Science and Bio/Technology (submitted)

Sproull, G.J., Bukowski, M., Mcnutt, N., Zwijacz-Kozica, T., Szwagrzyk, J., 2017. Landscape-Level Spruce Mortality Patterns and Topographic Forecasters of Bark Beetle Outbreaks in Managed and Unmanaged Forests of the Tatra Mountains. Polish Journal of Ecology 65, 24–37. https://doi.org/10.3161/15052249PJE2017.65.1.003

Stadelmann, G., Bugmann, H., Wermelinger, B., Bigler, C., 2014. Spatial interactions between storm damage and subsequent infestations by the European spruce bark beetle. Forest Ecology and Management 318, 167–174. https://doi.org/10.1016/j.foreco.2014.01.022

Storch, T., Honold, H.-P., Chabrillat, S., Habermeyer, M., Tucker, P., Brell, M., Ohndorf, A., Wirth, K., Betz, M., Kuchler, M., Mühle, H., Carmona, E., Baur, S., Mücke, M., Löw, S., Schulze, D., Zimmermann, S., Lenzen, C., Wiesner, S., Aida, S., Kahle, R., Willburger, P., Hartung, S., Dietrich, D., Plesia, N., Tegler, M., Schork, K., Alonso, K., Marshall, D., Gerasch, B., Schwind, P., Pato, M., Schneider, M., De Los Reyes, R., Langheinrich, M., Wenzel, J., Bachmann, M., Holzwarth, S., Pinnel, N., Guanter, L., Segl, K., Scheffler, D., Foerster, S., Bohn, N., Bracher, A., Soppa, M.A., Gascon, F., Green, R., Kokaly, R., Moreno, J., Ong, C., Sornig, M., Wernitz, R., Bagschik, K., Reintsema, D., La Porta, L., Schickling, A., Fischer, S., 2023. The EnMAP imaging spectroscopy mission towards operations. Remote Sensing of Environment 294, 113632. https://doi.org/10.1016/j.rse.2023.113632

Stříbrská, B., Hradecký, J., Čepl, J., Tomášková, I., Jakuš, R., Modlinger, R., Netherer, S., Jirošová, A., 2022. Forest margins provide favourable microclimatic niches to swarming bark beetles, but Norway spruce trees were not attacked by Ips typographus shortly after edge creation in a field experiment. Forest Ecology and Management 506, 119950. https://doi.org/10.1016/j.foreco.2021.119950

Trubin, A., Kozhoridze, G., Zabihi, K., Modlinger, R., Singh, V.V., Surový, P., Jakuš, R., 2023. Detection of susceptible Norway spruce to bark beetle attack using PlanetScope multispectral imagery. Front. For. Glob. Change 6, 1130721. https://doi.org/10.3389/ffgc.2023.1130721

Trubin, A., Kozhoridze, G., Zabihi, K., Modlinger, R., Singh, V.V., Surový, P., Jakuš, R., 2024. Detection of Green Attack and Bark Beetle Susceptibility in Norway Spruce Trees using PlanetScope Multispectral Imagery. Manuscript under review.

Trubin, A., Mezei, P., Zabihi, K., Surový, P., Jakuš, R., 2022. Northernmost European spruce bark beetle Ips typographus outbreak: Modelling tree mortality using remote sensing and climate data. Forest Ecology and Management 505, 119829. https://doi.org/10.1016/j.foreco.2021.119829

Vošvrdová, N., Johansson, A., Turčáni, M., Jakuš, R., Tyšer, D., Schlyter, F., Modlinger, R., 2023. Dogs trained to recognise a bark beetle pheromone locate recently attacked spruces better

than human experts. Forest Ecology and Management 528, 120626. https://doi.org/10.1016/j.foreco.2022.120626

Weed, A.S., Ayres, M.P., Hicke, J.A., 2013. Consequences of climate change for biotic disturbances in North American forests. Ecological Monographs 83, 441–470. https://doi.org/10.1890/13-0160.1

Wermelinger, B., 2004. Ecology and management of the spruce bark beetle Ips typographus— a review of recent research. Forest Ecology and Management 202, 67–82. https://doi.org/10.1016/j.foreco.2004.07.018

Wermelinger, B., Jakoby, O., 2022. Bark Beetles, in: Wohlgemuth, T., Jentsch, A., Seidl, R. (Eds.), Disturbance Ecology, Landscape Series. Springer International Publishing, Cham, pp. 271–293. https://doi.org/10.1007/978-3-030-98756-5_12

White, T.C.R., 2015. Are outbreaks of cambium-feeding beetles generated by nutritionally enhanced phloem of drought-stressed trees? J Applied Entomology 139, 567–578. https://doi.org/10.1111/jen.12195

Winter, M.-B., Baier, R., Ammer, C., 2015. Regeneration dynamics and resilience of unmanaged mountain forests in the Northern Limestone Alps following bark beetle-induced spruce dieback. Eur J Forest Res 134, 949–968. https://doi.org/10.1007/s10342-015-0901-3

Wulder, M.A., White, J.C., Bentz, B., Alvarez, M.F., Coops, N.C., 2006. Estimating the probability of mountain pine beetle red-attack damage. Remote Sensing of Environment 101, 150–166. https://doi.org/10.1016/j.rse.2005.12.010

Zabihi, K., Surovy, P., Trubin, A., Singh, V.V., Jakuš, R., 2021. A review of major factors influencing the accuracy of mapping green-attack stage of bark beetle infestations using satellite imagery: Prospects to avoid data redundancy. Remote Sensing Applications: Society and Environment 24, 100638. https://doi.org/10.1016/j.rsase.2021.100638

Zeppenfeld, T., Svoboda, M., DeRose, R.J., Heurich, M., Müller, J., Čížková, P., Starý, M., Bače, R., Donato, D.C., 2015. Response of mountain *Picea abies* forests to stand-replacing bark beetle outbreaks: neighbourhood effects lead to self-replacement. J Appl Ecol 52, 1402–1411. https://doi.org/10.1111/1365-2664.12504

Zhang, J., Cong, S., Zhang, G., Ma, Y., Zhang, Y., Huang, J., 2022. Detecting Pest-Infested Forest Damage through Multispectral Satellite Imagery and Improved UNet++. Sensors 22, 7440. https://doi.org/10.3390/s22197440

7. Supplementary material

Supplementary materials are included in the electronic version of this PhD thesis and comprise the supplementary data from the three published papers discussed. The first two papers contain supplementary data. The supplementary content is as follows:

7.1 Article I (chapter 3.1)

Supplemental table 1 | Mean and standard deviations of Susceptible and Healthy samples of individual bands and SVI for all imagery

The Supplementary Material for this article can be found online at: https://www.frontiersin.org/articles/10.3389/ffgc.2023.1130721/full#supplementary-material

7.2 Article IV (chapter 3.4)

Table S1 - Proposed 102 best GAM regression models with which to study annual changes of tree cover loss for a 10-year period.

Figure S1. The result of fitting the most parsimonious model (Table 4) for the relation between the bark beetle spots initialisation and May average monthly air temperature in the current year, average yearly precipitation in the previous year, and June wind speed in the current year over a 10-year span in the study area.

Figure S2. The result of fitting the most parsimonious model (Table 7) for the relation between the bark beetle spot spreading and Average yearly precipitation in the previous year, sum duration of solar radiation in the previous year in April and June over a 10-year span in the study area.

Figure S3. The result of fitting the most parsimonious model (Table 10) for the relation between the annual tree cover loss change and Average yearly precipitation in the previous year, May amount of precipitation in the current year, and May wind speed in the current year over a 10-year span in the study area.

The Supplementary Material for this article can be found online at: https://ars.els-cdn.com/content/image/1-s2.0-S0378112723009003-mmc1.docx